MITOCHONDRIAL LOCALISATION AND CELLULAR UPTAKE *IN VITRO* USING NOVEL 'MITOCHONDRIOTROPIC' LIPOSOMES

BY

NICOLISHA NARAINPERSAD

Submitted in fulfilment of the academic requirements for the degree of

DOCTOR OF PHILOSOPHY

In the School of Life Sciences,

University of KwaZulu-Natal, Westville Campus.

December 2016

As the candidate's supervisor and co-supervisors respectively, we have approved submission of this thesis.

Supervisor: **Professor M. Singh**

Signed: _____ Date: _____

Co-Supervisor: **Professor M. Ariatti**

Signed: _____ Date: _____

Co-Supervisor: **Dr. B. Masola**

ABSTRACT

Mitochondrial research has made tremendous strides since the 1980/90s when mitochondrial DNA mutations were first identified as a primary cause for human diseases and the organelle's role in apoptosis was elucidated. These mutations of the mitochondrial genome have been implicated in a spectrum of clinical disorders especially involving the muscle and central nervous system. This makes the mitochondrion a prime candidate for organelle-specific delivery of exogenous materials such as therapeutic DNA and drugs, for therapy of diseases caused by mitochondrial dysfunction. However, reports of mitochondrial targeted delivery systems are limited. Hence vector design and development is of paramount importance. The success of liposomes viz. cationic liposomes, in chromosomal gene therapy make them potential vectors for mitochondrial gene targeting.

In this investigation novel 'mitochondriotropic' liposomes were synthesised to evaluate their cellular uptake and mitochondrial localisation activity *in vitro* using four different mammalian cell culture models. Cationic cholesterol derivative, 3β [N-(N',N'-dimethylaminopropane)-carbamoyl] cholesterol (CHOL-T) was formulated with dioleoylphosphatidylethanolamine (DOPE) to produce cationic liposomes, to which a mitochondrial targeting sequence (MTS) and octaarginine (R8) peptides were attached via two different novel cholesterol-derived cross-linking agents. Size, zeta potential, shape and lamellarity of liposomes and corresponding lipoplexes were assessed by the innovative technique, Nanoparticle Tracking Analysis (NTA) and cryogenic transmission electron microscopy. Their ability to bind, condense and protect plasmid DNA (pCMV-*luc*), was determined using the band shift, dye displacement and nuclease protection assays repectively. *In vitro* cytotoxicity and mechanism of cell death prompted by these novel liposomal preparations was determined using the MTT, AlamarBlue® and acridine orange and ethidium bromide (AO/EB) dual staining assays respectively, in the hepatocyte-derived human cell line (HepG2), human embryonic kidney cells (HEK293), the human intestinal cell line (Caco-2) and human cervical carcinoma (HeLa-Tat *luc*) cells. Fluorescently labelled DNA was used to determine cellular uptake and mitochondrial targeting and localisation ability of these cationic mitochondriotropic liposomal formulations in the target organelles, mitochondria using fluorescence microscopy and the quantitative evaluation of fluorescence in the mitochondrial fraction of cell homogenate cocktails.

These mitochondriotropic liposomes successfully bind, condense and protect plasmid DNA in the presence of serum, are fairly well tolerated by all cell lines tested in culture with cell death observed to be apoptotic and not necrotic in nature. The liposomes were shown to successfully enhance cellular uptake in all cell culture models tested. Furthermore, results demonstrate positive mitochondrial targeting and localisation activity facilitated by the presence of MTS peptide and a combination of MTS and R8 peptides on the liposomal surface for all four of these novel liposomal nanovectors.

Key words: cationic liposome, mitochondriotropic, cytotoxicity, targeting, localisation

PREFACE

The experimental work described in this thesis was carried out in the School of Life Sciences, University of KwaZulu-Natal (Westville Campus), Durban, South Africa from August 2010 to December 2016, under the supervision of Professor M. Singh and the co-supervision of Professor M. Ariatti and Dr B. Masola.

These studies represent original work by the author and have not otherwise been submitted in any form for any degree or diploma to any tertiary institution. Where use has been made of the work of others it is duly acknowledged in the text.

DECLARATION 1 – PLAGIARISM

I, Nicolisha Narainpersad declare that

1. The research reported in this thesis, except where otherwise indicated, is my original research.

2. This thesis has not been submitted for any degree or examination at any other university.

3. This thesis does not contain other persons' data, pictures, graphs or other information, unless specifically acknowledged as being sourced from other persons.

4. This thesis does not contain other persons' writing unless specifically acknowledged as being sourced from other researchers. Where other written sources have been quoted, then:

   a. Their words have been re-written but the general information attributed to them has been referenced.

   b. Where their exact words have been used, then their writing has been placed in italics and inside quotation marks, and referenced.

5. This thesis does not contain text, graphics or tables copied and pasted from the internet, unless specifically acknowledged, and the source being detailed in the thesis and in the Reference Section.

Signed: _____

Declaration Plagiarism 22/05/08 FHDR Approved

DECLARATION 2 - PUBLICATIONS

DETAILS OF CONTRIBUTION TO PUBLICATIONS that form part and/or include research presented in this thesis (include publications in preparation, submitted, *in press* and published and give details of the contributions of each author to the experimental work and writing of each publication.

Publication: Peer Reviewed Published Abstract

Narainpersad N., Ariatti M., and Singh M. (2013). *Mitochondrial Gene Targeting in Mammalian Systems using Novel 'Mitochondriotropic' Liposomes*. Human Gene Therapy **24(12):** A1-A172. (Appendix B)

Manuscripts

Narainpersad N., Singh M., and Ariatti M. *Macromolecule delivery to mitochondria: A review of delivery strategies. In Preparation* (Appendix B)

Signed: _____

Declaration Publications FHDR 22/05/08 Approved

TABLE OF CONTENTS

LIST OF FIGURES

– MS04 0.3, RM product = 0.05, SP-CHOL = 0.2;Plate **B** – MS04 = 0.4, RM product = 0.3, GM-CHOL = 0.4. Solvent system: $CHCl_3$: MeOH (95:5, $^{v}/_{v}$)

Figure 4.4: Schematic structure and composition of the cationic liposome (+) used in this study and its electrostatic interaction with anionic DNA (–) to form a liposome-DNA complex called a lipoplex.

Figure 4.5: Schematic of the two most common lipoplex structures **(A)** lamellar structure (L^{C}_{α}) where DNA is sandwiched between lipid bilayers, and **(B)** inverted hexagonal structure (H^{C}_{II}) where DNA is coated with lipid monolayer arranged in a hexagonal lattice. Adapted from Dan (2015).

Figure 4.6: Gel retardation analysis of the binding interaction of varying amounts of cationic mitochondriotropic liposome preparations in a total of 10 µl reaction mixture while pCMV-*luc* DNA was kept constant at 0.5 µg per well. **(A)** SP-CHOL-MTS, **(B)** GM-CHOL-MTS, **(C)** SP-CHOL-MTS-R8 and **(D)** GM-CHOL-MTS-R8. Samples from left to right are as follows, lane 1: 0.5 µg of naked pDNA (0 µg of cationic liposome); lanes 2 – 8: the respective liposome-DNA complexes prepared using various liposome mass (µg) as indicated. Numbers in red and arrows indicate the point of electroneutrality.

Figure 4.7: Nuclease protection assay of cationic mitochondriotropic liposome-DNA complexes of **(A)** SP-CHOL-MTS, **(B)** GM-CHOL-MTS, **(C)** SP-CHOL-MTS-R8 and **(D)** GM-CHOL-MTS-R8 in a total of 10 µl reaction mixture while pCMV-*luc* DNA was kept constant at 1 µg per well. Samples from left to right are as follows, lane 1: 1 µg of untreated naked pCMV-*luc* DNA (control 1); lane 2: 1 µg of FBS-treated naked pCMV-*luc* DNA (control 2); lanes 3 – 8: the respective liposome-DNA complexes prepared at different liposome mass (µg) as indicated.

Figure 4.8: Schematic representation of DNA supercoiling followed by formation of anticlockwise (–) -coiling and clockwise (+) -coiling of circular DNA needed for condensation and compaction (Bugreev and Nevinsky, 2009).

Figure 4.9: Diagram showing **(A)** Ethidium bromide and **(B)** the process of intercalation, illustrating the lengthening and untwisting of the DNA helix. Adapted from www.technologyinscience.blogspot.com (accessed 19/07/2015).

Figure 4.10: EtBr intercalation displacement assay where percentage relative fluorescence was plotted as a function of µgrams of liposome **(A)** MTS only liposomes and **(B)** MTS and R8 liposomes. Cationic mitochondriotropic liposome was systematically added to an EtBr/pCMV-*luc* (1.2 µg) solution until a plateau in fluorescence was attained.

Figure 4.11: Transmission electron micrographs of cationic mitochondriotropic liposomes as follows: **(A)** SP-CHOL-MTS, **(B)** GM-CHOL-MTS, **(C)** SP-CHOL-MTS-R8 and **(D)** GM-CHOL-MTS-R8. Bar = 100 or 200 nm.

Figure 4.12: Transmission electron micrographs of cationic mitochondriotropic lipoplexes [prepared at optimal binding liposome-DNA or N/P ratios as determined by electrophoretic mobility shift assays]. **(A)** SP-CHOL-MTS 7.5:1, **(B)** GM-CHOL-MTS 4.8:1, **(C)** SP-CHOL-MTS-R8 2.1:1 and **(D)** GM-CHOL-MTS-R8 1.6:1. Bar = 100 or 200 nm.

Figure 4.13: Schematic diagram of zeta potential for nanoparticles depicting the potential difference as a function of distance from the charged surface of a particle suspended in adispersion medium. (http://www.pharmainfo.net/characterization-nanoparticles/zeta; accessed 08/04/2015).

Figure 4.14: Schematic of the optical configuration used in NTA and two-dimensional Stokes-Einstein equation. The sample in the chamber is illuminated by a laser beam. The particle movement is recorded via light scattering by a sCMOS camera and the software tracks each particle and determines the diffusion coefficient of the Brownian motion. Combining Stokes–Einstein equation

and two dimensional mean square displacement, the particle size is then calculated as the mean-squared displacement $(x, y)^2$, K_B as the Boltzmann's constant, T as the absolute temperature, t as the measurement time, η as the viscosity and d as the hydrodynamic diameter. Adapted from (Gross *et al*., 2016; NanoSight, 2015a; Dragovic *et al*., 2011).

Figure 4.15: Screen shot from video showing light scatter from liposomal particles moving under Brownian motion.

Figure 4.16: Cell lines used in this study: **(A)** HEK293, **(B)** HepG2, **(C)** Caco-2 and **(D)** HeLa-Tat *luc.* Here cells were viewed as a monolayer at semi-confluence under 100 x magnification with an inverted microscope (Olympus CKX41, Tokyo, Japan).

Figure 4.17: Chemical structure of MTT and its reduced coloured insoluble formazan product. Adapted from Stockert *et al*. (2012).

Figure 4.18: *In vitro* MTT cytotoxicity analysis of cationic mitochondriotropic liposome-pCMV-*luc* DNA complexes toward HepG2, HEK293, Caco-2 and HeLa-Tat *luc* cell lines. Lipoplexes (containing 1 µg of pCMV-*luc* DNA) were prepared at various liposome-DNA ratios ($^{w}/_{w}$) as indicated above. **(A)** SP-CHOL-MTS, **(B)** GM-CHOL-MTS, **(C)** SP-CHOL-MTS-R8 and **(D)** GM-CHOL-MTS-R8. A control sample containing only cells was assumed to have 100% survival. Results are presented as a percentage of the control sample and represent the mean ± SD, n = 3. Statistical analysis was performed using one-way ANOVA followed by Dunnett multiple comparison *post hoc* test. *P<0.05 and **$P<0.01$ as compared to the control.

Figure 4.19: Chemical structure of non-fluorescent blue dye, resazurin and its reduction to strongly fluorescent pink resorufin by viable cells. Adapted from Stoddart (2011).

Figure 4.20: AlamarBlue® cytotoxicity assay showing percentage (%) reduction of resazurin as cell viability in HepG2 (♦), HEK293 (■), Caco-2 (●) and HeLa-Tat *luc* (▲) cell lines as function liposome-pCMV-luc DNA ratios. Lipoplexes (containing 1 µg of pCMV-*luc* DNA) were prepared at various liposome-DNA ratios ($^{w}/_{w}$) as indicated above. **(A)** SP-CHOL-MTS, **(B)** GM-CHOL-MTS, **(C)** SP-CHOL-MTS-R8 and **(D)** GM-CHOL-MTS-R8. A control sample (------) containing only cells were assumed to have 100% survival. Results represent the mean ± SD, n = 3.

Figure 4.21: Apoptotic index calculated as a percentage (%) from results of the AO/EB dual staining apoptosis assay. SP-CHOL-MTS, GM-CHOL-MTS, SP-CHOL-MTS-R8 and GM-CHOL-MTS-R8 mitochondriotropic lipoplexes (containing 1 µg of pCMV-*luc* DNA) prepared at optimal binding ratios were incubated with HepG2, HEK293, Caco-2 and HeLa-Tat *luc* cell lines. A control of untreated cells for each cell line was utilised. Results represent the mean ± SD, n = 2. Statistical analysis was performed using one-way ANOVA followed by Dunnett multiple comparison *post hoc* test. *$(P<0.05)$ **$(P<0.01)$ and ***$(P<0.001$) indicate a significant difference compared to the respective controls.

Figure 4.22: Apoptosis assay using AO/EB dual staining and fluorescent microscopy illustrating morphological changes induced by SP-CHOL-MTS, GM-CHOL-MTS, SP-CHOL-MTS-R8 and GM-CHOL-MTS-R8 mitochondriotropic lipoplexes (containing 1 µg of pCMV-*luc* DNA) prepared at optimal binding ratios in HepG2, HEK293, Caco-2 and HeLa-Tat *luc* cell lines as indicated. A control of untreated cells for each cell line was utilised. **L**: Live cells stained green; **EA**: early apoptotic cells with condensed yellow-green nuclei; **LA**: late apoptotic cells stained orange with condensed nuclei; **N**: necrotic cells with uniform orange fluorescence and **MB**: membrane blebbing, a feature of apoptosis. Bar = 100 µm.

Figure 4.23: Representative images showing intracellular co-localisation by CLMS. Left panel: mitochondria stained green byMitoTracker® Green FM; Central panel: red fluorescence from rhodamine-tagged DNA delivered by the nanoparticles; Right panel: merged left and central panels.

Yellowish colour indicates co-localisation of the rhodamine-tagged DNA with the MitoTracker® Green FM. Bar = 10μm

Figure 4.24: Schematic representation of mitochondrial delivery of MTS only and MTS and R8 liposomes. Lipoplexes enter the cell via endocytosis or macropinocytosis respectively. Disruption of endosome and macropinosome allows escape of respective liposome-DNA complexes which then translocate to the mitochondria to which it binds via MTS and a combination of MTS and R8.

Figure 4.25: Intracellular co-localisation by fluorescence microscopy of SP-CHOL-MTS, GM-CHOL-MTS, SP-CHOL-MTS-R8 and GM-CHOL-MTS-R8 mitochondriotropic lipoplexes (containing 1 μg of rhodamine-labelled pCMV-*luc* DNA) prepared at optimal binding ratios in **(A)** HepG2, **(B)** HEK293, **(C)** Caco-2 and **(D)** HeLa-Tat *luc* cell lines. Two controls containing cells only and cells exposed to naked rhodamine-tagged DNA were used. Left panel: red fluorescence from rhodamine-tagged DNA delivered by the nanoparticles; Central panel: mitochondria stained green by MitoTracker® Green FM; Right panel: merged left and central panels. Yellowish colour indicates co-localisation of the rhodamine-tagged DNA with the MitoTracker® Green FM. Magnification = 200x.

Figure 4.26: Evaluation of mitochondrial targeting of mitochondriotropic liposomes SP-CHOL-MTS, GM-CHOL-MTS, SP-CHOL-MTS-R8 and GM-CHOL-MTS-R8 in four different cell homogenates. Lipoplexes (containing 1 μg of fluorescein-labelled pCMV-*luc* DNA) were prepared at optimal binding ratios. Two controls, comprising untreated cells and cells exposed to naked DNA were utilised. Results represent the mean ± SD, $n = 3$. Statistical analysis was performed using one-way ANOVA followed by Dunnett multiple comparisons *post hoc* test. *($P<0.05$) and ***($P<0.001$) indicate a significant difference.

LIST OF TABLES

ABBREVIATIONS AND SYMBOLS

Å	Ångström
Amp^r	Ampicillin resistance
ADP	Adenosine diphosphate
AD	Alzheimer's disease
ALS	Amyotrophic lateral sclerosis
AO/EB	Acridine orange/ ethidium bromide
AONs	Antisense oligonucleotides
ATP	Adenosine triphosphate
BSA	Bovine serum albumin
cDNA	Complementary DNA
CHOL-T	3β-[*N*-(*N'*, *N'*-Dimethylaminopropane)-carbamoyl] cholesterol
CLSM	Confocal Laser Scanning Microscopy
CMV	Cytomegalovirus promoter
cryo-TEM	Cryogenic-transmission electron microscopy
CPP	Cell penetrating peptide
DCM	dichloromethane
DC-CHOL	3β[N,N',N'-dimethylaminoethane)-carbamoyl] cholesterol
DMAPA	3-Dimethylaminopropylamine
DMSO	Dimethyl sulfoxide
DNA	Deoxyribonucleic acid
DOGS	dioctadecylamidoglycyl-spermine
DOPE	dioleoylphosphatidylethanolamine
DOTAP	1,2-Dioleoyl-3-trimethylammonium-propane
DOTMA	N-[1-(2,3-dioleyloxy)propyl]-N,N,N-trimethylammonium chloride
EMEM	Eagle's Minimum Essential Medium
EtBr	Ethidium bromide
FBS	Foetal bovine serum
GMBS	*N*-γ-maleimidobutyryl-oxysulfosuccinimide ester
GM-CHOL	3β-[N-(hydrazino-γ-maleimidobutyryl)-carbamoyl] cholesterol
H^C_{II}	Inverted hexagonal structure
HBS	HEPES buffered saline
HD	Huntington's disease
HEPES	2-[4-(2-Hydoxyethyl)-1-piperazinyl] ethanesulfonic acid
Lα	Lamellar phase
luc	Luciferase
MIB	Mitochondrial Isolation Buffer
mol%	Mole percentage
MPS	Mononuclear phagocyte system
MS04	Cholesterylformylhydrazide
MS09	*N*, *N*-Dimethylaminopropylaminylsuccinylcholesterylformylhydrazide

MTT	3-(4, 5-Dimethyl-2-thiazolyl)-2, 5-diphenyl-2H-tetrazolium bromide
MΩ	Megaohm
MTS	Mitochondrial Targeting Sequence
MtDNA	Mitochondrial DNA
nDNA	Nuclear DNA
N/P	Amine to phosphate ratio
NTA	Nanoparticle Tracking Analysis
OD	Optical density
OXPHOS	Oxidative phosphorylation system
PBS	Phosphate buffered saline
pDNA	Plasmid DNA
PD	Parkinson's disease
PEG	Polyethylene glycol
PEI	Polyethyleneimine
PLL	Poly-L-lysine
SD	Standard deviation
SE	Standard error
SDS	Sodium dodecyl sulphate
SP-CHOL	3β-[N-(hydrazino 3-{2-pyridyldithio} propionate)-carbamoyl] cholesterol
SPDP	Succinimidyl 3-(2-pyridyldithio) propionate
TAT	Trans-activated transcription
TCA	Cycle tricarboxylic acid cycle
TLC	Thin layer chromatography
TIM	Translocator inner membrane
TOM	Translocator outer membrane
tRNA	Transfer RNA
R8	Octaarginine
RES	Reticuloendothelial system
ROS	Reactive oxygen species
TPP	Triphenylphosphonium
v/v	Volume to volume ratio
w/v	Weight to volume ratio
w/w	Weight to weight ratio
λ	Wavelength (lambda)
ζ	Zeta potential

ACKNOWLEDGEMENTS

I wish to express my sincere thanks and appreciation to the following people:

- My supervisor, Professor Moganavelli Singh and co-supervisor, Professor Mario Ariatti, for their invaluable supervision, guidance and patience during the course of this study as well as their vast array of scientific knowledge.
- My parents, Mr and Mrs Narainpersad, my brothers, sisters-in-law, my nephew and the rest of my family and friends for their constant support, encouragement, assistance and kindness during the course of this study.
- The National Research Foundation (NRF) for financial support.
- Dr. J. Wesley-Smith (Electron Microscopy) his immeasurable assistance with electron microscopy.
- Ms. Lorika Beukes (Microscopy & Microanalysis Unit) for help with CLSM.
- My colleagues and friends from the Discipline of Biochemistry for their support and help.
- My husband, Nicholas Naidoo, for his care, love, patience, encouragement and support throughout the completion of this thesis.

CHAPTER ONE

INTRODUCTION

1.1. BACKGROUND OF STUDY

The efficient and site-specific distribution of therapeutic agents is a vitally important issue in nanotechnology. Many reports have detailed nanocarriers directed to specific cells and tissues however there is a distinct lack of development in nanocarriers that target a specific organelle, such as mitochondria, the endoplasmic reticulum and the Golgi apparatus, all of which represent promising potential targets for therapeutic agents. Of these organelles, mitochondria are of immense interest due to its association with several human diseases, in addition to playing a key role in apoptosis in mammalian cells. Mitochondria are DNA-containing organelles found in almost all eukaryotic cells. They contain a small circular 16,6 kb DNA molecule that resides inside the matrix space and are the prime ATP energy generating sites in eukaryotic cells. They are intimately involved in maintaining the homeostasis of vital physiological functions, in addition to its array of other functions ranging from apoptosis, calcium signalling, intermediary metabolism to aging (D'Souza *et al*., 2007; Scheibye-Knudsen *et al*., 2014).

Mitochondrial research has made a giant leap since early 1988 and 1990s respectively, when mitochondrial DNA mutations were first identified as a primary cause for human diseases and the organelle's role in apoptosis was elucidated (Horobin *et al*., 2007). However there is much that is still not fully understood about diseases caused by mitochondrial dysfunction. It has been reported by a number of studies that mutations or genetic defects in mitochondrial DNA (mtDNA) are linked to mitochondrial diseases or dysfunctions leading to human disorders such as diabetes mellitus, increased susceptibility to cancer, and neurodegenerative diseases such as Alzheimer's, Huntington's and Parkinson's disease, (Yamada *et al*., 2015; Salvado *et al*., 2015). In fact, the prevalence of pathogenic mitochondrial DNA mutations is extremely high, and recently estimated to occur in every 1 of 200 adults (Tischner and Wenz, 2015). Currently, treatment options for mitochondrial diseases are limited to being palliative and supportive with no cure available. Effective therapies for these diseases caused by

mitochondrial dysfunction remain elusive as human mitochondria within living cells have limited accessibility to direct physical, biochemical and pharmacological manipulation. Therefore, incursion of nanotechnologies such as gene therapy into mitochondrial research by targeting of genetic material or drugs to the mitochondria could hold the promise of assisting to overcome these obstacles, and are promising candidates for the therapeutic treatment of mitochondrial diseases.

Presently, there have been reports of numerous systems for delivery of nucleic acids, including several successful gene therapies, to the nucleus and cytosol, however, far less progress has been made concerning mitochondrial gene delivery nanovectors (Yamada *et al*., 2015). Hence, there has been a paucity of information about mitochondrial targeted delivery using nanoparticles, although there have been reports of mitochondrial delivery of various biomolecules in isolated mitochondria and cell homogenates (Yamada and Harashima, 2013). However, it is significant to note that in respect to successful nuclear gene therapies, mitochondrial gene therapy has never been achieved (Yamada *et al*., 2015). This is because of the lack of an optimal mitochondrial targeting system that can sophistically regulate cellular uptake, endosomal escape and mitochondrial targeting. Thus, it appears that the need for an ideal vector for mitochondrial targeting has become a rate-limiting step.

To this end, modification of strategies that made chromosomal gene therapy successful could be utilised for mitochondrial targeting. Although conceptually simple, the translation of gene therapy into effective therapies has proven to be extremely challenging, featuring many decades of scientific development, failed clinical trials and numerous other setbacks. Through this all, gene therapy has still emerged as a new paradigm for the treatment of human disease, and is considered by many as a potential revolution in modern day molecular medicine. Until fairly recently, most gene therapy experimental designs have made use of viruses as delivery vehicles, however increased inflammatory-type toxicities attributed to the activation of adaptive and innate immune responses in hosts in response to the viral-based vectors were observed. This led to non-viral vectors being the delivery vehicle of choice, particularly, liposomes. The success of phospholipid vesicles or liposomes, more specifically cationic liposomes, as gene delivery vehicles for chromosomal gene therapy have made them a potentially attractive vector for mitochondrial targeting.

This study aims to address the need for a safe and efficient mitochondrial targeted nanovector system, by developing a non-toxic, cationic mitochondriotropic liposomal delivery system for specific mitochondrial targeting and localisation. It is hoped that the development of an ideal vector system able to successfully target therapeutic genes and agents to the mitochondria in a clinical setting will open up a new window into the treatment and possible cure of mitochondrial diseases and mitochondrial associated diseases such as cancer, Parkinson's and Alzheimer's disease.

1.2. SCOPE OF STUDY

Mitochondrial gene and drug delivery is a field still in its infancy, due in part, to the absence of an ideal delivery vehicle to facilitate mitochondrial localisation and subsequent delivery. There is currently a search for a model vector system for gene/drug delivery that can specifically localise to the site of mitochondria of cells i.e. it is mitochondriotropic. This vector system should ideally be biodegradable, non-toxic, stable to storage, display low immunogenicity as well as have high therapeutic efficacy. To this end, non-viral vectors, specifically cationic liposomes, meet all prerequisites for an ideal delivery vehicle which they have proven to be with their considerable success in traditional nuclear gene delivery. However, their design and application in mitochondrial localisation requires streamlining. Accordingly, this study evaluates the ability of four novel cationic mitochondriotropic liposomal formulations to improve the efficacy of cellular uptake and mitochondrial localisation of plasmid DNA in four different cell line models.

1.2.1. Hypothesis

Cationic liposome-based delivery systems comprising the cytofectin, 3 β [*N-(N', N'*-dimethylaminopropane)-carbamoyl] cholesterol (CHOL-T); cross-linking agents, 3β-[N-(hydrazino 3-{2-pyridyldithio} propionate)-carbamoyl] cholesterol (SP-CHOL) and 3β-[N-(hydrazino-γ-maleimidobutyryl)-carbamoyl] cholesterol (GM-CHOL); mitochondria targeting ligand, mitochondrial targeting sequence (MTS) and octaarginine (R8) peptides display minimal toxicity in various cell lines as well as efficiently and effectively enhances cellular uptake and mitochondrial localisation of model plasmid DNA in selected mammalian cell lines.

1.2.2. Aim

The main aim of this investigation was the development of mitochondrial targeting vectors in the form of four cationic mitochondriotropic liposomal formulations and the evaluation of their chemical and biophysical characteristics, cytotoxicity, cellular uptake as well as their mitochondrial targeting and localisation activity in four cell lines.

1.2.3. Objectives

The following objectives form the basis to test the hypothesis and achieve the aim:

- Preparation of four cationic liposomes (CHOL-T), two incorporating the cholesterol-derived cross-linker, SP-CHOL and two containing GM-CHOL. Each of these is made mitochondriotropic by the addition of the MTS peptide only or a combination of MTS and R8 peptides.
- Preparation of liposome-pDNA complexes and characterisation of these lipoplexes in terms of size and zeta potential by Nanoparticle Tracking Analysis (NTA), and morphologically utilising cryogenic-transmission electron microscopy (cryo-TEM).
- Determination of binding capacity and serum stability of resultant lipoplexes using gel retardation, nuclease protection and ethidium bromide intercalation assays.
- Evaluation of cytotoxicity in selected mammalian cell lines *in vitro* by employing the 3-(4, 5-Dimethyl-2-thiazolyl)-2, 5-diphenyl-2H-tetrazolium bromide (MTT) growth inhibition and AlamarBlue® assays; detection of apoptosis by acridine orange and ethidium bromide (AO/EB) staining.
- Determination of cellular uptake and mitochondrial localisation by fluorescent microscopy and quantification of mitochondrial targeting activity.

1.3. NOVELTY OF STUDY

The synthetic cationic cholesterol-derived cytofectin, CHOL-T was previously synthesised in our laboratory (Singh *et al.*, 2001). Liposomes were formulated with a constant 50 mol% composition of CHOL-T, a varying mole percentage of dioleoylphosphatidylethanolamine (DOPE) and 5 or 10 mol% of either novel cholesterol-derived cross-linking agents, SP-

CHOL or GM-CHOL. The novelty of these previously synthesized liposomes is that they were taken a step further and made mitochondriotropic by the addition of MTS and R8 peptides. There have been no previous studies documented involving this novel combination of lipids and peptide additives. Accordingly, this study aims to assess the ability of these novel liposomal formulations to facilitate cellular uptake as well as mitochondrial localisation and targeting activity in the chosen cell lines.

1.4. OUTLINE OF THESIS

Chapter One

This chapter provides an introduction and background to the study. It highlights the challenges of mitochondrial gene delivery and non-viral gene delivery systems. Additionally, it outlines the rationale, scope, aim and objectives of the investigation.

Chapter Two

This chapter reviews in depth the relevant literature. Firstly, it details non-viral gene delivery nanovectors. Secondly, it highlights the mitochondria, types of mitochondrial diseases and their implications. Lastly, it explores the experimental strategies currently being investigated to correct mitochondrial defects and the feasibility thereof.

Chapter Three

The contents of this chapter details the experimental design and describes the laboratory methods undertaken. The syntheses of the cationic cytofectin and the cholesterol-derived cross-linkers and their subsequent formulation into cationic liposomes are described. Thereafter, the process of attaching the respective peptides to the surface of liposomes to generate mitochondriotropic liposomes is discussed, followed by determination of DNA binding and nuclease protection by gel retardation, ethidium bromide intercalation and nuclease protection assays respectively. Thereafter, further physical characterisation of liposomes and corresponding lipoplexes facilitated by the innovative technique of NTA and cryo-TEM is illustrated. Lastly, *in vitro* cell culture studies examining the cytotoxicity profile and mechanism of cell death initiated by these novel liposomal formulations was

conducted using the MTT, AlamarBlue® and apoptosis assays in HepG2, HEK293, Caco-2 and HeLa-Tat *luc*, cell lines, followed by a description of fluorescent studies used to establish cellular uptake, mitochondrial localisation and targeting activity.

Chapter Four

Chapter four details all the results acquired, together with a comprehensive discussion on the interpretation of these results and their implications providing perspective to this study.

Chapter Five

This final chapter concludes the study by emphasising outcomes which are significant to the aim and objectives of the investigation. Contributions of the study to the area of mitochondrial research are documented and assessed, while possible limitations and inadequacies of the study are evaluated. Finally, recommendations for further research to optimise the current system for clinical studies are made.

CHAPTER TWO

LITERATURE REVIEW

2.1. GENE THERAPY: AN OVERVIEW

The use of nucleic acids as therapeutically useful molecules, offers a fundamental approach to the treatment of a variety of diseases of acquired or genetic origin (Smith, 1999; Huang *et al*., 1999). The concept of gene therapy has provided a new paradigm for the treatment of human diseases and is considered by many as a potential revolution in medicine. This is because the ultimate goal of gene therapy is to eliminate the causes of diseases by adding, correcting or replacing genes whereas most current treatment of diseases is by simply treating the symptoms not the causes (Mountain, 2000; Huang *et al.*, 1999). Gene therapy is a promising therapeutic strategy centred on correcting chronic ailments, such as cancer, and other pathogenic diseases through genetic modification. The basis of this therapy requires the introduction of an exogenous nucleic acid molecule, such as DNA, mRNA, miRNA, and RNAi molecules, such as siRNA or small hairpin RNAs (shRNA), and antisense oligonucleotides (AONs), into the cell to achieve the desired therapeutic benefit with the nucleic acid molecule serving as a 'drug' (Lasic, 1997; Hill *et al.,* 2016).

The basic ideas for gene therapy were first expressed in the 1960's when Amos (1961) found that the uptake of nucleic acid molecules into cultured cells was enhanced when RNA was complexed with protamine (Huang *et al.,* 1999). Following that initial discovery, several other articles were published which clearly established that complexation of DNA or RNA with agents such as gelatin, methylated protein, polylysine and polyarginine increased transfection and/or infectivity (Huang *et al.*, 1999). In 1972, a discussion of gene therapy was offered in which it was proposed that a set of ethicoscientific criteria be formulated to guide the clinical application and development of gene therapy techniques (Friedmann and Roblin, 1972). Since then a number of advances and discoveries, such as the development of retroviral vectors with almost 100% transfection efficiency in 1982, have been made leading to the first therapeutic study involving gene therapy in 1990. This study was conducted in

patients with adenosine deaminase deficiency. Mullen and co-workers used a retrovirus to insert the gene that codes for adenosine deaminase into lymphocytes *ex vivo* (Mullen *et al*., 1996). A summary of some of the key events in the development of gene therapy is seen in Table 2.1.

TABLE 2.1: Summary of key events in the development of gene therapy (Adapted from Huang *et al*., 1999 and Wirth *et al*., 2013).

YEAR	EVENT
1944	First description that genetic material is carried in the form of DNA
1953	Watson and Crick describe the double-helix structure of DNA
1956	Viral genomes can be permanently incorporated in cell genomes
1961-2	Foreign DNA can integrate stably into mammalian cellular genomes
1972	A discussion of gene therapy was offered
1981-2	Retroviral vectors were developed to transfer foreign DNA to essentially 100% of exposed mammalian cells
1987	Synthesis of cationic lipid, DOTMA
1990	Adenosine deaminase gene therapy trial was initiated
1992	First gene therapy trial using DC-CHOL/DOPE cationic liposomes
1990s	Other gene delivery systems were developed
2003	China becomes the first country to approve a gene therapy based product for clinical use
2009	First successful gene therapy phase III gene therapy clinical trial in the EU
2012	EMA recommended a gene therapy product for approval in the EU

In the last two decades a number of gene therapy trials, involving genetic diseases such as cystic fibrosis, acquired diseases such as cancer and infectious diseases such as AIDS, have been initiated (Nishikawa and Huang, 2001). Some examples of diseases targeted by gene therapy are given below (Table 2.2).

TABLE 2.2: Examples of some disease applications of gene therapy (Lasic, 1997; Hill *et al.*, 2016).

DISEASE
Cystic fibrosis
Sickle cell anemia
Gaucher's disease
Duchenne muscular dystrophy
Cancer
HIV-1
Parkinson's disease
Alzheimer's disease
Arthritis
Atherosclerosis
Hemophilia B
β-Thalassemia major
Painful diabetic neuropathy

Currently, there are more than 1800 approved, ongoing or pending clinical trials worldwide (Wirth *et al*., 2013) (Figure 2.1). More than 60% of these trials are directed at cancer with most of the remainder targeted to monogenetic disorders, cardiovascular and infectious diseases.

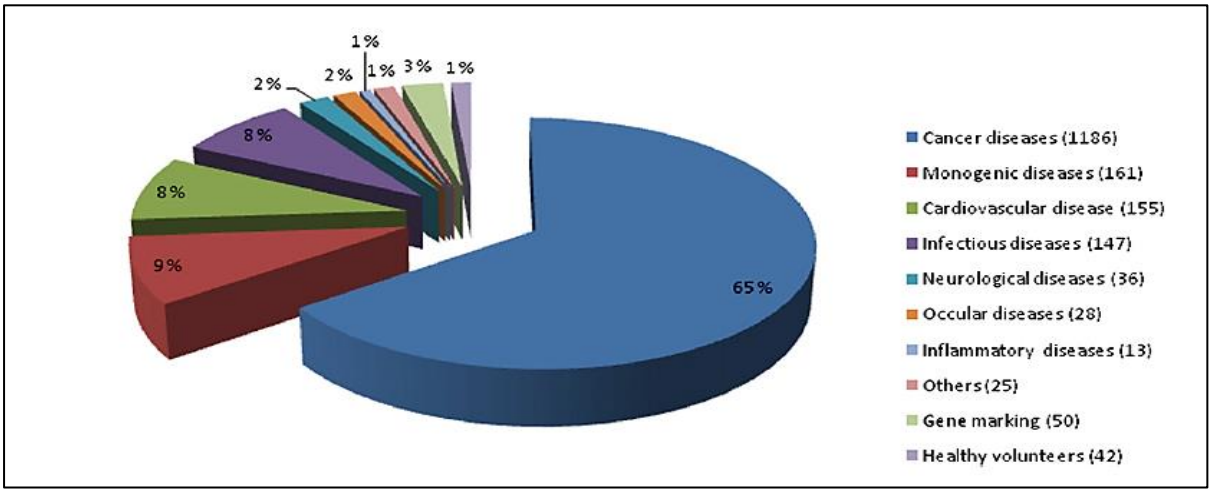

Figure 2.1: Graphical representation of indications of diseases/disorders addressed by worldwide gene therapy clinical trials [The Journal of Gene Medicine, Wiley and Sons (http://www.abedia.com/wiley/index.html) accessed 03/03/2016].

Almost 50 years after its 'discovery', gene therapy has had modest success. In 2007 University College London's Institute of Opthalmology reported a clinical trial for inherited retinal disease using a recombinant adeno-associated virus. The subject showed a moderate increase in vision and no apparent side effects (Bainbridge *et al.*, 2008). China became the first country to approve a gene therapy based product for clinical use in 2003 with Gendicine™, an adenoviral vector with human p53 cDNA for treatment of head and neck squamous cell carcinoma. Oncorine™, another adenoviral vector for treatment of late-stage refractory nasopharyngeal cancer, was also approved, in China in 2005 (Wirth *et al*., 2013). The European Medicines Agency (EMA) recommended, for the first time, approval of a gene therapy product, Glybera, in the EU in July 2012. Glybera is an adeno-associated viral vector manufactured to express lipoprotein lipase in the muscle tissue for the management of severe lipoprotein lipase deficiency (Wirth *et al*., 2013). Other gene delivery based products include Rexin G and Neovasculgen (Hill *et al.*, 2016).

Even with this very moderate success, 95% of clinical trials evaluating gene delivery technology have failed to progress beyond Phase II trials, demonstrating that there are still compelling challenges to producing clinically relevant, effective gene therapies (Hill *et al.*, 2016). Some of these include identification of diseases and access to target tissue, gene defect identification, stable and prolonged expression of newly introduced genes, immune response of the body, long and short term toxicity and probably the most limiting of all, the development of a vector that can selectively and efficiently deliver a gene to target cells with minimal toxicity (Smith, 1999; Li and Ma, 2001).

The scientific community have been constantly looking into ways of overcoming these hurdles and have taken up the challenge to develop a safe and efficient vector that can be employed in gene therapy both *in vitro* and *in vivo* with no restrictions and side effects. Hence to date, a great deal of interest has been focused on basic research into finding an ideal gene delivery system.

2.2. GENE DELIVERY VECTORS

In traditional gene therapy, in order for genes to be expressed they must be able to enter the nucleus of the cell. Genes or nucleic acids are generally incapable of entering a cell by itself

for two reasons: large size and repulsion due to their anionic charges (Ropert, 1999; Hill *et al.*, 2016). Hence, the need for a suitable vector to 'carry/transport' the nucleic acid or biomacromolecule. An ideal vector is regarded as one that should be safe, stable, easy to produce and proficient at achieving efficient, extended and cell or tissue specific gene expression (Li and Ma, 2001). Gene delivery systems generally fall into two categories: viral and non-viral. Viral vectors include all viruses used in the delivery of genes while non-viral vectors encompass all other methods of gene delivery. The advantages and disadvantages of these vectors are detailed in Table 2.3.

TABLE 2.3: Summary of advantages and disadvantages of gene delivery systems (Adapted from Mountain, 2000; Nayerossadat *et al*., 2012).

Vector	Advantages	Disadvantages
Adenovirus	Very high transfection efficiency *ex vivo* and *in vivo* Transfects both dividing and non-dividing cells Substantial clinical experience Characterized by complexity, stability, and integrity	Acute and strong immune responses Transgene size limit of 7.5 kb Manufacture and storage are moderately difficult Short duration of expression
Retrovirus	Fairly prolonged expression High transfection efficiency *ex vivo* Substantial clinical experience Low immunogenicity	Low transfection efficiency *in vivo* Transgene size limit of 8 kb Transfects only dividing cells Safety concerns of mutagenesis
Adeno-associated virus	Efficiently transfects a wide variety of cells *in vivo* Very prolonged expression *in vivo* Low immunogenicity High stability, safety and efficacy	Transgene limit of 4.8 kb Manufacture and production is very difficult Little clinical experience Safety concern of mutagenesis Repeat dosing affected by neutralising antibodies
Naked DNA	Manufacture, storage are simple and safe Very low immunogenicity Very good safety profile Clinical efficacy demonstrated in critical limb ischemia	Very short duration of expression in most tissues Very inefficient transfection *in vivo* Retargeting transfection very difficult Has to be applied directly
Cationic liposomes	Relatively simple manufacture and storage Efficient transfection *ex vivo* and *in vitro* Low immunogenicity and antigenicity Good safety profile	Inefficient transfection *in vivo* Short duration of expression and rapid clearance by Little clinical experience Retargeting transfection difficult
Cationic polymers	Relatively simple manufacture and storage Efficient transfection *ex vivo* and *in vitro* Low immunogenicity Good safety profile Retargeted transfection demonstrated	Inefficient transfection *in vivo* Very short duration of expression Non-biodegradable nature of PEI No clinical experience

2.2.1. Viral Vectors

Viral vectors are replication-deficient viruses with part of their viral sequence modified by deletion and replaced by therapeutic genes (Li and Ma, 2001). Generally most viral vectors are highly efficient gene transfer vehicles as they contain all of the necessary characteristics for successful gene transfer such as cell adhesion, membrane translocation, efficient transcription and translation (Cristiano *et al.*, 1993). In addition, their ability to stably integrate exogenous DNA into host chromosomes and their high specificity are among the major reasons why viral vectors were employed in more than 90% of clinical gene therapy trials (Singh *et al*., 2006; Walther, 2000; Hill *et al.*, 2016). However several limitations are inherent in their use. Depending on the type of viral vector, these could include toxicity, high immunogenicity, low viral titres, limited transgenic capacity size and provocation of mutagenesis and carcinogenesis in hosts (Huang *et al.*, 1999; Liu and Huang, 2002; Nayerossadat *et al*., 2012). In 1999, the worst case scenario for viral vectors became a reality when an 18 year old patient taking part in a gene therapy clinical trial died as a direct result of the adenovirus used for the treatment, highlighting safety issues with viral vectors and necessitating further investigation regarding overcoming technical limitations and improving biosafety (Wirth *et al*., 2013; Mertena and Gaillet, 2016).

Retroviruses are the most extensively used vectors. They are single-stranded RNA viruses which are constructed into viral vectors by replacing all viral genes required for replication with therapeutic genes. This type of viral vector randomly incorporates the gene directly into the host chromosome leading to safety concerns such as mutagenesis and carcinogenesis (Lasic, 1997; Smith, 1999). Adenoviruses are less hazardous as they do not integrate into the host chromosome so gene expression is short-lived (Huang *et al.*, 1999). This vector can be produced at high viral titres but suffers in that it often induces an inflammatory response from the host making repeat doses impossible (Huang *et al.*, 1999). These limitations can be overcome by the use of ‘gutless’ or ‘helper dependent’ adenoviruses, which lack all viral coding sequences (Józkowicz and Dulak, 2005). Adeno-associated viruses are small non-pathogenic DNA viruses that require a helper virus to replicate. They infect both dividing and non-dividing cells and like retroviruses, the wild type version can integrate into the host chromosome in contrast to the recombinant adeno-associated virus vectors for which integration in chromosomes is rare and random (Mertena and Gaillet, 2016). The major drawbacks of adeno-associated viruses are that they have a small transgene capacity of less

than 5 kb and produce low titres (Smith, 1999; Huang *et al.*, 1999; Nayerossadat *et al*., 2012). Other viral vectors include the Herpes simplex viruses (HSV), the main disadvantage of which is their cytotoxicity; lentiviruses which suffer from low infectivity and the pox viruses which, although possessing a large transgene capacity, have a complex biology and structure, are immunogenic and provide only transient expression (Huang *et al.*, 1999; Nayerossadat *et al*., 2012).

As mentioned above, the safety concerns related to the use of these viruses in humans far outweigh their advantages making non-viral delivery systems an attractive alternative.

2.2.2. Non-viral Vectors

Advantages of non-viral vectors include their simplicity of use, lack of specific immune response, low acute toxicity, no limitation in transgene capacity for most of the vectors and ease of large scale production (Li and Huang, 2000; Huang *et al.*, 1999; Nayerossadat *et al*., 2012). These gene delivery vehicles have the potential to provide nucleic acid-based therapeutics that strongly resemble traditional pharmaceuticals in that the products may be capable of repeat dosages with minimal toxicity, be able to be produced in large quantities at an acceptable cost, have high reproducibility and lastly be stable to enable storage (Davis, 2002). Non-viral gene delivery vectors can be non-targeted or targeted to a specific cell or tissue type (Singh, 1998). Several non-viral delivery methods exist and they can be broadly divided into two categories, naked DNA delivery by a physical method or DNA delivery by complexation with a cationic carrier (Nishikawa and Huang, 2001; Nayerossadat *et al*., 2012). These methods will be discussed in brief.

2.2.2.1. Naked DNA Injection

The direct transfer of DNA into the nucleus of cells by microinjection is the simplest system for DNA delivery (Nishikawa and Huang, 2001). The DNA used can be produced on a large scale by cultivation of plasmid harbouring *Escherichia coli.* Direct DNA transfer by this method is not feasible as it is difficult for the naked DNA to enter cells due to their large size, it cannot be done on a large scale, gene expression levels are low and it is fairly limited to

only a few tissues i.e. the skeletal muscle, the heart muscle, liver and solid tumours (Singh, 1998; Huang *et al.,* 1999; Manjila *et al*., 2013). However, they are more suitable as 'DNA vaccines' (Li and Ma, 2001).

2.2.2.2. Gene Gun Method

This method is also referred to as the ballistic method, the particle acceleration method or DNA coated particle bombardment (Lasic, 1997; Manjila *et al*., 2013). This physical method involves shooting gold, tungsten or silver microparticles coated with pDNA into target cells or tissues with a gene gun (Nishikawa and Huang, 2001; Manjila *et al*., 2013). The gene gun method allows for DNA to penetrate directly into the cell thereby bypassing enzymatic degradation by the endosomal pathway (Li and Huang, 2000). A major drawback of this type of gene delivery is that the target tissues have to be surgically exposed and there is only low level of gene product (Huang *et al.,* 1999; Nishikawa and Huang, 2001). A possible application for the gene gun method is genetic or DNA vaccinations.

2.2.2.3. Electroporation and Nucleofection

Electroporation was first described in the 1965 by Coster. This method involves the application of short, intense bursts of controlled electrical pulses to induce transient membrane destabilisation of the target cells, thereby allowing the DNA to enter the cytoplasm. After initial permeabilisation, the pores on the membrane close trapping the DNA inside the cell (Nishikawa and Huang, 2001; Nayerossadat *et al*., 2012). To date, this technique has been applied to the skin, liver, lung, muscle and in tumour treatment but the parameters associated with optimal gene expression differ from tissue to tissue making implementation of this method on a large scale difficult (Nishikawa and Huang, 2001).

Nucleofection is a further development of electroporation. It follows the same principle as electroporation however this cell-type specific technique depends on less harmful electrical pulses and specialised solutions optimised for specific cell types (Gresch *et al.,* 2004).

2.2.2.4. Cationic Polymers

High molecular weight, long chain polymers bearing cationic groups have been used to condense DNA via electrostatic interaction and thus facilitate gene transfer (Huang *et al.,* 1999; Mountain, 2000). The complexes formed between cationic polymers and DNA are referred to as 'polyplexes' (Felgner *et al.,* 1997). The complexation between the polymer and DNA protects the nucleic acid molecule from degradation, increases the stability of DNA, enhances endocytosis or cellular uptake and enters the nucleus to release the nucleic acid molecule (Manjila *et al*., 2013). Commonly used polymers include polyethylenimines (PEI), poly-L-lysine (PLL), poly-L-ornithine and chitosan (Nishikawa and Huang, 2001; Oku *et al.,* 2001). These polymers can be readily chemically synthesised, making them amenable to scalable synthesis. There has recently been a surge in the use of polymer-based vectors, possibly due to the growing understanding of polymer gene-delivery mechanisms.

2.2.2.5. Liposomes

Liposomes have been described as vesicular colloidal particles that are composed of self-assembled amphiphilic molecules (Lasic, 1997). These 'liposomal particles' were first developed by Bangham in 1965 and due to their resemblance to cell membranes they have been extensively used as model membrane systems (Smith *et al.,* 1993).

Liposomes are vesicles consisting of one or more concentric bilayers alternating with aqueous compartments, within which a variety of lipid soluble or water soluble substances can be enclosed (Bangham *et al.,* 1972). Although, they are usually composed of biodegradable, reusable phospholipids, their design and structure is dependent on their intended function (Singh, 1998). Due to their relatively simple design and ease of formulation techniques, these vectors are easily synthesised on a large scale. Prior to their application to gene therapy, liposomes were widely used as carriers for a variety of drugs (Wang *et al.,* 2006). These artificial phospholipid vesicles are able to trap hydrophilic drugs in the inner aqueous space and lipophilic drugs in the phospholipid bilayer. Liposome research has been the most successful at developing US FDA approved therapeutics such as Doxil®, the first liposome-based drug formulation, and since then, others such as AmBiosome®, DaunoXome® and DepoCyte® have entered the market (D'Souza and Weissig,

2009; Durazo and Kompella, 2011). Additional applications of liposomes include a role in cosmetics and the possible use of liposomes in genetic vaccinations (Lasic, 1997; Gregoriadis *et al.*, 2002). As vehicles for the delivery of nucleic acid molecules, liposomes can offer a protective, biocompatible and biodegradable delivery system, safe from endogenous enzymes, which can further enhance their cellular uptake. Liposome mediated gene delivery is known to exhibit a number of desirable advantages over viral vectors such as lack of mutagenesis, reproducibility and ease of use, significant transgene expression and decreased immunogenicity and toxicity, thus safety in their use (Koumbi *et al.*, 2006; Percot *et al.*, 2004; Shim *et al.*, 2013). Liposomes serving as nanocarriers are currently the most represented class of nanoparticles used clinically (Hwang *et al.*, 2015).

Liposomes in general can interact with cells through four different mechanisms (Figure 2.2). These can be distinguished as (1) Adsorption, with extracellular release of the liposomal contents; (2) Adsorption with lipid exchange; (3) Endocytosis and (4) Fusion of the vesicle with the cell membrane (Torchilin, 2003). The two types of adsorption lead to the contents of the liposomes entering the cell without the uptake of the intact liposome. In the first type, the water soluble contents are released into the extracellular environment with the subsequent passive or active transport of the molecules into the cell. The second type involves the selective transfer of lipophilic material from the liposomal membrane to the cell membrane.

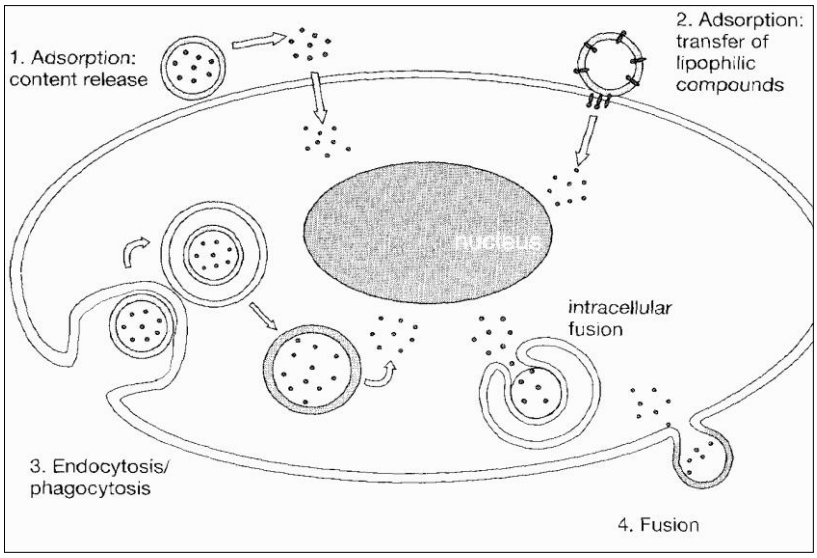

Figure 2.2: Four mechanisms of liposome-cell interactions by which liposomes can deliver their contents (Torchilin, 2003).

The process of fusion involves the complete mixing of the liposomal membrane with the cell membrane and, thereby release of the contents of the liposome into the cytoplasm of the cell (Torchilin, 2003). The occurrence of any of these interactions depends largely on the characteristics of the liposome, such as size, composition, charge, the presence of targeting ligands, and the type of cell (Torchilin, 2003). Endocytosis has been established as the principal mechanism of entry for non-viral nanoparticles. Endocytosis can further be classified into different endocytic routes including phagocytosis, macropinocytosis, clathrin dependent endocytosis and clathrin independent endocytosis, which includes caveolae-mediated internalisation (Figure 2.3). Clathrin-dependent/-mediated endocytosis is the major route of lipoplex entry into cells. Briefly, upon binding to the cell surface via electrostatic interactions; the liposome undergoes endocytotic internalisation followed by possible intracellular degradation via the endolysosomal pathway, and subsequent intracellular release of the liposomal content. In order to achieve gene transfer, the DNA has to escape the endosome to avoid lysosomal degradation (Hoekstra *et al.*, 2007). This is facilitated by the destabilisation of the endosomal membrane by a number of methods but mostly by the incorporation of DOPE in the structure of the liposome (Liu and Huang, 2002). Recently, macropinocytosis has received attention as an efficient entry route for gene delivery as it displays some expedient features such as an increased uptake of biomolecules, evasion of lysosomal degradation and subsequent ease of escape from macropinosomes as a result of their inherently leaky nature (Khalil *et al.*, 2006b). To this end, a succinct description is

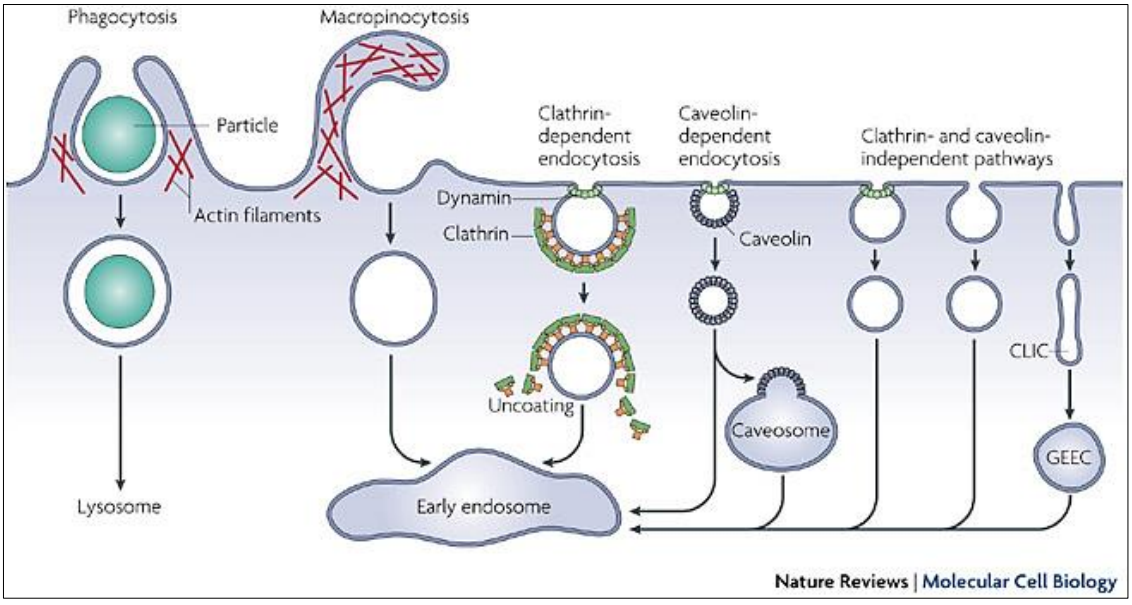

Figure 2.3: Schematic detailing different endocytic pathways of entry into cells. (Mayor and Pagano, 2007).

warranted. Macropinocytosis is a non-selective form of endocytosis that internalises particles like liposomes by the actin-driven formation of membrane ruffles and the succeeding engulfment of fluid that results in the formation of large macropinosomes. These macropinosomes are relatively leaky and allow the escape of lipoplexes thus avoiding lysosomal degradation (Khalil *et al*., 2006b; Vercauteren *et al.*, 2012).

Liposomes can be divided into four different classes as defined with respect to their functionality (Figure 2.4).

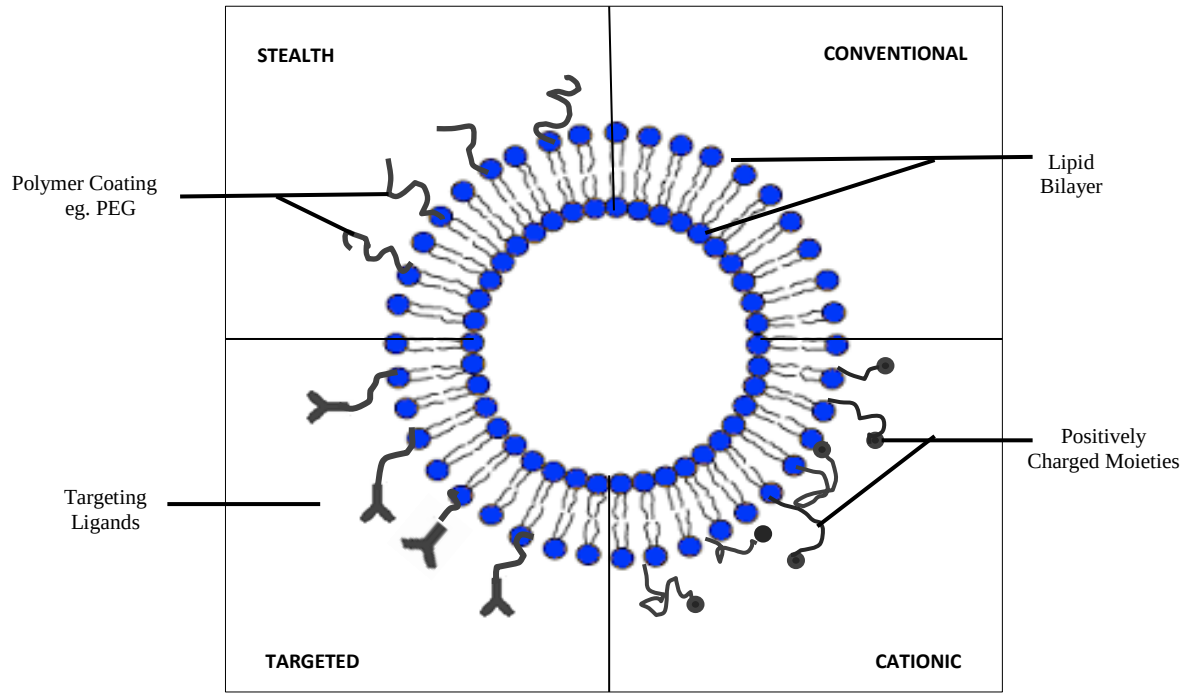

Figure 2.4: Four classes of liposomes as defined by their functionality.

Conventional or anionic liposomes are characterised by their non-specific interactions with the environment (Lasic, 1997). They are composed of neutral or anionic phospholipids. This type of liposome encapsulates macromolecules such as plasmid DNA within their aqueous environment. As a rule, they are not considered very efficient gene delivery vectors as they have relatively small packing capacities that limit the size of plasmid DNA that can be entrapped (Zhdanov *et al.*, 2002).

Targeted liposomes have ligands or targeting moieties such as monoclonal antibodies, peptides, lectins, growth factors, glycoproteins, receptor ligands, cell penetrating peptides, simple molecules such as carbohydrates and bioactive small molecules such as folic acid attached to the liposomal surface allowing for targeting to a specific cell type or tissue and thus increasing the cellular uptake of the liposome by target cells (Lasic, 1997; Immordino *et al.,* 2006; Shim *et al.,* 2013; Allen and Cullis, 2013).

Stealth or long-circulating liposomes are terms adopted to apply to liposomes sterically stabilised with polymers such as polyethylene glycol (PEG). The incorporation of a lipid derivative of PEG, into the bilayer of liposomes have been reported to improve their stability, inhibit protein adsorption onto the surface of the liposome and prevent opsonisation *in vivo.* This limits the liposomal recognition by the reticuloendothelial system (RES), consequently leading to an increase in the liposome systemic circulation time (Gabizon, 2001; Garinot, *et al.,* 2007; Allen and Cullis, 2013).

2.2.2.5.1. Cationic Liposomes

Cationic liposomes were not extensively studied in the first 20 years of liposome research due to their apparent high toxicity (Lasic, 1997). However since 1987 when Felgner and colleagues reported the first successful *in vitro* transfection with their synthesised cationic lipid, N-[1-(2,3-dioleyloxy)propyl]-N,N,N-trimethylammonium chloride (DOTMA), containing a monovalent cationic head group and two hydrocarbon tails [Figure 2.5 (a)], a number of other cationic lipids have been produced and have proven to be significant tools for cellular delivery of nucleic acids, including DNA, oligonucleotides, siRNA, miRNA (Li and Ma, 2001; Singh, 1998; Shim *et al*.,2013). These include, N-[1-(2,3-dioleoyloxy)propyl]-N,N,N-trimethylammonium methyl sulphate (DOTAP) [Figure 2.5 (b)]; 3β[N,N',N'-dimethylaminoethane)-carbamoyl] cholesterol (DC-CHOL), dioctadecylamidoglycyl-spermine (DOGS) and more recently, N',N'-dioctadecyl-N-4,8-diaza-10-aminodecanoyl glycine amide to name a few. All cationic lipids have a common structure, a positively charged polar head group, one/two hydrophobic chains or steroid structures and a linker region connecting the two (Lonez *et al.,* 2008; Shim *et al*., 2013).

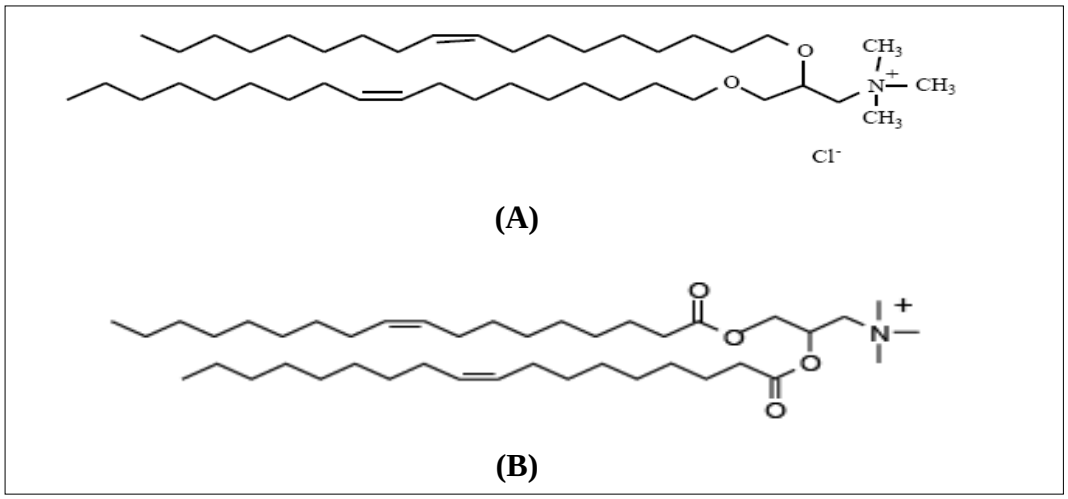

Figure 2.5: Structure of cationic lipids, **(A)** DOTMA and **(B)** DOTAP (Martin *et al.*, 2005; Immordino *et al.*, 2006).

A typical cationic gene delivery system comprises three components: the cationic lipid, a neutral helper lipid such as dioleoylphosphatidylethanolamine (DOPE) and a nucleic acid such as plasmid DNA, siRNA, oligonucleotides or miRNA (Huang *et al.*, 1999; Ju *et al*., 2016). The cationic lipid together with a neutral co-lipid forms the cationic liposome. These positively charged liposomes can interact with negatively charged DNA through electrostatic forces to form a cationic liposome-DNA complex, known as a 'lipoplex' (Felgner *et al.*, 1997). Several studies have suggested that successful nuclear gene transfer involves: 1) packaging of nucleic acid, 2) nonspecific interaction between the nanosystem and the cell surface, 3) internalisation of nucleic acid by endocytosis, 4) nucleic acid molecule escape from endosomes and 5) translocation of the nucleic acid and subsequent expression in cell nuclei (Hui *et al*., 1996; Nayerossadat *et al*., 2012). Hence, cationic liposomes have been fairly successful gene delivery vehicles since their first deployment in this role in 1987. To date, numerous cationic liposomes have been synthesised and used for the delivery of nucleic acid molecules into cultured cells, in animals and even in patients undergoing phase I and II clinical trials (Lonez *et al.*, 2008).

Cationic liposomes are the most extensively employed non-viral gene transfer agents as they offer distinct advantages over other non-viral methods (Singh *et al.*, 2006; Ju *et al.*, 2016). They are easily prepared, there is virtually no size limitation on the DNA or nucleic acid to be transferred, and owing to their positive charge, they interact favourably with the negatively charged cell membrane to promote cellular delivery (Li and Ma, 2001; Hwang *et al*., 2015).

There are, however, several drawbacks related to the use of cationic liposomes *in vivo*. These include low delivery efficiency, cytotoxicity, their undesired interaction with negatively charged serum proteins and components leading to opsonisation, complement activation and their rapid clearance from circulation and accumulation in cells of the mononuclear phagocyte system (MPS) or reticuloendothelial system (RES) (Rejman *et al.*, 2004; Zalipsky *et al.*, 1996; Shim *et al*., 2013).

2.3. SUB-CELLULAR ORGANELLE TARGETING

Subcellular targeting is an expansion on traditional gene/drug therapy, which was discussed above. This targeting involves engineered nanovector intracellular interactions, processing, and trafficking and is a rapidly emerging frontier of biomedical innovation (Huang *et al*., 2011).

Most methods of intracellular delivery focus on traversing the cellular membrane without identifying a specific intracellular target or controlling the distribution of the nanoparticle once inside the cell (Heller *et al*., 2012). Biomedical nanotechnology advancement would be enhanced by nanocarriers that target a specific organelle, such as the nucleus, mitochondria, Golgi apparatus or the endoplasmic reticulum, all of which are promising targets for therapeutics (Kawamura *et al*., 2013). The potential clinical effect of this type of nanoparticle subcellular targeting may be appreciated when taking into consideration the potential of effective gene therapies, molecular imaging devices and treatments for organelle-specific diseases (Huang *et al*., 2011). An example of this subcellular targeting is directing therapeutics such as nucleic acids to mitochondria, which is discussed in 2.3.1

2.3.1. Mitochondrial DNA Targeting

The term Mitochondria comes from the combined Greek words *mitos* (filament) and *chondrion* (granule) and was coined in 1898 by Karl Benda, German doctor, to describe filamentous-type cell organelles, which were first detected in the 1850s by Swiss physiologist Albert Von Kölliker (Von Stockum *et al*., 2016).

The mitochondrion is a membrane-bound DNA containing intracellular organelle present in almost all eukaryotic cells. Cell biology and mitochondrial biology have advanced considerably since Philip Siekevitz first coined the mitochondrion as the "powerhouse of the cell" in 1957 (Siekevitz, 1957). This organelle is vital for the regulation of programmed cell death, as the cell's "arsenal" (Chen *et al*., 2015). However, to state that this encompasses all that mitochondria does would be a gross oversimplification. Milane *et al*. (2015) uses the analogy of the cell as a city, where the mitochondria can be regarded as: the electrical company due to it being the metabolic centre and involved in production of adenosine triphosphate (ATP), the waste containment company with its involvement in reactive oxygen species (ROS) containment, the moving company with its assistance in cell movement and trafficking intracellularly and extracellularly, the department of defence with its association with inflammation, immunity, the stress response and cell danger response, the historical society with evolutionary tracking through mitochondrial DNA (mtDNA) and lastly the grim reaper through involvement in apoptosis regulation.

Research studies about and on mitochondria have been ongoing with considerable success for over a century. In fact, since the publication of two papers in 1988, one in Science and the other in Nature revealed that mutations in the mitochondrial genome could cause human disease, mitochondrial gene targeting in gene therapy is steadily emerging to show great potential (Horobin *et al*., 2007). Mitochondrial research is currently one of the fastest growing disciplines in biomedicine, so much so that it has given rise to the development of new sub-disciplines such as Mitochondrial Medicine, Mitochondrial Pharmaceutics and Mitochondrial Pharmacology (Weissing *et al*., 2004).

The uniqueness of mitochondria must first be considered before commencing on a discussion regarding gene or macromolecule delivery to the organelle. Mitochondria are different from other subcellular organelles in that they are DNA-containing and comprise a complex two membrane structure. Their primary function is energy production through the mitochondrial respiratory chain, which consists of four enzymatic complexes, namely complexes I, III and IV which are energy coupling centres. These complexes, together with the electron carriers cytochrome c and ubiquinone, and complex V make up the oxidative phosphorylation (OXPHOS) system which synthesises ATP according to the cell's needs (Salvado *et al*., 2015). Additionally, as mentioned above, mitochondria play important roles in a number of processes ranging from regulating calcium and iron homeostasis, nitrogen metabolism and

aging to apoptosis (Pearce *et al*., 2013; D'Souza *et al*., 2007). This multitude of roles makes the mitochondrion a candidate of significant interest for organelle-specific delivery of exogenous materials such as DNA, drugs and other macromolecules (Horton *et al*., 2008). Importantly, the formation of the OXPHOS system is under the influence of two separate genetic systems, the nuclear and the mitochondrial genomes. As a consequence of this, genetic defects of either nuclear or mitochondrial DNA can compromise ATP production and potentially cause human pathology at any age, with any symptoms, and by any mode of inheritance (Pearce *et al*., 2013).

2.3.2. Mitochondrial Form and Function

2.3.2.1. Double Membrane and Matrix Space

Mitochondria are composed a double membrane, both of which are largely composed of phospholipids arranged in bilayers with proteins embedded in them. As there are two membranes, two distinct aqueous compartments are defined. The space between the membranes is called the intermembrane space while the inner most one is called the matrix space (Figure 2.6). It has been suggested that the mitochondrion originated by, and is a result of endosymbiosis about 1.5 billion years ago (DiMauro, 2007). Research on mtDNA supports this theory and show similarities between mitochondria and α-proteobacteria (Gray *et al*., 2004).

The outer membrane, which has a lipid to protein ratio of 1:1 does not provide a barrier to small molecules (<5 kDa) which can simply diffuse through pores in the membrane formed by membrane-spanning channel proteins called porins (Mukhopadhyay and Weiner, 2007; Yamada and Harashima, 2008). Larger molecules gain access past the outer membrane by using unique protein import machinery. An example of this would be the presequence mitochondrial targeting signal peptide (MTS) which delivers many proteins to mitochondria via protein import machinery (Yamada *et al*., 2007). Other protein import pores on the outer membrane include the sorting and assembly machinery (SAM), and translocase of the outer membrane (TOM). These provide passage for the majority of mitochondrial proteins that are encoded by nuclear DNA and imported through these pores (Milane *et al*., 2015).

As ATP synthesis via the OXPHOS system, β-oxidation of fatty acids and the TCA cycle all occur in the matrix space, the inner membrane, in contrast to the outer membrane, is highly impermeable i.e. it is far more selective regarding what enters the organelle. This inner membrane is characterised by invaginations that fold back into pockets to form cristae to increase surface area so that the mitochondrial respiratory capacity can be significantly amplified. It also has a high content of membrane proteins compared to the outer membrane and it further contains a unique lipid viz. the phospholipid, cardiolipin (Weissig, 2005; Von Stockum *et al*., 2016). In order for specific compounds to reach the matrix space, proteins in the inner membrane function as transporters, with each having a specific ligand to shuttle across the membrane. For example, the ATP/ADP carrier (AAC) allows ADP to cross the inner membrane, while simultaneously transferring ATP out of the matrix space. In addition to metabolite transport proteins, the inner membrane also hosts mostly proteins that are components of the respiratory chain complex and ATP synthase (Mukhopadhyay and Weiner, 2007; Yamada and Harashima, 2008). The impermeability of the inner membrane is a necessity in creating a discrepancy in proton distribution between the mitochondrial matrix and the cytosol, which is the chief motive for ATP synthesis (Weissig, 2005).

The mitochondrial matrix space formed within the inner membrane encompasses the mitochondrial DNA (mtDNA) which is a circular, double-stranded molecule of approximately 16,659 nucleotide base pairs (Figure 2.7). The genome comprises 37 genes arranged end to end with no introns present (Pearce *et al*., 2013). The 37 genes code for 13 hydrophobic polypeptides, seven of them (ND1-ND6 and ND4L) form part of the 46 subunits of complex I, one (cytochrome b) is part of the 3 subunits of complex III, three (COX I, COX II and COX III) are found in the 13 subunits of complex IV and two (A6 and A8) are located in the 16 subunits of ATP synthase (Andalib *et al*., 2014; Salvado *et al*., 2015). The other 24 genes encode for 22 transfer RNAs and 2 ribosomal RNAs that are necessary for their protein expression within the organelle (Pearce *et al*., 2013). The matrix space is also the site for other major biochemical pathways including the urea cycle, fatty acid oxidation and the TCA cycle. The unique features of the inner membrane allows for simple diffusion of hydrophobic molecules. Triphenylphosponium (TPP) ion, rhodamine 123 and JC1 are examples of cationic hydrophobic molecules that can cross the mitochondrial membrane. This property of TPP has been exploited by investigators to diffuse drugs attached to TPP across the mitochondrial membranes. Additionally, ions with delocalised charge can also diffuse across

the membrane while ions with a localised charge (eg. Na^{+} or Ca^{2+}) require transporters (Mukhopadhyay and Weiner, 2007).

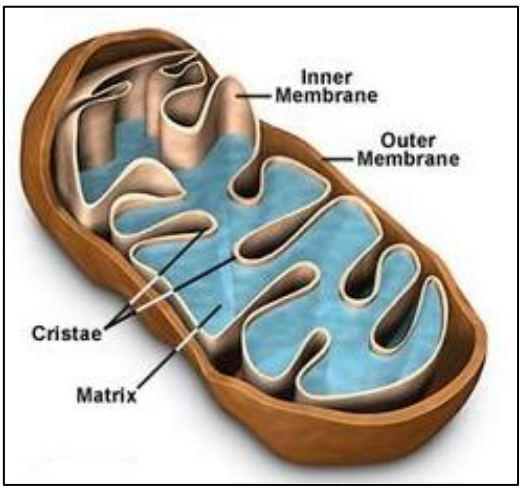

Figure 2.6: Graphical representation of human mitochondria depicting structural features www.rachithscellanalogy.weebly.com (accessed 21/11/2015).

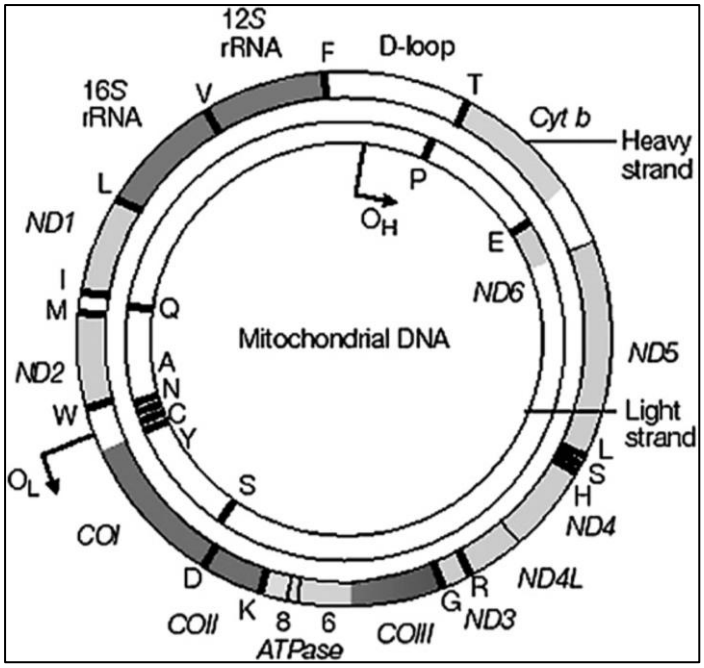

Figure 2.7: A schematic diagram of human mitochondrial DNA encoding 13 polypeptides (ND1-ND6, ND4L, CYT b, COX I-III, ATPase6 and ATPase8), rRNAs, and 22 tRNAs. The tRNas are depicted as single letter amino acid code. (Mukhopadhyay and Weiner, 2007; Pearce *et al*., 2013).

2.3.2.2. Transporters and Translocators

As mentioned above, for larger proteins to enter mitochondria, a translocator is required. As the majority of mitochondrial proteins are coded for by nuclear genes, they have to be translocated to the organelle. To achieve this, receptor-translocator complexes exist on both membranes to allow these proteins to enter mitochondria (Neupert and Herrmann, 2007). These mechanisms include the transfer system on the outer membrane abbreviated TOM (translocator outer membrane) and the TIM (translocator inner membrane) located on the inner membrane (Mukhopadhyay and Weiner, 2007). These nuclear encoded proteins possess a N-terminal leader sequence that is recognised by the receptor-translocator complexes (Dolezal *et al*., 2006). Attachment of this leader sequence to virtually any protein will enable this protein to be translocated into mitochondria. Exploitation of this mechanism allows for fragments of DNA or RNA fused to the leader to be taken up by mitochondria (D'Souza *et al*., 2003).

2.3.2.3. Mitochondria and Apoptosis

It is well known that mitochondria are involved in apoptotic programmed cell death. Cysteine proteases called caspases are the central mediators of apoptosis (Milane *et al.*, 2015). These caspases can be activated to induce apoptosis by two general routes: the extrinsic and intrinsic pathways. The extrinsic pathway is initiated by extracellular ligand binding to death receptors on the cell surface (Yamada and Harashima, 2008; Milane *et al.*, 2015). The intrinsic pathway, also known as the mitochondrial or Bcl-2 inhibitable pathway, involves the destabilisation of the mitochondrial membrane, and release of mitochondrial apoptotic proteins such as cytochrome c, apoptosis inducing factor (AIF) and HtRA2. This leads to a cascade of events in the cytosol and forming of an apoptosome which then activates the effector caspases that eventually leads to partial self-digestion of the cell and eventually cell death. The proteins of the Bcl-2 family regulate the intrinsic pathway with proteins that are pro-apoptotic (Bax, Bak, Bid, Bad, Puma, Bim) and those that are anti-apoptotic (Bcl-2, Bcl-X_L) (Yamada and Harashima, 2008; Milane *et al.*, 2015).

2.3.2.4. The Electron Transfer System and ATP Synthesis

Mitochondria are the principal mediators of cellular energy production. They produce adenosine 5′-triphosphate (ATP) though the process of oxidative phosphorylation (OXPHOS), which accounts for 80 to 90% of ATP generation in major mammalian tissues (Yamada and Harashima, 2008; Milane *et al.*, 2015). The mitochondrial respiratory chain or OXPHOS pathway consists of a group of five multi-protein enzyme complexes (complexes I-V) and two electron carriers (coenzyme Q10 and cytochrome c) embedded in the inner mitochondrial membrane (Chinnery and Schon, 2011; Milane *et al.*, 2015). Reduced cofactors (NADH and $FADH_2$) derived from the tricarboxylic acid cycle (TCA cycle; Krebs cycle) donate electrons to complex I and II and these electrons flow between the complexes down an electro-chemical gradient shuttled by the electron carriers and complexes III and IV. The freed energy is used by complexes I, III and IV to establish a proton gradient (chemiosmotic potential), that is utilised by complex V to generate the production of ATP from adenosine diphosphate (ADP) and inorganic phosphate (Chinnery and Schon, 2011; Milane *et al.*, 2015). Perhaps the most important mitochondrial function is the synthesis of ATP. Dysfunction of ATP production is associated with large number of mitochondrial diseases (Yamada and Harashima, 2008).

2.3.3. Diseases of Mitochondrial Origin and Mitochondrial Dysfunction in Disease

Mitochondrial diseases comprise a heterogeneous group of metabolic disorders characterized by the common link of compromised energy production resulting from defects in mitochondrial OXPHOS system protein synthesis (Pearce *et al*., 2013). The biochemical evidence of the concept of these mitochondrial diseases or dysfunctions such as loose coupling of oxidation and phosphorylation was first observed in Stockholm in 1962 by Luft *et al.* in a young lady with non-thyroid hypermetabolism (Luft syndrome) (DiMauro, 2004a). The molecular age of mitochondrial diseases, as it was described by DiMauro (2004b), commenced in 1988 with a critical break-through regarding our future understanding of "mitochondrial myopathies" in the report of point mutations and pathogenic deletions in mtDNA (Larsson and Luft, 1999; DiMauro, 2004b).

Mitochondrial diseases or disorders are considered unique from a genetic viewpoint because the respiratory chain is the only metabolic pathway in the cell that is under the dual influence of both the mitochondrial and nuclear genomes (DiMauro, 2004a).

Since it was discovered that mtDNA mutations could cause human disease, a number of disorders have been reported to be associated with defects in the mitochondrial genome. Up to 2007, 347 distinct mitochondrial disorders have been identified (Weissig *et al*., 2007). Mutations in mtDNA genes are a regular cause of mitochondrial cytopathy resulting in a large variety of clinical phenotypes connected to severe metabolic dysfunctions (Salvado *et al*., 2015). In fact, the prevalence of mitochondrial disease is so high that according to the United Mitochondrial Disease Foundation, a child is born with mitochondrial disease or may develop one by age five every 15 minutes (Weissig *et al*., 2007). Additionally, the prevalence of pathogenic mitochondrial DNA mutations was recently estimated to be 1 in 200 adults (Tischner and Wenz, 2015). In addition, mutations in mitochondrial genes are related to Parkinson, Huntington's and Alzheimer's diseases, diabetes and also have a greater susceptibility to develop cancer (Salvado *et al*., 2015).

To date, over 300 pathogenic mutations have been identified in the human mtDNA (http://www.mitomap.org; accessed 20/05/2016). These refer to point mutations in tRNA or rRNA genes, missense mutations in protein-coding genes and duplications or deletions (Niazi *et al*., 2012) (Table 2.4).

Mitochondria contain an estimated 1500 proteins, of which only 13 are mitochondrial genome coded (Doyle and Chan, 2008). Therefore, as stated above, mitochondrial diseases can arise from defects in both or either the nuclear and mitochondrial genomes. Since both mitochondrial DNA and nuclear DNA (nDNA) encode constituents of the mitochondrial respiratory chain and ATP synthase, mitochondrial diseases typically affect tissues that are highly metabolically active with an elevated ATP demand such as muscular, cardiac, neuronal tissues and endocrine and renal systems (Murphy and Smith, 2000).

Mitochondrial DNA diseases comprise a varied range of conditions that are usually progressive, and are often accountable for severe disorders and premature mortality. Many complex and unidentified factors unfortunately contribute to the pathophysiology of mtDNA diseases (Doyle and Chan, 2008). Phenotypically mitochondrial disorders can be extremely

diverse and variable, so much so that an identical mutation produces immensely different phenotypes between two individuals, or, the same phenotype is caused by different mutations. Thus mitochondrial diseases are extremely heterogeneous and difficult to categorise into groups or classes (Doyle and Chan, 2008). However, from a genetic perspective, mitochondrial diseases can be classified into two major categories: (i) primary mitochondrial diseases caused by mutations in the mitochondrial genome, which include homo- and heteroplasmic point mutations and large scale rearrangements or deletions; (ii) mitochondrial diseases caused by mutations in nuclear genes involved in mitochondrial function and the respiratory chain (Farrar *et al*., 2013; Viscomi *et al.*, 2015). It was suggested that a third (iii) category be included that comprises secondary disorders that arise from accumulation of mitochondrial damage over time, and could include neurodegenerative disorders that encompass mutations of either or both mitochondrial or nuclear DNA (Farrar *et al*., 2013).

2.3.3.1. Pathogenic Mitochondrial DNA Mutations and Mitochondrial Diseases

Most eukaryotic cells except erythrocytes contain hundreds to thousands of mitochondria, depending on the energy demand of that cell or tissue (Milane *et al*., 2015). Thus a typical cell would also contain hundreds or thousands of mtDNA copies. This difference in mtDNA copy number per mitochondria, per cell or per tissue is termed *polyplasmy* (DiMauro, 2004a; Milane *et al*., 2015). In normal tissue, all mtDNA molecules are identical and of the wild type (*homoplasmy*). MtDNA mutations can occur in all copies of the genome and is called *homoplasmic*, or in only some copies which is termed *heteroplasmic* (where both mutated and wild type mtDNA co-exist within the cell). In heteroplasmy, due to the number of copies of mtDNA in the cell, the ratio of mutated to wild type mtDNA molecules needs to increase to a level where the wild type mtDNA can no longer compensate for the biochemical defect, before the mutated species can begin to manifest tissue dysfunction and clinical symptoms. This phenomenon is known as the *threshold effect*. This threshold level varies based on mutation and tissue type. Generally, single large scale mtDNA deletions require a lower threshold value (~ 60%) of mutated to wild type mtDNA than point mutations which is normally greater than 80% (Mancuso *et al*., 2007; Tuppen *et al*., 2010; Pearce *et al*., 2013; Russell and Turnbull, 2014).

In addition to cellular polyploidy, mitochondrial genetics differ from Mendelian genetics in a number of ways; firstly, mtDNA is exclusively maternally inherited because mitochondria are derived from the oocyte as mitochondria from spermatozoa degenerate soon after fertilisation, secondly, it deviates from the standard genetic code and lastly, during cellular division, the proportion of mutant mtDNA molecules in daughter cells may be distributed randomly and the phenotype may change accordingly. This phenomenon, called *mitotic segregation*, describes how certain patients with mitochondrial disorders may actually manifest different mitochondrial diseases at different stages of their lives (DiMauro, 2004a; Tuppen *et al*., 2010; Pearce *et al*., 2013).

Mutations that occur in the mitochondrial genome can be maternally inherited or occur sporadically. The mutation rate of mtDNA is disproportionately high and is approximately 17-fold higher than in nuclear DNA, and it is highly vulnerable to mutation and oxidative damage (Mazunin *et al*., 2010). This is due to a number of factors including, the specific structural organisation of the mitochondrial genome, its lack of histones, replication errors with insufficient repair mechanisms, mutations of nuclear genes whose protein products function in mitochondria and lastly, mtDNA damage and resultant mutations that arise from the availability of ROS from increased electron leak of the respiratory chain that is in close proximity to the mtDNA molecules (Mazunin *et al*., 2010; Andalib *et al.*, 2014). As mentioned above, there are commonly two types of mutations that occur in mtDNA: point mutations and mtDNA rearrangements.

2.3.3.1.1. Point Mutations

Pathogenic mtDNA point mutations have been noted to occur in protein encoding, tRNA and rRNA genes, causing a wide range of diseases. They are mostly maternally inherited and multisystemic, but some are sporadic and tissue specific (DiMauro, 2004a; Tuppen *et al*., 2010). Protein encoding genes account for two-thirds of the mtDNA sequence; however, the majority (> 50%) of pathogenic mtDNA point mutations causing human disease are located on mitochondrial tRNA genes, which only comprise 10% of the genome (Pearce *et al*., 2013). Phenotypically, these tRNA mutations, and to some extent the rRNA point mutations, may impair total mitochondrial translation by decreasing the availability of functional tRNAs and rRNAs, whereas point mutations in mitochondrial protein encoding genes only specifically

affect the function of the OXPHOS complex to which the corresponding protein belongs. Point mutations exhibit substantial clinical heterogeneity and are mostly heteroplasmic but homoplasmic mutations do occur (Tuppen *et al*., 2010). Transfer RNA point mutations display a variety of clinical phenotypes such as, myopathies, encephalopathies, hearing impairment and diabetes mellitus (Pearce *et al*., 2013). The most common mtDNA and best studied mitochondrial tRNA mutation is the A3243G mutation in $tRNA^{Leu(UUR)}$ which was described by Goto *et al*. in 1990, and is responsible for 80% of patients with mitochondrial encephalopathy, lactic acidosis and stroke-like episode (MELAS) syndrome. Patients often present with progressive encephalomyopathy characterised by repeated stroke-like episodes with seizures typically involving posterior cerebral areas, vomiting, exercise intolerance recurrent migraine-like headaches and lactic acidosis are other frequent clinical features (Pearce *et al*., 2013; Russell and Turnbull, 2014). Although this mutation is famously known for its association with MELAS, a recent study showed that this mutation can also phenotypically manifest as maternally inherited diabetes and deafness (MIDD) or a combination of the MELAS/MIDD syndrome (Russell and Turnbull, 2014). Other common mitochondrial diseases associated with mitochondrial tRNA mutations include myoclonus epilepsy with ragged red fibres (MERRF) and cardiomyopathy (DiMauro, 2004a; Pearce *et al*., 2013).

Of the point mutations in protein encoding genes, Leber hereditary optic neuropathy (LHON) is the most common phenotype. There are three primary LHON mtDNA mutations (G11778A, G3460A, and T14484C), which are present in at least 95% of LHON patients. This mitochondrial disease is characterised by acute or sub-acute impairment of vision in young adults, more commonly males, due to bilateral optic atrophy. LHON is usually due to homoplasmic mtDNA mutation that is maternally inherited (DiMauro, 2004a; Tuppen *et al*., 2010). Other common mitochondrial diseases associated with mitochondrial protein encoding gene point mutations include maternally inherited Leigh syndrome (MILS) and NARP (neuropathy, ataxia, retinitis pigmentosa) (Table 2.4) (Tuppen *et al*., 2010).

2.3.3.1.2. MtDNA Rearrangement Mutations

Rearrangements of mtDNA can be deletions or duplications, with deletions being more commonly associated with mitochondrial diseases. The majority of mtDNA rearrangement

mutations are large scale deletions, which show a variable size range from 1.3 to 8 kb, and span several genes (Tuppen *et al*., 2010; Russell and Turnbull, 2014). These large scale deletions are typically sporadic and occur early in development, with the identical deletion present in all cells within affected tissues. These deletions are thought to occur during replication and/or repair of the genome. Recent studies have suggested that patients have a~5 kb deletion in a similar area of the mitochondrial genome, the so called "common deletion", and that the size of the deletion and its heteroplamsy is linked to disease severity (Mancuso *et al.,* 2007; Tuppen *et al*., 2010; Russell and Turnbull, 2014). The main clinical syndromes due to single large scale deletions are Kearns Sayre Syndrome (KSS), a multisystem disease, characterised by development of retinitis pigmentosa and chronic progressive opthalmoplegia; Pearson syndrome, a rare disorder of infancy associated with sideroblastic anaemia and exocrine pancreatic failure; and chronic progressive external ophthalmoplegia (CPEO), a phenotype characterised by progressive paralysis of the eye muscles leading to limitation of eye movements, palpebral ptosis and generalized weakness (Table 2.4). CPEO is one of the most common manifestations of mtDNA disease in adults (Mancuso *et al.,* 2007; Tuppen *et al*., 2010; Russell and Turnbull, 2014).

2.3.3.2. Pathogenic Nuclear DNA Mutations and Mitochondrial Diseases

As noted above, there are about 1500 proteins that make up the OXPHOS system, of which only a minute portion is encoded by the mtDNA; the vast majority of these proteins are encoded by the nuclear genome. As such, it is clear that mutations in nuclear DNA may cause mitochondrial diseases (Mazunin *et al*., 2010). Nuclear DNA mutations have been discovered in a large number of genes either directly or indirectly connected to the respiratory chain. Direct association refers to mutations in nDNA genes that encode the structural subunits of the respiratory chain complexes including subunits of complex I, III, IV, V and all subunits of complex II, as well as primary coenzyme Q10 (CoQ10) and cytochrome c. Indirect association refers to mutations in nDNA genes encoding proteins that are not constituents of the respiratory chain, but are required for the correct assembly and functionality of respiratory chain complexes in addition to other roles of mitochondria. These include the assembly factor proteins of the respiratory complexes; proteins engaged in the mtDNA maintenance and replication machinery; components of the mtDNA transcription and translation apparatuses; mitochondrial import and export transport equipment, and proteins of

pathways such as apoptosis and other enzymatic cycles viz. TCA cycle and fatty acid β-oxidation (DiMauro, 2004a; Mazunin *et al*., 2010; Viscomi *et al.*, 2015). Mitochondrial disorders that occur because of defective nuclear encoded proteins comprise severe alcoholic liver disease, pyruvate dehydrogenase deficiency, human deafness dystonia syndrome and type 1 primary hyperoxaluria. Numerous other mitochondrial diseases arise from mutations in nuclear encoded mitochondrial proteins, such as those involved in mtDNA maintenance/ or replication and mtDNA polymerase (Yamada and Harashima, 2008). However, nuclear DNA mutations that cause mitochondrial diseases is beyond the scope of this investigation which focuses primarily on mtDNA defects.

TABLE 2.4: Classification of common mtDNA mutations and associated disorders (Adapted from Mukhopadhyay and Weiner, 2007; Pearce *et al*., 2013).

	Mutation	**Phenotype**
Protein synthesis genes		
tRNA	A3243G ($tRNA^{Leu}$)	MEALS, MIDD , PEO
	A3243T ($tRNA^{Leu}$)	Encephalomyopathy
	A3252G ($tRNA^{Leu}$)	Dementia, diabetes
	A3260G ($tRNA^{Leu}$)	Myopathy, cardiomyopathy
	A8344G ($tRNA^{Lys}$)	MERRF, myopathy, Leigh's syndrome
	G8363A ($tRNA^{Lys}$)	MERRF, cardiomyopathy
	A583G ($tRNA^{Phe}$)	MEALS
	5537T insert ($tRNA^{Trp}$)	Ataxia, Leigh's syndrome
	T14709C ($tRNA^{GLu}$)	Myopathy and diabetes
rRNA	A1555G 12S rRNA	SNHL
Large-scale rearrangements	Deletion/duplication/triplication	KSS, CPEO, Pearson syndrome, MIDD, ataxia
Protein coding genes		
Multisystemic	G3460A (ND1)	LHOM
	G11778A (ND4)	
	T14484C (ND6)	
	T8993C/G (ATPase 6)	MILS/NARP
Tissue specific	Point mutation or deletion (CYT b)	Exercise intolerance

CPEO, chronic progressive external ophthalmoplegia; CYT b, cytochrome b; KSS, Kearns–Sayre syndrome; LHON, Leber hereditary optic neuropathy; MELAS, mitochondrial myopathy, encephalopathy, lactic acidosis, and stroke-like episodes; MERRF, myoclonic epilepsy with ragged-red fibers; MIDD, maternally-inherited diabetes and deafness; MILS, maternally-inherited Leigh syndrome; NARP, neuropathy, ataxia, and retinitis pigmentosa; ND1/4/6, NADH dehydrogenase subunits 1/4/6; SNHL, sensorineural hearing loss.

2.3.3.3. Mitochondrial Mutations, Cancer and Neurodegenerative Diseases

Recently, mitochondrial genetics, specifically mtDNA mutations and/or polymorphism variance, have been related to several other common human diseases, including diabetes, autism spectrum disorders, neurodegenerative disorders including Alzheimer's disease (AD), Parkinson's disease (PD), Huntington's disease (HD) and amyotrophic lateral sclerosis (ALS) in addition to greater susceptibility to develop cancer (Moreira *et al.*, 2010; Dowling, 2014).

Neurodegenerative disorders are broadly characterised by the loss of adult neuronal cells through their dysfunction and eventual pre-emptive death (Milane *et al*., 2015). Additionally, there have been multiple demonstrations of mtDNA defects in neurodegenerative disorders, comprising large-scale deletions, point mutations, nucleic acid modifications, and diminished mtDNA copies. Impaired mtDNA gives rise to deficient mitochondrial key enzymes leading to defects in mitochondrial respiration, excessive ROS generation, increased mitophagy and ultimately apoptosis and cell death (Du and Yan, 2010).

Studies have suggested that complex I defects and other mtDNA mutations or variations may result in mitochondrial dysfunction that leads to PD, however this tenuous association has yet to be definitively proven (Chaturvedi and Beal, 2013; Andalib *et al*., 2014). Several reports have proposed that mtDNA defects such as reduced mtDNA ND6 transcript expression, decreased mtDNA copy numbers and point mutations in mtDNA encoded cytochrome c oxidase subunits I, II and III genes were observed in AD patients. However these defects have not yet been identified as AD specific mutations that lead to pathogenesis. A substantial body of evidence also suggests the involvement of mtDNA mutations in HD and ALS, but similar to the other neurodegenerative diseases mentioned above, these mutations have not been conclusively proven to cause pathogenesis (Chaturvedi and Beal, 2013).

Mitochondrial DNA mutations such as insertions or deletions have been noted in many varieties of human cancer. Atypical metabolic processes, increased ROS production, and failure to induce apoptosis in cancerous cells are believed to be as a result of these mutations, and are hypothesised to be involved in tumourigenesis in some cases (Chatterjee *et al*., 2006; Akouchekian *et al.*, 2011; Yu, 2012). Mitochondrial functional impairments have also been observed due to irregular expression of mtDNA encoded proteins as a result of defective oxidative phosphorylation. However, further studies and investigations are necessary to

elucidate the functional role of the different mitochondrial mutations in the initiation, progression and aetiology of human cancer (Chatterjee *et al*., 2006; Yu, 2012).

2.3.4. Strategies for Correcting Mitochondrial Defects

Current therapies for treating mitochondrial diseases are palliative and supportive not curative. These include supplementation with vitamins, anti-oxidants, CoQ10, creatine, l-carnitine, controlled nutrition and exercise therapy; that ultimately only treat symptoms of the disorders (DiMauro and Mancuso, 2007; Tischner and Wenz, 2015). The other common strategy that is employed is to force a shift in heteroplasmy i.e. decreasing the ratio of mutant to wild type mtDNA (DiMauro and Mancuso, 2007). As mentioned above, in a heteroplasmic cell, the mutant and wild type mtDNA molecules exist in a particular ratio; above which mitochondrial diseases result. This strategy can be achieved by use of agents such as restriction enzymes and peptide nucleic acids (PNA) that destroy mutant mtDNA molecules, or selectively inhibit their replication. This leads to a decrease in the number of mutant mtDNA genomes, ultimately causing a shift in the ratio to below the threshold level (Doyle and Chan, 2008; Adhya *et al.*, 2011; Tischner and Wenz, 2015). However, there are several limitations to this therapy, viz. (i) it is a short-term solution, (ii) there are limited target mutations for restriction enzymes, (iii) there are insufficient binding sites for the PNA and (iv) it is only heteroplasmic specific and therefore not compatible with homoplasmic disorders (Doyle and Chan, 2008).

As stated above, there is essentially no clearly defined genotypic-phenotypic relationship among mitochondrial DNA disorders. Taking this into consideration and the existing largely inadequate and ineffective treatments outlined above, the development of mitochondrial gene therapy to treat mtDNA diseases represents a potentially exciting and promising approach. The underlying goal of this gene therapy is to rectify the defects of the OXPHOS chain itself, on a genetic level, the one commonly shared distinguishing feature among all mtDNA disorders. It is a practical and valuable tool to treat a diverse and vast array of clinical phenotypes as the focal point is on the actual cause of the disorder. The use of this therapeutic genetic intervention ultimately involves efficient and effective delivery of therapeutic molecules to and into mitochondria. To this end, there are currently two

approaches to genetically modify the impaired proteins of the OXPHOS chain: the "indirect" method also known as allotopic expression and the "direct method".

2.3.4.1. Allotopic Expression

This indirect method of mitochondrial gene therapy involves the delivery of a wild type version of the mtDNA encoded gene that is mutated or impaired via an appropriate vector, to the nucleus of recipient cells. This mtDNA gene would have to first be recoded from the mitochondrial code to a nuclear genetic code before delivery to the nucleus. After transcription in the nucleus, the corresponding mRNA is translated in the cytosol and the protein imported into mitochondria (Figure 2.8). In order to facilitate mitochondrial uptake, a N-terminal signal sequence or mitochondrial targeting sequence (MTS) is attached on the gene. This allotopically expressed wild type protein is transported into the mitochondria, freed of the MTS peptide and incorporated into the specific subunit of the respiratory chain, in lieu of the original mutated gene product (D'Souza and Weissig, 2004; DiMauro and Mancuso, 2007; Adhya *et al.*, 2011). This allotopic expression has been demonstrated *in vitro* by Manfredi *et al*. (2002).

Although the method has had some success, there are shortcomings. In addition to the need to recode the wild type mitochondrial gene to be efficiently translated, and the need for the preprotein to be fused to a cleavable MTS peptide, the mitochondrial encoded proteins are highly hydrophobic, and the allotopic method might be limited to those that are amphiphilic enough to permit importation into the organelle via the protein import machinery (D'Souza *et al*., 2007; Adhya *et al.*, 2011; Tischner and Wenz, 2015).

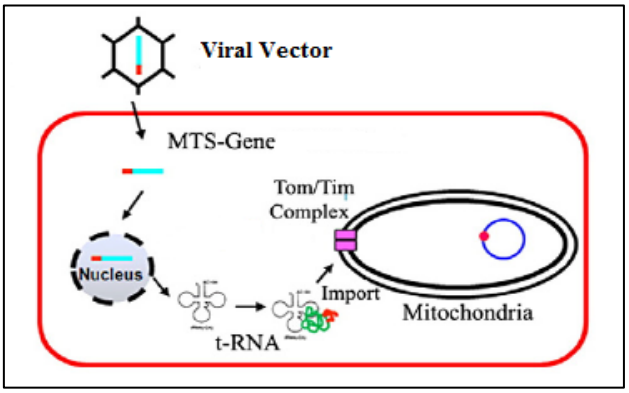

Figure 2.8: Graphical representation of allotopic expression.

2.3.4.2. Direct Delivery of DNA/Macromolecules into Mitochondria

Due to the central role of mitochondria in health and disease, as discussed in 2.3.2 and 2.3.3 above, mitochondria are attractive targets for pharmaceutical and therapeutic intervention. However effective therapies for diseases, caused by mitochondrial DNA defects described in section 2.3.3.1, remain elusive as human mitochondria within living cells have limited accessibility to direct physical, biochemical and pharmacological manipulation. Hence, targeting of genetic material or drugs to the mitochondria could hold the promise of assisting to overcome these obstacles. To make this vision a future reality, basic *in vitro* and *in vivo* research in the laboratory in search of new and improved vectors for mitochondrial gene/macromolecule delivery has to be undertaken and accomplished. Hence this makes vector system design and development, and gene transfer efficiency of paramount importance.

Adhya *et al*. (2011) suggested three conditions that must be satisfied in order for mitochondrial gene therapy to be successful. Firstly, the method or vector system should be able to deliver nucleic acids to the inner most mitochondrial space, the mitochondrial matrix. For this to occur, the cargo must (i) be taken up by the recipient cell through a specific method of internalisation such as endocytosis; (ii) once internalised, the nucleic acid cargo must be preferably transported to mitochondria (mitochondriotropism) and not other intracellular organelles; (iii) the nucleic acid should be transported to the matrix where the mitochondrial genome and gene expression machinery is located. Secondly, the nucleic acid cargo should have a significantly beneficial influence on mitochondrial function, and thirdly, the alteration of mitochondrial function through mitochondrial gene therapy should occur *in vivo,* and have a substantial constructive effect on the progress of the disorder or disease.

In the multifaceted and complicated narrative of mitochondrial gene therapy, only the first condition has been marginally met, since this type of organelle-specific gene therapy is still in its infancy when compared to traditional nuclear gene therapy. Current work is mostly centred on finding a suitable nanovector system that should ideally be mitochondriotropic (an agent or system that localises to the site of mitochondria), biocompatible, non-toxic, safe, stable, show low immunogenicity and have high therapeutic efficacy (Severino *et al.*, 2015; Milane *et al*., 2015). To date, a number of reports of vector systems delivering cargoes to the

mitochondria have been described but they are not ideal (Yamada and Harashima, 2012). These common vector systems will be discussed in brief.

2.3.4.2.1. Lipophilic Molecules

Delocalised lipophilic cations are small membrane-permeable cationic molecules with delocalised positive charges that target the highly negative membrane potential of mitochondria and enter these organelles through electrostatic interactions (Zhang *et al*., 2011). Triphenylphosphonium (TPP), is the most common lipophilic cation that has been used for mitochondrial targeting. TPP has been investigated extensively for the delivery of small bioactive molecules such as vitamin E (MitoVitE) and ubiquinol (MitoQ) and conjugated to other nanoparticles. These particles are conjugated to TPP and gain entry into the organelle by exploiting the mitochondriotropism of TPPs delocalised charge which facilitates entry into the cell, and accumulation in the mitochondrial matrix (Doyle and Chan, 2008; Milane *et al*., 2015). Rhodamine 123 is another lipophilic cation that can selectively accumulate in the mitochondria of cells because of its delocalised charge centre. However, it has mostly been used as flurophore in biological imaging, to visualise mitochondria and not extensively utilised as a mitochondriotropic residue for nanoparticles (Zhang *et al*., 2011; Milane *et al.,* 2015).

2.3.4.2.2. Mitochondrial Targeting Sequences

Mitochondrial targeting sequences (MTS), or as they are also known, mitochondrial leader sequences are presequences found on proteins encoded by the nuclear genome, translated in the cytosol and actively transported into mitochondria via the protein import machinery. These MTS peptides guide trafficking to and facilitate import into the mitochondria. They are 10-80 amino acids in length, rich in positively charged and hydroxylated resides, contain no negatively charged residues, are located on the N-terminus of the precursor protein and they can be cleaved in 1 or 2 proteolytic steps once inside mitochondria (Yamada *et al*., 2007; Doyle and Chan., 2008; Zhang *et al*., 2011). The use of a MTS peptide makes it possible to selectively deliver a variety of proteins, chemicals, oligonucleotides and linear DNA to mitochondria (Yamada *et al*., 2007; Yamada and Harashima, 2013). The MTS

peptide can be directly conjugated to plasmid DNA (pDNA) to co-localise with the mitochondria when delivered to mammalian cells by DQAsomes (D'Souza *et al*., 2005). The use of MTS is the most studied approach to transport DNA into mitochondria. Some of these approaches include direct coupling of MTS to the pDNA or indirect coupling whereby the MTS molecule is conjugated to a carrier such as PEI or PNA (peptide nucleic acids) (Won *et al*., 2011). Flierl *et al.* (2003) described the use of MTS conjugated onto PNA-oligonucleotide complexes to successfully localise these complexes into mitochondria. These particles with MTS were targeted to mitochondria via the MTS import machinery. The use of MTS as a mitochondriotropic vector is severely limited by the size and physiochemical properties of the cargo that it can import into mitochondria through the MTS translocator (Yasuzaki *et al*., 2010; Zhang *et al*., 2011). However, the potential of MTS peptides may lie in their use as mitochondriotropic ligands coupled to an efficient carrier system like cationic liposomes.

2.3.4.2.3. Mitochondriotropic Vesicles

2.3.4.2.3. (a) DQAsomes

Dequalinium is a dicationic amphiphilic compound with a delocalised charge centre that has been shown to accumulate in the mitochondria of living cells in response to the mitochondrial membrane potential. Dequalinium and its derivatives are self-assembling molecules that resemble 'bola'-form electrolytes. These 'bola'-form like amphiphiles are able to form liposome-like cationic vesicles, which the investigators termed 'DQAsomes' (Weissig *et al*., 2001; D'Souza *et al*., 2003; Weissig *et al*., 2006). The DQAsomes, based on the intrinsic mitochondriotropism of its constituents, were used to deliver DNA into, firstly, isolated rat mitochondria, following which, mitochondria of living cells. DQAsomes have been further utilised to mediate delivery of both plasmid DNA and oligonucleotides, conjugated to the MTS peptide, to facilitate nucleic acid uptake via the mitochondrial protein import machinery (D'Souza *et al.*, 2007; Doyle and Chan, 2008). Employing immunofluorescence, and a combination of a variety of molecular-based and immunohistochemical techniques, it was finally demonstrated that DQAsomes are capable of transporting an artificial mini-mitochondrial genome, into mitochondria of a range of cell culture models including a mouse macrophage cell line (Lyrawati *et al*., 2011; Weissig, 2011). DQAsomes are still regarded as

one of the most promising candidates for future functional mitochondrial gene or drug delivery.

2.3.4.2.3. (b) MITO-Porter

MITO-Porter is a liposome based carrier system that can deliver macromolecular cargoes into mitochondria via a membrane fusion mechanism. It was pioneered by Yamada *et al*. (2008), and represents an advancement in mitochondrial gene and drug delivery due to the MITO-Porter system's success in delivering cargoes to the mitochondrial matrix. It is composed of fusogenic lipids in an optimised ratio (9:2:1) of DOPE (Dioleoylphosphatidylethanolamine), SM (Sphingomyelin), and STR-R8 (Stearyl octaarginine). The presence of octaarginine (R8) on the surface of the molecule, firstly, functions to facilitate cellular uptake and, secondly, its electrostatic interactions with mitochondria allow cargo entry while the lipid composition aids with liposome fusion with mitochondria, permitting matrix delivery (Yasuzaki *et al*., 2010; Milane *et al*., 2015). The investigators confirmed delivery to the mitochondrial matrix by preparing a MITO-Porter containing encapsulated propidium iodide, a membrane-impermeable fluorescent dye that binds nucleic acids, to detect the mtDNA. The fluorescence detected from the propidium iodide-mtDNA conjugates demonstrated that the MITO-Porter successfully delivered its cargo to the mitochondrial matrix (Yasuzaki *et al*., 2010; Milane *et al*., 2015).

The authors have expanded the MITO-Porter system to include DF-MITO-Porter, an improvement on the original, in which the cargo is coated with two mitochondria-fusogenic inner membranes and two endosome-fusogenic outer membranes, as well as octaarginine. This system was also proven effective in delivering molecular cargo to the mitochondrial matrix (Yamada *et al*., 2011). The MITO-Porter and DF-MITO-Porter systems were further modified with a mitochondrial import signal of tRNA and MTS, respectively, to enhance mitochondrial targeting, which proved successful (Kawamura *et al.*, 2013; Furukawa *et al*., 2015). Even though the MITO-Porter system has significantly progressed mitochondrial gene and drug delivery, there are still a number of questions regarding the harmfulness of the fusogenic lipid composition. Hence, the creation of safety and toxicity profiles would be beneficial (Milane *et al*., 2015).

2.3.4.2.3. (c) Cationic Liposome-based Nanocarriers

The success of phospholipid vesicles or liposomes, more specifically cationic liposomes, as gene delivery vehicles for chromosomal gene therapy have made them a potentially attractive vector for mitochondrial gene targeting. Liposomes, as mentioned above, are comprised of lamellar phospholipid bilayers that surround aqueous compartments. Their composition can be modified accordingly to control targeting, distribution, toxicity and nucleic acid/drug delivery (Knudsen *et al.*, 2015).

Cationic liposomes, as mentioned earlier are composed of cationic lipids, which are amphipathic molecules that usually consist of a hydrophobic head group attached via a linker or spacer to cholesterol derivatives or double hydrocarbon chains. This lipid composition allows for the liposome surface to interact with the negatively charged molecules of nucleic acids to provide delivery of the cargo to target cells (Sanitt *et al*., 2016). Liposomes and cationic liposomes are suggested to have immense translational potential for mitochondrial nucleic acid/drug delivery as they are largely considered biocompatible and non-toxic with many years of research in the field of liposomes and their use in drug delivery and gene therapy. This makes liposomes pharmaceutically relevant and therefore the most investigated class of nanocarriers for mitochondrial targeted therapeutics (Durazo and Kompella, 2011; Shim *et al*., 2013). This statement has proven accurate, so much so that the most successful mitochondrial targeted nanosystems to date, DQAsomes and MITO-Porter, being liposome based, with the MITO-Porter considered cationic as it contains octaarginine. The versatility of liposomes lies in the fact that they can be easily modified to become mitochondriotropic, by the addition on the liposomal surface, of mitochondriotropic residues such as MTS, R8 rhodamine 123 or TPP. This was demonstrated by Boddapati *et al*. (2008) with the construction of stearyl triphenylphosphonium (STPP) functionalised liposomes for ceramide to specifically target the mitochondria. Thus liposomes show great potential for future successful mitochondrial delivery of therapeutics.

The chapters that follow detail an investigation into the physicochemical characterisation, cytotoxic profile, cellular uptake and mitochondrial localisation and targeting potential of novel cationic mitochondriotropic liposomes modified with MTS and octaarginine (R8) peptides.

CHAPTER THREE

MATERIALS AND METHODS

3.1. SYNTHESES AND LIPOSOME FORMULATON

3.1.1. Chemicals and Reagents

Cholesteryl chloroformate ($C_{28}H_{45}ClO_2$), 3-dimethylaminopropylamine (DMAPA, $C_5H_{14}N_2$), and dioleoylphosphatidylethanolamine (DOPE, $C_{41}H_{78}NO_8P$) were purchased from the Sigma-Aldrich Chemical Company (St Louis, MO, USA). Succinimidyl 3-(2-pyridyldithio) propionate (SPDP, $C_{12}H_{12}N_2O_4S_2$) and *N*-γ-maleimidobutyryl-oxysulfosuccinimide ester (GMBS, $C_{12}H_{12}N_2O_6$) were obtained from Thermo Scientific (Waltham, MA, USA). Mitochondrial Targeting Sequence peptide [H-Met-Leu-Ser-Asn-Leu-Arg-Ile-Leu-Leu-Asn-Lys-Ala-Ala-Leu-Arg-Lys-Ala-His-Thr-Ser-Met-Val-Arg-Asn-Phe-Arg-Tyr-Gly-Lys-Pro-Val-Gln-Cys-OH (MTS, $C_{168}H_{286}N_{54}O_{42}S_3$)] and octaarginine [H-Arg-Arg-Arg-Arg-Arg-Arg-Arg-Arg-Cys-OH] (R8, $C_{51}H_{103}N_{33}O_{10}S_1$) were acquired from GL Biochem, (Shanghai) Ltd. (Shanghai, China). 2-[4-(2-hydoxyethyl)-1–piperazinyl] ethanesulphonic acid (HEPES, $C_8H_{18}N_2O_4S$), dichloromethane (DCM, CH_2Cl_2), hydrazine (N_2H_4), chloroform ($CHCl_3$), methanol (MeOH, CH_4O), absolute ethanol (EtOH, C_2H_6O), sulphuric acid (H_2SO_4) and silica gel $60F_{254}$ chromatography plates were purchased from Merck (Damstadt, Hesse, Germany). Ultrapure 18 MΩ water (Milli-Q50) was used throughout. All other chemicals were of analytical purity grade or higher and purchased commercially.

3.1.2. Cationic Cholesterol-derived Cytofectin (CHOL-T)

The first step in this study involved the synthesis of the cationic cholesterol derivative, CHOL-T (3β [*N*-(*N', N'*-dimethylaminopropane)-carbamoyl] cholesterol), formulated from the starting material cholesteryl chloroformate. This cytofectin is a positively charged amphiphilic molecule containing an amine cationic polar head group attached via a linker, and spacer region to a cholesterol derivative. The resultant cationic lipid was incorporated

into the formulation of cationic liposomes for DNA binding, condensation and subsequent delivery.

CHOL-T was prepared according to the protocol reported previously by Singh *et al.* (2001). Briefly, to a solution of cholesteryl chloroformate (90 mg, 0.2 µmols) in 1 ml DCM was added DMAPA (62.8 µl, 0.11 µmols) dropwise while stirring. This synthesis reaction was allowed to proceed for 1 hour at room temperature (Figure 3.1) and monitored by thin layer chromatography (TLC) on silica gel $60F_{254}$ chromatographic plates developed in $CHCl_3$:MeOH (9:1, $^{v}/_{v}$) (results not shown). The solvent (DCM and excess unreacted DMAPA) was subsequently removed by rotary evaporation under vacuum in a Büchi Rotavapor-R-300 (Büchi, Switzerland), leaving behind a thin film layer in the reaction vessel. This resultant residue was dissolved in absolute EtOH and allowed to crystallise overnight at 4ºC. The product was then recrystallised from EtOH, filtered under a stream of dry nitrogen gas and further dried by rotary evaporation under vacuum to yield the product as white coloured crystals. Melting point determinations: 103 – 105°C.

3.1.3. Cholesterol-derived Cross-linking Agents

This step involved the synthesis of two different hetero-bifunctional cross-linking agents, 3β-[N-(hydrazino 3-{2-pyridyldithio} propionate)-carbamoyl] cholesterol (SP-CHOL) and 3β-[N-(hydrazino-γ-maleimidobutyryl)-carbamoyl] cholesterol (GM-CHOL), conjugated to a cholesterol derivative to facilitate their incorporation into the liposome bilayer. The two cross-linkers used were SPDP (succinimidyl 3-(2-pyridyldithio) propionate) and GMBS (*N*-γ-maleimidobutyryl-oxysulfosuccinimide ester) and the cholesterol derivative was cholesterylformylhydrazide (MS04), a novel intermediary compound in the synthesis of the cationic cytofectin *N*, *N*-dimethylaminopropylaminylsuccinylcholesterylformylhydrazide (MS09) as reported by Singh and Ariatti (2006). In brief, MS04 was prepared as follows: Solutions of cholesteryl chloroformate (1.13 g, 2.5 mmols) in $CHCl_3$ (5 ml) and hydrazine (0.24 g, 7.5 mmols) in $CHCl_3$:MeOH (3.6 ml, 5:1, $^{v}/_{v}$) were prepared and cooled to 0°C. The cholesteryl chloroformate solution was progressively added to the hydrazine solution and stirred for 1 h at room temperature (Figure 3.2). The resultant reaction mixture was stored at room temperature for 24 h and subsequently concentrated under vacuum to form a crystalline

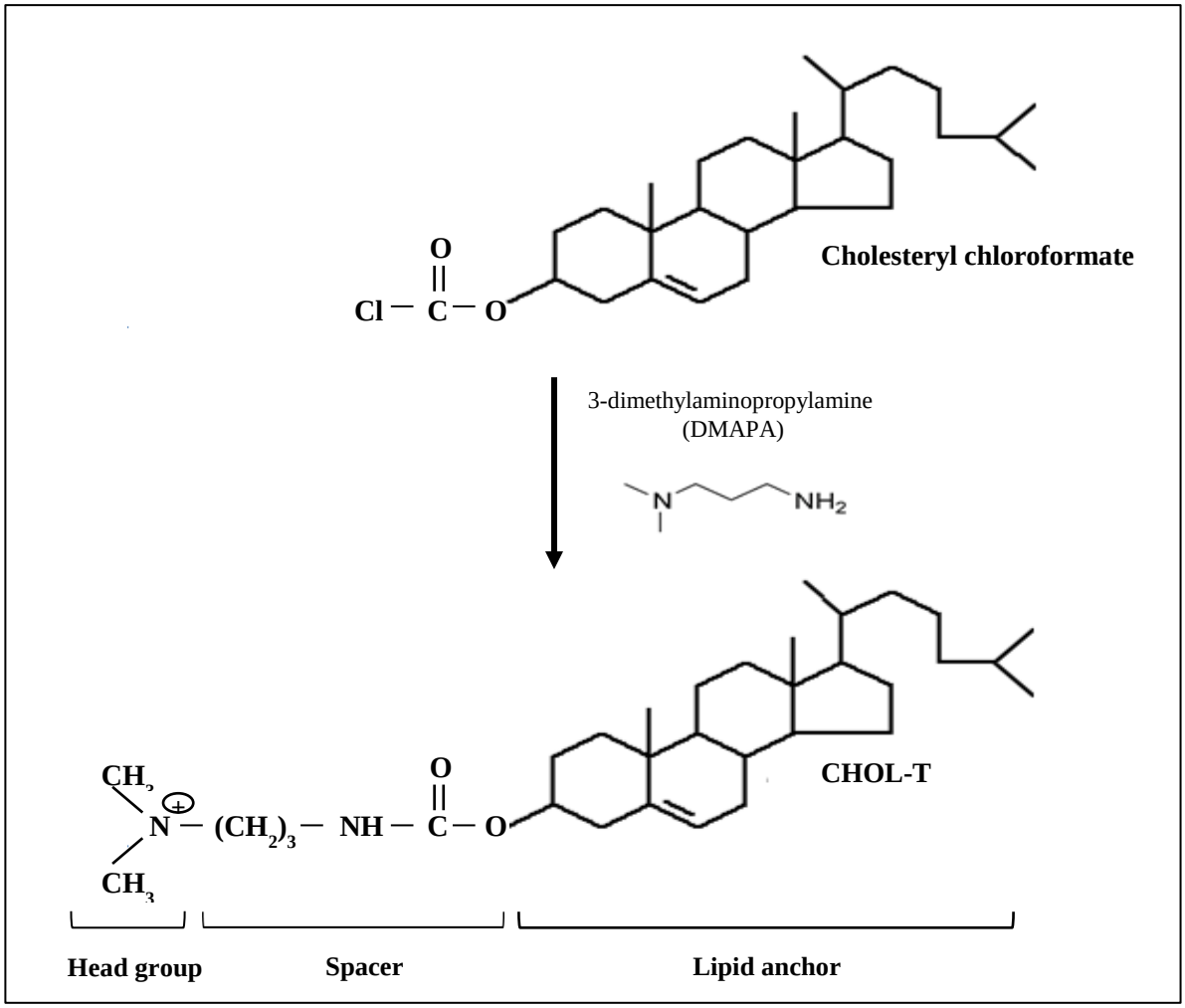

Figure 3.1: Synthesis reaction scheme of CHOL-T from starting material cholesteryl chloroformate with the addition of DMAPA.

product. This was then further recrystallised in $CHCl_3$:MeOH (125 mL, 4:1, $^{v}/_{v}$), and the crystals were isolated by filtration and dried under vacuum. Melting point: 225 – 227°C.

The two solutions containing either MS04 (13.8 mg, 0.03 mmols) or MS04 (23 mg, 0.05 mmols) in 500 µl $CHCl_3$ and SPDP (14.3 mg, 0.045 mmols) or GMBS (14 mg, 0.05 mmols, respectively, in 500 µl $CHCl_3$ were initially maintained at room temperature for 24 h in the dark and thereafter overnight at 4°C (Figure 3.3). Thereafter, the solvents of both reaction mixtures were evaporated *in vacuo* and the resultant residues were dissolved in 150 µl $CHCl_3$ and compared by TLC against the starting materials on silica gel $60F_{254}$ plates developed in $CHCl_3$:MeOH (95:5, $^{v}/_{v}$). Cholesterol-containing compounds were visualised as brown to purple spots upon spraying with H_2SO_4 (33%, $^{v}/_{v}$) and heating to 100°C. Bands presenting the respective products were scraped off, extracted with $CHCl_3$:MeOH (2:1, $^{v}/_{v}$) and filtered three times *in vacuo* through a sintered glass funnel. The solvent of resultant filtrates were

evaporated and the residues once again dissolved in $CHCl_3$:MeOH (2:1, $^{v}/_{v}$), and passed through a pipette containing a cotton plug, into weighted round bottom flasks. The solvent was evaporated by rotary evaporation using a Büchi Rotavapor-R300 and the products further dried using a pistol drier (Büchi-TO, Büchi, Switzerland) under vacuum to yield whitish coloured powdery products.

SP-CHOL: 13.5 mg GM-CHOL: 20.5 mg

3β-[N-(hydrazino 3-{2-pyridyldithio} propionate)-carbamoyl]cholesterol: ^{1}H NMR (300 MHz, $CDCl_3$) : δ 0.65 (s, 3H, C-*C*H_3), 0.83 (d, 6H, *J* = 6.0 Hz, 26-H, 27-H, CH-(*C*H_3)$_2$), 0.89 (d, 3H, *J* = 5.5 Hz, 21-H, CH-*C*H_3), 0.98 (s, 3H, 19-H, C-*C*H_3), 2.65 (t, 2H, *J* = 6.2 Hz, CO-*C*H_2), 3.07 (t, 2H, *J* = 6.1 Hz, S-*C*H_2), 4.55 (m, 1H, 3$_\alpha$-H), 5.35 (d, 1H, *J* = 4.8 Hz, 6-H), 7,13 (t, 1H, *J* = 5.2 Hz, 5'-H pyr), 7.50 (m, 1H, 3'-H pyr), 7.60 (m, 1H, 4'-H pyr), 8.55 (d, 1H, 6'-H pyr).

3β-[N-(hydrazino-γ-maleimidobutyryl)-carbamoyl]cholesterol: ^{1}H NMR (300 MHz, $CDCl_3$) : δ 0.67 (s, 3H, C-*C*H_3), 0.85 (d, 6H, *J* = 5.0 Hz, 26-H, 27-H, CH-(*C*H_3)$_2$), 0.91 (d, 3H, *J* = 6.5 Hz, 21-H, CH-*C*H_3), 1.00 (s, 3H, 19-H, C-*C*H_3), 2.20 (d, 2H, *J* = 7.0 Hz, CO-*C*H_2), 3.69 (d, 2H, *J* = 6.1 Hz, N-*C*H_3), 4.55 (m, 1H, 3$_\alpha$-H), 5.37 (d, 1H, *J* = 4.8 Hz, 6-H), 6.72 (s, 2H, *CH=CH* maleimido).

3.1.4. Mitochondriotropic Liposome Preparation

All cationic liposomes were synthesised by the thin-film evaporation method adapted from that of Gao and Huang (1991). In brief, stock solutions of the liposome components were individually prepared before liposomes formulation, according to the molar ratios outlined in Table 3.1. The total reaction mixture contained 4 µmoles of lipid. The cationic lipid, CHOL-T was kept constant (2 µmols) in all liposomes, the remaining 2 µmols of each preparation comprised the neutral lipid, DOPE and either 5 or 10 mol% of SP-CHOL or GM-CHOL. Each cationic liposome lipid solution in $CHCl_3$ was rotary evaporated to dryness at reduced pressure with a thin flow of moisture-free nitrogen gas at room temperature to produce a thin film deposit on the inside of the glass tube. The samples were further dried under vacuum by a pistol drier to eliminate all traces of solvent. Thereafter the thin film layers were rehydrated overnight at 4°C in 1 ml sterile HEPES buffered saline (HBS, 20 mM HEPES, 150 mM NaCl, pH 7.5). The hydrated lipid dispersions were then vortexed (Vortex Genie 2, Scientific Industries, Bohemia, USA) then sonicated (for 5 min at room temperature) using a

Transsonic T 460/H bath-type sonicator (Elma GmbH & Co., Singen, Germany), to generate small unilamellar liposomes which were stored at 4°C.

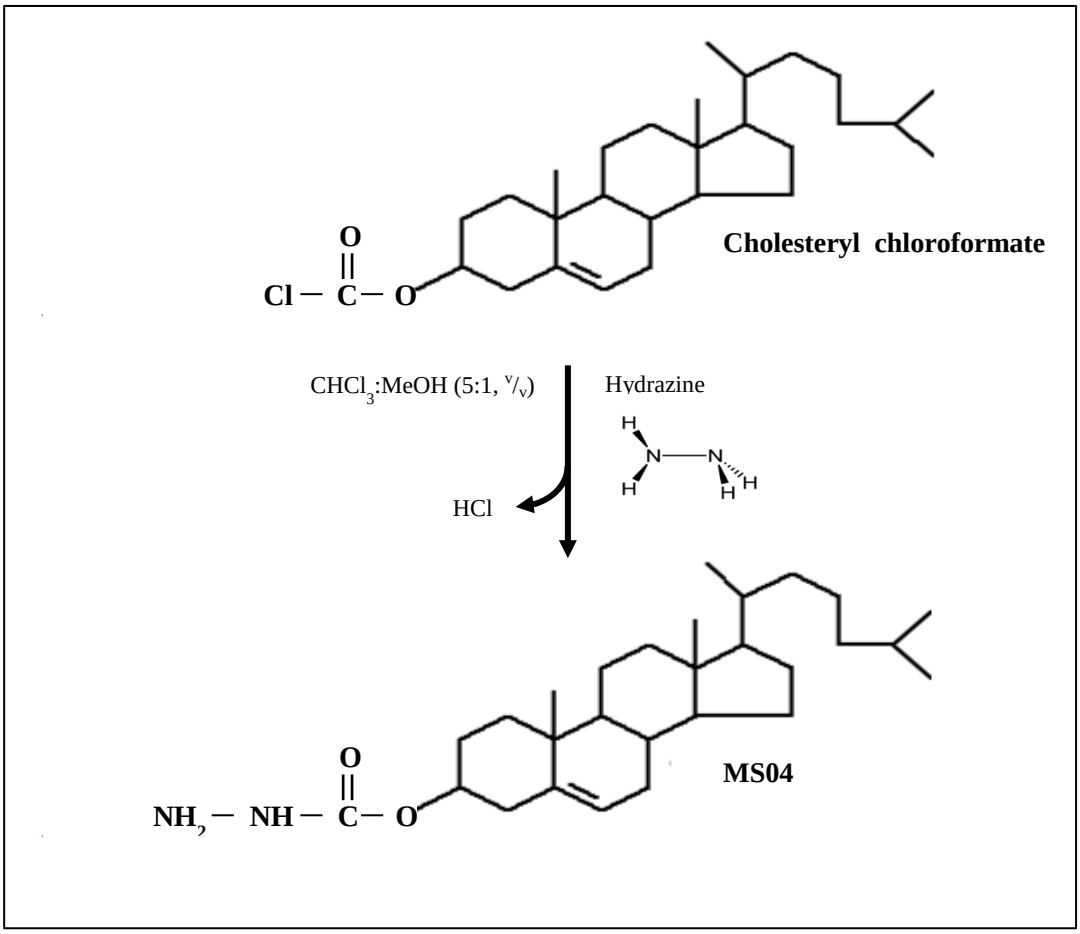

Figure 3.2: Synthesis reaction scheme of MSO4. Cholesteryl chloroformate was converted to MSO4 using hydrazine.

TABLE 3.1: Lipid composition and molar ratios of components of cationic mitochondriotropic liposomes.

Mitochondriotropic Liposome	**Molar Ratios (µmoles/1 ml)**			**Total Lipid Content (µg/µl)**	**Peptide Component**
	CHOL-T	**DOPE**	**SP-CHOL/ GM-CHOL**		
SP-CHOL-MTS	2	1.8	0.2	2.50	MTS
GM-CHOL-MTS	2	1.8	0.2	2.49	MTS
SP-CHOL-MTS-R8	2	1.6	0.4	2.48	MTS + R8
GM-CHOL-MTS-R8	2	1.6	0.4	2.46	MTS + R8

Abbreviations: **CHOL-T**; 3β-[*N*-(*N'*, *N'*-dimethylaminopropane)-carbamoyl] cholesterol, **DOPE**; Dioleoylphosphatidylethanolamine, **SP-CHOL**; 3β-[N-(hydrazino 3-{2-pyridyldithio} propionate) carbamoyl] cholesterol, **GM-CHOL**; 3β-[N-(hydrazino-γ-maleimidobutyryl)-carbamoyl] cholesterol, **MTS**; mitochondrial targeting signal, **R8**; octaarginine.

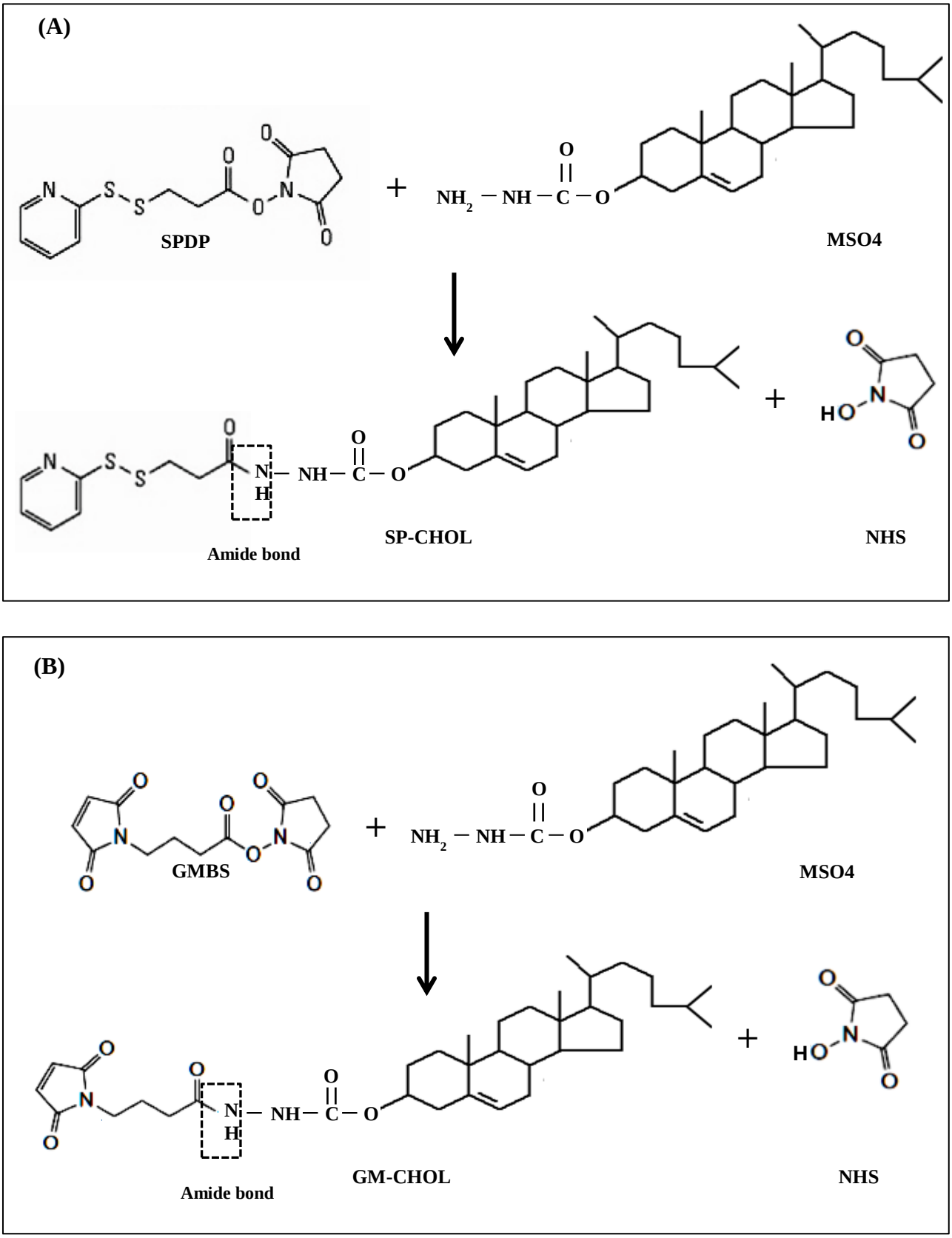

Figure 3.3: Synthesis reaction scheme of **(A)** 3β-[N-(hydrazino 3-{2-pyridyldithio} propionate)-carbamoyl] cholesterol (SP-CHOL) and **(B)** 3β-[N-(hydrazino-γ-maleimidobutyryl)-carbamoyl] cholesterol (GM- CHOL). MSO4 = cholesterylformylhydrazide, SPDP = succinimidyl 3-(2-pyridyldithio) propionate, GMBS = *N*-γ-maleimidobutyryl-oxysuccinimide ester and NHS = *N*-hydroxysuccinimide.

In order to make the cationic liposomes mitochondriotropic, the mitochondrial targeting signal (MTS) peptide was grafted onto the surface of the liposomes. This was achieved by incubation of the MTS peptide (5 mg, 1.3 µmols) in 1 ml sterile HBS with the liposome preparations SP-CHOL-MTS and GM-CHOL-MTS which contain MTS only. Each of these liposomes received 500 µl of the MTS solution and was subsequently incubated in the dark at room temperature overnight and thereafter for a further 24 h at 4°C. Liposome preparations containing both MTS and octaarginine (R8) peptides, SP-CHOL-MTS-R8 and GM-CHOL-MTS-R8, were formulated as above, with the exception that the MTS peptide was in 500 µl HBS, and included the addition of an equimolar quantity of R8 (1.78 mg, 1.3 µmols) in 500 µl HBS. The MTS and R8 solutions were added alternately to the liposomes and thereafter incubated as above. Following incubation periods, liposomes were then dialysed against HBS over 3 days with 3 additional buffer changes to eliminate any unbound peptides. The resultant liposome preparations were volume adjusted, stored at 4°C and sonicated prior to use.

3.2. CHARACTERISATION OF LIPOSOMES AND LIPOSOME-DNA COMPLEXES

3.2.1. Chemicals and Reagents

E. coli strain JM109 was obtained from Promega Corp. (Dübendorf, Zürich, Switzerland). Molecular biology grade UltraPure™ agarose was acquired from Invitrogen (Carlsbad, CA, USA). The gel loading buffer components (glycerol, bromophenol blue, xylene cyanol), ethidium bromide (EtBr), ethylenediaminetetraacetic acid (EDTA disodium salt, $C_{10}H_{16}N_2O_8$), sodium dodecyl sulphate (SDS, $C_{12}H_{25}SO_4Na$), Tris [(hydroxymethyl)-aminomethane, $C_4H_{11}NO_3$] and sodium dihydrogen phosphate (NaH_2PO_4) were purchased from Merck (Darmstadt, Hesse, Germany). Uranyl acetate dehydrate, depleted of radioactivity, was obtained from Ted Pella Inc. (Redding, CA, USA). *Label* IT® Tracker™ TM-Rhodamine and Fluorescein kits were purchased from Mirus (Madison, WI, USA). Gamma-irradiated foetal bovine serum (FBS) was supplied by Highveld Biological (Pty) Ltd. (Lyndhurst, Gauteng, RSA). Ultrapure 18 MΩ water (Milli-Q50) was used throughout. All other chemicals were of analytical purity grade or higher and purchased commercially.

3.2.2. Plasmid DNA Preparations

3.2.2.1. Amplification of pCMV-*luc* DNA

Plasmid pCMV-*luc* (6.2kbp) (Figure 3.4), driven by the cytomegalovirus (CMV) promoter, was purchased from Plasmid Factory (Bielefeld, North Rhine-Westphalia, Germany). The plasmid was amplified using *E. coli* strain JM109, grown in LB medium at 37°C and shaken at 150 rpm for 24 h. The plasmid was then isolated according to the Promega protocol. DNA purity and concentration was determined spectroscopically using the NanoDrop 2000c spectrophotometer (Thermo Scientific, Wilmington, DE, USA). The isolated plasmid DNA was run on a 1% agarose gel against a control pCMV-*luc* DNA sample to confirm purity and identify the different forms of DNA. The plasmid preparations displaying an $OD^{260}/_{280}$ value of 1.8 or higher were used. Working stock concentrations of 0.25 µg/µl were prepared with ultrapure 18 MΩ water (Milli-Q50) and stored at –20°C.

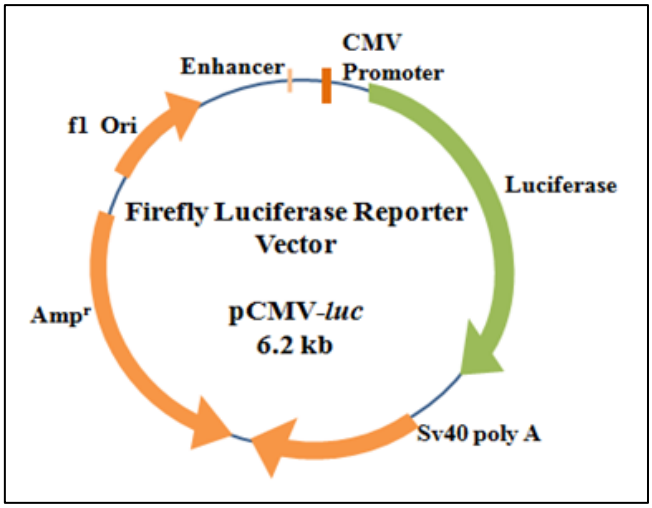

Figure 3.4: Plasmid map of pCMV-*luc* vector. The pCMV-*luc* vector contains the cDNA of the firefly luciferase (*luc*) gene and a beta-lactamase for ampicillin resistance (Amp^r). Adapted from http://www.plasmidfactory.com (accessed 20/02/2013).

3.2.2.2. Fluorescent Labelling of Plasmid DNA

Both rhodamine and fluorescein labelling of pCMV-*luc* DNA was carried out using the Mirus *Label* IT® Tracker™ TM-Rhodamine and Fluorescein kits respectively. Briefly, 325 µl sterile water, 50 µl 10x labelling buffer A, 100 µl 0.5 µg/µg pCMV-*luc* and 25 µl *Label* IT® Tracker™ reagent were added together in a 1.5 µl microcentrifuge tube and incubated at 37ºC for 1 h. The reaction mixture was quickly centrifuged after 30 min to minimise the effect of

evaporation and to maintain the concentration of reaction components at appropriate levels. Following the incubation period, the unreacted *Label* IT® Tracker™ reagent was removed by ethanol precipitation with the addition to the reaction mixture of 0.1 volume of 5 M NaCl and 2 volumes of ice cold 100% ethanol which was mixed well and further incubated for 1 h at -80ºC. Thereafter, the reaction mixture was centrifuged at 4ºC for 10 min to pellet out the labelled DNA. This labelled DNA pellet was washed with 500 µl 70% ethanol, further centrifuged and air dried to remove all traces of ethanol. The resultant dried pellet was resuspended in 100 µl sterile ultrapure 18 MΩ water (Milli-Q50). Labelled DNA purity and concentration was determined spectroscopically using the NanoDrop 2000c spectrophotometer, and DNA stored at –20°C.

3.2.3. Preparation of Mitochondriotropic Liposome-DNA Complexes

Liposome preparations were vortexed for 2 min and thereafter sonicated for 5 min prior to use. The plasmid DNA (0.5 or 1 µg of pCMV-*luc*) was mixed with varying amounts of the appropriate liposome suspension to attain specific ranges of mass ($^{w}/_{w}$) or N/P ($^{+}$/-) ratios. These suspensions were brought up to a volume of 10 µl with sterile HBS, vortexed for 30 s and allowed to incubate for 30 min at room temperature to afford DNA binding and complex formation. Lipoplexes were freshly prepared before each assay.

3.2.4. DNA Binding Studies of Mitochondriotropic Liposomes and Nuclease Protection Assays

3.2.4.1. Gel Retardation Assay

In this study, liposome-DNA complex formation was monitored by gel retardation or electrophoretic mobility shift assays, that were originally devised by Fried and Crothers for studying protein-DNA interactions (Scott *et al.*, 1994). Lipoplexes were freshly made, as described in 3.2.3 above, by incubating 0.5 µg pCMV-*luc* DNA with increasing amounts of cationic liposome preparations at various mass ratios (liposome-pDNA, $^{w}/_{w}$) as shown in Table 3.2, brought up to a total volume of 8 µl with HBS (pH 7.4), vortexed gently and allowed to mature for 30 min at room temperature. Following the incubation period, 2 µl of

gel loading buffer (50% glycerol, 0.05% bromophenol blue, 0.05% xylene cyanol) was added to all the samples. The samples (10 µl) were then subjected to electrophoresis on 1% agarose gels (0.2 g agarose, 18 ml deionised 18 MΩ water, 2 ml of 10 x running buffer, $^{w}/_{v}$), containing 1 µg/ml EtBr, in a Mini-Sub® electrophoretic system (BioRad Laboratories, Richmond, USA) containing electrophoresis buffer (36 mM Tris-HCl, 30 mM sodium dihydrogen phosphate, 10 mM EDTA pH 7.5) at room temperature for 90 minutes at 50 volts. The gels were viewed and analysed under UV_{300nm} transillumination and images captured using the Vacutec Syngene G:Box BioImaging system (Syngene, Cambridge, UK).

TABLE 3.2: Mitochondriotropic liposome mass range assayed for DNA binding studies. pCMV-*luc* DNA was kept constant at 0.5 µg for each lipoplex tested.

Mitochondriotropic Liposome	**Liposome Test Range (µg)**							
SP-CHOL-MTS	0	11.5	12	12.5	13	13.5	14	14.5
GM-CHOL-MTS	0	6.5	7	7.5	8	8.5	9	9.5
SP-CHOL-MTS-R8	0	2	2.5	3	3.5	4	4.5	5
GM-CHOL-MTS-R8	0	1	1.5	2	2.5	3	3.5	4

3.2.4.2. Nuclease Protection Assay

DNA degradation is known to be a major limiting factor in the application of gene transfer, and any non-viral gene delivery vector used has to be able to effectively protect the DNA cargo from nuclease digestion and degradation. The role of mitochondriotropic lipoplexes in protecting the pDNA from attack by serum nucleases was assessed by *in vitro* nuclease protection assays using agarose gel electrophoresis. Three mass ratios ($^{w}/_{w}$), as determined after analysis of gel retardation studies, of cationic mitochondriotropic liposomes (Table 3.3) were added to a constant amount of pCMV-*luc* DNA (1 µg). This was made up to a volume of 10 µl with HBS. The samples were allowed to incubate for 30 minutes at room temperature, as described in section 3.2.3. Foetal bovine serum (FBS) was thereafter added to the complexes to a final concentration of 10%. Two controls were employed, a positive control containing pCMV-*luc* DNA only with no liposome or FBS and a negative control comprising naked pCMV-*luc* DNA and FBS. The reaction mixtures were then incubated for 4 h at 37ºC in a digital temperature-controlled water bath (TriLab Scientific, Johannesburg,

Gauteng, RSA). After the incubation period, ethylenediaminetetraacetic acid (EDTA) was added to the samples to a final concentration of 10 mM and sodium dodecyl sulphate (SDS) to a final concentration of 0.5% ($^{w}/_{v}$), to terminate the enzymatic reaction and disassociate the lipoplexes, respectively. The samples were then incubated for a further 20 minutes at 55ºC. Thereafter, gel loading buffer (4 µl) was added and the samples subjected to electrophoresis on a 1% agarose gel for 120 minutes at 50 volts and imaged as described in section 3.2.4.1 for the band shift assays.

TABLE 3.3: Varying amounts of mitochondriotropic liposome preparations and corresponding charge ratios tested for nuclease protection, MTT, AlamarBlue®, imaging, sizing and fluorescent assays. pCMV-*luc* DNA was constant at 1 µg.

Mitochondriotropic Liposome	**Liposome Amount (µg) and Charge Ratio (N/P) (+/-)**		
SP-CHOL-MTS	27 (7.2)	28 (7.5)	29 (7.7)
GM-CHOL-MTS	17 (4.5)	18 (4.8)	19 (5.1)
SP-CHOL-MTS-R8	7 (1.9)	8 (2.1)	9 (2.4)
GM-CHOL-MTS-R8	5 (1.4)	6 (1.6)	7 (1.9)

3.2.4.3. Ethidium Bromide Intercalation Assay

The mitochondriotropic liposome-DNA association was further explored to determine the ability of the liposomes to efficiently compact DNA by the dye displacement or ethidium bromide intercalation assay. This assay was conducted on a GloMax®-Multi Detection System (Promega BioSystems, Sunnyvale, CA, USA) set at excitation and emission wavelengths of 520 nm and 600 nm, respectively. Initially 2 µl (0.2 µg) of an ethidium bromide stock solution (100 µg/ml) was added to 100 µl of HBS in a single well of 96-well FluorTrac flat-bottom black plate to establish a baseline measurement that was recorded as a relative fluorescence of 0. Subsequently, 4.8 µl (1.2 µg) of pCMV-*luc* DNA was added to the mixture and a representative 100% relative fluorescence was ascertained. Following this, 1 µl (± 0.8 – 2.5 µg) aliquots of a given liposome preparation were systematically added to the mixture until a plateau in fluorescence readings was achieved. In order to promote uniform dispersion and to ensure an accurate reading, the suspension was mixed for 5 seconds prior to each measurement recording. The results obtained were plotted relative to the 100% fluorescence value. This procedure was conducted for all liposome preparations.

3.2.5. Imaging and Sizing

3.2.5.1. Characterisation of Particles by Transmission Electron Microscopy (TEM)

The structural and physical features of the mitochondriotropic liposomes and lipoplexes were examined using cryogenic-transmission electron microscopy (cryo-TEM). Liposomes were vortexed for 2 min and sonicated for 5 min prior to use, after which the liposome preparations were diluted 1:5 ($^{v}/_{v}$) with HBS to promote fluidity of the samples to be imaged. Aliquots of diluted samples (1 µl) were placed onto 200-mesh Lacey Formvar carbon coated copper grids (Ted Pella Inc., Redding, CA, USA), contrasted 1:1 ($^{v}/_{v}$) with 4% uranyl acetate negative stain and allowed to stand for 3-5 min, and the excess liquid was blotted off with Whatman No. 5 filter paper paper (Sigma-Aldrich Chemical Co., St. Louis, MO, USA). The grids were immediately vitrified by plunging into liquid propane (-180°C) cooled by liquid nitrogen, using an injector spring-loaded Leica Microsystems EM CPC Cryo system (Leica, Vienna, Austria). The rapid freezing of the samples by the liquid propane protects against ice crystal formation and freeze-thaw damage. Grids containing samples were maintained in liquid nitrogen and mounted in a cyrotransfer system (Gatan Inc., München, Bavaria, Germany). Samples were examined at -170°C on a Cryo-TEM JEOL JEM-1010 electron microscope (Jeol, Tokyo, Japan) operating under low electron dose to minimise electron beam radiation damage at an accelerating voltage of 100 kV. Images were captured using a Soft Imaging Systems (SIS) MegaView III side-mounted 3 megapixel digital camera and subsequently visualised and selected using SIS iTEM software (Olympus, Münster, North Rhine-Westphalia, Germany) for final image processing. Mitochondriotropic liposome-DNA complexes were also examined by cryo-TEM. Lipoplexes were prepared as described in section 3.2.3 above, according to their optimal binding capacities. The lipoplex dispersions were diluted 1:5 ($^{v}/_{v}$) with HBS to promote fluidity and were observed and imaged using the protocol as described above.

3.2.5.2. Particle Size and Zeta Potential Analysis

Mitochondriotropic liposomes and lipoplexes preparations were studied for size and zeta potential determination using an innovative technique called Nanoparticle Tracking Analysis (NTA), facilitated by the Nanosight NS500 (Malvern Instruments, Malvern, Worcestershire,

UK) containing a sample chamber of around 0.25 ml, a laser wavelength of 430 nm and a sCMOS camera. For data capturing and analysis, the NTA 3.2 analytical software was used. Liposomes were vortexed for 2 min and sonicated for a further 5 min, thereafter the dispersions were diluted 1:1000 with 3% sterile HBS. Lipoplex preparations were prepared as described in section 3.2.3 and according to Table 3.3. The different lipoplexes were diluted 1:100 with 3% sterile HBS. The lipoplexes were also additionally subjected to analysis with 3% sterile HBS containing 5% FBS ($^{v}/_{v}$). All liposome and lipoplex sample preparations were mixed thoroughly prior to analysis.

3.3. *IN VITRO* CELL CULTURE STUDIES

3.3.1. Chemicals and Reagents

Eagle's Minimum Essential Medium (EMEM) with L-glutamine (4.5 g/l) together with the trypsin-versene mixture and antibiotics (100x) comprising penicillin (10 000 U/ml), streptomycin (10 000 µg/ml) and amphoterin B (25 µg/ml) were purchased from Lonza BioWhittaker (Verviers, Liège, Belgium). Foetal bovine serum (FBS) was purchased from HyClone (Cramlington, Norththumberland, UK). 3-(4, 5-Dimethyl-2-thiazolyl)-2, 5-diphenyl-2H-tetrazolium bromide (MTT, $C_{18}H_{17}N_5S$), dimethyl sulphoxide (DMSO, $(CH_3)_2SO$) phosphate buffered saline (PBS) tablets, acridine orange (AO, $C_{17}H_{19}N_3$) and isopropanol (C_3H_8O) were acquired from Merck (Darmstadt, Hesse, Germany). AlamarBlue® cell viability reagent was obtained from Invitrogen (Carlsbad, CA, USA). Invitrogen, Molecular Probes® (Eugene, OR, USA) supplied MitoTracker® Green FM ($C_{34}H_{28}C_{l5}N_3O$). Cell lysis buffer (5 x) was purchased from Promega Corporation (Madison, WI, USA). All sterile tissue culture plastic ware and consumables were obained from Corning Incorporated (New York City, NY, USA). Ultrapure 18 MΩ water (Milli-Q50) was used throughout. All other chemicals were of analytical purity grade or higher and purchased commercially.

3.3.2. Routine Cell Culture and Cell Maintenance

Human embryonic kidney cells (HEK293) was obtained from the Anti-Viral Gene Therapy Unit, Medical School, University of the Witwatersrand, human hepatocellular carcinoma

cells (HepG2) and human epithelial colorectal adenocarcinoma cells (Caco-2) was purchased from Highveld Biological (Pty) Ltd. (Kelvin, Gauteng, RSA), and human cervical adenocarcinoma cells that stably express the firefly luciferase gene (HeLa-Tat *luc)* were provided by the Department of Physiology, University of KwaZulu-Natal, Westville, South Africa.

The different cell lines were propagated using 5 ml of complete EMEM supplemented with 10% ($^{v}/_{v}$) foetal bovine serum (FBS) and antibiotics (100 U/ml penicillin, 100 µg/ml streptomycin, 0.25 µg/ml amphotericin B) in 25 cm^2 culture flasks at 37°C in an incubator (ThermoElectron Corp. Steri-Cult CO_2 incubator, HEPA Class 100) under a humidified atmosphere. All cell culture procedures including preparation of complete medium and routine maintenance of cells were carried out aseptically in an Airvolution Class II biosafety cabinet (United Scientific (Pty) Ltd. Goodwood, Cape Town, RSA).

3.3.2.1. Reconstitution of Cells

Initially, ampoules of cryopreserved HEK293, HepG2, Caco-2 and HeLa-Tat *luc* cells were removed from the biofreezer (-80ºC) and placed in a 37ºC water bath to thaw. Once thawed, the vials were disinfected with ethanol, aseptically opened, the suspensions transferred to sterile centrifuge tubes and subjected to centrifugation (3000 rpm for 2 min) to pellet cells. The resultant supernatants containing DMSO were discarded and the pellets resuspended in 1 ml pre-warmed fresh complete medium (EMEM + 10% FBS + antibiotics). These 1 ml suspensions were transferred to cell culture flasks containing 5 ml complete medium (EMEM + 10% FBS + antibiotics) and the flasks placed in a 37ºC incubator. The medium was changed every two to three days and the different cell lines monitored daily using an inverted light microscope (Nikon TMS-F 6V, Tokyo, Japan), until they reached confluence.

3.3.2.2. Propagation and Subcultivation of Cells

Once the cells were at or near confluence, they were trypsinised to aid in propagation of the cell lines. Trypsin is a proteolytic enzyme that acts by digesting the proteins that allow cells to adhere to the culture flask. Briefly, spent medium from the culture flask was discarded

into a sterile waste bottle and the cells washed with sterile 5 ml phosphate buffered saline (PBS, pH 7.5) by gently shaking the culture vessel. Thereafter, the PBS was removed and 1 ml of pre-warmed trypsin-versene was added to dislodge the cells from the culture flask. This process was allowed to proceed for approximately 1-2 min at room temperature or 37ºC and observed under an inverted phase contrast light microscope until the cells had rounded off. Subsequently, 2 ml of complete medium was added to the flask to stop the trypsinisation procedure, following which, the cells were completely dislodged by firm tapping against the palm. The resultant cell suspension was either then seeded into multiwell plates for the various experimental assays or split at a desired ratio into culture flasks, each containing 5 ml of complete medium. These flasks were incubated at 37ºC and growth medium changed when necessary ensuring maintenance of pH and elimination of waste products. Once cells had reached confluence, they were again trypsinised and split as desired or alternately cryopreserved for future use.

3.3.2.3. Cryopreservation of Cells

Cells at or near confluence were trypsinised as described above. The resulting cell suspension was centrifuged at 1000 rpm for 5 minutes. The pelleted cells were resuspended in 0.9 ml complete medium (EMEM + 10% FBS + antibiotics) and 0.1 ml of the cryoprotective agent such as dimethylsulfoxide (DMSO), which lowers the freezing point of the medium and ensures a slower cooling rate, thereby lowering the risk of ice crystal development causing cell damage. This suspension was gently vortexed to promote homogeneity and was then aliquoted into 2 ml cryogenic vials. Vials containing cells were frozen at a rate of -1°C per minute in a Nalgene™ Mr Frosty Cryo 1°C freezing container containing isopropanol to a temperature of -70°C. The cryogenic ampoules of frozen cells were thereafter stored in a -80ºC biofreezer (Nuaire, Lasec Laboratory and Scientific Equipment, Ndabeni, Cape Town, RSA) for short term storage or in liquid nitrogen for long term storage.

3.3.3. Cytotoxicity Studies

3.3.3.1. MTT Growth Inhibition Assay

The cytotoxicity of the mitochondriotropic liposome formulations were quantified by the MTT reduction assay in the HEK293, HepG2, Caco-2 and HeLa-Tat *luc* cell lines. Confluent cells were separately trypsinised, seeded into a 48-well plate at a seeding density of 2.1 – 2.6 x 10^4 cells/well and incubated in 0.25 ml complete medium at 37ºC for 24 hours to allow for cells to adhere to the wells and grow to semi-confluence. The liposome-DNA complexes correlating with the sub-optimal, optimal and supra-optimal DNA binding ratios as determined from retardation studies were set up as in Table 3.3 and these lipoplexes were prepared as outlined in section 3.2.3. Cells were prepared by firstly removing the medium and replacing it with 0.25 ml fresh complete medium. Thereafter, the reaction complexes were added to the wells containing cells, and cells incubated at 37ºC for 48 hours. The assays were carried out in triplicate. Positive controls comprising untreated cells were also included in the assay. Following the incubation period, the spent medium in each well was discarded and replaced with 0.2 ml growth medium and 0.2 ml MTT reagent (5 mg/ml in sterile PBS, pH 7.4). The plates were allowed to incubate for a further 4 h at 37ºC. Thereafter, the medium containing MTT was extracted and 0.2 ml of DMSO was added to each well to allow for the solubilisation of the formazan crystals. Subsequently, absorbances were read on a Mindray MR-96A microplate reader (Vacutec, Hamburg, Germany) at 570 nm. Cell viability (%) was directly correlated to absorbance and was calculated as follows:

% cell survival = [OD_{570} Treated cells] / [OD_{570} Control] x 100.

3.3.3.2. AlamarBlue® Assay

Overall cellular metabolism of viable cells was quantified by use of the AlamarBlue® assay. This assay was used to determine the *in vitro* cell viability of HEK293, HepG2, Caco-2 and HeLa-Tat *luc* cells when exposed to mitochondriotropic lipoplexes tested. Cells were trypsinised as described above, seeded into 48-well plates (2.2 – 2.5 x 10^4 cells/well), incubated and allowed to attach to the wells. After 24 hours, medium was replaced with fresh growth medium (0.25 ml) and test lipoplexes (Table 3.3), prepared as outlined in section 3.2.3, were added in triplicate to cells in the wells. Controls comprising untreated cells (as in

3.3.3.1) were also included in the assay. The plates were incubated for 48 hours at 37ºC, after which, 25 µl (10%, $^{v}/_{v}$) of 10x AlamarBlue® reagent was added to the cells containing growth medium which were further incubated for 4 h at 37ºC. Following the incubation period, a GloMax®-Multi Detection System (Promega BioSystems, Sunnyvale, CA, USA) operated by Instinct software was used to measure fluorescence in 96-well FluorTrac flat-bottom black plates at excitation and emission wavelengths of 570 nm and 585 nm, respectively. The percentage of AlamarBlue® reduction was calculated as follows:

$[(\lambda_{570}$ Test $- \lambda_{585}$ Test) / (λ_{570} Control $- \lambda_{585}$ Control)] x 100

3.3.4. Apoptosis Detection by Acridine Orange and Ethidium Bromide (AO/EB) Staining

As most of cell death that occurs when cells are exposed to liposomes is apoptotic, this assay was used to detect apoptosis *in vitro* by the dual staining method using ethidium bromide and acridine orange (AO/EB). HEK293, HepG2, Caco-2 and HeLa-Tat *luc* cells were trypsinised as described above, seeded into 48-well plates (1.9 – 2.3 x 10^4 cells/well), incubated and allowed to attach to the wells. After 24 hours, medium was replaced with fresh growth medium (0.25 ml) and test mitochondriotropic lipoplexes at the optimal liposome-DNA ratios (Table 3.3) were prepared as described in section 3.2.3 and added into the wells. Controls containing cells only were also employed. The plates were incubated for 24 hours at 37ºC after which, medium was discarded and the cells stained with 20 µl of EB/AO solution (100 µg/ml of AO and EtBr in a 1:1 ratio) per well for 5 minutes. Following the incubation, the cells were washed with PBS and viewed using an inverted fluorescence microscope (Olympus CKX41, Tokyo, Japan) at 490 nm (excitation λ) and 516 nm (emission λ).

3.3.5. Detection of Mitochondrial Localisation by Fluorescent Studies

3.3.5.1. Fluorescence Microscopy

Confluent cells (HEK293, HepG2, Caco-2 and HeLa-Tat *luc*) were separately trypsinised, seeded into 48-well plates at seeding densities of 1.9 – 2.1 x 10^4 cells/well and incubated in 0.25 ml complete medium at 37ºC for 24 hours to allow for cells to adhere to the wells and

grow to semi-confluence. Thereafter, the spent medium was replaced with fresh complete medium. Test mitochondriotropic lipoplexes at the optimal liposome-DNA ratios (Table 3.3) were prepared as illustrated in section 3.2.3 with rhodamine-labelled pCMV-*luc* DNA (1 µg) and added into wells. Controls comprising untreated cells and untreated cells with naked rhodamine-DNA were also included in the assay. The culture plates were incubated for 24 hours at 37ºC following which, the medium was discarded and the cells stained with 200 µl 50 nM MitoTracker® Green FM (made up in serum-free growth medium) and allowed to incubate for 1 h at 37ºC. Thereafter, the stain was decanted; cells washed with PBS (pH7.5) to remove excess stain and then viewed using an inverted fluorescence microscope (Olympus CKX41, Tokyo, Japan). MitoTracker® Green FM was observed at 490 nm (excitation λ) and 516 nm (emission λ) while rhodamine-labelled pCMV-*luc* DNA was examined at 546 and 576 nm representing the excitation and emission wavelengths, respectively.

3.3.5.2. Quantitative Evaluation of Mitochondrial Targeting Activity

This method was adapted from Yamada and Harashima (2013). A homogenate solution was obtained from a total of 5 x 10^6 of cultured cells (HEK293, HepG2, Caco-2 and HeLa-Tat *luc*). The cells were trypsinised to dislodge them from the surface of the flasks. Thereafter, cells were washed with ice-cold PBS, resuspended in mitochondrial isolation buffer [MIB, (250 mM sucrose; 2 mM Tris-HCl)] and subjected to 20 strokes in a Dounce homogeniser on ice to yield a homogenate. Aliquots (10 µl) of lipoplexes (containing 1 µg of fluorescein-labelled pCMV-*luc* DNA) were prepared at the optimal liposome-DNA ratio ($^{w}/_{w}$) as illustrated in section 3.2.3 for each of the cationic mitochondriotropic liposome formulations. These were added in triplicate to the homogenates of the different cell lines in 90 µl of MIB, and the suspensions incubated for 30 minutes at 25°C. The resultant solution was designated Sample A. Following the incubation period, a differential centrifugation technique was used to obtain each organelle fraction from the homogenates. All steps were carried out on ice. Controls comprising untreated cells only and cells only containing naked fluorescein-DNA were also included in the assay. The homogenate solution was centrifuged at 700 x g at 4°C for 10 minutes and the resultant pellet, denoted P fraction which contained nuclei and fracted cells were resuspended in 100 µl MIB. The supernatant was further centrifuged at 16 000 x g at 4°C for 10 minutes and the resulting pelleted fraction was resuspended in was resuspended in 100 µl MIB to give the mitochondrial fraction. Sample A and the mitochondrial fraction

were solubilised by 1 x cell lysis buffer and the fluorescence intensities were measured in 96-well FluorTrac flat-bottom black plates at excitation and emission wavelengths of 492 nm and 518 nm respectively, using the GloMax®-Multi Detection System operated by Instinct software. Mitochondrial targeting activity (%) was calculated as follows:

Mitochondrial targeting activity (%) = F_{mt}/F_A x 100,

where F_A and F_{mt} represent the fluorescent intensity of Sample A and the mitochondrial fraction, respectively.

3.4. STATISTICAL ANALYSIS

All data are presented as mean ± standard deviation (SD, n = 3). One-way analysis of variance (ANOVA) was performed for all analyses followed by Dunnett and Tukey-Kramer *post hoc* tests for multiple comparisons between groups. All statistical analyses were performed using a 95% confidence interval and was considered significant when the P value was less than 0.05 $(P<0.05)$.

CHAPTER FOUR

RESULTS AND DISCUSSION

4.1. SYNTHESES AND LIPOSOME FORMULATON

4.1.1. Cationic Cholesterol-derived Cytofectin (CHOL-T)

3 β [*N-(N', N'*- dimethylaminopropane)-carbamoyl] cholesterol (CHOL-T) was previously successfully synthesised from cholesterol chloroformate (Singh *et al*., 2001). This cationic lipid has the general structure of most cationic lipids used today, i.e. it has four basic components: a hydrophobic lipid anchor, spacer arm, linker bond and a positively charged head group (Huang *et al*., 1999) (Figure 4.1).

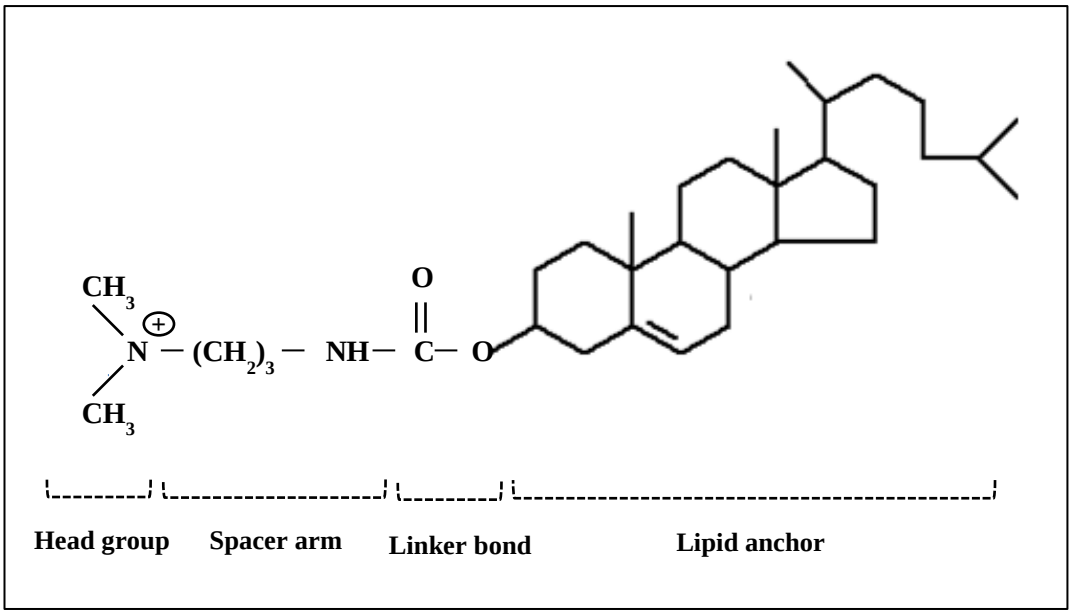

Figure 4.1: Structure of cationic lipid CHOL-T, showing the four components**.**

The cationic lipid in this study has a cholesterol ring anchor, a carbamoyl linker bond and a monovalent dimethylamino cationic head group. This lipid is amphiphilic and as such has both hydrophilic and lipophilic properties. The lipophilic portion, which is the cholesterol anchor, not only brings rigidity and stability to the liposome structure but it also seems to

influence membrane fluidity, the consequent effects on lipid mixing within the bilayers as well as determining other physical properties of the lipid bilayer (Huang *et al*., 1999; Lesage *et al.*, 2002). The hydrophilic segment is generally a charged head group, and in this cytofectin the cationic head group has an amine (R_3NH^+) functionality.

The linker bond of this cholesterol derivative is a carbamoyl bond and influences the chemical stability and biodegradability of the cationic lipid (Huang *et al*., 1999). The spacer arm length that joins the hydrophilic and hydrophobic portions may play a role in promoting DNA interaction with the charged head group i.e. a longer spacer arm would result in a decrease of steric hindrance between the polar head group and the hydrophobic cholesterol ring system (Singh, 1998).

The type of head group plays an important role in determining the transfection efficiency and cytotoxicity of the formulated liposomes. Monovalent cationic lipids, like CHOL-T, condense DNA less strongly than multivalent cationic lipids *in vitro*; however the presence of too many positive charges on the head group may result in an extremely secure interaction with the DNA and the subsequent decrease in transfection activity as this impedes the disassociation of the pDNA at the molecular level (Huang *et al.*, 1999). Cholesterol derivatives with a tertiary amino group, such a CHOL-T, generally have stronger transfection activities than quaternary derivatives (Farhood *et al.*, 1992). The terminal tertiary amino functionality of CHOL-T extends 6 Å from the 3-position of the fused perhydrocyclopentanophenanthrene ring system and additionally, a carbamoyl linkage connects the hydrophobic cholesteryl moiety and the 3-carbon propane spacer element (Singh *et al.*, 2011). This cholesterol-derived cytofectin formed the major structural constituent of the mitochondriotropic liposomal vesicles manufactured for this investigation.

4.1.2. Cholesterol-derived Cross-linking Agents

To make typical cationic liposomes mitochondriotropic, the mitochondrial targeting sequence (MTS) and octaarginine (R8) peptides were attached to the surface of the liposomes. To facilitate this attachment, the liposomes needed to possess a lipid with a hydrophobic anchor, a spacer arm and a reactive head group that will bind to the peptides, incorporated into the liposomal bilayer. To this end, two different cholesterol-derived cross-linking agents were

synthesised namely, 3β-[N-(hydrazino 3-{2-pyridyldithio} propionate)-carbamoyl] cholesterol (SP-CHOL) and 3β-[N-(hydrazino-γ-maleimidobutyryl)-carbamoyl] cholesterol (GM-CHOL) (Figure 4.2). The thin layer chromatographs confirmed the presence of the desired products, SP-CHOL and GM-CHOL (Figure 4.3). NMR data were consistant with structure assignment.

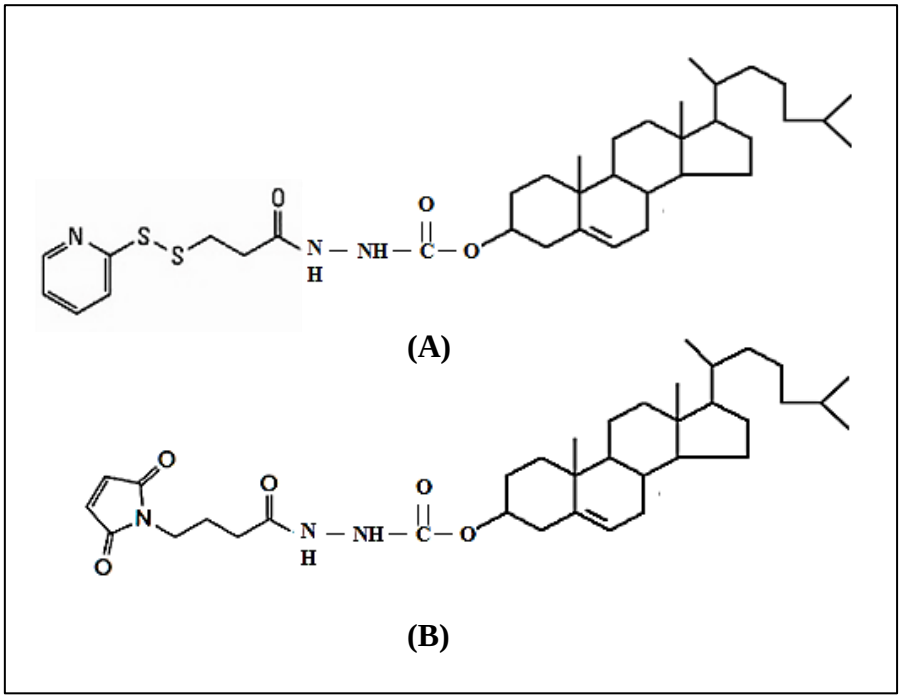

Figure 4.2: Structures of cholesterol-derived cross-linking agents **(A)** 3β-[N-(hydrazino 3-{2-pyridyldithio} propionate)-carbamoyl] cholesterol (SP-CHOL) and **(B)** 3β-[N-(hydrazino-γ-maleimidobutyryl)-carbamoyl]-cholesterol (GM-CHOL).

Sulphuric acid (33%, $^{v}/_{v}$) was sprayed onto the thin layer chromatograms to aid in colour development and visualisation. Dehydration of sterols such as free cholesterol and MS04 by the acid, results in a brown to purple colour. The reaction mixture (RM) as shown in Figure 4.3 (A and B) shows the product, some unreacted MS04 as well as *N*-hydroxysuccinimide (NHS) which is released by the reaction (Figure 3.3). The product lanes contained the desired crystalline products confirming that the purification process was successful.

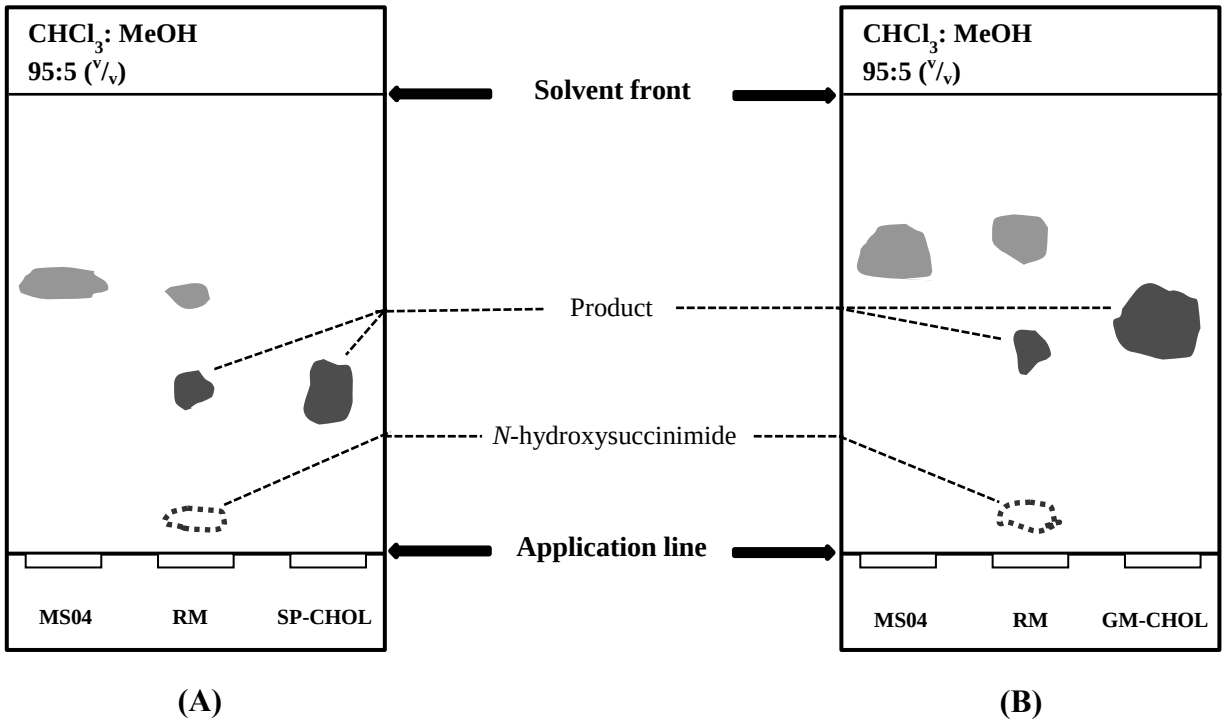

Figure 4.3: Representative TLC chromatographic plate illustrating the synthesis of **(A)** SP-CHOL and **(B)** GM-CHOL showing the stating material MS04, reaction mixture (RM) and as well as the purified products. The retention factor (R_f) of the reactants was calculated as the distance from point of application of analyte (mm) /distance from application line to solvent front (mm), as follows: Plate **A** – MS04 0.3, RM product = 0.05, SP-CHOL = 0.2; Plate **B** – MS04 = 0.4, RM product = 0.3, GM-CHOL = 0.4
Solvent system: $CHCl_3$: MeOH (95:5, $^v/_v$).

MS04 is the first step intermediary in the synthesis of the cationic cytofectin *N*-dimethylaminopropylaminylsuccinylcholesterylformylhydrazide (MS09). An excess amount of hydrazine, which acted as an electron/amino group donor activated the carbonyl group on cholesteryl chloroformate, which formed the hydrophobic anchor, yielding the product, cholesterylformylhydrazide (MS04), which contained the newly formed carbamoyl bond. This reaction was accompanied by the release of HCl (Figure 3.2). Thus MS04 lipid structure comprised a cholesterol anchor, a carbomyl bond and a terminal amino group.

The heterobifunctional cross-linkers used to synthesise the bioconjugates SP-CHOL and GM-CHOL have two different reactive groups at either end. SPDP contains NHS ester and pyridyldithiol reactive groups while GMBS comprises NHS ester and maleimide reactive groups. Both these reagents' cross-linking targets are amines through their NHS ester; and sulfhydryl groups through their pyridyldithiol or maleimide portions (Hemaprabha, 2012). In

the conjugation reaction with MS04, the NHS ester of both SPDP and GMBS reacts with the terminal amino group ($-NH_2$) of the MS04 to produce the cholesterol-derived cross-linking agents, SP-CHOL and GM-CHOL respectively (Figure 3.3) with the subsequent release of NHS as a by-product of the reaction. The cross-link formed by SPDP and MS04 is cleavable however the GMBS cross-link to MS04 is non-cleavable. As noted by the structures of SP-CHOL and GM-CHOL (Figure 4.2), they are essentially functionalised MS04 molecules with SP-CHOL containing a pyridyldithiol reactive group at one end and GM-CHOL boasting a maleimide reactive group at its end. These reactive groups allow for binding or bioconjugation of other molecules such as the MTS and R8 peptides through the SH groups of the C-terminal cysteine residues. SP-CHOL has a spacer arm of 6.8 Å containing a disulphide bond that extends from the amide bond to the pyridyldithiol reactive portion while GM-CHOL has a 7.3 Å alkane spacer arm length from said bond to its reactive maleimide segment. The hydrophobic cholesterol anchor was utilised for its natural interaction with, and stable incorporation into liposomal bilayers.

4.1.3. Formulation of Cationic Mitochondriotropic Liposomes

Conventional liposomes are lipid-based vesicular artificial macromolecular complexes usually composed of biodegradable, reusable amphiphilic molecules (Zhdanov *et al.,* 2002). These molecules have a hydrophilic group, the polar head, and a hydrophobic portion, which is the non-polar tail. Therefore these amphiphilic molecules self-assemble and form ordered structures, such as lipid bilayers, in aqueous solutions (Lasic, 1997). These lipid bilayers exist such that the polar surfaces shield the non-polar interior. However, as it is energetically unfavourable to have hydrophobic edges adjacent to water, the bilayer sheets self-close to form liposomes with the water both inside and outside the bilayer (Singh, 1998; Lasic, 1997) (Figure 4.4). As mentioned earlier, conventional liposomes can be easily modified. To this end, cationic lipids, which are positively charged amphiphilic molecules, can be incorporated into liposome structures to form cationic liposomes (Lonez *et al.,* 2008; Wasungu and Hoekstra, 2006).

Various methods have been utilised to prepare cationic liposomes. These include the original hand-shaken preparation producing multilamellar vesicles (Bangham *et al.*, 1965), ethanol or ether injection technique (Batzri and Korn, 1973; Campbell, 1995; Deamer and Bangham,

1976), reverse phase evaporation technique (Szoka and Papahadjopoulos, 1978), detergent depletion (Torchilin, 2003) and thin lipid film hydration (Gao and Huang, 1991). The latter method was employed for the successful preparation of the four cationic mitochondriotropic liposomes utilised in this study. Each of these four liposomes contained a constant 50% mole composition of the synthetic cationic cytofectin, CHOL-T to facilitate binding of negatively-charged pDNA as well as varying mole percentage of the helper lipid, dioleoylphosphatidylethanolamine (DOPE). The lipid composition of liposomes determines many physical features such as size, zeta potential and fluidity or rigidity of the bilayer as well as functional characteristics like cytotoxicity, binding capacity and transfection efficiency of the resultant liposomal vesicle. Lipid derivatives containing cholesterol produce liposomes with good membrane stabilisation and well-organised structure due to the presence of the cholesterol portion of the lipid (Lesage *et al.*, 2002; Briuglia *et al*., 2015). The presence of cholesterol and its derivatives in liposomal bilayers has been shown to have a number of advantages: it improves vesicle resistance to excessive aggregation and protein binding; it improves serum stability of the vector even when exposed to high serum concentrations; the mechanical strength of these delivery vehicles is enhanced; and finally, it increases the packing density of lipids via "ordering and condensing" effects which leads to a more ordered membrane structure and subsequently results in reduced permeability of the liposomal bilayer to non-electrolyte and electrolyte solutes (Yang *et al*., 2013; Magarkar *et al*., 2014; Briuglia *et al*., 2015).

The other major ingredient in all liposome preparations was the cephalin dioleoylphosphatidylethanolamine (DOPE). DOPE is a neutral zwitterionic phospholipid and is often used in liposome preparations as a helper or co-lipid. It tends to form a heterodimer with the cationic lipid through the interaction between the negatively charged phosphate on DOPE and the tertiary ammonium group on the cationic lipid (Felgner *et al.*, 1994). This helper lipid is also required to stabilise cationic liposome formulations as the cationic lipids tend repel each other (Dass, 2004). It is thought that this lipid improves cationic lipid mediated nuclear transfection efficiency by promoting the conversion of the lamellar lipoplex phase into a non-lamellar or inverted hexagonal phase (H_{II}) (Wasungu and Hoekstra, 2006; Kim *et al*., 2015). DOPE has a small head group and two bulky fatty acyl chains that give it a conical molecular shape (Figure 4.4). This shape favours robust intermolecular interactions between the phosphate and amine groups of its polar head, which explains why this lipid and other phosphatidylethanolamines are unable to organise themselves into bilayers by

themselves and instead prefer the H_{II} phase (Monteiro *et al*., 2016). It is this feature of DOPE that contributes to its fusogenic capacity that allows this neutral lipid to assist in endosomal membrane destabilisation and the subsequent release of DNA from the endosome during nuclear transfection (Li and Ma, 2001; Percot *et al.*, 2004). This natural fusogenic characteristic of DOPE is also exploited in mitochondrial targeted delivery of macromolecules such as DNA, proteins or drugs where DOPE-containing mitochondriotropic liposomes fuse with the mitochondrial membrane in order to facilitate delivery of cargoes (Yamada and Harashima, 2013; Kawamura *et* al., 2013a; Furukawa *et al*., 2015). It is for these favourable reasons that the fusogen DOPE was incorporated into the cationic mitochondriotropic liposomes used in this study.

To display MTS and R8 peptides on the surface of the liposome, 5 or 10 mol% of either SP-CHOL or GM-CHOL was also incorporated in the liposomal bilayer. The reactive groups (pyridyldithiol on SP-CHOL and maleimide on GM-CHOL) at the end of these lipid derivatives react with cysteine on MTS and cysteine on R8 when the liposomal suspensions are incubated with these peptides, thus enabling the binding of the respective peptides onto the liposomal surface and generating the resultant cationic mitochondriotropic liposomes. As mentioned earlier, MTS peptide has been shown to selectively deliver a wide range of proteins, chemicals, linear DNA and ODNs to mitochondria (Flierl *et al*., 2003; Yamada and Harashima, 2013). It was further reported by Yamada and Harashima (2013) that MTS was an efficient ligand for the selective mitochondrial delivery of the nanoparticle under investigation in cell homogenates, by virtue of their accumulation in the mitochondrial fraction. MTS peptide was added at 5 mol% of total lipid content as it was found that at higher concentrations, the MTS molecule caused excessive increases in surface charge and aggregation (Yamada and Harashima, 2013). Based on this evidence, it is expected that MTS has the potential to be an effective ligand for selective mitochondrial delivery, via mitochondrial import machinery, of the cationic mitochondriotropic liposomes in this study.

Octaarginine (R8) is a synthetic cationic cell penetrating peptide (CPP) that has been used extensively as vectors or ligands for the intracellular delivery of a variety of therapeutic molecules such as nucleic acids, proteins, peptides, fluorochromes, nanoparticles, micelles, small molecular drugs and liposomes (Yamada *et al*., 2008; Biswas and Torchilin, 2013; Layek *et al*., 2015; Boisguérin *et al*., 2015). Liposomes modified with high-density R8 have been shown to be internalised predominantly by macropinocytosis, a form of fluid-phase

endocytosis that allows vectors to more efficiently escape macropinosomes due to their inherent leaky nature, and thus evade lysosomal degradation (Khalil *et al*., 2006a; Yamada *et al*., 2008 Huang *et al*., 2011). It is thought that R8 and other CPPs mediate macropinocytosis by electrostatic interactions with anionic phospholipids and negatively charged sulphated proteoglycans such as glycosaminoglycans of cell membranes (Layek *et al*., 2015; Boisguérin *et al*., 2015; Imani *et al*., 2015). R8 mimics the TAT peptide derived from human immunodeficiency virus (HIV-1 protein) which has been shown to deliver some cargo to mitochondria, while Yamada and Harashima (2008) observed that R8 modified liposomes enhanced binding to mitochondria (Yamada *et al*., 2011). Thus, in this study, 5 mol% R8 surface modification of cationic mitochondriotropic liposomes, which is considered high density, was utilised primarily as a cellular uptake device as well as a possible mitochondrial targeting device.

4.1.4. Mitochondriotropic Liposome-DNA Complex Formulation

The term 'lipoplexes' was first used by Felgner *et al*. (1997) to describe the complex formed by the interaction of plasmid DNA (pDNA) with cationic liposomes or lipids. These so-called 'lipoplexes' have proven to be a viable alternative in the search for new DNA delivery agents.

The exact mechanism involved in the formation of cationic liposome-DNA constructs and structure of the lipoplexes is still not fully understood. What is known however, and holds true today is that complexation is achieved by simply mixing and incubating the cationic liposome preparation and the pDNA (Felgner *et al*., 1987). This process is dependent on a number of factors including charge ratio, type of cationic lipid, liposome concentration and nature of preparation, plasmid size and temperature to name a few (Barenholz, 2001; Wasungu and Hoekstra, 2006; Tros de Ilarduya *et al*., 2010). It is generally accepted that the cationic liposomes interact with pDNA through charge-charge attraction (Li and Ma, 2001). Cationic liposomes, when mixed with DNA, react by spontaneous self-assembly forming lipoplexes (Figure 4.4). The first step in this process involves an electrostatic interaction between the positively charged amine headgroup of the cationic lipid and the negatively charged phosphate backbone of the pDNA resulting in the formation of a liposome-DNA complex, a process during which the liposomes tend to retain their original shape

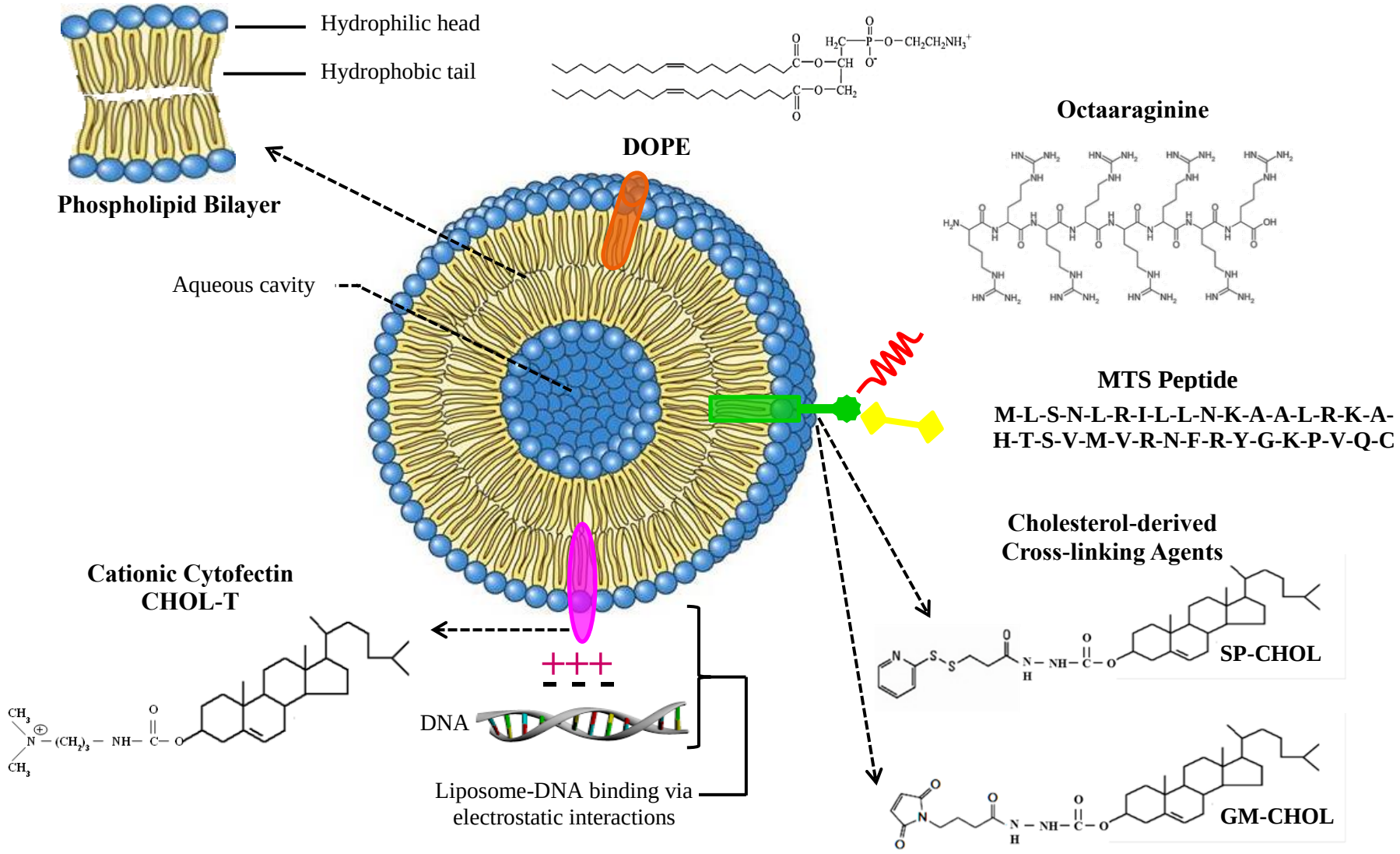

Figure 4.4: Schematic structure and composition of the cationic liposome (+) used in this study and its electrostatic interaction with anionic DNA (–) to form a liposome-DNA complex called a lipoplex.

This is an exothermic, rapid and reversible reaction (Ropert, 1999; Tros de Ilarduya *et al*., 2010) (Figure 4.4). The second step is irreversible, slower and endothermic involving the rearrangement and fusion of the liposome and pDNA such that the pDNA is compacted or condensed in a way that it is effectively shielded by the lipids of the liposome (Zhdanov *et al*., 2002; Wasungu and Hoekstra, 2006; Tros de Ilarduya *et al*., 2010).

Originally there were essentially two hypothetical models of liposome-DNA interactions that have been elucidated by the use of fluorescence, atomic force and electron microscopy techniques. These two models were the electrostatic model or 'external' model and the coated electrostatic or 'internal' model (Singh, 1998; Smith *et al*., 1993; Ma *et al*., 2007). The original electrostatic model was proposed by Felgner and Ringold in 1989 and is based on the probability that electrostatic forces underlie the successful interactions between DNA and cationic lipids where the DNA is adsorbed onto the surface of the cationic liposomal vesicle gaining a 'beads on a string' structure. The coated electrostatic model suggests that the DNA is coated by lipid bilayers due to the DNA being entrapped between the bilayers during liposome-DNA interactions (Ma *et al*., 2007; Tros de Ilarduya *et al*., 2010). As cationic liposomes and thus lipoplexes are frequently heterogeneous in terms of composition, preparation, size and shape, many varieties of morphologies have been reported such as spaghetti and meatballs structures, sliding columnar phase and map-pin structures. However, x-ray diffraction studies have shown two prevailing types of structures in plain lipoplexes, viz. multilamellar structure L^{C}_{α} where DNA monolayers are sandwiched between lipid bilayers characterised by regular spacing [Figure 4.5 (A)]; and the second is the inverted hexagonal structure H^{C}_{II} or 'honeycomb' phase with DNA encapsulated within lipid monolayer tubes [Figure 4.5 (B)] (Tros de Ilarduya *et al*., 2010; Dan, 2015; Motta *et al*., 2016). It has been reported that lipid properties of the bilayer determine which of the two above structures the resultant lipoplexes will form (Dan and Danino, 2014). Cationic lipoplexes may exhibit colloidal stability in three main zone allocations: zone A which has a negative N/P ratio and contains lipoplexes with uncondensed DNA surrounding them; zone B which comprises essentially uncharged complexes and is a region of colloidal instability and zone C which is a region of stable, positively charged lipoplexes with highly condensed DNA (Kreiss *et al*., 1999).

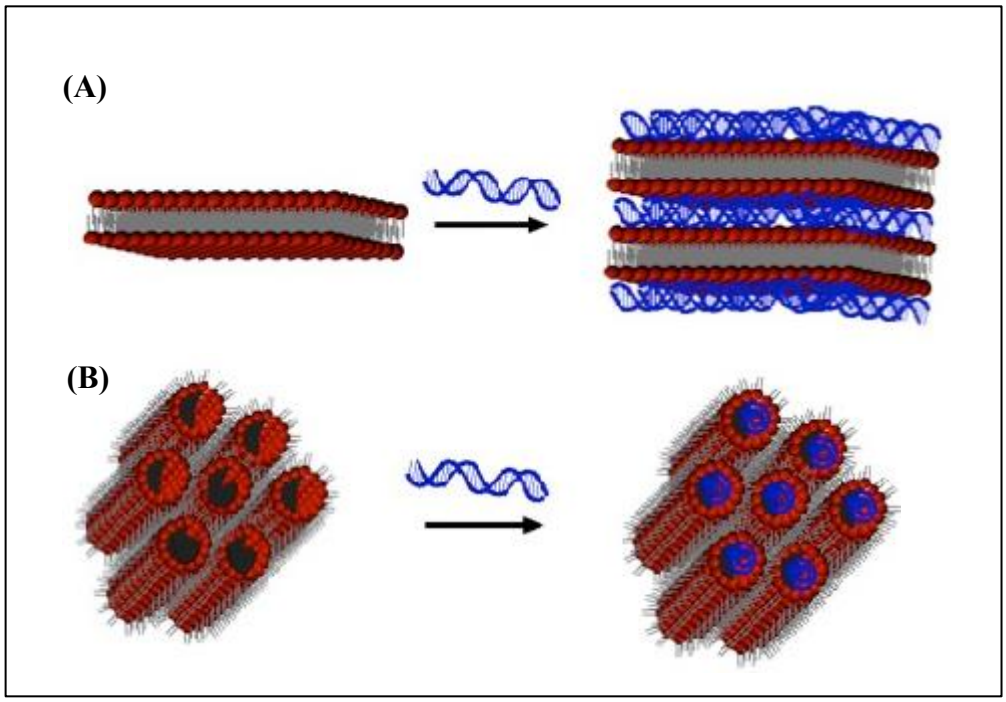

Figure 4.5: Schematic of the two most common lipoplex structures
(A) lamellar structure (L^{C}_{α}) where DNA is sandwiched between lipid bilayers, and
(B) inverted hexagonal structure (H^{C}_{II}) where DNA is coated with lipid monolayer arranged in a hexagonal lattice. Adapted from Dan (2015).

4.2. CHARACTERISATION OF LIPOSOMES AND LIPOSOME-DNA COMPLEXES

4.2.1. DNA Binding Studies of Mitochondriotropic Liposomes and Nuclease Protection Assays

As noted above, lipoplexes are formed by the mixing of cationic liposomes and anionic DNA, driven by electrostatic interactions between the two molecules. Characterisation of these resultant lipoplexes was conducted to determine the optimum binding ratios of the liposome-DNA complexes for *in vitro* analyses and mitochondrial localisation. Lipoplex formation was investigated using the gel retardation, ethidium bromide intercalation and nuclease digestion assays.

4.2.1.1. Gel Retardation Assay

The gel retardation or electrophoretic mobility shift (EMS) assay was originally devised by Fried and Crothers for studying protein-DNA interactions (Scott *et al*., 1994; Hellman and Fried, 2007). It was adapted for cationic liposome studies and the underlying principal of this assay is that the formation of complexes between plasmid DNA and cationic liposomes results in the retardation of the DNA electrophoretic migration. Agarose gel electrophoresis was used to demonstrate the binding efficiency or complex formation between the pDNA and the cationic liposomes. The amount of liposome-associated pDNA that is retained in the wells increases with increasing liposome concentration until complete DNA complexation is achieved, and the charge ratio (N/P) corresponding to this complexation can be thus estimated (Percot *et al*., 2004). This is the minimum mass of cationic liposome that is required to completely compact and bind a constant amount of pDNA, thereby forming a cationic lipoplex capable of gene delivery. Complete retardation suggests that the negative charges of the pDNA are completely titrated by the positive charges of the cationic mitochondriotropic liposomes. This yields electroneutral complexes that cannot migrate through the agarose gel matrix and can be seen fluorescing in the wells. At higher liposome-DNA ratios, precipitates may form and float out of the sample wells thus evading detection even after ethidium bromide staining (Singh, 1998). Naked pDNA, in the absence of liposome, would migrate in the gel matrix, however in the presence of increasing concentrations of cationic mitochondriotropic liposome; the anionic pDNA was neutralised resulting in complete DNA compaction by the liposomes and hence no further migration was observed and pDNA was finally retained in the wells. As can be seen from the results (Figure 4.6) all cationic liposome preparations successfully bound the pDNA, at various weight or N/P ratios.

The control lane containing 0.5 µg of naked or uncomplexed pCMV-*luc* generated the expected three conformations, i.e. supercoiled helical (migrates the furthest), linear and nicked circular (migrates the least). It was observed that all mitochondriotropic lipoplexes retarded the same amount of pDNA (0.5 µg) at varying liposome-DNA or N/P ratios regardless of the fact that all liposomal preparations comprised a constant amount (2 µmols) of the cationic lipid, CHOL-T. It can hence be suggested that the difference seen in binding efficiencies of the various lipoplexes was possibly attributed to the cholesterol-derived cross-linking agents, and the MTS and R8 peptides attached to the surface of the various liposomes.

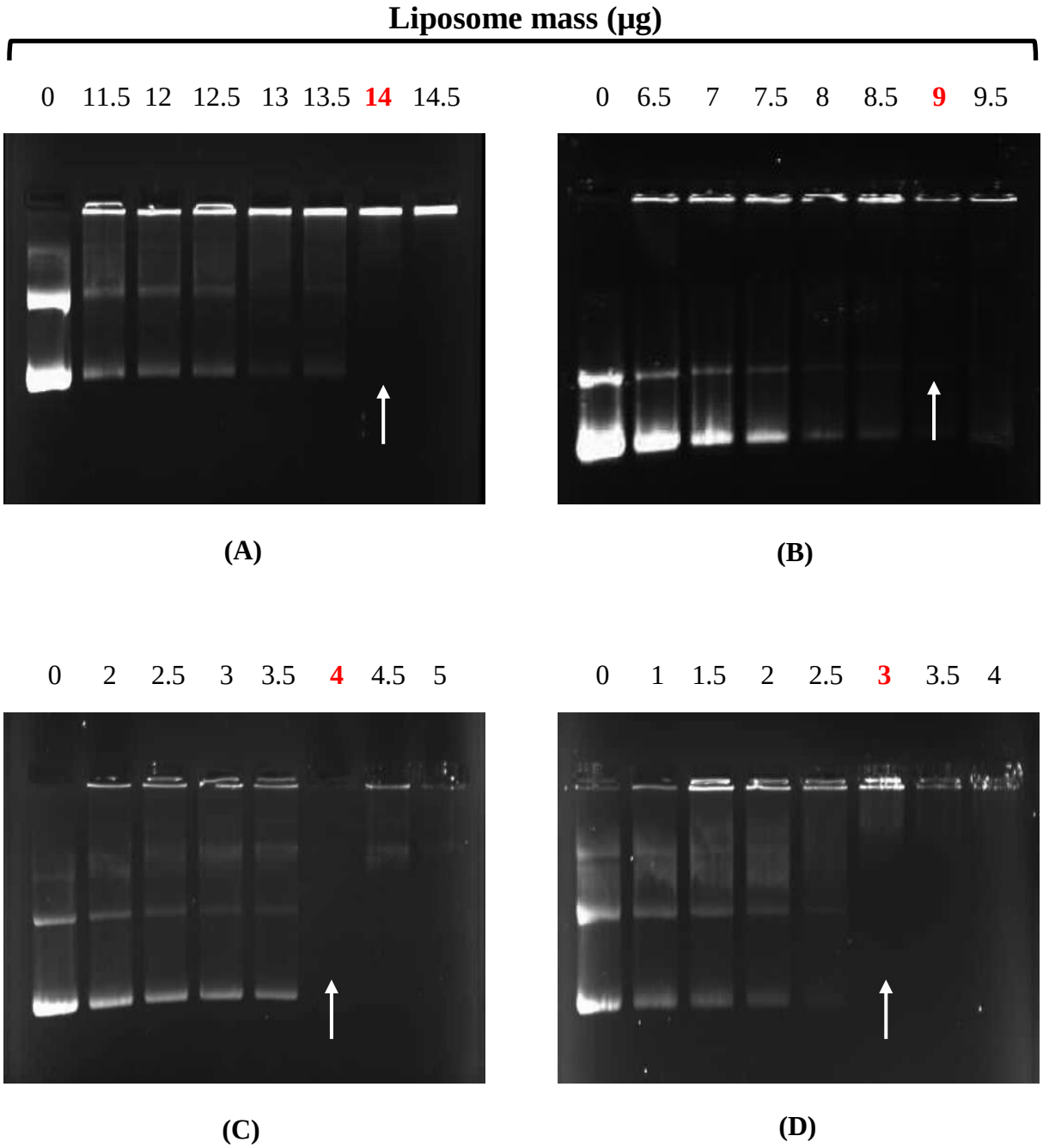

Figure 4.6: Gel retardation analysis of the binding interaction of varying amounts of cationic mitochondriotropic liposome preparations in a total of 10 µl reaction mixture while pCMV-*luc* DNA was kept constant at 0.5 µg per well.
(A) SP-CHOL-MTS, **(B)** GM-CHOL-MTS, **(C)** SP-CHOL-MTS-R8 and **(D)** GM-CHOL-MTS-R8. Samples from left to right are as follows, lane 1: 0.5 µg of naked pDNA (0 µg of cationic liposome); lanes 2 – 8: the respective liposome-DNA complexes prepared using various liposome mass (µg) as indicated. Numbers in red and arrows indicate the point of electroneutrality.

From the results obtained (Figure 4.6 and Table 4.1), it can be seen that mitochondriotropic liposomes containing SP-CHOL required more liposome to bind 0.5 µg pDNA compared to their respective GM-CHOL containing counterparts. SP-CHOL and GM-CHOL have lipid anchors that form part of the lipid bilayer of the liposome and the reactive portion of these agents structurally protrude out of the bilayer of the liposomes. The MTS and R8 peptide molecules attach to these bilayer projecting reactive portions of the respective agents to form the mitochondriotropic liposomes. SP-CHOL has a spacer arm of 6.8 Å while GM-CHOL has an arm length of 7.3 Å. This slight difference in spacer length could possibly account for the higher N/P ratios needed by SP-CHOL containing liposomes to retard DNA migration relative to the GM-CHOL containing liposome preparations. The shorter arm length of SP-CHOL means that MTS molecules in SP-CHOL-MTS and both MTS and R8 peptides in SP-CHOL-MTS-R8 bind to the liposome somewhat closer than would be observed in GM-CHOL containing liposomes, GM-CHOL-MTS and GM-CHOL-MTS-R8. This could possibly cause a shielding or masking effect whereby the positive charges of the liposomes are essentially blocked or shielded by the bound peptides thereby decreasing the 'available' overall positive charge or cationic cytofectin of the liposome and thus interfering with the binding of the cationic liposomes to the negatively charged DNA. A similar shielding effect was observed in a study by Meyer *et al.* (1998) in which the polymer blocked negative charges of liposome-bound oligodeoxyribonucleotides. The marginally larger spacer arm length of GM-CHOL could have ensured that the peptides bind to the liposome sufficiently further away such that the shielding effect is negated or reduced and the 'available' cationic charge is largely unaffected.

Another trend observed was that mitochondriotropic liposome preparations that contained the R8 peptide, SP-CHOL-MTS-R8 and GM-CHOL-MTS-R8 showed significantly lower amounts of liposome needed to bind 0.5 µg pDNA and hence lower N/P ratios in contrast to liposomes containing MTS only. R8, as noted above, is a cationic peptide molecule and as such when bound to the liposomes, it lends its positive charge to those liposomes thus increasing the overall theoretical cationic charge of the liposomal preparations. This could have consequently resulted in the requirement of lower amounts of those liposomes to completely bind the same amount of pDNA leading to the decreased N/P ratios detected. Additionally, MTS (33 amino acids) is a substantially larger peptide than R8 (8 amino acids). In liposome preparations that contain MTS only, SP-CHOL-MTS and GM-CHOL-MTS, MTS could exclusively bind to the reactive portions of the SP-CHOL and GM-CHOL thus

perhaps partially masking the positive charges of the liposomes because of its considerable size. In liposomes containing MTS and R8, SP-CHOL-MTS-R8 and GM-CHOL-MTS-R8, MTS peptides are in competition with R8 molecules to bind the reactive portions thus it is conceivable that fewer MTS peptides attach to the liposomes and this could have lessened any shielding influence that MTS peptides may have induced.

TABLE 4.1: Liposome-DNA ratios at which all plasmid DNA is lipoplex – associated (optimal ratio) and corresponding charge ratios for gel retardation and ethidium bromide intercalation assays.

Mitochondriotropic Liposome	Retardation			Ethidium Bromide Intercalation Assay	
	Liposome Amount (µg)	Liposome-DNA Ratio ($^{w}/_{w}$)	Charge Ratio (N/P)	Liposome-DNA Ratio ($^{w}/_{w}$)	Charge Ratio (N/P)
SP-CHOL-MTS	14	28:1	7.5:1	33:1	11.3:1
GM-CHOL-MTS	9	18:1	4.8:1	21:1	5.5:1
SP-CHOL-MTS-R8	4	8:1	2.1:1	9:1	2.4:1
GM-CHOL-MTS-R8	3	6:1	1.6:1	7:1	2.0:1

The data obtained has been used to facilitate the design of lipoplexes intended for cytotoxicity and mitochondrial localisation studies described in chapter three.

4.2.1.2. Nuclease Protection Assay and Stability in Serum

Serum has been widely proposed as one of the key barriers to cationic liposome meditated gene transfer with many studies having demonstrated the numerous adverse effects of serum on lipoplexes (Zhang and Anchordoquy, 2004; Betker *et al*., 2013a). Serum is a complex suspension derived from blood plasma. It comprises various proteins such as albumin, lipases, electrolytes, nucleases, lipoproteins and other exogenous constituents but does not contain any blood cells and fibrinogens. Serum has been reported to wield its inhibitory effect by interaction with cationic lipoplexes which results in alteration of their biophysical properties leading to possible decreases in lipoplex association with cells and consequent transfection efficiency as well as influencing the intracellular processing of lipoplexes (Madeira *et al*., 2008; Kim *et al*., 2014). In recent times, there have been observations and indications that serum-induced inhibition is mainly due to the serum components such as

lipoproteins, glycoproteins, apolipopriteins, immunoglobulins and albumin that associate with nanoparticles upon their interaction with biological fluids or serum (Caracciolo *et al*., 2010; Betker *et al*., 2013b). The association of these serum proteins with the lipoplex surface forms a protein rich layer called a protein corona (Caracciolo *et al*., 2010; Betker *et al*., 2013b; Kim *et al*., 2014; Caracciolo, 2015). The protein corona can have detrimental effects on the cationic lipoplex which leads to aggregation, structural reorganisation and/or destabilisation of complexes. Aggregation results in size increases and modifications in zeta potential while structural reorganisation and destabilisation affects electrostatic interactions with cell membranes and could also induce the dissociation of DNA from the complexes exposing the DNA to nucleases present in the serum and thus probable degradation (Xu and Anchordoquy, 2008; Marchini *et al*., 2009; Caracciolo *et al*., 2010; Yang *et al*., 2013). The formation of the protein corona around the lipoplex due to its interaction with serum, and its subsequent processing by the cells requires further investigation, as this key interaction may serve as an important predictive archetype for the possible *in vivo* efficiency of the nanoparticle. Hence stability in serum, both *in vitro* and *in vivo* and the ability of the lipid vector to protect and shield its DNA cargo is a major concern. DNA degradation is known to be a chief limiting factor in the application of gene transfer and any synthetic vector used has to be able to effectively protect the DNA cargo (Obata *et al*., 2009). The integrity of DNA in serum containing media is vitally important in gene delivery systems. Nucleic acid degradation by serum nucleases such as DNase I and other endonucleases is of particular concern as inefficient protection of DNA by a gene delivery vehicle is an undesirable trait in vector systems (Obata *et al*., 2009).

The role of the formulated lipoplexes in protecting the DNA from attack by serum nucleases was assessed by *in vitro* nuclease protection assays using agarose gel electrophoresis (Figure 4.7). In theory, DNA associated with cationic liposomes is able to withstand the degradative effects of serum nucleases as the DNA is condensed and compacted into highly organised supramolecular structures (Figure 4.8) together with the liposomal vesicles, whereas DNA unprotected by a cationic lipid coating is rapidly degraded (Singh *et al*., 2006; Caracciolo *et al*., 2010). As mentioned above, serum can also cause disruption of lipoplex structure resulting in DNA release and subsequent degradation. Therefore, liposomes have a dual role of not only protecting DNA from serum, but additionally forming a resilient, serum-resistant interaction with DNA so as to tolerate any adverse effects of serum on its structure.

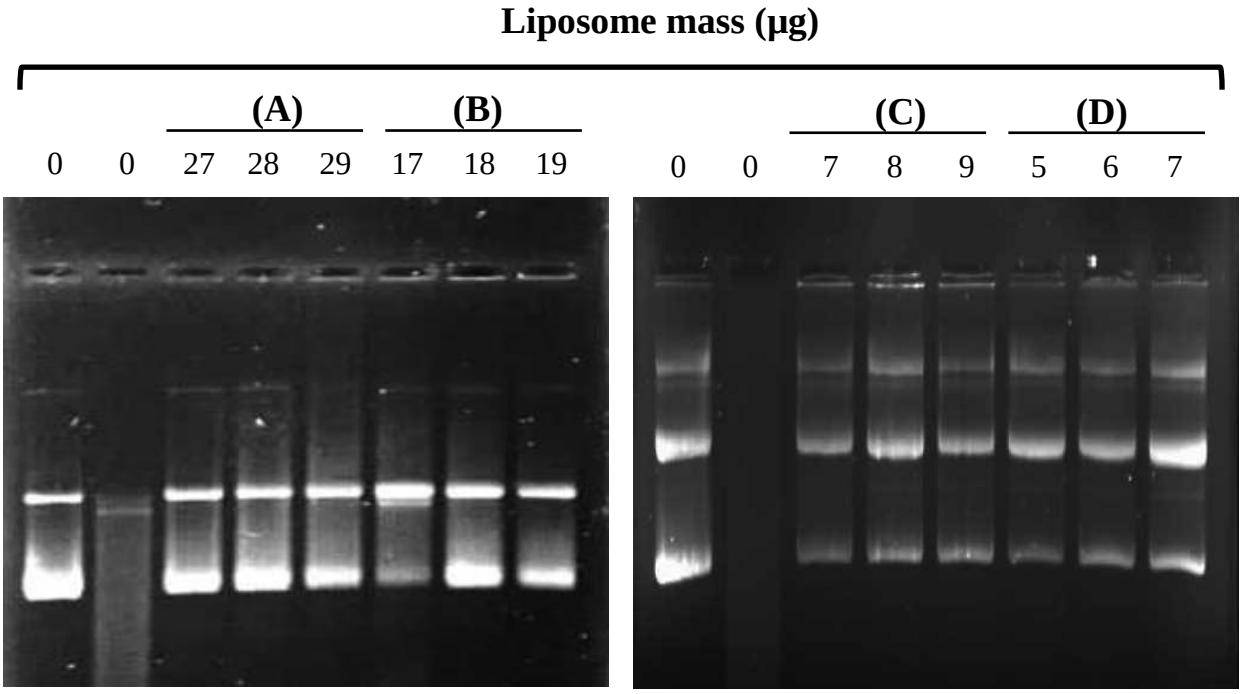

Figure 4.7: Nuclease protection assay of cationic mitochondriotropic liposome-DNA complexes of **(A)** SP-CHOL-MTS, **(B)** GM-CHOL-MTS, **(C)** SP-CHOL-MTS-R8 and **(D)** GM-CHOL-MTS-R8 in a total of 10 µl reaction mixture while pCMV-*luc* DNA was kept constant at 1 µg per well. Samples from left to right are as follows, lane 1: 1 µg of untreated naked pCMV-*luc* DNA (control 1); lane 2: 1 µg of FBS-treated naked pCMV-*luc* DNA (control 2); lanes 3 – 8: the respective liposome-DNA complexes prepared at different liposome mass (µg) as indicated.

Two controls were included in this investigation, namely, control 1: untreated naked marker pCMV-*luc* DNA displaying 3 species of DNA: an abundant high-mobility band, representing the compact supercoiled helical form (Figure 4.8); an intermediate band, showing the linear form and the least mobile band, indicating the nicked circular form; and control 2: naked unprotected pCMV-*luc* DNA treated with 10% FBS, to evaluate the degree of serum nuclease digestion on treated unprotected DNA compared to DNA in association with cationic mitochondriotropic liposomes. As observed from the results obtained, all mitochondriotropic liposome preparations were able to effectively protect their associated pDNA cargo from possible degradation by nucleases present in FBS across all liposome-DNA mass ratios ($^{w}/_{w}$) tested compared to the unprotected fully digested pDNA (control 2).

Cholesterol is known to increase the mechanical strength of membranes, affecting membrane elasticity and enhancing the packing density of phospholipids by 'ordering and condensing' effects. This leads to a reduced permeability of membranes to solutes, water, small

molecules and ions (Róg *et al*., 2009; Caracciolo *et al*., 2010; Magarkar *et al*., 2014; Briuglia *et al*., 2015). Due to these properties, cholesterol or cholesterol-derived lipids are often incorporated into liposomal preparations. It has also been reported that the preservation of liposomal stability in the presence of serum could also be attributed to the increased packing of phospholipids by cholesterol which inhibits their removal by high-density lipoproteins (Caracciolo *et al*., 2010). Furthermore, cholesterol-based liposomal preparations have been shown to resist serum-induced aggregation and dissociation possibly through the rigidity imparted by containing cholesterol in their structures; and additionally, cholesterol is effective in decreasing the quantity of serum proteins that adsorb to lipoplexes (Betker *et al*., 2013a; Betker *et al*., 2013b; Kim *et al*., 2014; Briuglia *et al*., 2015). Thus, cholesterol derivatives used in the formulation of mitochondriotropic liposomes in this study contributed to the conservation of liposomal integrity and stability in the presence of serum. As indicated by the gel patterns, it can be assumed that all cationic mitochondriotropic liposomes at the sub-optimal, optimal and supra-optimal ratios tested, were able to offer considerable protection of their pDNA cargo by forming stable liposome-DNA complexes.

SP-CHOL-MTS and GM-CHOL-MTS seemed to have afforded the best protection of pDNA across all ratios tested as the recovered DNA from these lipoplexes seemed to be almost completely intact when compared to banding patterns of the control marker DNA. SP-CHOL-MTS-R8 and GM-CHOL-MTS-R8 lipoplexes, however, seem to have undergone very minor partial DNA conformational change as there appeared to a slight increase in the relative amount of linear and decrease in amount of supercoiled helical DNA detected compared to the undigested control. Overall, these findings indicate that the cationic mitochondriotropic liposomes prepared in this study are suitable gene transfer vehicles as serum treatment of liposome-DNA complexes did not enhance nuclease accessibility, and liposomes afforded complete protection to their pDNA cargo from the nucleases.

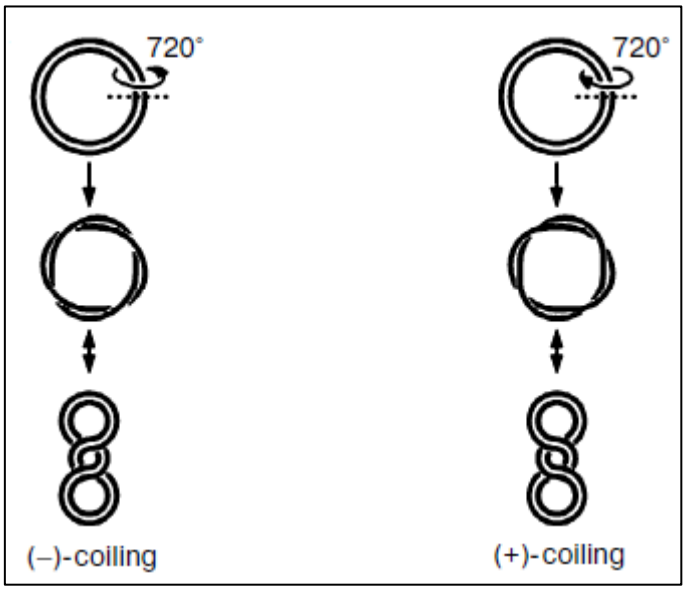

Figure 4.8: Schematic representation of DNA supercoiling followed by formation of anticlockwise (–) -coiling and clockwise (+) -coiling of circular DNA needed for condensation and compaction (Bugreev and Nevinsky, 2009).

4.2.1.3. Ethidium Bromide Intercalation Assay

The quantitative binding efficiency of cationic mitochondriotropic liposomes to pDNA as well as the corroboration of optimal ratios attained from retardation studies was investigated utilising a fluorescence quenching method based on ethidium bromide (EtBr), a monovalent cationic double-stranded DNA-intercalating dye (Geall and Blagbrough, 2000; Tros de Ilarduya *et al*., 2002). Ethidium bromide interacts with double-stranded DNA by occupying an effective binding site between two base pairs. An enhanced fluorescence is detected when EtBr binds to DNA due to the phenanthridium moiety of this agent intercalating DNA, an observation first reported by LePecq and Paoletti in 1967 (Geall and Blagbrough, 2000; Duarte *et al*., 2011). EtBr intercalation into DNA molecular modelling studies have shown that this binding results in a helical screw axis displacement of approximately +1 Å in the DNA structure which causes base pairs in the immediate vicinity to twist by 10°. This twisting consequently results in an angular unwinding of -26° and an 8° tilt in intercalated base pairs relative to each other (Figure 4.9) (Sobell *et al*., 1977; Geall and Blagbrough, 2000). Free EtBr in solution exhibits very low fluorescence in aqueous solvents owing to the excited-state proton transfer to water however when EtBr intercalates DNA, it enters the hydrophobic environment surrounding the DNA molecule which consequently drastically

slows down the rate of proton transfer to water molecules thus causing a resultant significant enhancement of fluorescence observed (Geall and Blagbrough, 2000).

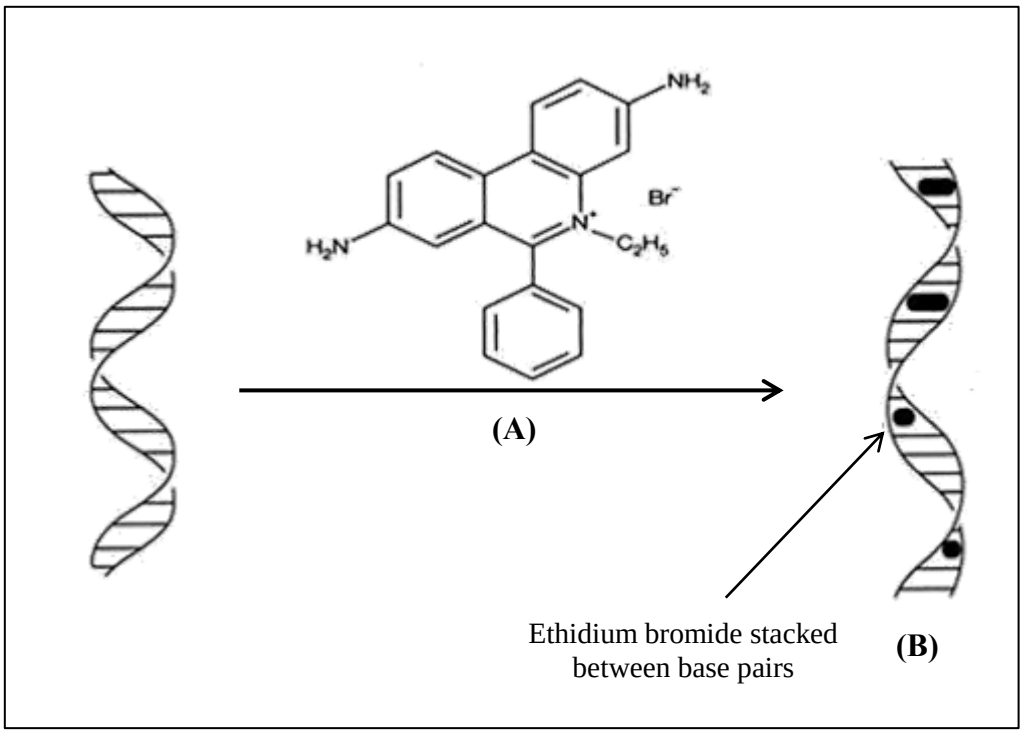

Figure 4.9: Diagram showing **(A)** Ethidium bromide and **(B)** the process of intercalation, illustrating the lengthening and untwisting of the DNA helix.
Adapted from www.technologyinscience.blogspot.com (accessed 19/07/2015).

As mentioned above, displacement of EtBr from DNA was employed in this study as confirmatory evidence of the binding ability of the cationic liposomes to pDNA. In accordance with the principle of the assay, EtBr fluorescence is intensely enhanced upon intercalating base pairs of DNA and is quenched when displaced by higher affinity compounds or by compaction and condensation of the DNA structure. The experimental parameter examined is the progressive decrease in fluorescence consequent to the increase in the concentration of cationic mitochondriotropic liposomes added i.e. as more liposome is added, resulting in DNA condensation; more EtBr molecules are displaced and replaced by the liposome resulting in a gradual decrease in fluorescence recorded (Xu *et al.*, 1999; Duarte *et al*., 2011; Banerjee *et al*., 2013). In agreement with this, all cationic mitochondriotropic liposome preparations were able to successfully displace intercalated ethidium bromide from pCMV-*luc* DNA. This was demonstrated by the continual decrease in fluorescence upon the

stepwise addition of cationic liposomes to the reaction mixture as illustrated in Figure 4.10 where percentage relative fluorescence was plotted as a function of micrograms of cationic mitochondriotropic liposomes. Varying amounts of cationic liposomes were added to the reaction mixture, forming a liposome-DNA complex, until the fluorescence values reached a plateau, commonly referred to as the point of inflection. This point represents the liposome-DNA ratio at which the liposome maximally displaced the ethidium bromide and completely bound as well as condensed the pDNA. The liposome-DNA mass ($^{w}/_{w}$) and N/P ratios representing these points are indicated in Table 4.1. Ethidium bromide fluorescence decreased with an increase in the amount of cationic liposomes added, indicating that this increase led to a greater degree of DNA condensation and protection. This action substantiates that DNA was compacted and condensed by the cationic liposomes to form lipoplexes, and this interaction is significantly stronger than that present between EtBr and DNA. As can be seen from the graphs, GM-CHOL containing liposomes produced a greater level of fluorescence decline compared to their SP-CHOL containing counterparts. This could possibly be because the shorter length of SP-CHOL which might produce a shielding effect, preventing interaction with DNA. Furthermore, R8 containing liposomal preparations [Figure 4.10 (B)] needed far less liposome to completely condense and displace EtBr until fluorescence decay plateaued, than the MTS only liposomes [Figure 4.10 (A)]. This is in keeping with the results obtained from the gel retardation assays conducted which showed that SP-CHOL-MTS-R8 and GM-CHOL-MTS-R8 required considerably lower amounts of liposome to bind 0.5 µg of pDNA. It could therefore be suggested, as mentioned in section 4.2.1.1, that the presence of R8 increases the overall theoretical cationic charge of these liposomes and probably enhanced their pDNA binding and compaction efficiencies.

Approximated percentage fluorescence decline for each mitochondriotropic liposome was: 37% (SP-CHOL-MTS), 39% (GM-CHOL-MTS), 33% (SP-CHOL-MTS-R8) and 42% (GM-CHOL-MTS-R8). GM-CHOL-MTS-R8 displaced the most amount of EtBr while SP-CHOL-MTS-R8 displaced the least demonstrating the weakest compaction of pDNA. High degrees of EtBr displacement and the inferred high compaction denote that DNA is tightly bound to the liposome which can be seen as either favourable or unfavourable for transfection or, in this study, mitochondrial localisation. Strong DNA-liposome binding and compaction would provide adequate protection and enable the liposome-DNA complex to securely transport its bound cargo to the target site but could prove detrimental if the bound

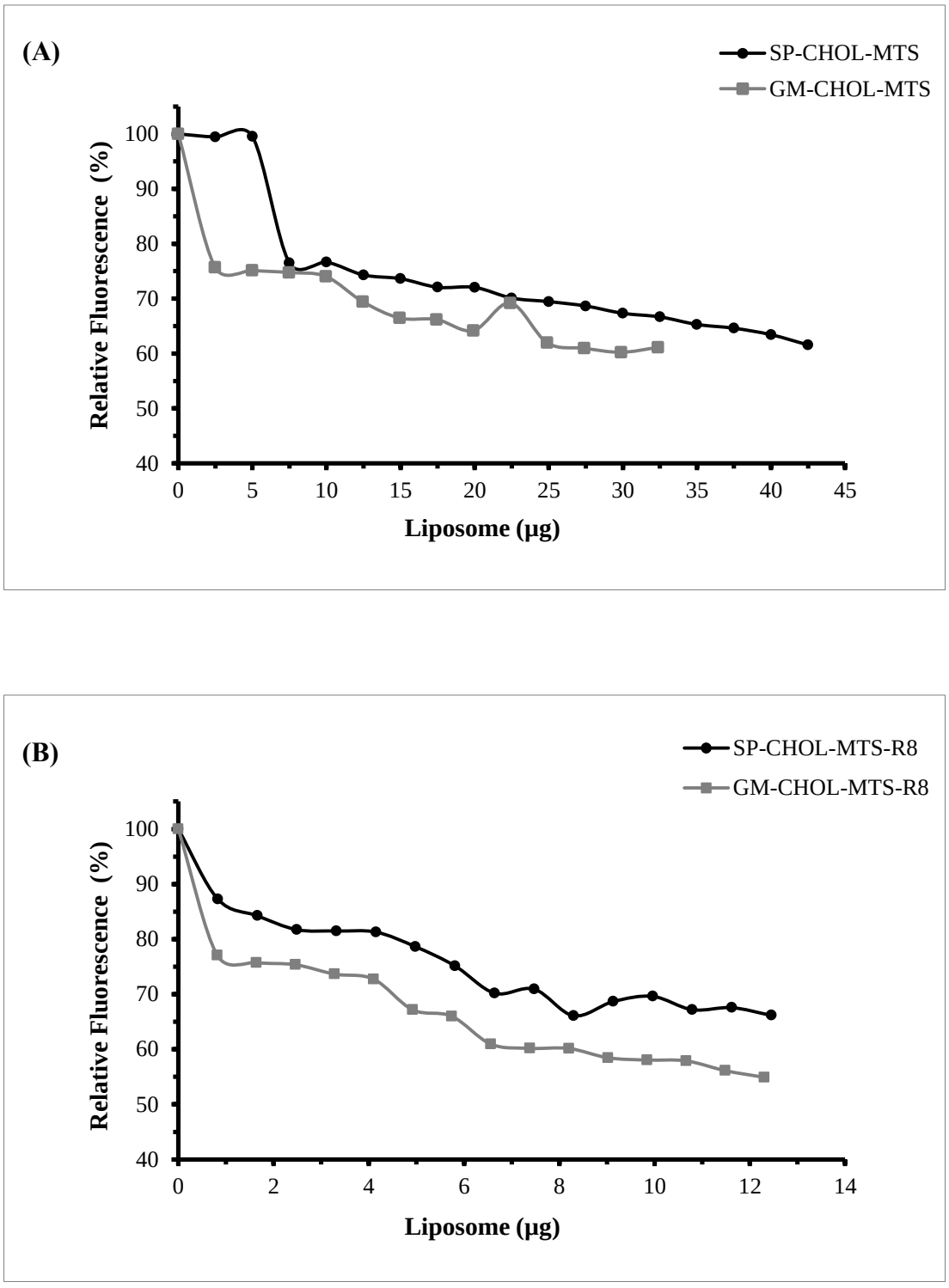

Figure 4.10: EtBr intercalation displacement assay where percentage relative fluorescence was plotted as a function of µgrams of liposome **(A)** MTS only liposomes and **(B)** MTS and R8 liposomes. Cationic mitochondriotropic liposome was systematically added to an EtBr/pCMV-*luc* (1.2 µg) solution until a plateau in fluorescence was attained.

DNA could not be timeously released to transfect the cell and subsequently be expressed. Conversely, weak DNA-liposome binding and compaction efficiency could result in disassociation of the lipoplex and likely degradation of the DNA cargo before it reaches its target cell. Thus, it seems that an intermediary degree of DNA-lipid compaction and binding strength, such as demonstrated by all the cationic mitochondriotropic liposomes tested, would be most beneficial to efficient transfection or mitochondrial localisation. A comparison of the liposome-DNA mass ($^{w}/_{w}$) and N/P ratios obtained here to that demonstrated by gel retardation assays (Table 4.1) display some minor discrepancies. A potential reason for these differences is that retardation studies are based exclusively on charge neutralisation i.e. the point at which the negative charges of the DNA are completely titrated by the positive charges of the cationic liposome whereas this assay is based on DNA condensation and compaction by the cationic liposome as well as charge neutralisation.

4.2.2. Imaging and Sizing

4.2.2.1. Characterisation of Particles by Transmission Electron Microscopy (TEM)

The nanostructure of cationic mitochondriotropic liposomes and lipoplexes were directly visualised by cryo-TEM which allows for the analysis of morphology and structure at the nanometer level. Additionally, cryo-TEM permits the examination of a sample in a frozen-hydrated state, i.e. very near its native state and with avoidance of fixation (Kuntsche *et al*., 2011; Helvig *et al*., 2015). As organic materials are known to give poor contrast in cryo-TEM, combining negative staining with cryo-TEM allows for an improvement in contrast (Kuntsche *et al*., 2011). In the most basic terms, TEM can be envisaged as an inverted light microscope where the 'light source' is an electron beam. This beam is concentrated by a system of electromagnetic lenses onto the sample surface after which the transmitted electrons are further magnified and focused by magnetic lenses to generate a projected image on a viewing screen (Bibi *et al*., 2011; Kuntsche *et al*., 2011). Sample preparation for cryo-TEM involves application of a droplet of diluted sample onto the grid, followed by use of a negative stain and finally the sample is plunge-frozen in a coolant resulting in the sample preparation being embedded in a layer of electron-transparent vitrified amorphous ice which is maintained in liquid nitrogen (Alfredsson, 2005; Friedrich *et al*., 2010). The negative stain attaches to the phosphate portion of phospholipids, poorly accessing the liposomal bilayer

which results in a darkly coloured outline of the liposome or lipoplex whilst the inner compartment is comparatively white (Bibi *et al*., 2011; Ruozi *et al*., 2011).

Figures 4.11 and 4.12 illustrate the cryo-TEM micrographs of cationic mitochondriotropic liposomes and lipoplexes, respectively. Overall, the morphologies observed for all liposome preparations were generally spherical; however some revealed a deformable nature with the presence of twisted and invaginated structures detected. This could be possibly attributed to the fluidity and flexibility of the liposomal membranes.

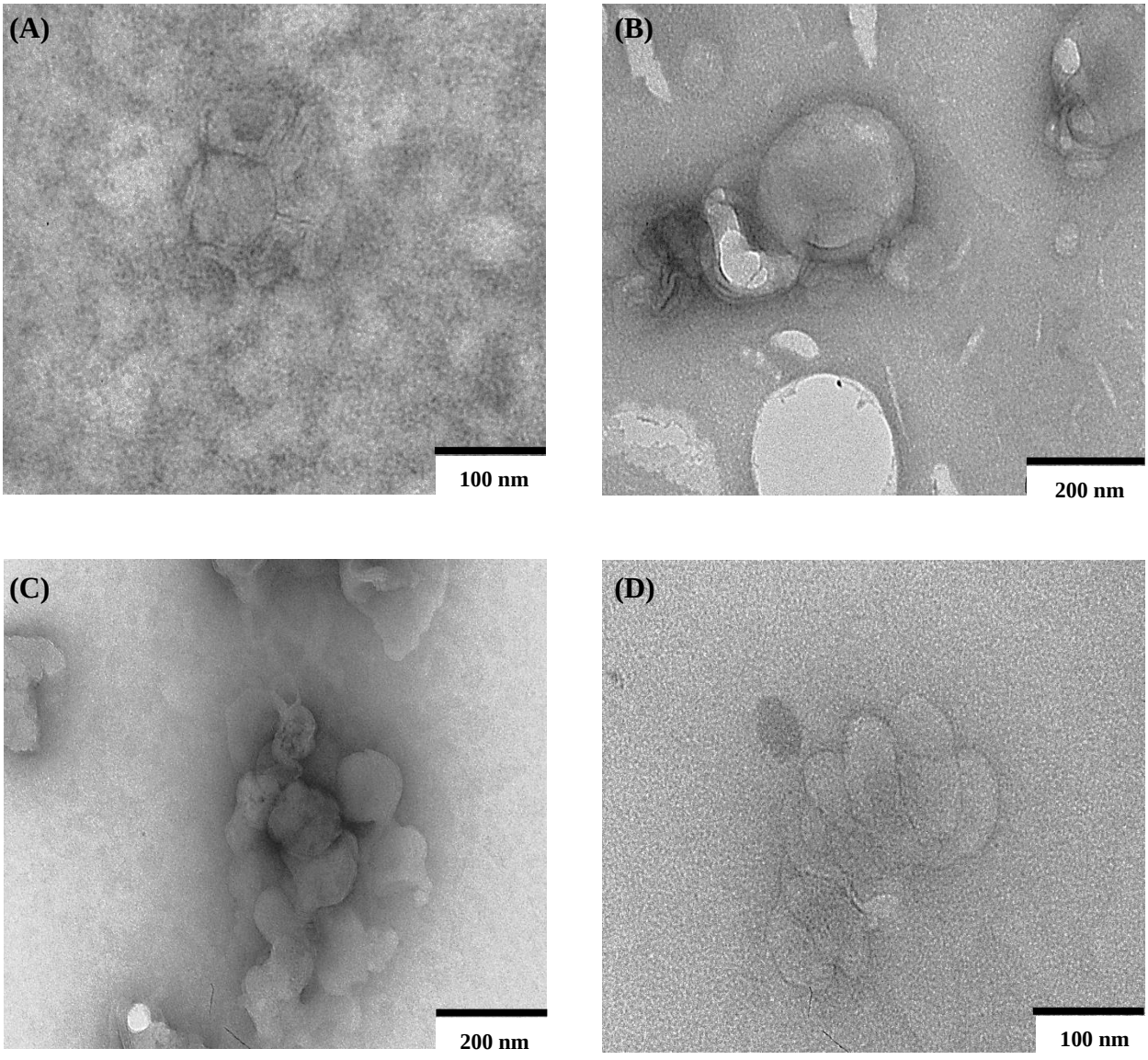

Figure 4.11: Transmission electron micrographs of cationic mitochondriotropic liposomes as follows: **(A)** SP-CHOL-MTS, **(B)** GM-CHOL-MTS, **(C)** SP-CHOL-MTS-R8 and **(D)** GM-CHOL-MTS-R8. Bar = 100 or 200 nm.

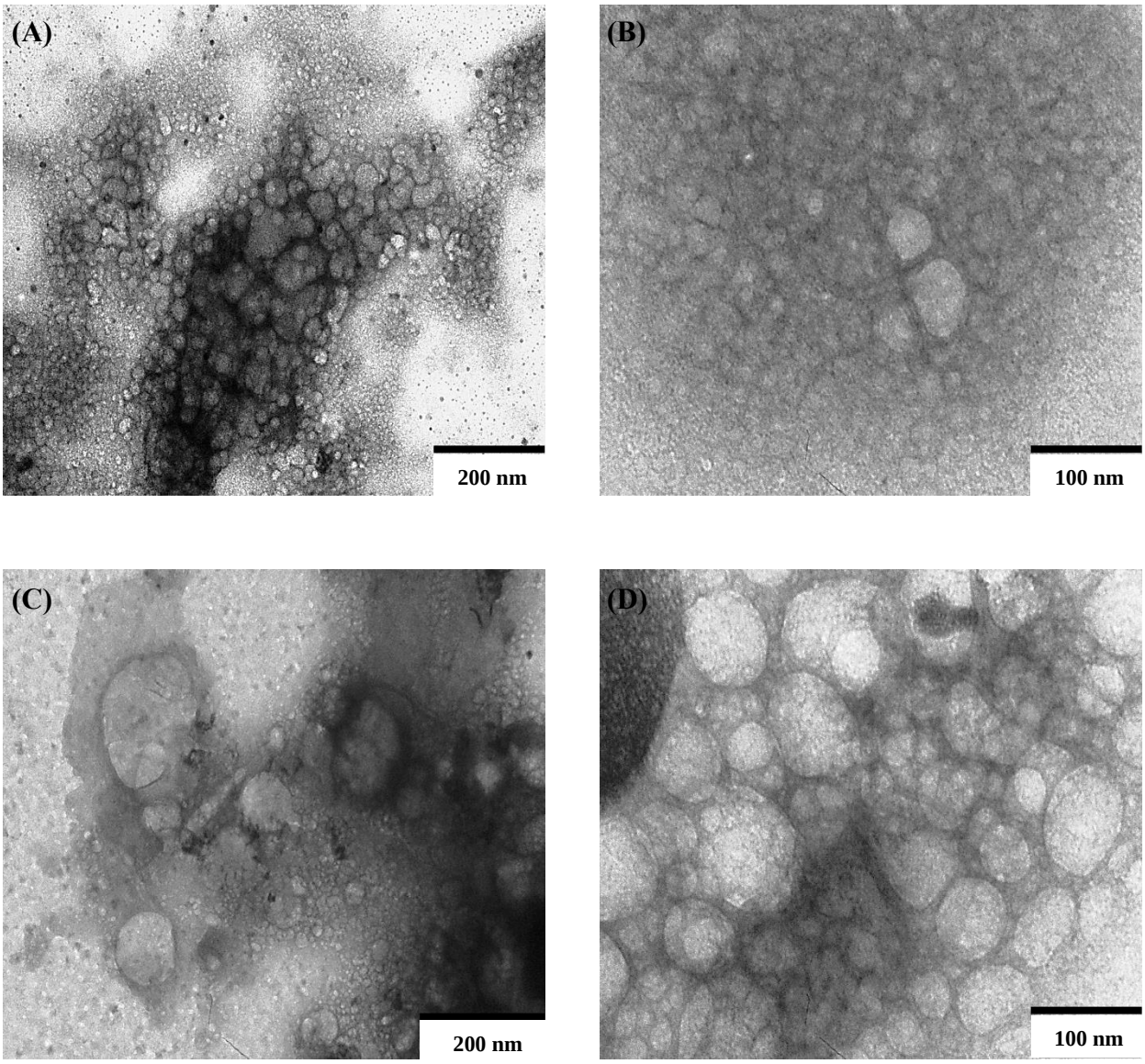

Figure 4.12: Transmission electron micrographs of cationic mitochondriotropic lipoplexes [prepared at optimal binding liposome-DNA or N/P ratios as determined by electrophoretic mobility shift assays]. **(A)** SP-CHOL-MTS 7.5:1, **(B)** GM-CHOL-MTS 4.8:1, **(C)** SP-CHOL-MTS-R8 2.1:1 and **(D)** GM-CHOL-MTS-R8 1.6:1. Bar = 100 or 200 nm.

The micrographs describe heterogeneous vesicles in which the negative stain makes it possible to highlight the existence of closed bilayer structures with free internal space. Some degree of vesicular structure distortion was identified; which could perhaps be artefacts due the interaction between the sample and the negative stain or dehydration as a result of exposure of samples to a vacuum in the viewing procedure. Additionally, processes like slow freezing and possible thawing may result in morphological changes accompanied by a reorganisation of the vesicle structure and thus inaccurately represented images (Kuntsche *et*

al., 2011; Ruozi *et al*., 2011). In general, all liposomes appear to be unilamellar in nature with the exception of SP-CHOL-MTS [Figure 4.11 (A)] which seems to show a multi-lamellar structure however, this could be either single-walled or unilamellar vesicles that layered atop one another or invaginated/folded unilamellar structures giving the illusion of multi-lamellarity (Almgren *et al*., 2000). Moreover, all cationic mitochondriotropic liposome preparations display a certain degree of clustering with some singular liposomes on the periphery of images. The images of the corresponding lipoplexes (Figure 4.12) revealed numerous largely unclear ill-defined multi-lamellar aggregates which appear to be intact and layered over each other. These aggregates are characteristic of lipoplexes and it has been suggested that oligonucleotides used in the formation of lipoplexes act as intermembrane bridges preventing the electrostatic repulsion of liposomal membranes hence forming aggregated lipoplexes (Alfredsson, 2005). The formation of lipoplexes was corroborated by the existence of large, intact aggregate assemblies. The presence of R8 did not seem to have any obvious morphological effects on either liposomes or lipoplexes. Although TEM does provide some information on the sizes of the liposomes and their complexes, we resorted to Nanoparticle Tracking Analysis (NTA) (4.2.2.2), which provides a more accurate picture on size distribution.

4.2.2.2. Particle Size and Zeta Potential Analysis

Particle size is a morphological parameter in nanoparticle development that is of great importance not only in its role in determining transfection efficiency but also in influencing circulatory half-lives and evasion of the reticuloendothelial system (RES) during *in vivo* applications. Lipoplex or nanoparticle size is thought to impact transfection effectiveness or, in this study, mitochondrial localisation by influencing the nature of the entry pathway of complexes into the cell by endocytosis i.e. either clathrin- or caveolin-mediated endocytosis or macropinocytosis (Ross and Hui, 1999; Ma *et al.,* 2007; Marchini *et al*., 2009; Akbarzadeh *et al*., 2013). Another feature of liposome-DNA complexes that is of significance is the zeta potential of the particle which is defined as a measure of the surface charge of given particles in a medium or suspension and which is further related to their stability by electrostatic forces (Figure 4.13). Zeta potential therefore acts as an indicator of the colloidal stability of the lipoplexes in suspension and can potentially affect the pharmacokinetic properties of the nanocomplexes during their interaction with cells (Xu, 2008; Griffiths *et al*., 2011; Honary and Zahir, 2013a).

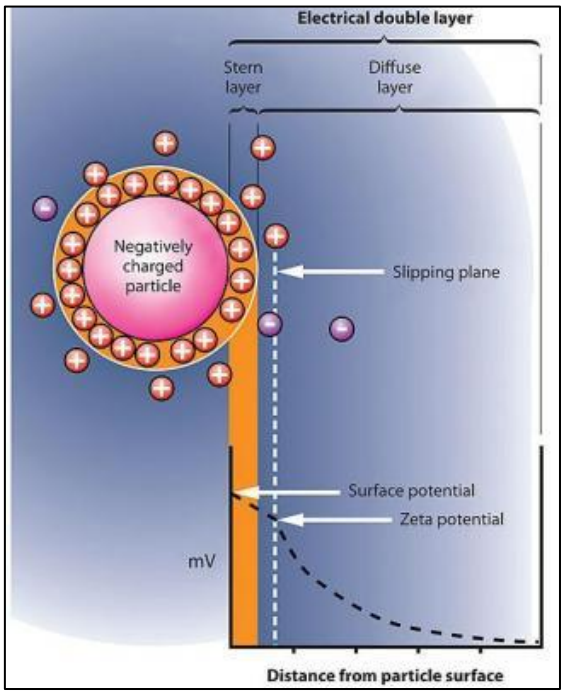

Figure 4.13: Schematic diagram of zeta potential for nanoparticles depicting the potential difference as a function of distance from the charged surface of a particle suspended in a dispersion medium.
http://www.pharmainfo.net/characterization-nanoparticles/zeta (accessed 08/04/2015)

The cationic mitochondriotropic liposomes and their corresponding optimal liposome-DNA complexes were evaluated for size and zeta potential by Nanoparticle Tracking Analysis (NTA). NTA is a relatively new technique that allows for the simultaneous multi-parameter analysis of nanoparticles in liquid suspensions for direct, real-time visualisation and examination of concentration, size and zeta potential. NTA utilises the well-understood principles of sizing by measuring both light scattering and Brownian motion of samples in liquid suspension to calculate the nanoparticle diffusion constant which is applied to estimate a spherical hydrodynamic diameter of the particle (Gross *et al*., 2016; NanoSight, 2015a). The measurement principles and methodology of NTA is extensive (Figure 4.14), but in short, the sample in suspension is pumped into a sample chamber where a laser beam (wavelength 430 nm) is passed through a prism edged glass flat within the sample chamber where the particles under investigation in the path of this beam scatter light in such a manner that they can easily be visualised and recorded at 90° via a 20x magnification microscope objective onto which is mounted a sCMOS camera. The camera then captures a video of the particles (Figure 4.15) moving under Brownian motion within the field of view of approximately 100 µm x 80 µm x 10 µm. This real-time video is then analysed on a frame-

by-frame basis and each particle centre is individually and simultaneously visualised and tracked by specific image tracking, evaluation and processing software (NTA 3.2 analytical software). The software tracks many particles individually and using the Stokes-Einstein equation (Figure 4.14) calculates their sphere equivalent hydrodynamic diameters. NTA tracks nanoparticles within a range of 10 – 1000 µm. As NTA permits each particle to be sized individually, irrespective of the others, the resulting data is not an intensity weighted mean but an absolute high resolution particle size analysis (NanoSight, 2015a, 2015b). The NTA instrument measures zeta potential in a way similar to sizing with certain additions. An electrophoresis system, facilitated by two platinum electrodes in the sample chamber, allows a variable electric current to be applied to the nanoparticle sample suspension causing motion of the particles under the influence of the electric field. The electrophoretic velocity of the particle movement is recorded, tracked and quantified in the same way as Brownian motion allowing for the resultant zeta potential to be calculated on a particle by particle basis (Griffiths *et al*., 2011; NanoSight). A representative NTA report is found in Appendix A.

Mean particle size distribution and zeta potential of the cationic mitochondriotropic liposomes and corresponding optimal liposome-DNA complexes are summarized in Table 4.2. As can be seen in these results, the hydrodynamic diameters calculated by NTA revealed nano-sized liposomes in the range of 121.0 – 246.55 nm. Their corresponding lipoplex sizes were in the 129.7 – 200.35 nm range while in the presence of 5% FBS, these same lipoplexes displayed a diminished size range of 55.35 – 132.75 nm.

TABLE 4.2: Mean particle size and zeta potential for liposomes and optimal liposome-DNA ratios.

Mitochondriotropic Liposome	**Mean Particle Size and Zeta Potentials (n=2)**					
	Liposome		**Lipoplex (3% HBS)[a]**		**Lipoplex (5% FBS)[b]**	
	Size (nm) ± SE	**ζ-Potential (mV) ± SE**	**Size (nm) ± SE**	**ζ-Potential (mV) ± SE**	**Size (nm) ± SE**	**ζ-Potential (mV) ± SE**
SP-CHOL-MTS	142.6 ±13.55	-29.05 ±2.05	175.8 ±15.02	-16.50 ±0.54	129.35 ±14.9	-18.70 ±1.0
GM-CHOL-MTS	121.0 ±11.6	-38.95 ±1.1	200.35 ±26.8	-17.90 ±0.85	132.75 ±33.5	-13.25 ±0.25
SP-CHOL-MTS-R8	246.55 ±11.3	-25.30 ±0.1	150.25 ±12.4	-17.35 ±0.55	55.35 ±2.80	-20.85 ±0.75
GM-CHOL-MTS-R8	226.05 ±67.2	-28.70 ±1.9	129.7 ±10.26	-19.05 ±0.65	55.50 ±2.25	-14.50 ±0.8

Abbreviations: SE; standard error
[a] Lipoplexes were diluted 1:100 with 3% filter-sterilised HBS.
[b] Lipoplexes were diluted 1:100 with 3% filter-sterilised HBS containing 5% FBS ($^{v}/_{v}$).

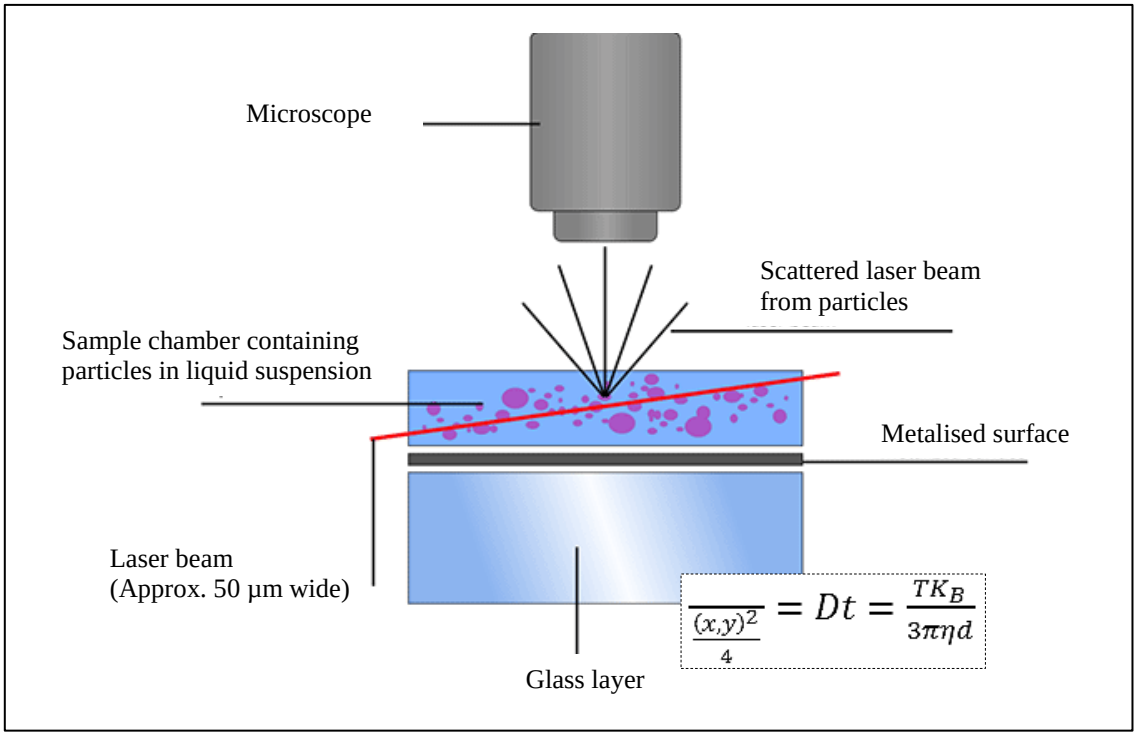

Figure 4.14: Schematic of the optical configuration used in NTA and two-dimensional Stokes-Einstein equation. The sample in the chamber is illuminated by a laser beam. The particle movement is recorded via light scattering by a sCMOS camera and the software tracks each particle and determines the diffusion coefficient of the Brownian motion. Combining Stokes–Einstein equation and two dimensional mean square displacement, the particle size is then calculated as the mean-squared displacement $(x, y)^2$, K_B as the Boltzmann's constant, T as the absolute temperature, t as the measurement time, η as the viscosity and d as the hydrodynamic diameter.
Adapted from (Gross *et al*., 2016; NanoSight, 2015a; Dragovic *et al*., 2011).

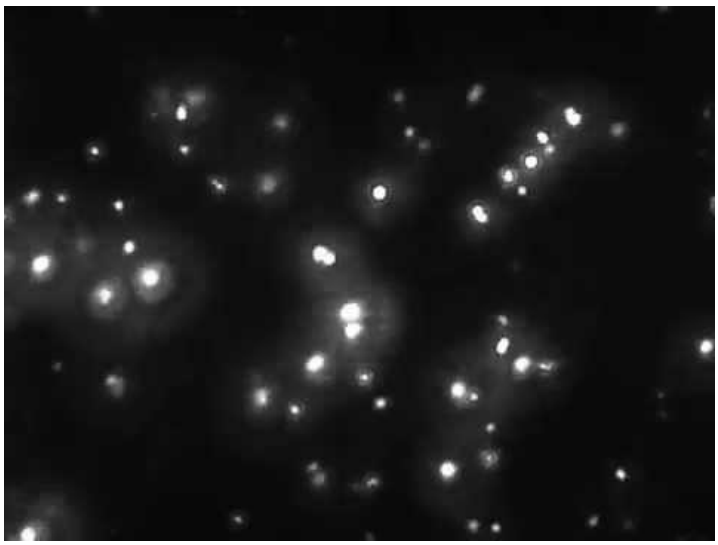

Figure 4.15: Screen shot from video showing light scatter from liposomal particles moving under Brownian motion.

The different diluents used also showed an impact on the sizes and zeta potential of the formulations (Table 4.2). The presence of 5% FBS in the diluent medium clearly had an effect on the liposome-DNA complex size resulting in more diminutive lipoplexes with only SP-CHOL-MTS-R8 and GM-CHOL-MTS-R8 liposome-DNA complexes displaying a significant *($P<0.05$)* decrease in size. These two R8 containing liposomal suspensions also showed larger sizes for the free liposomes, in contrast to their MTS only containing counterparts. Furthermore, the lipoplexes in 3% HBS that they generated were comparatively smaller in size than their liposomes, whereas the MTS only liposomal suspensions, SP-CHOL-MTS and GM-CHOL-MTS, produced relatively larger lipoplexes in 3% HBS compared to their respective free liposome sizes. This could be attributed to the presence of R8 which could have made the liposomes bulkier but when combined with DNA to form lipoplexes, the compaction and condensation that would have occurred, in part because of the cationic charge of R8, caused a shift to smaller nanoparticle sizes. This was reinforced by the results of the gel retardation assays (Table 4.1) where lower amounts of these liposomes were needed to completely bind a constant amount of DNA. These gel retardation assays also indicated that far greater amounts of MTS only containing liposomal suspensions were required to bind the same amount of DNA and this probably contributed to the larger sized lipoplexes observed for these liposomes.

Previous studies have inferred a direct correlation between lipoplex size and their effectiveness in transfection (Zuhorn *et al*., 2002; Ross and Hui, 1999). Although, some authors believe that there to be little or no association with the size of lipoplexes and transfection efficiency, there is general consensus that lipoplex size definitely plays a role in determining the entry pathway into cells, the so-called size-dependent entry mechanism of lipoplexes (Zuhorn *et al*., 2002; Ma *et al*., 2007; Marchini *et al*., 2009). Studies have revealed that lipoplexes larger than 300 nm were preferentially internalised by caveolae-mediated pathways while smaller ones mainly entered cells via clathrin-mediated endocytosis (Marchini *et al*., 2009; Ramezani *et al*., 2009). Furthermore, there also seems to be little consensus on which size array is optimal to garner effective entry into the cells or produce efficient transfection or a combination of both. Conflicting reports have been published claiming larger complexes are better for improved transfection while others suggest that smaller lipoplexes are superior (Ma *et al*., 2007; Marchini *et al*., 2009; Masotti *et al*., 2009; Wang *et al*., 2012). For mitochondrial localisation/delivery, studies have shown that liposomes and liposome-DNA complexes are relatively successful at a variable size range of

below 100 µm to about 300 µm (Khalil *et al*., 2006a; Yamada and Harashima, 2013; Kawamura *et al*., 2013a). The cationic mitochondriotropic lipoplexes used in this study are proposed to enter cells via a combination of clathrin-mediated endocytosis and macropinocytosis, a non-specific form of endocytosis that allows for a broad range of particles sizes, up to 5 µm, to be internalised (Hirota and Terada, 2012). Therefore, the concept of size of the liposome-DNA complex might not be most vital or limiting parameter in determining efficient mitochondrial localisation *in vitro* but could have significant importance *in vivo* by affecting circulation times of the nanocomplexes.

The zeta potential is the overall charge that a nanoparticle acquires in a particular medium. It is a measure of the electric potential at the slipping/shear plane between the attached layer of diluent molecules surrounding the nanoparticle and the bulk solution (Figure 4.13). It states the potential difference between the bound layer of fluid attached to the dispersed particle and the dispersion medium. Thus, zeta potential can be defined as the electrokinetic value correlating a realistic level of surface charge (Honary and Zahir, 2013a). A higher level of zeta potential is desired as nanoparticles with zeta potential values greater than +25 – 30 mV or less than -25 – -30 mV typically have superior degrees of stability owing to their high mobility in solution and greater electrostatic repulsion between nanoparticles thus minimising aggregation effects (Griffiths *et al*., 2011). From the results obtained (Table 4.2), it was firstly observed that all samples had zeta potentials that were negative and secondly, that free liposomes had higher zeta potential values than their corresponding lipoplex formulations in both 3% HBS and 5% FBS implying that the liposomes had greater colloidal stability than the lipoplexes. There is also a change in zeta potential detected in lipoplexes sampled in HBS only compared to those in 5% FBS and HBS. This change is significant *($P<0.05$)* for GM-CHOL-MTS, SP-CHOL-MTS-R8 and GM-CHOL-MTS-R8 liposome-DNA complexes but not SP-CHOL-MTS lipoplexes. These changes in zeta potential could likely be attributed to effects of serum on the nanocomplexes with the possible binding of serum proteins to the complexes, forming a protein corona around the formulations. The ionic strength of the diluent is one of the important factors affecting the zeta potential, with increasing ionic strength resulting in increased zeta potential. As to the negative charge observed by the lipoplexes, previous literature has suggested that this might not be a huge deterrent to cellular binding and subsequent internalisation of the liposome-DNA complexes as studies have shown that nanoparticles with negative zeta potential have been successful in cellular uptake through the formation of nanoparticle clusters and the process of non-specific nanoparticle

adsorption on the cell membrane (Honary and Zahir, 2013a). Additionally, Honary and Zahir (2013b) indicated that both cationic and anionic charges are known to enhance the delivery of liposomes to cells and that negatively charged particles showed lower cytotoxicity and longer circulation half-times in rats than positively charged ones. Furthermore, nanoparticles with a high positive charge can combine with plasma proteins in the blood system *in vivo* and hence increase cellular toxicity. Thus, these liposomes and lipoplexes with negative zeta potentials were low in cytotoxicity as evidenced from the MTT and AlamarBlue® assays (4.3.2.1-4.3.2.2). Lastly, Xu (2008) stated that as zeta potential is a parameter that involves not only nanoparticle but also their environment, the zeta potential values measured may differ greatly from their true values in the experimental or test environment and therefore may be trivial to practical usefulness.

4.3. *IN VITRO* CELL CULTURE STUDIES

4.3.1. Cell Lines

Human embryonic kidney cells (HEK293), human hepatocellular carcinoma cells (HepG2), human epithelial colorectal adenocarcinoma (Caco-2) and human cervical adenocarcinoma cells that stably express the firefly luciferase gene (HeLa-Tat *luc)* were used in this study (Figure 4.16). HEK293 cell are semi-adherent cells that grow as a monolayer in culture. These cells were derived by the exposure of mechanically sheared fragments of DNA of adenovirus type 5 (AD5) to the human primary embryonic kidney cell culture of an aborted embryo (Thomas and Smart, 2005; Stepanenko and Dmitrenko, 2015). The HepG2 cell line is one of several cell lines isolated from the liver biopsies of hepatoblastoma and hepatocellular carcinomas (Aden *et al.,* 1979). They are epithelial in morphology and are known to exhibit the same biosynthetic capabilities as well as several genotypic and phenotypic characteristics of normal liver parenchymal cells and thus produce a large number of serum proteins such as albumin, transferrin, α-fetoprotein, fibrinogen and β-lipoprotein to name but a few (Knowles *et al.,* 1980; Santos *et al.,* 2016). The Caco-2 cell line is a continuous line of heterogeneous epithelial cells cultivated through research conducted by Dr. Jorgen Fogh (Fogh and Trempe, 1977). It is a well-known and widely accepted *in vitro* model of the human intestinal epithelium that in culture, spontaneously differentiate resulting in a monolayer of cells that display numerous morphological and functional characteristics of

mature enterocytes (Liu and Chen, 2004; Sambuy *et al*., 2005). HeLa cells were the first immortal cell line to be cultured. They were discovered by Dr George Gey in 1951 and were taken from a biopsy sample of cervical carcinoma from a patient named Henrietta Lacks (Lucey *et al*., 2009). HeLa cells are adherent, large and triangular in shape and they tend to proliferate unusually rapidly in a single layer. The HeLa-Tat *luc* cells used in this study were stably transfected with the TAT protein together with reporter plasmid LTR-*luc* under the control of HIV-1 LTR promoter. It therefore stably expresses the firefly luciferase gene but has all the characteristics of parental cells, HeLa wild.

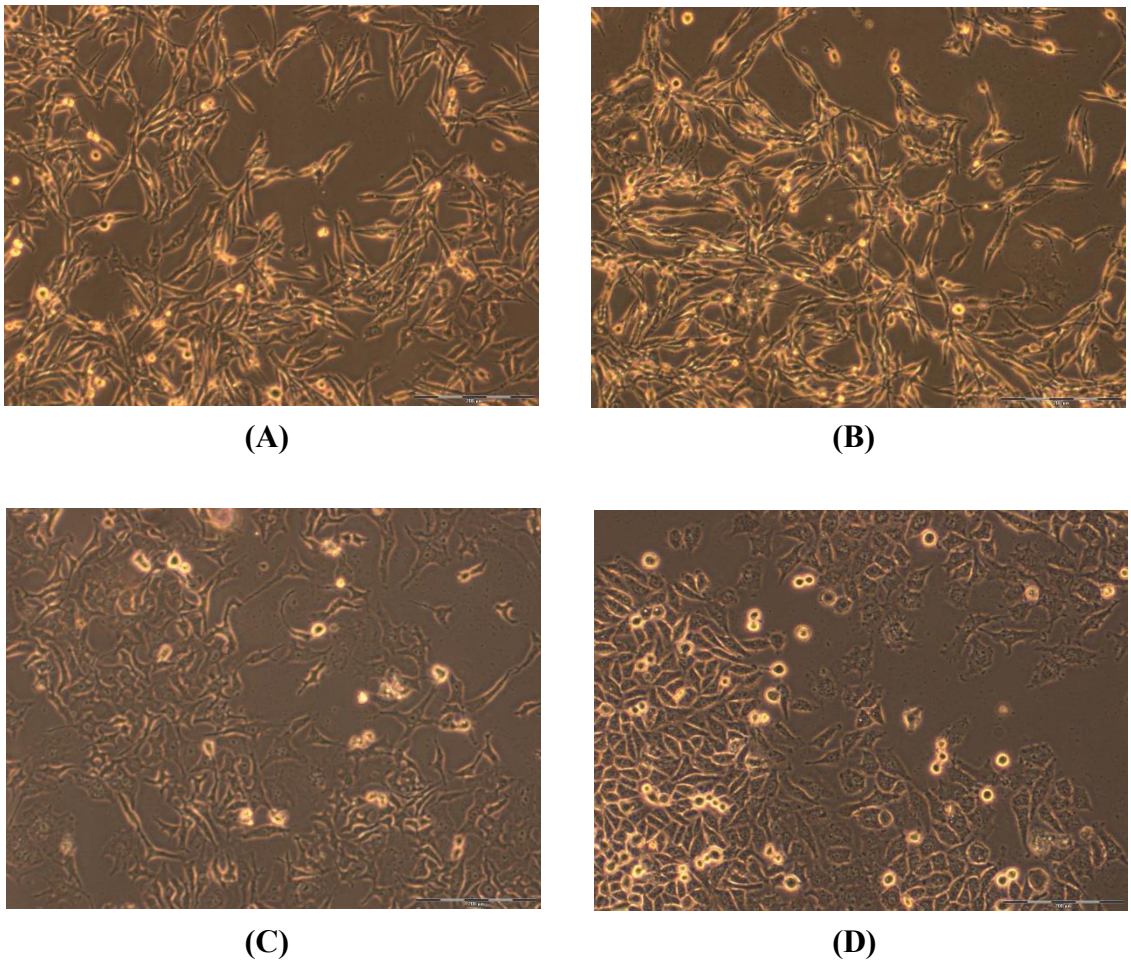

(A) **(B)**

(C) **(D)**

Figure 4.16: Cell lines used in this study: **(A)** HEK293, **(B)** HepG2, **(C)** Caco-2 and **(D)** HeLa-Tat *luc*. Here cells were viewed as a monolayer at semi-confluence under 100 x magnification with an inverted microscope (Olympus CKX41, Tokyo, Japan).

When mammalian cells are cultured *in vitro*, the aim is to reproduce the cells' original physiological environment as closely as possible. In order to accomplish this, the appropriate

nutrient environment, temperature, gas and humidity levels need to be maintained. To this end, the cell culture medium provides the nutrients needed such as vitamins, glucose, amino acids and salts as well as supplemented growth factors from FBS and it also helps in the regulation of the pH of the culture. Most adherent cell lines grow as a single layer (monolayer) attached to the culture vessel and once the accessible surface is covered by cells, cell growth is reduced which leads to growth suppression and possible cell death. To avoid this and keep cells healthy and optimally growing, it is necessary to passage or subdivide them regularly as well as replenish with fresh cell medium when required.

All four cell lines were successfully reconstituted and cultured in complete medium (EMEM + 10% FBS + antibiotics) over the period of study. Initial cell growth was slow with cells only reaching confluence after 4 to 5 days. This was expected as reconstituted cells have an initial growth rate that is slower than normal. Eventually cell numbers increased probably due to the amplified levels of growth factors secreted by the propagating cells. The cell lines were trypsinised and subdivided 1:3 or 1:2 splits every 3 to 4 days.

4.3.2. Cytotoxicity Studies

Cell lines are well established as valuable alternative assay systems for toxicological analyses (Santos *et al.*, 2016). In this investigation, two cell viability assays viz. the MTT reduction and AlamarBlue® assays were utilised to determine the levels of *in vitro* cytotoxicity that the cationic mitochondriotropic liposomal delivery systems had induced in the HEK293, HepG2, Caco-2 and HeLa-Tat *luc* cell lines. Cells were exposed to the liposome-DNA complexes correlating to the sub-optimal, optimal and supra-optimal DNA binding ratios and allowed to incubate for 48 hours.

4.3.2.1. MTT Growth Inhibition Assay

This is a colorimetric assay that measures the reduction of yellow MTT in aqueous solution by reducing agents and dehydrogenases in viable metabolically active cells to yield purple formazan crystals that are water insoluble (Figure 4.17) (Stockert *et al.*, 2012). When cells are no longer viable, they lose their ability to reduce MTT into formazan and thus the colour detection gives an indication of the number of viable cells (Riss *et al.*, 2013). The formazan

is solubilised and its concentration as reflected by optical density values serves as indicator of viable cells. Early literature speculated that MTT is reduced in the mitochondria of cells by mitochondrial succinic dehydrogenases and that this assay is a fitting indicator of mitochondrial function and activity however, recent evidence reveals that MTT is mainly metabolised in the cytoplasm by NADH, nicotinamide co-enzymes and other dehydrogenases associated with the plasma membrane, the endoplasmic reticulum and lysosome vesicles (Stockert *et al*., 2012; Angius and Floris, 2015). Taking this into consideration, the MTT assay was only used to assess cell viability and not as an inference to mitochondrial activity or integrity.

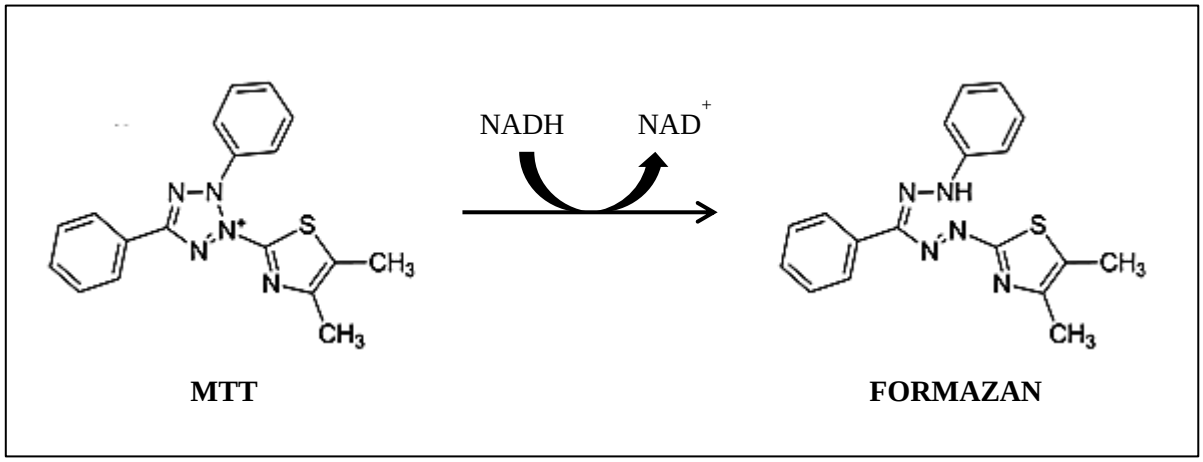

Figure 4.17: Chemical structure of MTT and its reduced coloured insoluble formazan product. Adapted from Stockert *et al*. (2012).

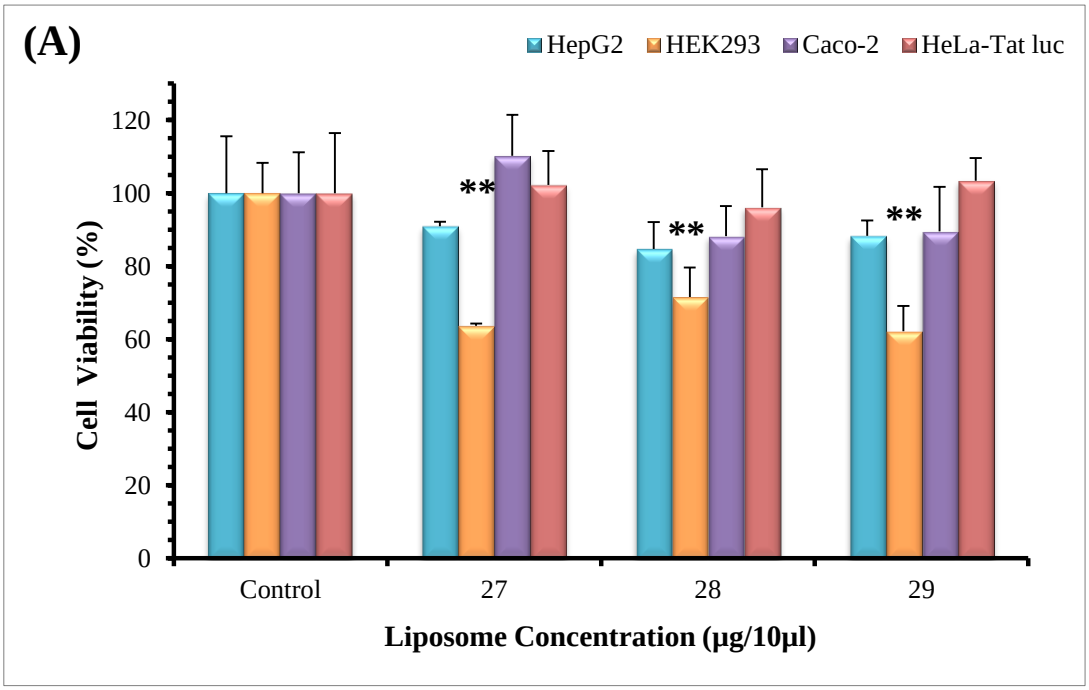

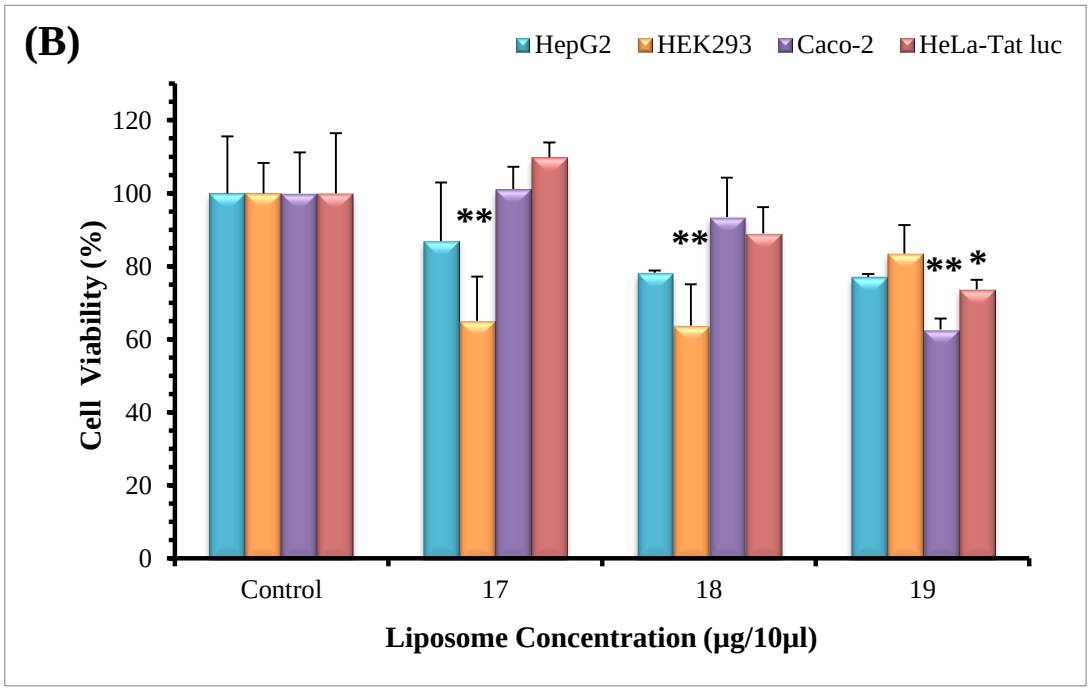
(B)
HepG2
HEK293
Caco-2
HeLa-Tat luc
Cell Viability (%)
120
100
80
60
40
20
0
**
**
** *
Control
17
18
19
Liposome Concentration (µg/10µl)

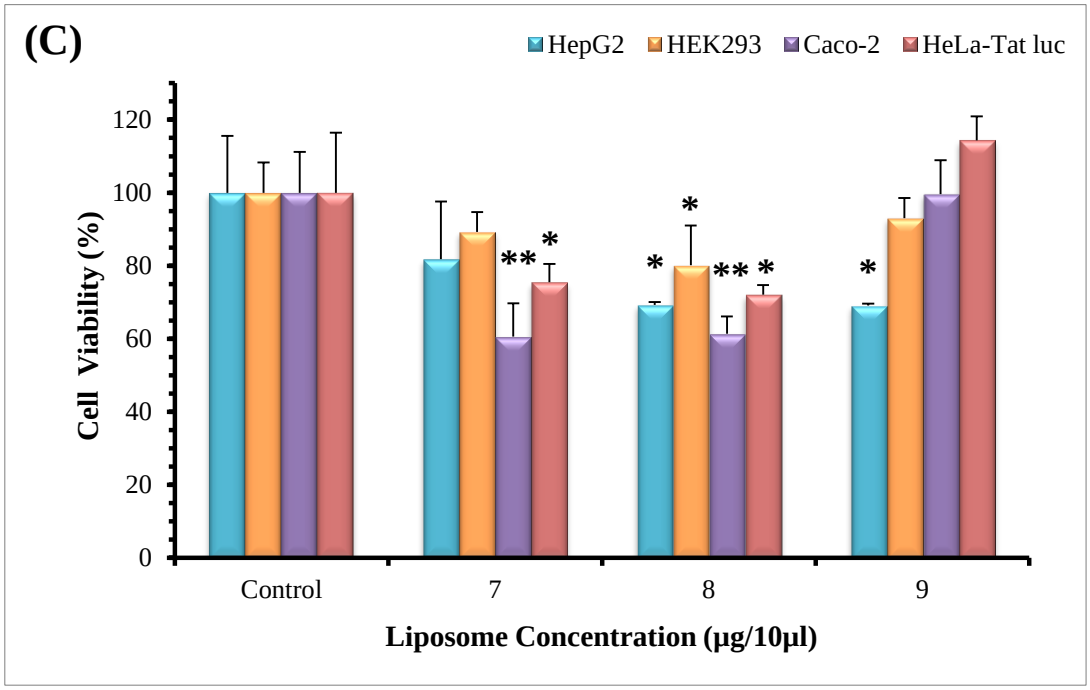
(C)
HepG2
HEK293
Caco-2
HeLa-Tat luc
Cell Viability (%)
120
100
80
60
40
20
0
** *
* * ** *
*
Control
7
8
9
Liposome Concentration (µg/10µl)

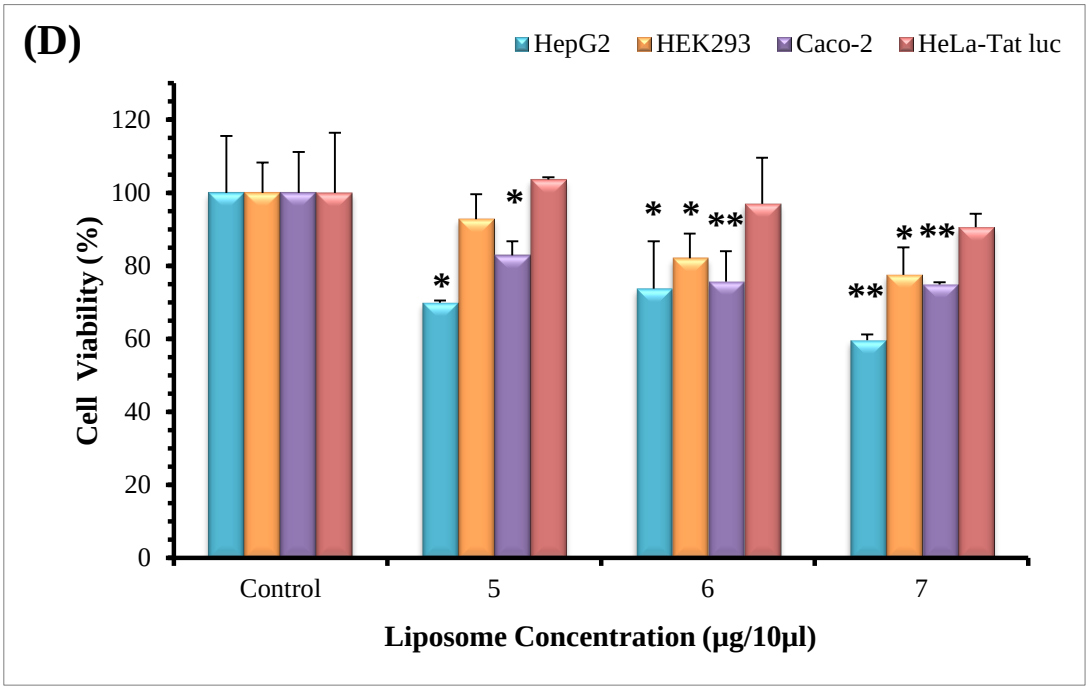

Figure 4.18: *In vitro* MTT cytotoxicity analysis of cationic mitochondriotropic liposome-pCMV-*luc* DNA complexes toward HepG2, HEK293, Caco-2 and HeLa-Tat *luc* cell lines. Lipoplexes (containing 1 µg of pCMV-*luc* DNA) were prepared at various liposome-DNA ratios ($^{w}/_{w}$) as indicated above. **(A)** SP-CHOL-MTS, **(B)** GM-CHOL-MTS, **(C)** SP-CHOL-MTS-R8 and **(D)** GM-CHOL-MTS-R8. A control sample containing only cells was assumed to have 100% survival. Results are presented as a percentage of the control sample and represent the mean ± SD, $n = 3$. Statistical analysis was performed using one-way ANOVA followed by Dunnett multiple comparison *post hoc* test. *$P<0.05$ and **$P<0.01$ as compared to the control.

Figure 4.18 (A-D) shows the plot of percentage cell viability as a function of liposome-DNA ratios ($^{w}/_{w}$). As shown from the results obtained all cationic mitochondriotropic lipoplexes were relatively well tolerated, some more than others, over the lipid concentration range tested. The general trend observed for most of the cell lines tested seems to reveal a decrease in cell viability with an increase in liposome-DNA ratios with the maximum reduction in viability observed at the highest (supra-optimal) lipoplex ratio for most of the liposome formulations in all four cell lines. At higher liposome-DNA ratios and therefore higher N/P ratios, there is a slight decrease in viability observed. A similar trend was observed by Masotti *et al*. (2009) in a study that investigated different cationic liposomes and commercially available liposomes. This is expected as greater charge ratios are expected to be more harmful to cells with the excess free liposomes competing with the nanocomplexes for binding and subsequent uptake by target cells (Xu *et al*., 1999). Of the four cell lines evaluated, HEK293 cells seem to be most susceptible to toxic effects ($P<0.01$) of all cationic mitochondriotropic lipoplexes, with significant decreases in viability exhibited. The HeLa-

Tat *luc* cell line was the most resilient demonstrating very little cytotoxicity for the different mitochondriotropic lipoplexes as well as across all the complex ratios. The HepG2 and Caco-2 cell lines were intermediate in their response to the lipoplexes. Overall, the results show that the cationic mitochondriotropic lipoplexes were well tolerated by all the cell lines over a range of liposome-DNA ratios ($^{w}/_{w}$) with cell survival staying over 60% across the board. Cell viabilities of the cell line, HepG2, HEK293, Caco-2 and HeLa-Tat *luc*, respectively were as follows: SP-CHOL-MTS (90-85; 72-62; 110-88 and 103-96) %, GM-CHOL-MTS (87-77; 83-64; 101-63 and 110-74) %, SP-CHOL-MTS-R8 (82-69; 93-80; 100-61 and 114-73) % and GM-CHOL-MTS-R8 (74-60; 93-77; 83-75 and 104-91) %. Of the lipoplex preparations, GM-CHOL-MTS-R8 prompted the greatest level of toxicity observed, in HepG2 cells, with 40% reduction in cell viability however it was very well tolerated in the other cell lines. Therefore, from the results, there seems to be no clear indication of which liposome preparation caused the most cytotoxicity as they all affected the different cell lines dissimilarly with a liposomal formulation having a pronounced cytotoxic effect on one cell line but also causing an increase in cell numbers in another cell line. Cationic lipids are known to be cytotoxic and level of toxicity is dependent on the structure of the cationic lipid. Cholesterol-based cationic lipids are known to exhibit lower toxicities compared to the lipids with aliphatic chains and additionally cationic lipids with a quaternary amine headgroup is more toxic compared to a tertiary one (Lv *et al*., 2006; Yang *et al*., 2013; Kim *et al*., 2014). DOPE-containing liposomes were also shown to display low toxicity in HepG2 cells (Lv *et al*., 2006). It can therefore be suggested that the presence of the cationic cholesterol-derived cytofectin, CHOL-T and DOPE in the mitochondriotropic liposomal formulations tested probably influenced their biocompatibility and stability and led to the relatively low toxicities detected.

4.3.2.2. AlamarBlue® Assay

The perfect test for *in vitro* cytotoxicity should be one that is a rapid, simple, sensitive, efficient, consistent, cost effective and safe measurement of cell viability (O'Brien *et al*., 2000). Hence, the MTT assay falls short of some the above mentioned characteristics, prompting the additional use of the AlamarBlue® assay to test the cationic mitochondriotropic lipoplexes for any harmful effects toward the cell lines utilised. The MTT assay is a technique that is an indirect indicator of cell viability that monitors cell membrane integrity

following drug or test compound exposure which can impede or damage the cell's functioning and is thus considered a terminal assay which does not allow for the further investigations or follow-up using the same cell cultures (Al-Nasiry *et al*., 2007; Rampersad, 2012). The AlamarBlue® assay, on the other hand, seems to fit all the requirements of the ideal *in vitro* cytotoxicity test; it is safe, sensitive, non-toxic for cells, one-step and cost-effective. AlamarBlue® circumvents many of the issues that the MTT assay has and offers advantages over it as well, that include higher sensitivity, better stability and a non-toxic nature, solubility in medium and also allows for continuous monitoring of cultures (Al-Nasiry *et al*., 2007). The active ingredient in AlamarBlue® is resazurin, a water soluble, cell permeable redox indicator that is used to monitor the reducing environment of living cells and hence measure the proliferation of viable cells (Rampersad, 2012; Bonnier *et al*., 2015). Resazurin (oxidised form) is a blue, non-fluorescent dye that is reduced to the highly fluorescent, pink resorufin (Figure 4.19) which can be quantitatively measured either as colorimetric or fluorometrically, with the latter being the more sensitive. Thus, similar to the MTT assay principal, by assessing the changes in the fluorescence of the dye, the number of metabolically active cells can be identified and measured with the quantity of resorufin product being proportional to the number of viable cells (Riss *et al*., 2013; Bonnier *et al*., 2015). AlamarBlue® is reduced by mitochondrial reductases and cytochromes as well as other enzymes located in the cytosol and mitochondria such as diaphorases, NAD(P)H:quinone oxidoreductases and flavin reductase, to name a few. Therefore AlamarBlue® reduction may indicate damage of cellular metabolism and is not necessarily indicative of a break of the electron transport chain and mitochondrial dysfunction (Rampersad, 2012).

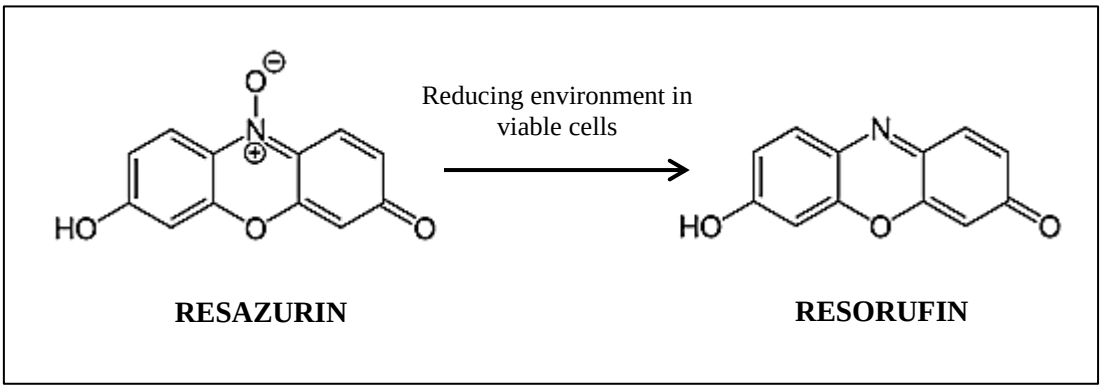

Figure 4.19: Chemical structure of non-fluorescent blue dye, resazurin and its reduction to strongly fluorescent pink resorufin by viable cells. Adapted from Stoddart (2011).

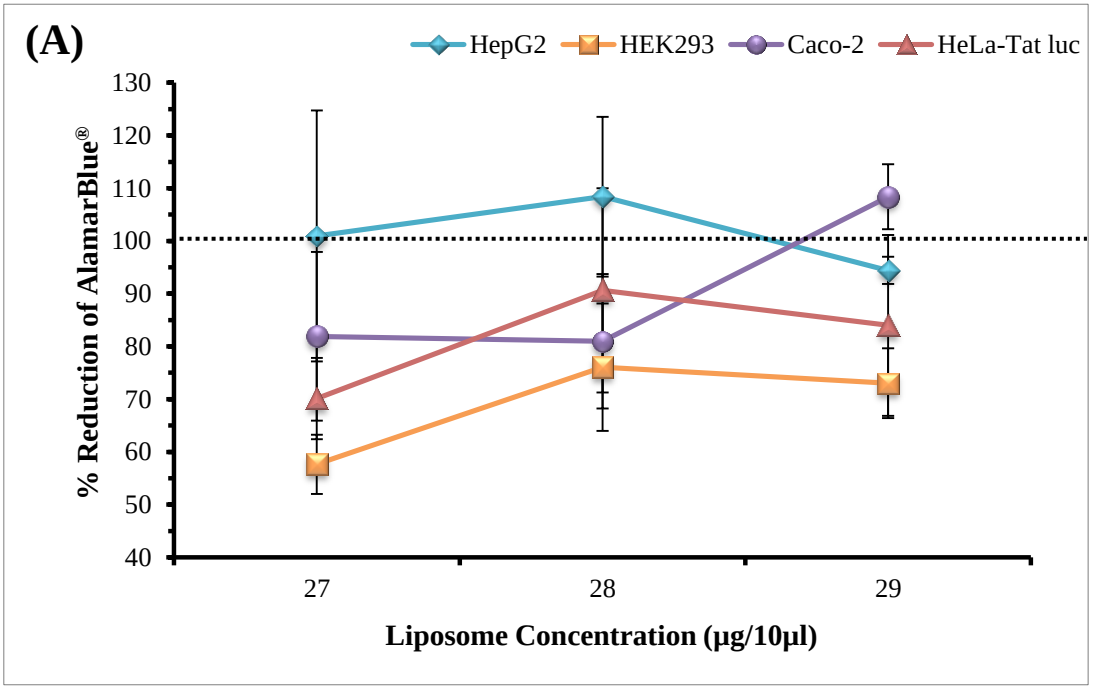
(A)
HepG2
HEK293
Caco-2
HeLa-Tat luc
% Reduction of AlamarBlue®
130
120
110
100
90
80
70
60
50
40
27
28
29
Liposome Concentration (µg/10µl)

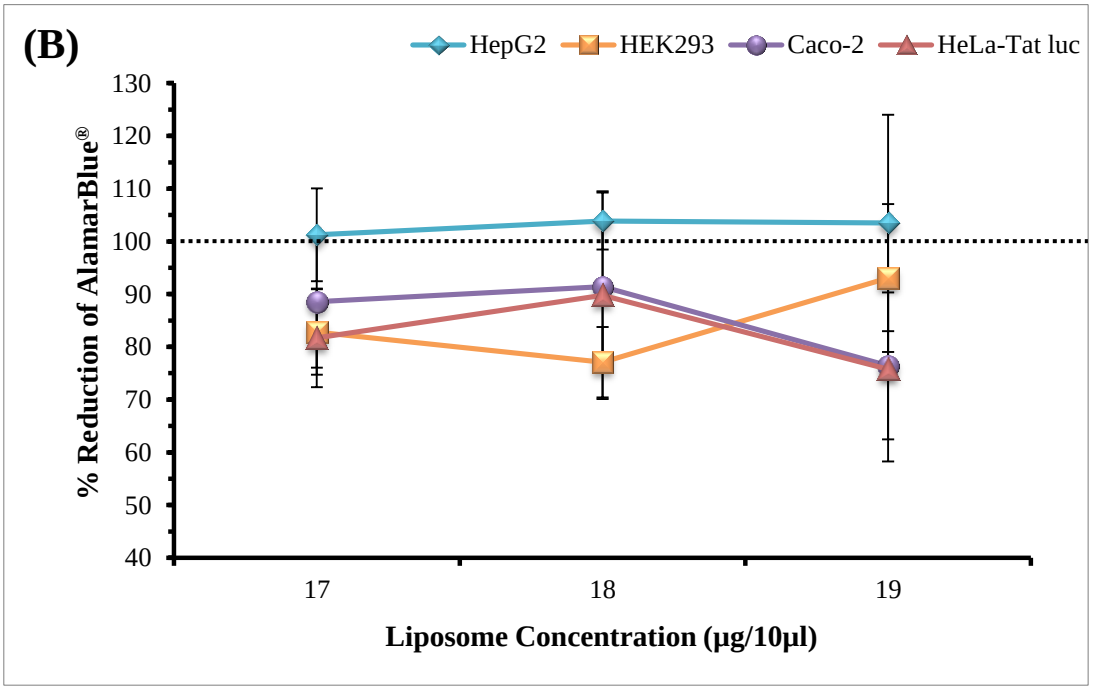
(B)
HepG2
HEK293
Caco-2
HeLa-Tat luc
% Reduction of AlamarBlue®
130
120
110
100
90
80
70
60
50
40
17
18
19
Liposome Concentration (µg/10µl)

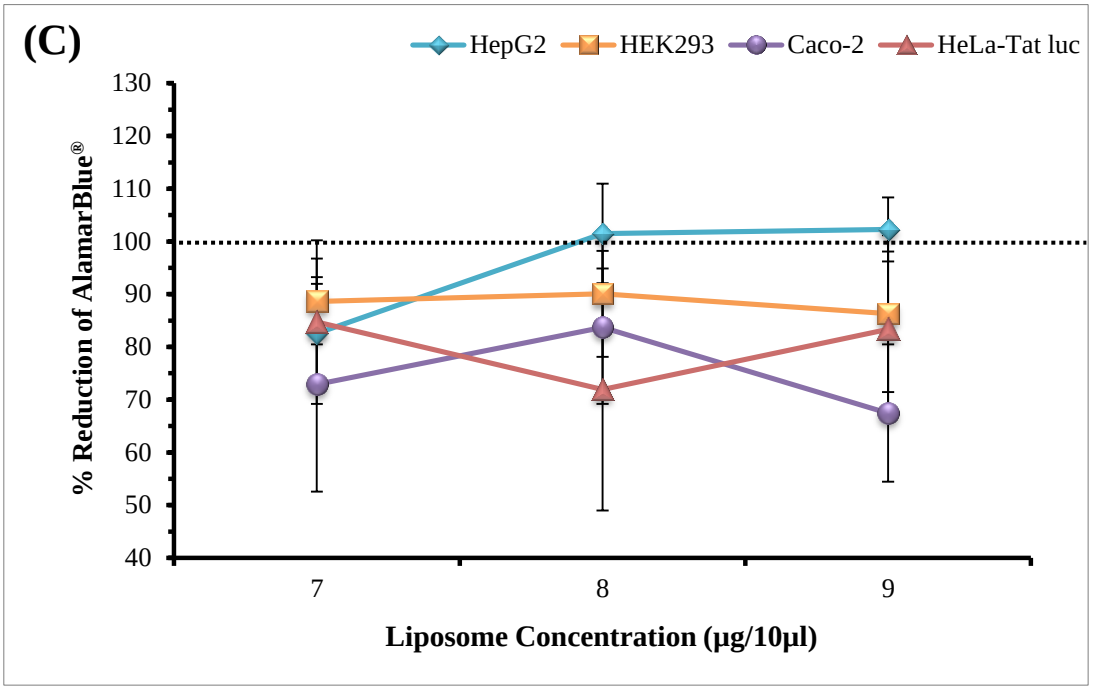

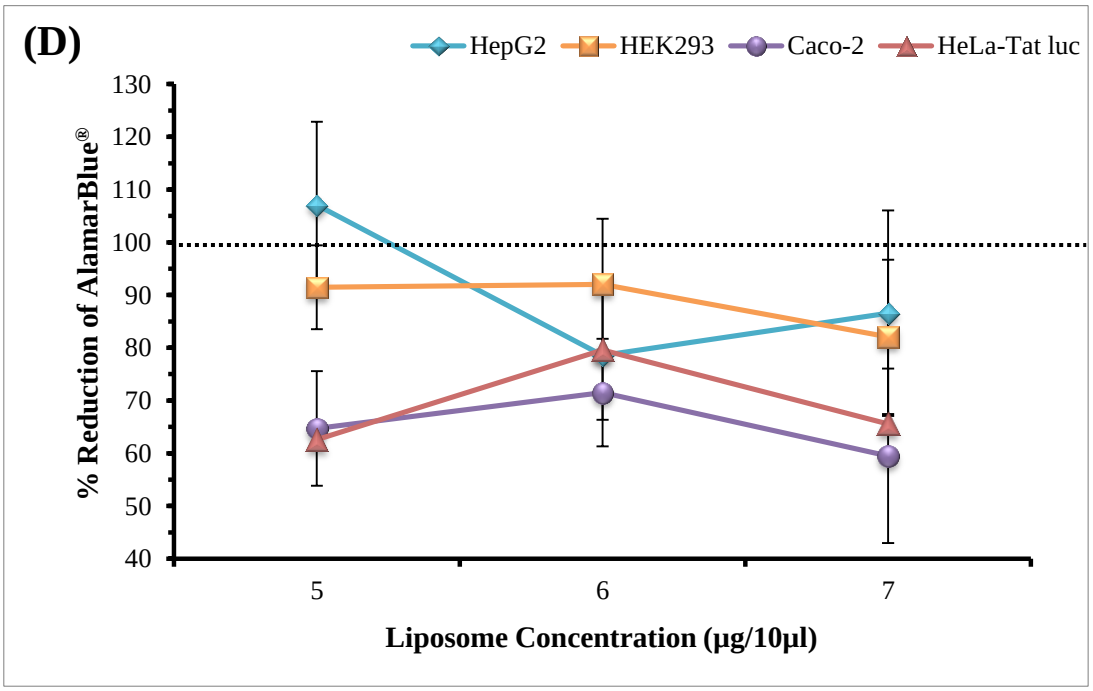

Figure 4.20: AlamarBlue® cytotoxicity assay showing percentage (%) reduction of resazurin as cell viability in HepG2 (♦), HEK293 (■), Caco-2 (●) and HeLa-Tat *luc* (▲) cell lines as function liposome-pCMV-luc DNA ratios. Lipoplexes (containing 1 µg of pCMV-*luc* DNA) were prepared at various liposome-DNA ratios ($^{w}/_{w}$) as indicated above. **(A)** SP-CHOL-MTS, **(B)** GM-CHOL-MTS, **(C)** SP-CHOL-MTS-R8 and **(D)** GM-CHOL-MTS-R8. A control sample (·····) containing only cells were assumed to have 100% survival. Results represent the mean ± SD, n = 3.

Figure 4.20 displays the percentage reduction of AlamarBlue® as a function of liposome-DNA ratios ($^{w}/_{w}$), in HepG2, HEK293, Caco-2 and HeLa-Tat *luc* cell lines. As can be seen by the results, all the mitochondriotropic lipoplexes across all liposome-DNA ratios were fairly well tolerated. As with the MTT assay, there seems to be a decrease in cell viability with a corresponding increase in liposome-DNA ratios, with the maximum decline in viability observed at the highest (supra-optimal) lipoplex ratio for most (75%) of the liposome formulations in the four cell lines tested. However, dissimilar to that observed in the MTT assay, the response of the different cells lines differed, with HepG2 cells displaying the most resistance to the cytotoxic effects of the lipoplexes. In fact, it showed virtually no cytotoxicity in response to most of the liposomal formulations and in some cases proliferation of cells actually increased to higher than that of the control cells represented by (----) line in the graph. HeLa-Tat *luc* and Caco-2 cell lines were the most susceptible while HEK293 cells were intermediate in their reaction. Generally, this assay showed a much higher reduction of AlamarBlue® for all liposomal formulations, and therefore a greater level of cell viability compared to the MTT assay probably owing to AlamarBlue® assay's superior degree of sensitivity. Conversely, this assay also presented the most inhibitory effect with a 42% decrease in cell survival observed in HeLa-Tat *luc* cells for SP-CHOL-MTS at lipid-DNA ratio ($^{w}/_{w}$) of 27:1. GM-CHOL-MTS elicited the lowest overall cytotoxic response from all four cell lines.

Both cytotoxicity assays demonstrated results that are consistent with other lipid-based gene delivery nanoparticles (Naicker *et al*., 2014). The AlamarBlue® has an advantage as it is more sensitive and non-toxic and thus probably more accurate than the MTT assay. None the less, neither of these bioassays may be very predictive of *in vivo* outcomes and careful analysis of data is necessary.

4.3.3. Apoptosis Detection by Acridine Orange and Ethidium Bromide (AO/EB) Staining

Apoptosis is a type of genetically controlled programmed cell death whereby individual cells of multicellular organisms undergo self-destruction in reaction to an assortment of stimuli that includes an emergency response to viral infections, anomalous growth of cells, cells undergoing a period of stress or those that are severely damaged beyond repair. Apoptosis is also responsible for the elimination of cells during normal development when they have

become redundant or once they have reached the end of their lifespan (Hong and Wu, 2002; Stoddart 2011; Liu *et al*., 2015). The alternate mechanism of cell death is necrosis which is considered unprogrammed and results in the premature death of cells due to pathological conditions such as trauma and toxins and is additionally, almost always detrimental (Rock and Kono, 2008). The process of apoptosis results in distinct morphological characteristics such as chromatin condensation, nuclear fragmentation, cell shrinkage, loss of membrane integrity and membrane blebbing that can be identified visually by the use of fluorescent microscopy and the differential uptake of fluorescent DNA binding dyes such as AO/EB dual staining (Cury-Boaventur *et al*., 2004; Ribble *et al*., 2005).

Studies in adherent cells and macrophages have shown that cytotoxicities caused by liposomes are mostly attributed to apoptosis (Bednarek *et al*., 2002; Takano *et al*., 2003). In this investigation, the MTT growth inhibition and AlamarBlue® assays indicated cytotoxicity induced by the cationic mitochondriotropic liposomal preparations. In an effort to evaluate whether cell death was mostly apoptotic or necrotic, the AO/EB dual staining technique was employed. Mitochondriotropic liposome-DNA complexes prepared at optimal ratios were incubated for 24 hours with the HepG2, HEK293, Caco-2 and HeLa-Tat *luc* cell lines and thereafter stained with AO/EB, the results of which are illustrated in Figure 4.22. Acridine orange is a vital nucleic acid selective fluorescent dye that stains both live and dead cells. Ethidium bromide, on the other hand, stains only cells that have lost their cytoplasmic membrane integrity thereby allowing EtBr to enter the cells to intercalate the DNA. Therefore, live cells appear evenly green with a circular nucleus in the centre of the cell while early apoptotic cells look green with bright yellow-green dots located on one side in the nuclei as a result of chromatin condensation and fragmentation. Late apoptotic cells stain nuclei orange as the EtBr incorporates into the cells but these nuclei appear fragmented and condensed in contrast to necrotic cells that also stain orange but have a structurally normal nucleus reminiscent of viable cells and an increased cell volume (Ribble *et al*., 2005; Kasibhatla *et al*., 2006; Liu *et al*., 2015). From the morphological observations made after evaluation of the fluorescent images, an apoptotic index (AI), which is defined as the percentage of apoptotic cells within the total population of cells, was calculated and plotted as a function of the respective cells lines, HepG2, HEK293, Caco-2 and HeLa-Tat *luc* (Figure 4.21). As can be seen from the results, HepG2 cells had the highest level of apoptosis observed followed by HEK293, Caco-2 and HeLa-Tat *luc* cells in this assay with all the mitochondriotropic lipoplexes displaying much greater levels of apoptosis than their

respective controls *(P<0.05; P<0.01; P<0.001)* which is to be expected. No definitive trend can be observed as to which liposomal formulation has the greatest influence on apoptosis as all the lipoplexes had induced programmed cell death to varying degrees in the different cell lines. These results do not exactly correlate with the cytotoxicity values obtained from the MTT and AlamarBlue® assays, with some values obtained here comparatively much higher. This can be possibly explained by the fact that this assay does not examine any metabolic activity of cells to determine their viability, just morphological observations based on their death. Ćurčić *et al*. (2012) suggested that differences in cell viability detected between metabolic activity-testing cytotoxicity assays, such as MTT, and apoptosis indicating assays such as the AO/EB dual staining, could be attributed to the fact that the former ones would detect cell death far earlier and the latter only identifies it later in the process. This assay was therefore conclusive in proving that cell death induced by liposomes was apoptotic and not necrotic in nature. However, the results as they relate to actual cytotoxicity of the liposomes should be regarded with caution as this assay's principal purpose is to distinguish and quantify the type of cell death and morphological features related to that and not to determine the actual cytotoxicity of the nanoparticle or drug under investigation.

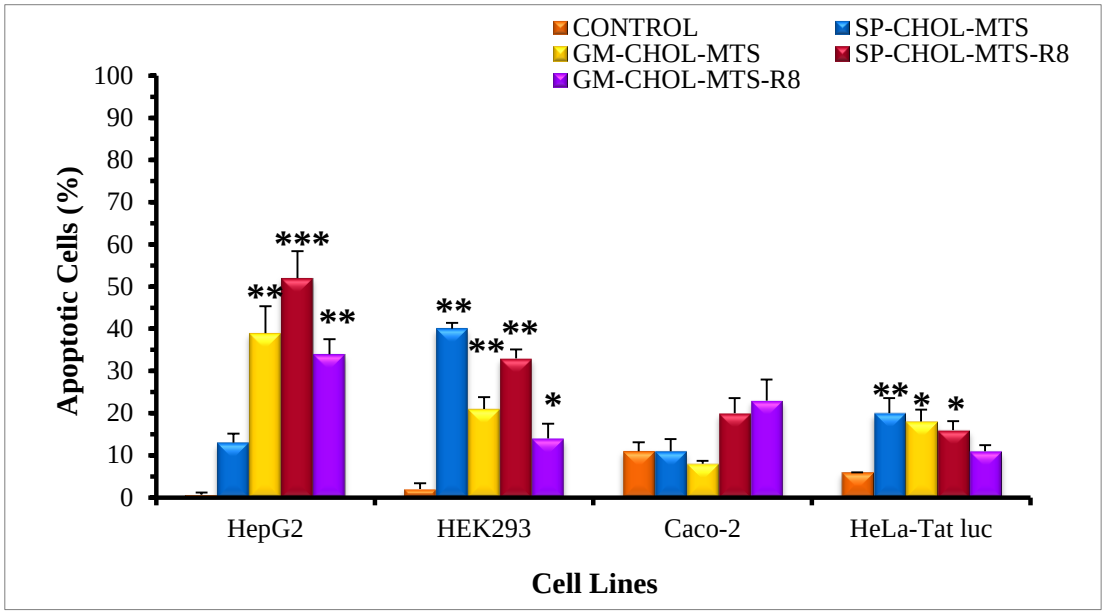

Figure 4.21: Apoptotic index calculated as a percentage (%) from results of the AO/EB dual staining apoptosis assay. SP-CHOL-MTS, GM-CHOL-MTS, SP-CHOL-MTS-R8 and GM-CHOL-MTS-R8 mitochondriotropic lipoplexes (containing 1 µg of pCMV-*luc* DNA) prepared at optimal binding ratios were incubated with HepG2, HEK293, Caco-2 and HeLa-Tat *luc* cell lines. A control of untreated cells for each cell line was utilised. Results represent the mean ± SD, n = 2. Statistical analysis was performed using one-way ANOVA followed by Dunnett multiple comparison *post hoc* test. **(P<0.05)* ***(P<0.01)* and ****(P<0.001*) indicate a significant difference compared to the respective controls.

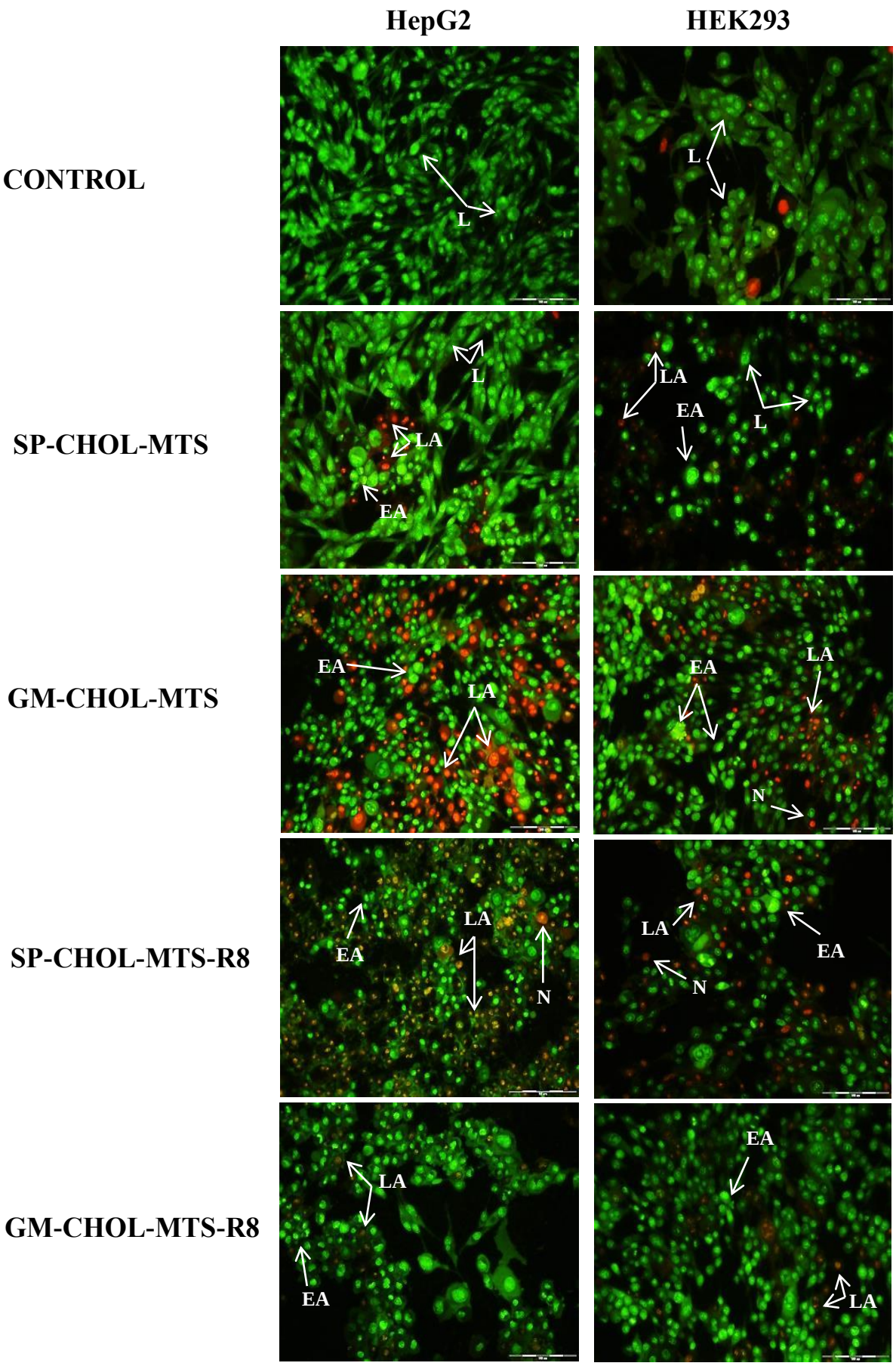
HepG2
HEK293
CONTROL
SP-CHOL-MTS
GM-CHOL-MTS
SP-CHOL-MTS-R8
GM-CHOL-MTS-R8
L
LA
EA
N

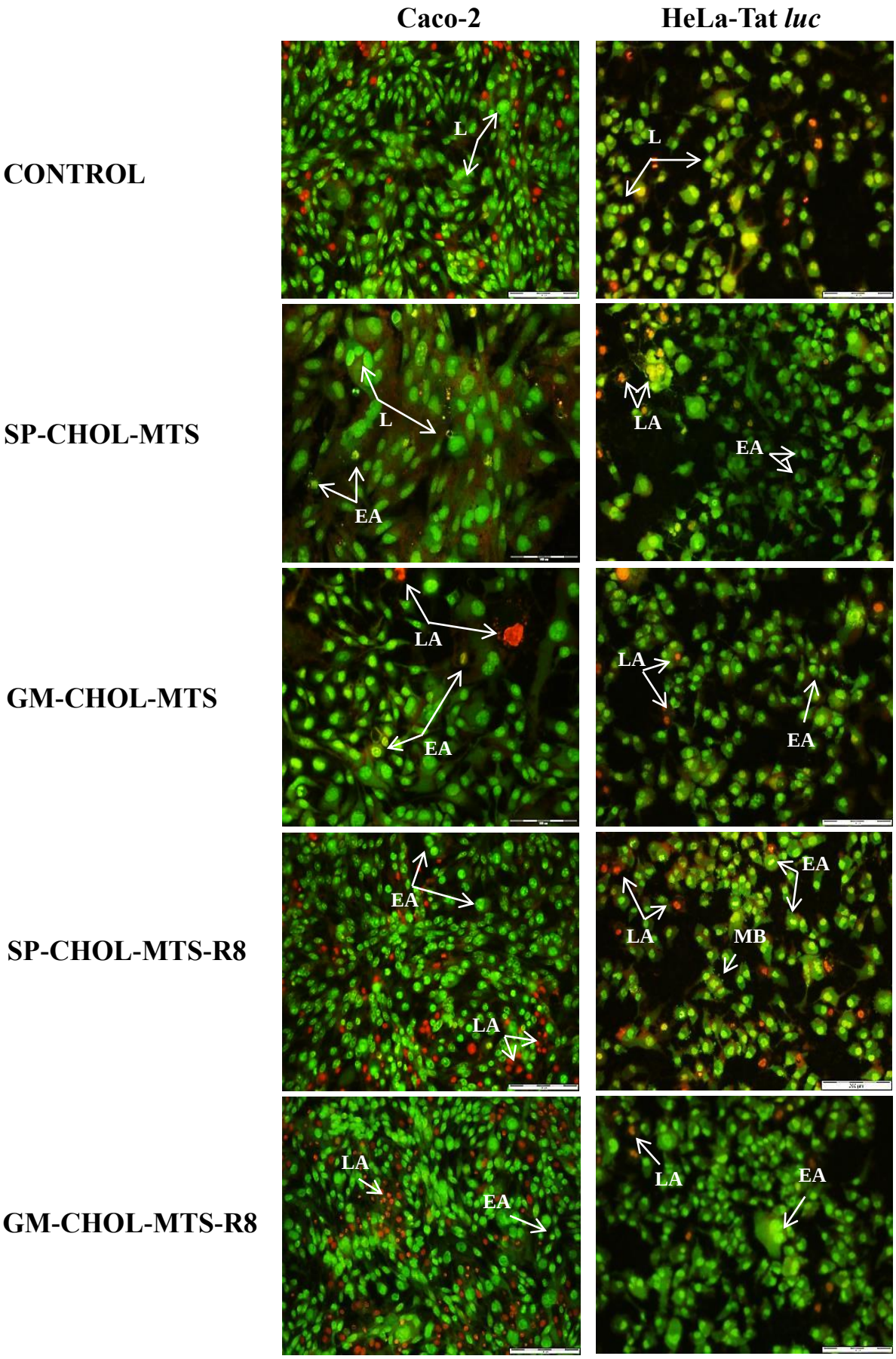
Caco-2
HeLa-Tat *luc*
CONTROL
SP-CHOL-MTS
GM-CHOL-MTS
SP-CHOL-MTS-R8
GM-CHOL-MTS-R8
L
LA
EA
MB

Figure 4.22: Apoptosis assay using AO/EB dual staining and fluorescent microscopy illustrating morphological changes induced by SP-CHOL-MTS, GM-CHOL-MTS, SP-CHOL-MTS-R8 and GM-CHOL-MTS-R8 mitochondriotropic lipoplexes (containing 1 µg of pCMV-*luc* DNA) prepared at optimal binding ratios in HepG2, HEK293, Caco-2 and HeLa-Tat *luc* cell lines as indicated. A control of untreated cells for each cell line was utilised. **L**: Live cells stained green; **EA**: early apoptotic cells with condensed yellow-green nuclei; **LA**: late apoptotic cells stained orange with condensed nuclei; **N**: necrotic cells with uniform orange fluorescence and **MB**: membrane blebbing, a feature of apoptosis. Bar = 100 µm.

4.3.4. Evaluation of Cellular Uptake and Mitochondrial Localisation by Fluorescent Studies

4.3.4.1. Fluorescence Microscopy

DNA was labelled with rhodamine using the Mirus *Label* IT® Tracker™ Kit. The reagents in this kit covalently bind marker molecules such as rhodamine to nucleic acids in an uncomplicated one-step chemical reaction, which yields fully intact fluorescently-tagged DNA for *in vitro* tracking experiments. This DNA was used to make up the optimal (electroneutral) liposome-DNA ratios, as determined by gel retardation assays, for each of the mitochondriotropic liposomes (SP-CHOL-MTS, GM-CHOL-MTS, SP-CHOL-MTS-R8 and GM-CHOL-MTS-R8), which were then incubated with the different cell lines for 24 hours. Thereafter, the cells were stained with MitoTracker® Green FM, a cell-permeant probe that comprises a mildly thiol-reactive chloromethyl moiety that allows it to covalently bind to mitochondrial matrix proteins by interacting with free thiol groups of cysteine residues thereby labelling mitochondria. As there are hundreds to thousands of mitochondria that are part of an extensive continuous and dynamic cytoskeleton in cells, MitoTracker® Green would stain all of them and therefore make the entire cell appear green in images similar to that observed in the central panels of Figure 4.25.

Prior to utilising fluorescent microscopy for this assay, confocal laser scanning microscopy (CLSM) was employed to attain higher resolution images so as to better evaluate the assay and its practical potential in attaining the desired result. Representative images, similar to that of fluorescence microscopy were acquired (Figure 4.23), leading to the decision that fluorescent microscopy could indeed be used to garner the desired result.

The ability of the cationic mitochondriotropic liposomes to localise rhodamine-labelled pCMV-*luc* DNA (1 µg) intracellulary in the vicinity of mitochondria was examined in living HepG2, HEK293, Caco-2 and HeLa-Tat *luc* cell lines using fluorescent microscopy. The intracellular targeting potential of the mitochondriotropic liposome-rhodamine-labelled pCMV-*luc* DNA complexes (red) was observed after staining mitochondria green with MitoTracker® Green FM. The yellowish fluorescence indicated in the merged fluorescent images represents the co-localisation of the rhodamine-labelled pCMV-*luc* DNA with the MitoTracker® Green FM (Figure 4.25, right panels). Controls containing cells only and cells only incubated with naked rhodamine-labelled pCMV-*luc* DNA were employed. As can be seen there is no fluorescence detected in these control images. This is an expected result as the cells alone should not have any discernible fluorescence and the naked rhodamine-tagged DNA would have been likely degraded by the serum nucleases present in the medium. From the results, it appears that MitoTracker® Green was effective in staining the mitochondria of cells because, as mentioned above, the hundreds of these organelles present in a cell would have picked up the dye and consequently made the whole cell seem green. It can also be said that all mitochondriotropic lipoplexes were successful in the intracellular delivery of the rhodamine-DNA cargo. This is evidenced by the red fluorescence seen in the left panels of Figure 4.25 where the DNA appears to be localised almost exclusively inside the cells and not in the matrix around the cells. The artefacts that can be seen brightly fluorescing are remnants of the MitoTracker® Green dye. The proposed mechanism of cellular uptake for SP-CHOL-MTS and GM-CHOL-MTS liposomal formulations is non-specific clathrin-mediated endocytosis (Figure 4.24) while SP-CHOL-MTS-R8 and GM-CHOL-MTS-R8 are purported to employ macropinocytosis via electrostatic interactions of cellular uptake device, R8, with the cell membrane (Figure 4.24). Both these mechanisms appear to have been effective as the results clearly show that there is definite intracellular co-localisation observed in all cell lines and for all cationic mitochondriotropic liposome formulations, between the green fluorescence of MitoTracker® Green and the red fluorescence of the rhodamine-labelled DNA as depicted in the merged images in the right panels of Figure 4.25. It also appears that all lipoplexes (SP-CHOL-MTS, GM-CHOL-MTS, SP-CHOL-MTS-R8 and GM-CHOL-MTS-R8) prepared at optimal liposome-DNA ratios were efficient in firstly, enhancing cellular uptake in all four cell lines and secondly, effecting the co-localisation observed in the four cell lines tested even though these nanocomplexes were shown to have negative zeta potentials. It therefore seems that the zeta potential did not affect the performance of the complexes.

This efficiency indeed posed an issue as it is virtually impossible to evaluate which one of them was most proficient. Both MTS and R8 were shown to successfully target mitochondria using MITO-Porter and DF-MITO-Porter in a series of studies (Yasuzaki *et al*., 2010; Yamada *et al*., 2011; Yamada and Harashima, 2013; Kawamura *et al*., 2013a; Kawamura *et al*., 2013b) Another concern encountered is that it is not possible to conclusively say that the rhodamine-DNA is localised exclusively to mitochondria as this cannot be elucidated by these images alone. This observation was also made by Santos *et al*. (2014) in their investigation of plasmid nanoparticles. However, at this point it is fair to speculate that this microscopy study certainly supports the notion of the mitochondriotropic nanoparticles cell internalisation and directed selective delivery to the mitochondria. To further investigate this, an attempt to quantify fluorescence was made utilising cell homogenates, which is discussed below.

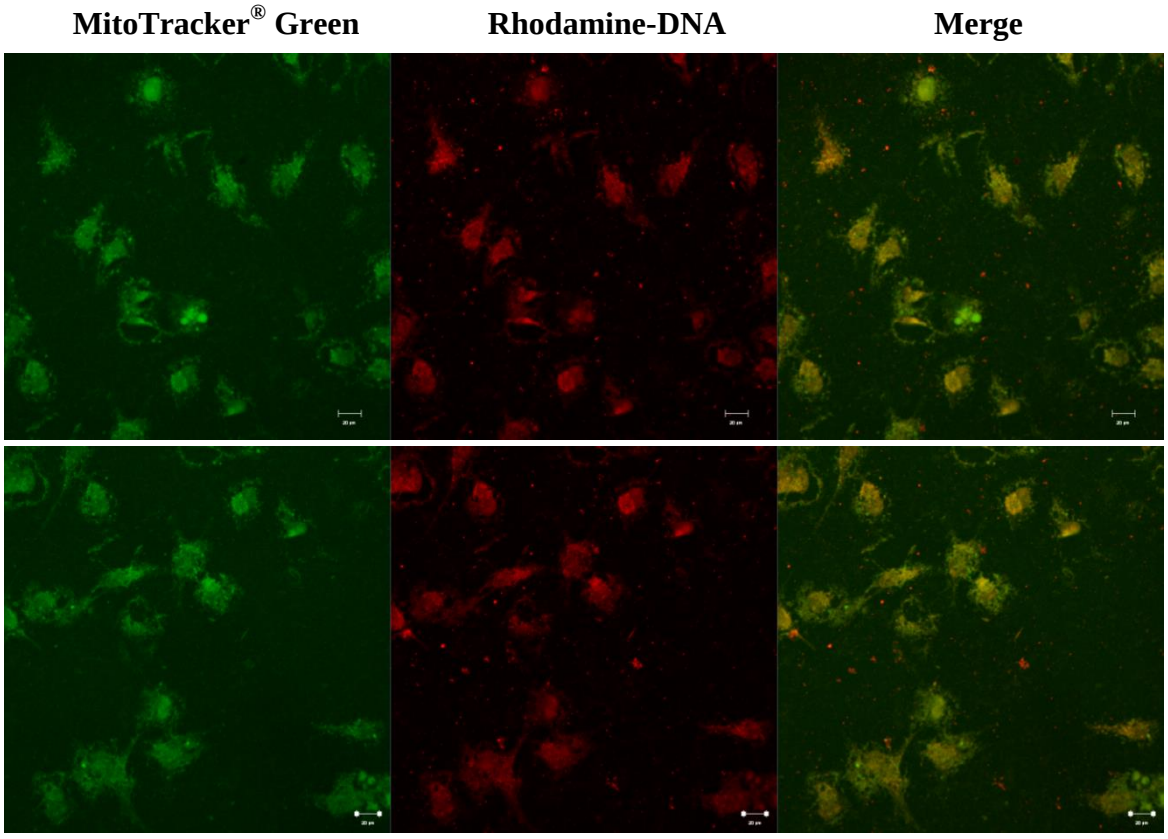

Figure 4.23: Representative images showing intracellular co-localisation by CLMS. Left panel: mitochondria stained green byMitoTracker® Green FM; Central panel: red fluorescence from rhodamine-tagged DNA delivered by the nanoparticles; Right panel: merged left and central panels. Yellowish colour indicates co-localisation of the rhodamine-tagged DNA with the MitoTracker® Green FM. Bar = 10µm.

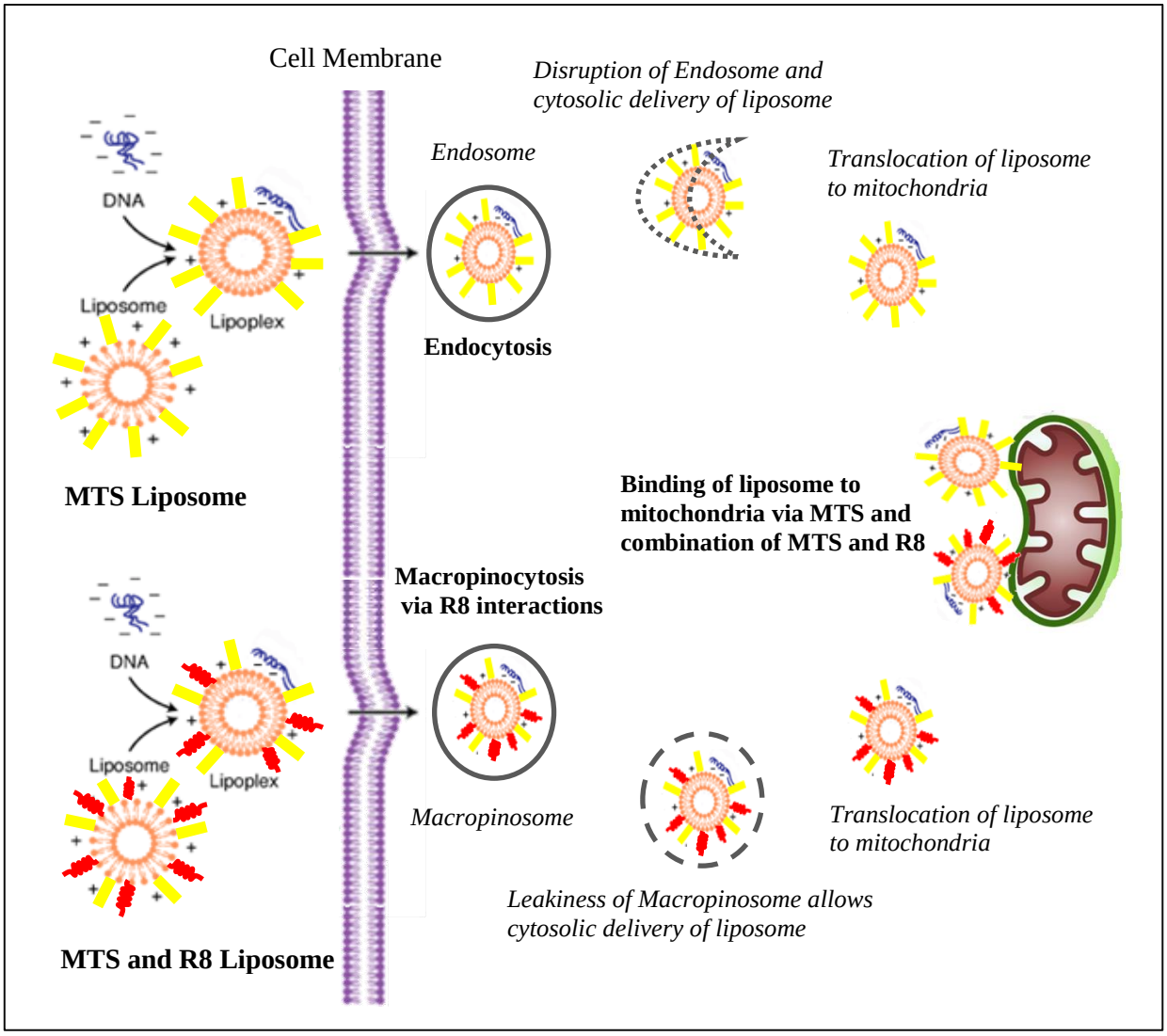

Figure 4.24: Schematic representation of mitochondrial delivery of MTS only and MTS and R8 liposomes. Lipoplexes enter the cell via endocytosis or macropinocytosis respectively. Disruption of endosome and macropinosome allows escape of respective liposome-DNA complexes which then translocate to the mitochondria to which it binds via MTS and a combination of MTS and R8.

(A)

HepG2

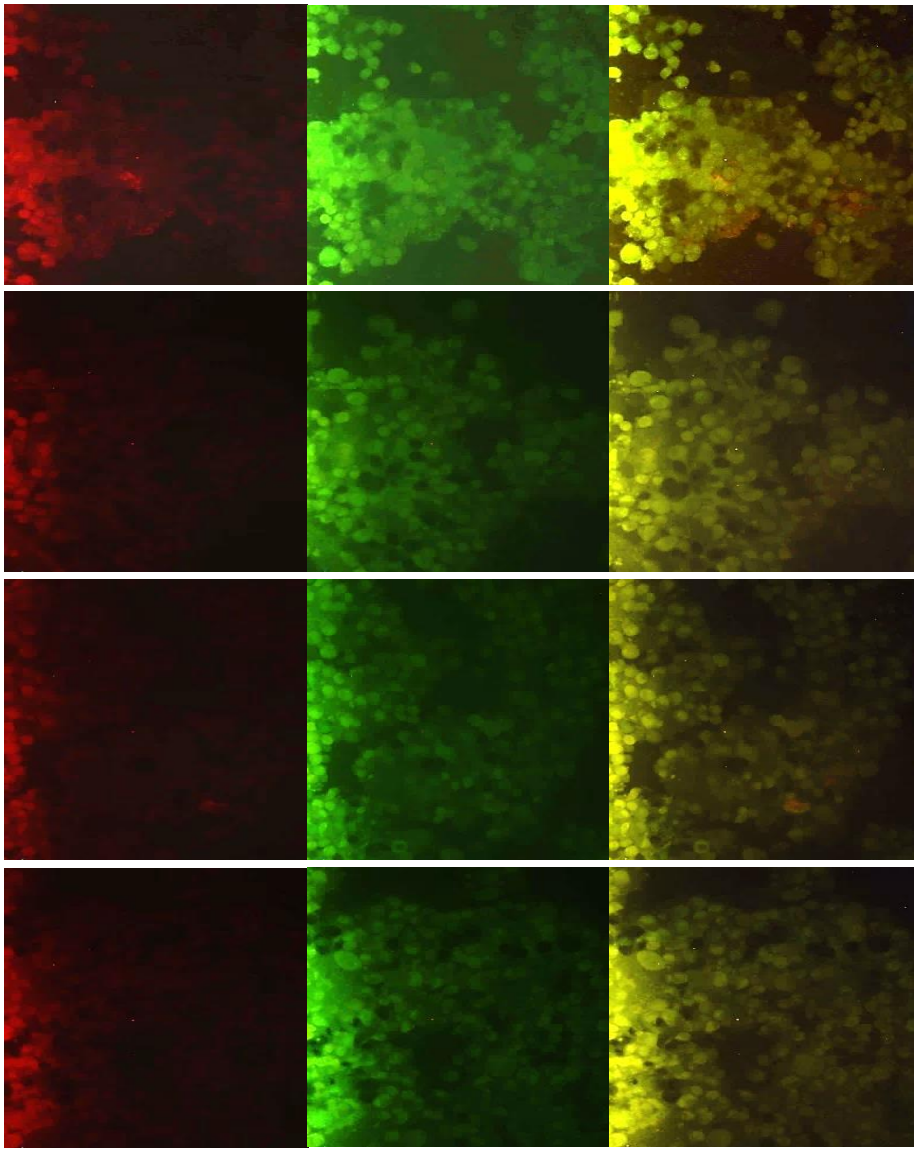

Controls

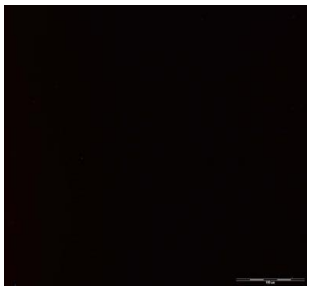

Cells only

Naked DNA

(B)

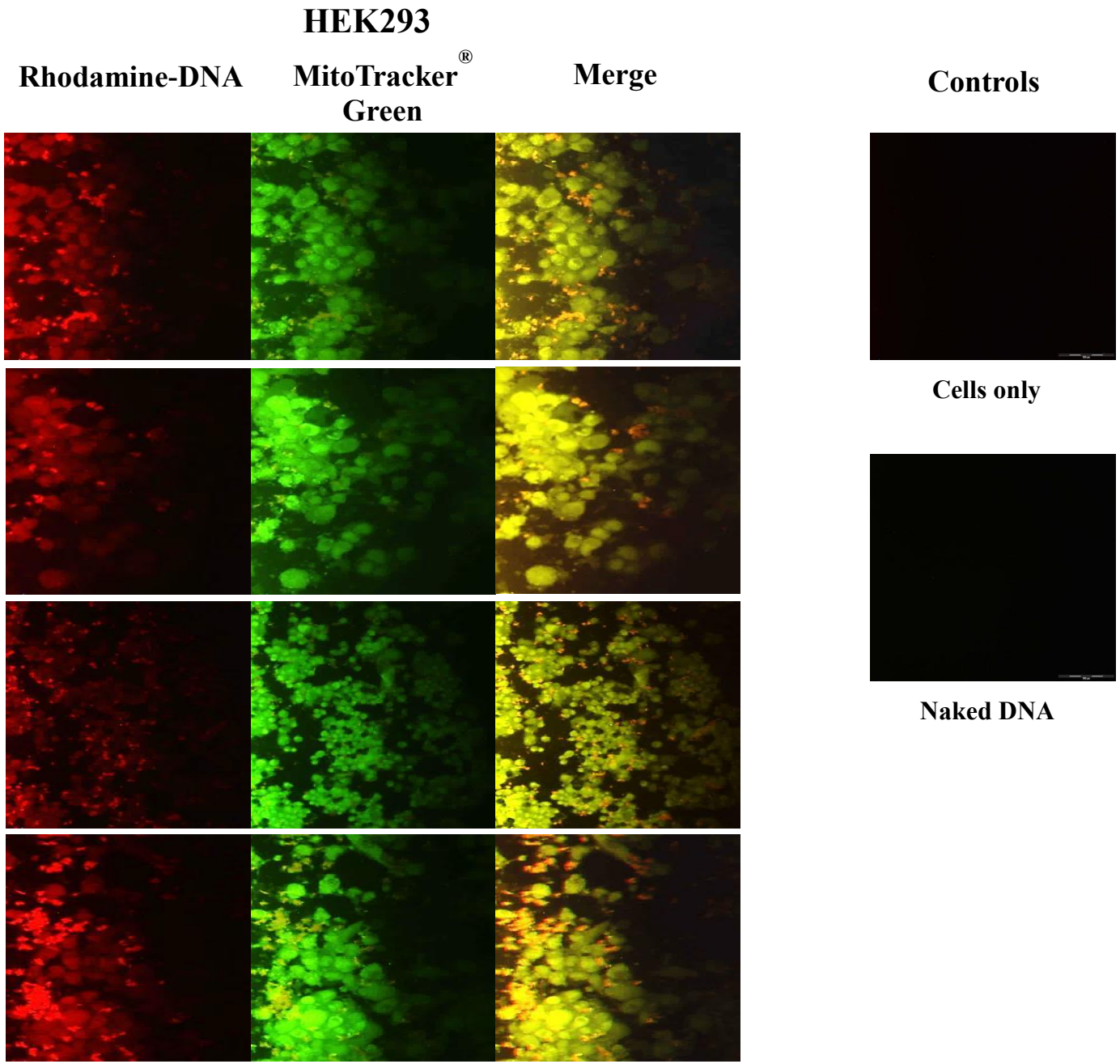
HEK293
Rhodamine-DNA
MitoTracker® Green
Merge
Controls
SP-CHOL-MTS
GM-CHOL-MTS
SP-CHOL-MTS-R8
GM-CHOL-MTS-R8
Cells only
Naked DNA

(C)

Caco-2

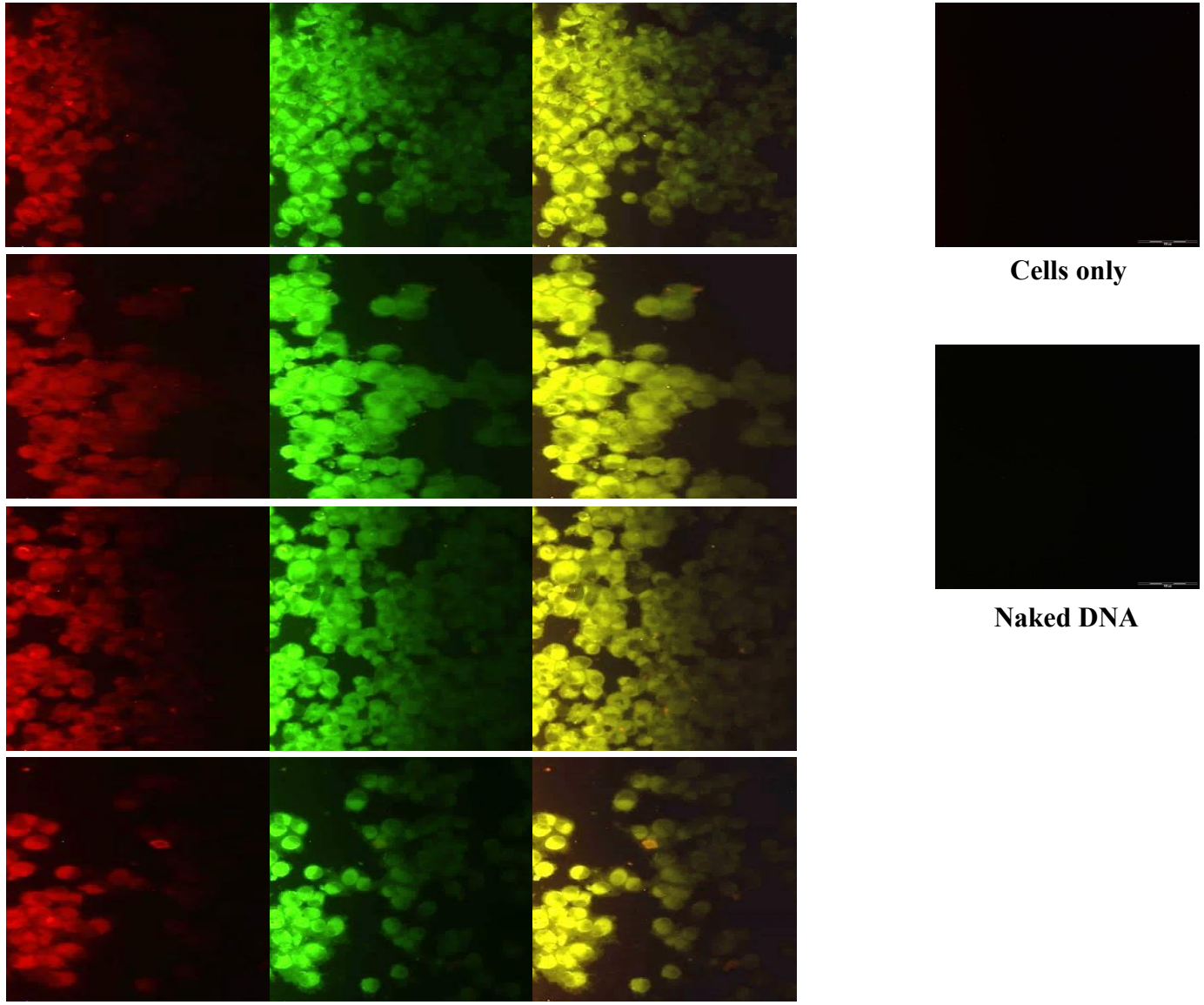

Controls

Cells only

Naked DNA

(D)

HeLa-Tat *luc*

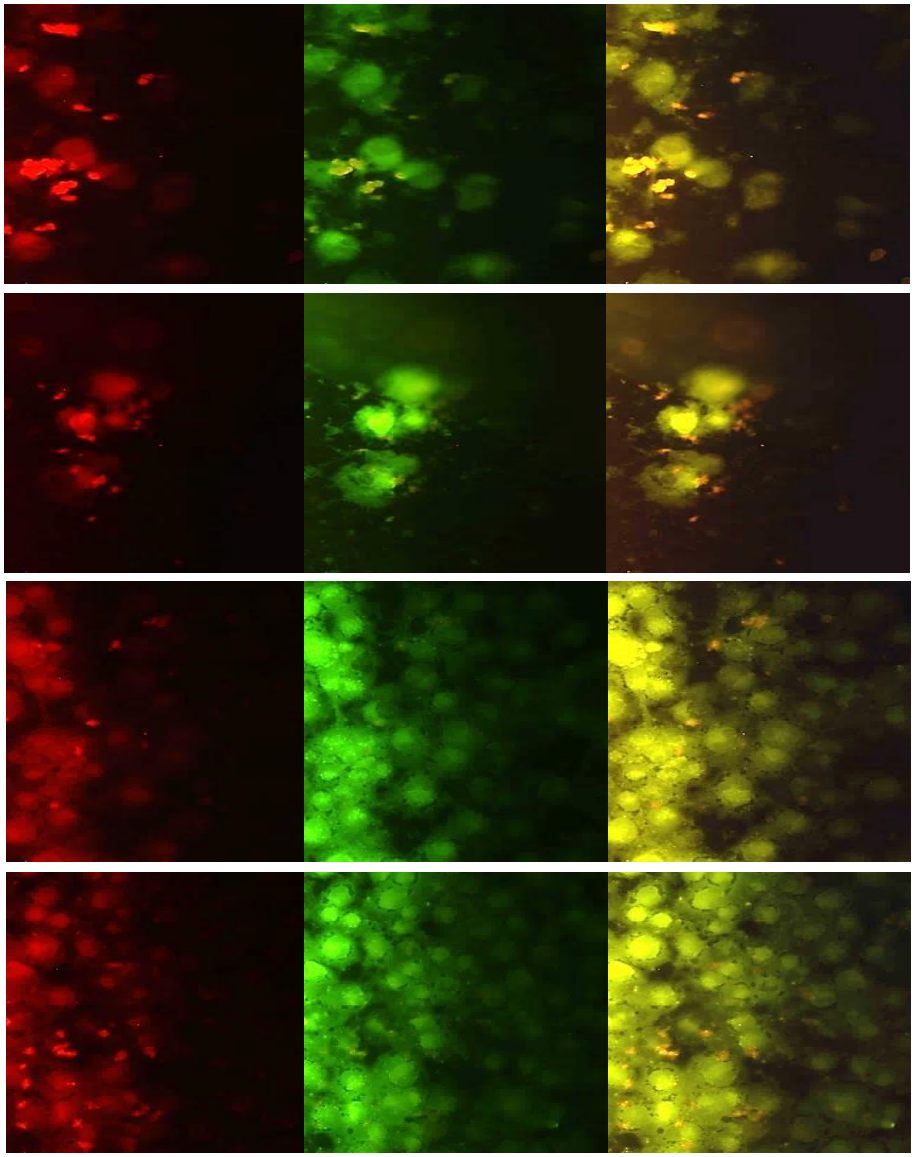

Controls

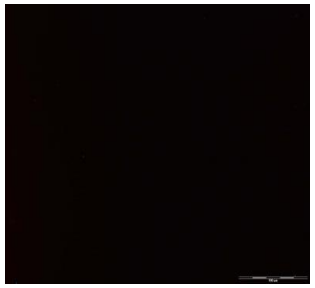

Cells only

Naked DNA

Figure 4.25: Intracellular co-localisation by fluorescence microscopy of SP-CHOL-MTS, GM-CHOL-MTS, SP-CHOL-MTS-R8 and GM-CHOL-MTS-R8 mitochondriotropic lipoplexes (containing 1 µg of rhodamine-labelled pCMV-*luc* DNA) prepared at optimal binding ratios in **(A)** HepG2, **(B)** HEK293, **(C)** Caco-2 and **(D)** HeLa-Tat *luc* cell lines. Two controls containing cells only and cells exposed to naked rhodamine-tagged DNA were used. Left panel: red fluorescence from rhodamine-tagged DNA delivered by the nanoparticles; Central panel: mitochondria stained green by MitoTracker® Green FM; Right panel: merged left and central panels. Yellowish colour indicates co-localisation of the rhodamine-tagged DNA with the MitoTracker® Green FM. Magnification = 200x.

4.3.4.2. Quantitative Evaluation of Mitochondrial Targeting Activity

The plasmid DNA pCMV-*luc* was labelled with fluorescein using the Mirus *Label* IT® Tracker™ Kit. This fluorescein-tagged DNA (1 µg) was used to form mitochondriotropic lipoplexes at the optimal binding ratios of each of the four liposomal formulations (SP-CHOL-MTS, GM-CHOL-MTS, SP-CHOL-MTS-R8 and GM-CHOL-MTS-R8). These lipoplexes were then added to cell homogenates of the HEK293, HepG2, Caco-2 and HeLa-Tat *luc* cell lines to examine their mitochondrial targeting ability. Cell homogenates were used as they are a better model of living cells than isolated mitochondria since they contain other organelles (Yamada and Harashima, 2013). In the previous experiment, living cells were used however no conclusive answer was acquired as to whether the presence of MTS and/or R8 increased the interaction between liposomes and mitochondria. To satisfy this enquiry, it was decided that homogenates were a superior model system to living cells. The ability of cationic MTS-modified liposomes (SP-CHOL-MTS and GM-CHOL-MTS) to selectively target mitochondria was evaluated by assessing the mitochondrial targeting activity of these nanoparticles. The mitochondrial targeting activity of MTS and R8 modified liposomes (SP-CHOL-MTS-R8 and GM-CHOL-MTS-R8) was also studied. MTS peptide is well known to have a high mitochondrial targeting activity but it has not been tested with these novel liposomal formulations and in dual surface modification with R8.

As mentioned above, lipoplexes prepared at the optimal binding ratios of these liposomes and comprising fluorescein-tagged DNA were incubated with the respective cell homogenates. The fluorescent level of the fluorescein-tagged DNA and therefore the liposomes themselves in the mitochondrial fraction was determined after subcellular fractionation by differential centrifugation. This was calculated to be the mitochondrial targeting activity of the tested liposomes and is summarised in Figure 4.26.

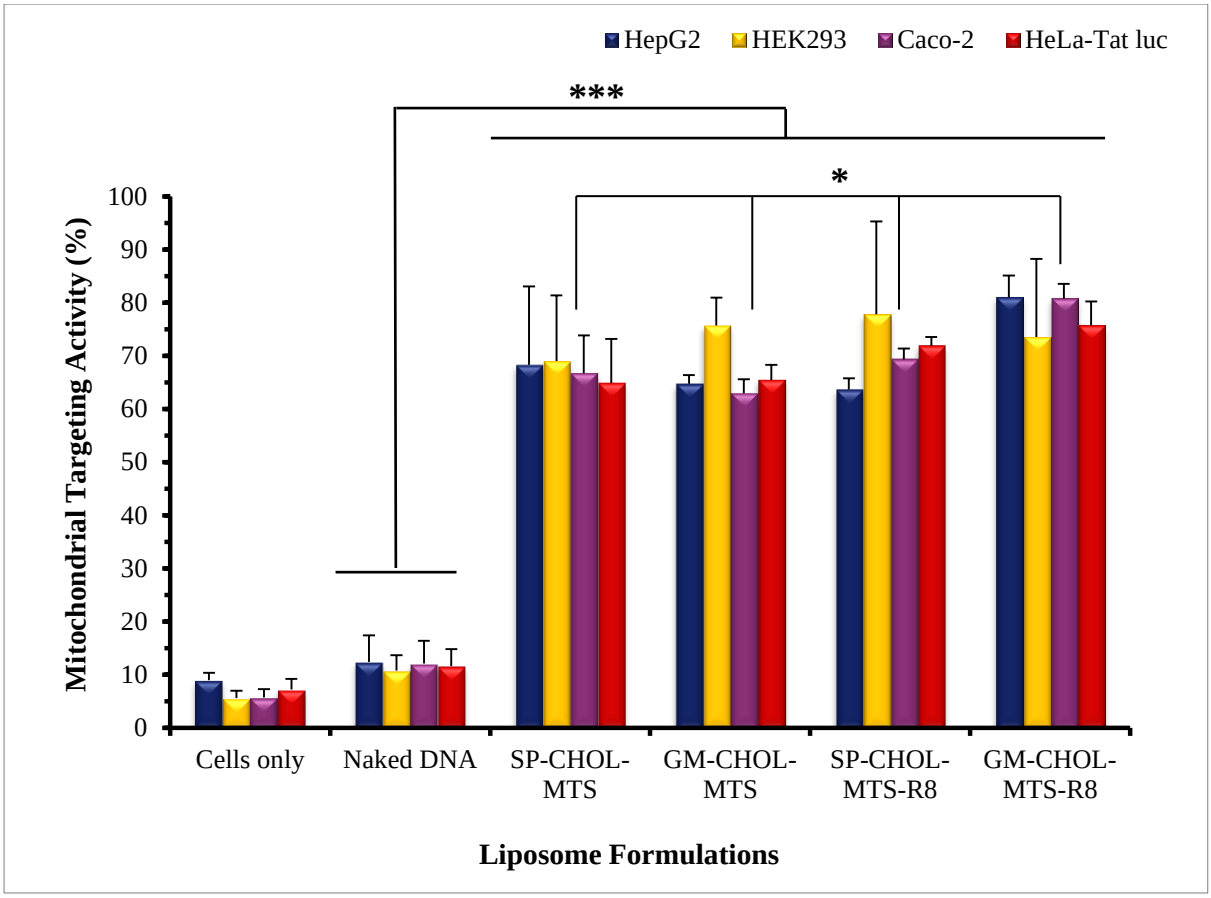

Figure 4.26: Evaluation of mitochondrial targeting of mitochondriotropic liposomes SP-CHOL-MTS, GM-CHOL-MTS, SP-CHOL-MTS-R8 and GM-CHOL-MTS-R8 in four different cell homogenates. Lipoplexes (containing 1 µg of fluorescein-labelled pCMV-*luc* DNA) were prepared at optimal binding ratios. Two controls, comprising untreated cells and cells exposed to naked DNA were utilised. Results represent the mean ± SD, $n = 3$. Statistical analysis was performed using one-way ANOVA followed by Dunnett multiple comparisons *post hoc* test. *($P<0.05$) and ***($P<0.001$) indicate a significant difference.

From the results, it was observed that both MTS alone and MTS in combination with R8 definitely improved the mitochondrial targeting of nanoparticles that were larger than 150 nm (Table 4.2). Lipoplexes prepared at optimal binding ratios of MTS only (SP-CHOL-MTS and GM-CHOL-MTS) and MTS and R8 (SP-CHOL-MTS-R8 and GM-CHOL-MTS-R8) liposomes displayed much greater mitochondrial targeting efficiencies *($P<0.001$)* than the two controls employed in the HepG2, HEK293, Caco-2 and HeLa-Tat *luc* cell homogenates. The two controls showed little fluorescence, as was expected as the cells alone were untreated and the naked fluorescein-tagged DNA would have likely been degraded by nucleases. In terms of the differences observed between the MTS only liposomes (SP-CHOL-MTS and GM-CHOL-MTS), and the MTS and R8 liposomes (SP-CHOL-MTS-R8

and GM-CHOL-MTS-R8), the MTS and R8 nanocomplexes seem to have a slight though not statistically significant advantage, except in the case of GM-CHOL-MTS-R8 in the Caco-2 cell homogenates ($P<0.05$), over their MTS only counterparts. This could be as a result of the R8, as recent studies reported that R8 also serves as a mitochondrial targeting device via electrostatic interactions with the mitochondria, which has a highly negative potential. This gives R8 the ability to deliver certain cargoes to the mitochondria (Khalil *et al*., 2006a; Yamada *et al*., 2012). However, in another study conducted by the same authors they postulated that R8 had non-specific binding to the mitochondria, and R8 modified liposomes performed poorly compared to MTS modified liposomes in mitochondrial targeting (Yamada and Harashima, 2013). Conversely, in a more recent study, the authors once again suggested that R8 had mitochondrial targeting properties (Yamada *et al*., 2015).

In line with these findings, in this study the presence of R8 together with MTS appeared to have a beneficial effect. No significant difference was detected between the majority of the liposomes containing the SP-CHOL and GM-CHOL cholesterol-derived cross-linking agent, except in the case of GM-CHOL-MTS-R8 where a significant increase ($P<0.05$) can be noted in mitochondrial targeting activity of this liposome in the Caco-2 cell homogenates. This could possibly be from the slightly longer spacer in the cross-linker structure that may give the MTS and R8 peptides attached to it an added advantage in mitochondrial targeting. No significant difference was observed between the liposomes performances the different cell homogenates. Interestingly, this assay does not indicate whether or not the delivered pDNA entered the mitochondria, just that it was targeted or localised to mitochondria which as suggested by Niazi *et al*. (2013) is adequate for mitochondrial gene therapy considering that these authors speculated that mitochondrial competence for DNA uptake is an intrinsic property of the organelle and has the potential capability to support mitochondrial transfection in living cells. Overall, mitochondrial targeting and localisation analysis of this assay's results revealed that both MTS only and a combination of MTS and R8 can function as mitochondrial targeting devices in combination with liposomes, leading to enhanced mitochondrial targeting of these novel liposomal formulations observed in a variety of cell homogenates.

CHAPTER FIVE

CONCLUSION

5.1. CONCLUDING REMARKS

Mitochondria are organelles that are of mounting interest in pharmaceutical and nanomedical research, since it was discovered that dysfunction of these organelles contribute to numerous diseases and pathologies, each with a different clinical manifestation. To date, not much is understood about these defects and their implications in mitochondrial diseases. It is speculated that nanotechnology, specifically gene therapy will shed more light on these dysfunctions. However, mitochondrial gene therapy is a field still in its early developmental stages, but has immense potential in finally elucidating, observing and manipulating the mitochondria and its genome to clarify its role in common diseases such as Alzheimer's disease, Parkinson's disease, cancer, neurodegeneration and ageing. Additionally, it would serve to increase our understanding of defects and dysfunctions present in mitochondrial disease leading to more efficient treatment and possibly cure. This stagnicity in mitochondrial research is, in part, due to the non-existence of an efficient, safe and biocompatible mitochondrial targeting nanovector. Therefore, the development of a non-toxic and effective mitochondrial targeting system is required but this still remains a fairly arduous challenge.

This study evaluated the ability of four novel cationic mitochondriotropic lipid-based delivery systems to improve the efficacy of cellular uptake and mitochondrial localisation of model plasmid DNA in four different cell line models. The cationic cytofectin, CHOL-T, together with the neutral lipid, DOPE; the cholesterol-derived cross-linkers, SP-CHOL and GM-CHOL, and the MTS and R8 peptides were able to form mitochondriotropic liposomes capable of successfully binding and additionally, protecting pDNA from the effects of serum nucleases. The liposomes and their corresponding optimal lipoplexes also presented with relatively favourable particle sizes and zeta potential measurements as well as being morphologically spherical in shape. These nanovectors were reproducible and stable to long-term storage at 4°C with nominal aggregation observed.

In vitro cell culture studies examining the cytotoxicity profile of these novel liposomal formulations revealed them to be well tolerated by, and display minimal toxicity to, the HepG2, HEK293, Caco-2 and HeLa-Tat *luc*, cell lines tested. Additionally, evaluation of the mechanism of cell death induced by these delivery vehicles indicated that apoptosis was the predominant process.

Initial studies into the cellular uptake and co-localisation of the liposome-rhodamine tagged DNA complex with mitochondria in living cells was conducted using CLSM as a proof of principle of the technique and subsequent studies were performed utilising fluorescent microscopy. Fluorescent images demonstrated that the mitochondriotropic liposomes did indeed overwhelmingly enhance cellular uptake, in the presence of serum, as can be inferred by the obvious and substantial co-localisation observed between green stained mitochondria of cells and the red rhodamine-tagged DNA delivered by the nanovectors, compared to the two controls employed which showed no detectable fluorescence. However, the images could not provide detailed definitive evidence that the rhodamine-tagged DNA was exclusively localised specifically to mitochondria in these living cells.

In an attempt to further elucidate mitochondrial localisation and targeting ability of the MTS only (SP-CHOL-MTS and GM-CHOL-MTS) and MTS and R8 (SP-CHOL-MTS-R8 and GM-CHOL-MTS-R8) liposomes, cell homogenates were employed. Efficient accumulation of the MTS modified and MTS and R8 modified liposomes on mitochondria was confirmed using these various cell homogenate cocktails. This strongly suggested that the presence of MTS on the liposomal surface did indeed significantly increase ($P<0.001$) the mitochondrial localisation and targeting ability of the liposomes as evidenced by the increased presence of fluorescence in the mitochondrial fraction of the homogenates for all cell lines tested. The dual surface modification of MTS and R8 peptides of the liposomes appeared to perform better than their MTS only counterparts with the GM-CHOL-MTS-R8 liposomal preparation performing the best in terms of mitochondrial localisation and targeting. So it can be assumed that R8 contributed to the mitochondrial targeting ability of the liposome. This particular liposome also displayed low toxicity and high DNA compaction and binding affinity as indicated by the MTT, AlamarBlue® and ethidium bromide intercalation assays respectively.

These results reflect the potential of these four cationic mitochondriotropic liposomes in accomplishing cellular uptake and mitochondrial targeting and localisation. These findings support the hypothesis that these MTS only and a combination of MTS and R8 modified liposomes have the ability for future corrective and restorative mitochondrial gene delivery. However, even though all four nanovectors proved to be competent at achieving cellular uptake and mitochondrial targeting to varying degrees, it can be reasoned that the GM-CHOL-MTS-R8 liposome holds the most potential for further development and eventual establishment as a clinically applicable vector system for effective mitochondrial delivery of therapeutic genes and bioactive molecules.

Possible limitations to this study include the lack of; firstly, an available mitochondria-specific reporter gene system that will allow for easy expression and simple identification inside mitochondria and secondly, advanced bioassays that can definitely establish the presence of delivered DNA inside mitochondria. The absence of these confirmatory assays greatly contributed to the inconclusive fluorescence microscopy results of this study that could not categorically determine if rhodamine-tagged DNA was exclusively co-localised to mitochondria in living cells. Until these bioassays are developed, all mitochondrial targeted delivery systems have to rely on indirect methods of demonstrating mitochondrial targeting of DNA.

Future studies include, improvement of the vector system, possibly by incorporating a fluorescent component into its structure so as to better visualise it in living cells and, evaluating the ability of these cationic mitochondriotropic liposomes to target mitochondria in an animal model *in vivo*. Additional work to confirm mechanisms of cell internalisation and endosomal escape may be investigated to give a superior understanding of intracellular trafficking. To conclude, taking into consideration their relatively non-toxic nature and stability in serum *in vitro*, these novel cationic mitochondriotropic liposomes appear to be a viable and attractive option as a promising optimal mitochondrial targeting system *in vivo*.

REFERENCES

Aden D.P., Fogel A., Damjanov S., Plotkin B., and Knowles B.B. (1979). *Controlled synthesis of HBsAg in a differential human liver carcinoma-derived cell line*. Nature **282:** 615-616.

Adhya S., Mahato B., Jash S., Koley S., Dhar G., and Chowdhury T. (2011). *Mitochondrial gene therapy: The tortuous path from bench to bedside.* Mitochondrion **11:** 839-844.

Akbarzadeh A.,Rezaei-Sadabady R., Davaran S., Joo S.W., Zarghami N., Hanifehpour Y., Samiei M., Kouhi M., and Nejati-Koshk K. (2013). *Liposome: classification, preparation, and Applications.* Nanoscale Research Letters **8:** 102.

Akouchekian M., Houshmand M., Akbari M.H.H., Kamalidehghan B., and Dehghan M. (2011). *Analysis of mitochondrial ND1 gene in human colorectal cancer.* Journal of Research in Medical Sciences **16:** 50-55.

Alfredsson V. (2005). *Cryo-TEM studies of DNA and DNA–lipid structures*. Current Opinion in Colloid & Interface Science **10:** 269-273.

Allen T.M., and Cullis P.R. (2013). *Liposomal drug delivery systems: From concept to clinical applications.* Advanced Drug Delivery Reviews **65:** 36-48.

Almgren M., Edwards K., and Karlsson G. (2000). C*ryo transmission electron microscopy of liposomes and related structures.* Colloids and Surfaces A: Physicochemical and Engineering Aspects **174:** 3-21.

Almofti M.R., Harashima H., Shinohara Y., Almofti A., Li W., and Kiwada H. (2003). *Lipoplex size determines lipofection efficiency with or without serum.* Molecular Membrane Biology **20:** 35-43.

Al-Nasiry S., Geusens N., Hanssens M., Luyten C and Pijnenborg R. (2007). *The use of Alamar Blue assay for quantitative analysis of viability, migration and invasion of choriocarcinoma cells*. Human Reproduction **22:** 1304-1309.

Andalib S., Vafaee M.S., and Gjedde A. (2014). *Parkinson's disease and mitochondrial gene variations: A review*. Journal of the Neurological Sciences **346:** 11-19.

Angius F., and Floris A. (2015). *Liposomes and MTT cell viability assay: An incompatible affair*. Toxicology *in Vitro* **29:** 314-319.

Banerjee A., Singh J., and Dasgupta D. (2013). *Fluorescence spectroscopic and calorimetry based approaches to characterize the mode of interaction.* Journal of Fluorescence **23:** 745-752.

Bangham A.D., Standish M.M., and Watkins J.C. (1965). *Diffusion of univalent ions across the lamellae of swollen phospholipids*. Journal of Molecular Biology **13:** 238-252.

Barenholz Y. (2001). *Liposome application: problems and prospects*. Current Opinion in Colloid & Interface Science **6:** 66-77.

Batzri S., and Korn E.D. (1973). *Single bilayer liposomes prepared without sonication*. Biochimica et Biophysica Acta **298:** 1015-1019.

Bednarek I., Czajka M., and Wilczok T. (2004). *Efficiency of lipofection of adherent cells is limited by apoptosis*. Folia Histochemica and Cytobiologica 4**0:** 133-134.

Betker J.L., Kullberg M., Gomez J., and Anchordoquy T.J. (2013a). *Cholesterol domains enhance transfection.* Therapeutic Delivery **4:** 453-462.

Betker J.L., Gomez J., and Anchordoquy T.J. (2013b). *The effects of lipoplex formulation variables on the protein corona and comparisons with in vitro transfection efficiency.* Journal of Control Release **171:** 261-268.

Bibi S., Kaur R., Henriksen-Lacey M., McNeil S.E., Wilkhu J., Lattman E., Christensen E., Mohammed R.A., Perrie Y. (2011). *Microscopy imaging of liposomes: From coverslips to environmental SEM.* International Journal of Pharmaceutics **417:** 138-150.

Biswas S., and Torchilin V.P. (2014). *Nanopreparations for organelle-specific delivery in cancer*. Advanced Drug Delivery Reviews **66:** 26-41.

Boisguérin P., Deshayes S., Gait M.J., O'Donovan L., Godfrey C., Betts C.A., Wood M.J.A., and Lebleu B. (2015). *Delivery of therapeutic oligonucleotides with cell penetrating peptides.* Advanced Drug Delivery Reviews **87:** 52-67.

Bonnier F., Keating M., Wrobel T.P., Majzner K., and Baranska M. (2015). *Cell viability assessment using the Alamar blue assay: A comparison of 2D and 3D cell culture models*. Toxicology *in Vitro* **29:** 124-131.

Briuglia M., Rotella C., McFarlane A.,and Lamprou D.A. (2015). *Influence of cholesterol on liposome stability and on in vitro drug release*. Drug Delivery and Translational Research **5:** 231-242.

Bugreev D.V., and Nevinsky G.A. (2009). *Structure and mechanism of action of type IA DNA topoisomerases.* Biochemistry (Moscow) **74:** 1467-1481.

Campbell M.J. (1995). *Lipofection reagents prepared by a simple ethanol injection technique*. Biotechniques **18:** 1027-1032.

Caracciolo G. (2015). *Liposome–protein corona in a physiological environment: Challenges and opportunities for targeted delivery of nanomedicine*s. Nanomedicine: Nanotechnology, Biology, and Medicine **11:** 543-557.

Caracciolo G., Callipo L., Candeloro De Sanctis S., Cavaliere C., Pozzi D., and Laganà A. (2010). *Surface adsorption of protein corona controls the cell internalization mechanism of DC-Chol–DOPE/DNA lipoplexes in serum.* Biochimica et Biophysica Acta **1798:** 536-543.

Chatterjee A., Mambo E., and Sidransky D. (2006). *Mitochondrial DNA mutations in human cancer.* Oncogene **25:** 4663-4674.

Chaturvedi R.K., and Beal M.F. (2013). *Mitochondrial diseases of the brain.* Free Radical Biology and Medicine **63:** 1-29.

Chen Z., Zhang L., Song Y., He J., Wu L., Zhao C., Xiao Y., Li W., Cai B., Cheng H., and Li W. (2015). *Hierarchical targeted hepatocyte mitochondrial multifunctional chitosan nanoparticles for anticancer drug delivery.* Biomaterials **52:** 240-250.

Chinnery P.F., and Schon E.A. (2003). *Mitochondria.* Journal of Neurology, Neurosurgery & Psychiatry **74:** 1188-1199.

Christiano R.J., Smith L.C., Kay M.A., Brinkly B.R., and Woo, S.L.C. (1993). *Hepatic gene therapy: efficient gene delivery and expression in primary hepatocytes utilizing a conjugated adenovirus-DNA complex*. Proceedings of the National Academy of Sciences, USA **90:** 11548-11552

Ćurčić M.G., Stanković M.S., Mrkalić E.M., Matović Z.D., Banković D.D., Cvetković D.M., Đačić D.S., and Marković S.D. (2012). *Antiproliferative and proapoptotic activities of methanolic extracts from Ligustrum vulgare L. as an individual treatment and in combination with palladium complex.* International Journal of Molecular Sciences **13:** 2521-2534.

Cury-Boaventura M.F., and Rui Curi C.P. (2004*). A simple technique for quantifying apoptosis in 96-well plates. Comparative toxicity of oleic acid and linoleic acid on Jurkat cells*. Clinical Nutrition **23:** 721-732.

D'Souza G.G.M., and Weissig V. (2004). *Approaches to mitochondrial gene therapy*. Current Gene Therapy **4:** 317-328.

D'Souza G.G.M., and Weissig V. (2009). *Subcellular targeting: A new frontier for drug-loaded pharmaceutical nanocarriers and the concept of the magic bullet*. Expert Opinion on Drug Delivery **6:** 1135-1148.

D'Souza G.G.M., Boddapati S.V., and Weissig V. (2007). *Gene therapy of the other genome: The challenges of treating mitochondrial DNA defects*. Pharmaceutical Research **24:** 228-238.

D'Souza G.G.M., Rammohan R., Cheng S., Torchilin V.P., and Weissig V. (2003). *DQAsome-mediated delivery of plasmid DNA toward mitochondria in living cells*. Journal of Controlled Release **92:** 189-197.

Dan N. (2015). *Lipid-nucleic acid supramolecular complexes: Lipoplex structure and the kinetics of formation.* AIMS Biophysics **2:** 163-183.

Dan N., and Danino D. (2014). *Structure and kinetics of lipid–nucleic acid complexes.* Advances in Colloid and Interface Science **205:** 230-239.

Dass C.R. (2004). *Lipoplex-mediated delivery of nucleic acids: factors affecting in vivo transfection*. Journal of Molecular Medicine **82:** 579-591.

Davis M.E. (2002). *Non–viral gene delivery systems*. Current Opinion in Biotechnology **13:** 128-131.

Deamer D., and Bangham A.D. (1976). *Large volume liposomes by ether vaporisation method*. Biochimica et Biophysica Acta **443:** 629-624.

DiMauro S. (2004a). *Mitochondrial diseases.* Biochimica et Biophysica Acta **1658:** 80-88.

DiMauro S. (2004b). *Mitochondrial medicine.* Biochimica et Biophysica Acta **1659:** 107-114.

DiMauro S. (2007). *Mitochondrial DNA Medicine*. Bioscience Reports **27:** 5-9.

DiMauro S., and Mancuso M. (2007). *Mitochondrial diseases: Therapeutic approaches*. Bioscience Reports **27:** 125-137.

Dolezal P., Likic V., Tachezy J., Lithgow T., (2006). *Evolution of the molecular machines for protein import into mitochondria.* Science **313:** 314-318.

Dowling D.K. (2014). *Evolutionary perspectives on the links between mitochondrial genotype and disease phenotype*. Biochimica et Biophysica Acta **1840:** 1393-1403.

Doyle S.R., and Chan C.K. (2008). *Mitochondrial Gene Therapy: An evaluation of strategies for the treatment of mitochondrial DNA disorders*. Human Gene Therapy **19:** 1335-1348.

Dragovic R.A., Gardiner C., Brooks A.S., Tannetta D.S., Ferguson D.J.P., Hole P., Carr B., Redman C.W.G., Harris A.L., Dobson P.J., Harrison P., and Sargent I.L. (2011). *Sizing and phenotyping of cellular vesicles using Nanoparticle Tracking Analysis.* Nanomedicine **7:** 780-788.

Du H., and Yan S.S. (2010). *Mitochondrial medicine for neurodegenerative diseases.* The International Journal of Biochemistry and Cell Biology **42:** 560-572.

Duarte S., Faneca H., Pedroso de Lima M.C. (2011). *Non-covalent association of folate to lipoplexes: A promising strategy to improve gene delivery in the presence of serum.* Journal of Controlled Release **149:** 264-272.

Durazo S.A., and Kompella U.B. (2011). *Functionalized nanosystems for targeted mitochondrial delivery*. Mitochondrion **12:** 190-201.

.

Farhood H., Bottega R., Epand R.M., and Huang L. (1992). *Effect of cationic cholesterol derivatives on gene transfer and protein kinase C activity*. Biochimica et Biophysica Acta **1235:** 289-295.

Farrar G.J., Chadderton N., Kenna P.F., and Millington-Ward S. (2013). *Mitochondrial disorders: aetiologies, models systems, and candidate therapies*. Trends in Genetics **29:** 488-97.

Felgner J.H., Kumar R., Sridhar C.N., Wheeler C.J., Tsai Y.J., Border,R., Ramsey P., Martin M., and Felgner P.L. (1994). *Enhanced gene delivery and mechanism studies with a novel series of cationic lipid formulations.* Journal of Biological Chemistry **269:** 2550-2561.

Felgner P.L., and Ringold G.M. (1989). *Cationic liposome mediated transfection*. Nature **337:** 387-388.

Felgner P.L., Barenholz Y., Behr J.P., Cheng S.H., Cullis P., Huang L., Jesse J.A., Seymour L., Szoka Jr F.C., Thierry A.R., Wagner E., and Wu G. (1997). *Nomenclature for synthetic gene delivery systems.* Human Gene Therapy **8**: 511-512.

Felgner P.L., Gadek T.R., Holm M., Roman R., Chan H.W., Wenz M., Northrop J.P., Ringold J.M., and Danielsen M. (1987). *Lipofection: A highly efficient, lipid-mediated DNA-transfection procedure.* Proceedings of the National Academy of Sciences, USA **88:** 7413-7417.

Flierl A., Jackson C., Cottrell B., Murdock D., Seibel P., and Wallace D.C. (2003). *Targeted delivery of DNA to the mitochondrial compartment via import sequence conjugated peptide*. Molecular Therapy **7:** 550-557.

Fogh J., and Trempe G. (1975). *New human tumor cell lines*. In Human Tumor Cells *in vitro.* Fogh J., ed. New York. Plenum Publishing Corp: 115- 141.

Friedmann T., and Roblin R. (1972). *Gene therapy for human genetic disease*. Science **175:** 949-955.

Friedrich H., Frederik P.M., de With G., and Sommerdijk N.A.J.M. (2010). *Imaging of self-assembled structures: Interpretation of TEM and Cryo-TEM images*. Angewandte Chemie International Edition **49:** 7850-7858.

Furukawa R., Yamada Y., Kawamura E., and Harashima H. (2015). *Mitochondrial delivery of antisense RNA by MITO-Porter results in mitochondrial RNA knockdown, and has a functional impact on mitochondria*. Biomaterials **57:** 107-115.

Gabizon A.A. (2001). *Stealth liposomes and tumor targeting: one step further in the quest for the magic bullet*. Clinical Cancer Research **7:** 223-225.

Gao X., and Huang L. (1991). *A novel cationic liposome reagent for efficient transfection of mammalian cells*. Biochemical Biophysical Research Communications **179:** 280-285.

Garinot M., Mignet N, Largeau C, Seguin J., Scherman D., and Bessodes M. (2007). *Amphiphilic polyether branched molecules to increase the circulation time of cationic particles*. Bioorganic and Medicinal Chemistry **15:** 3176-3186.

Geall A.J., and Blagbrough I.S. (2000). *Rapid and sensitive ethidium bromide fluorescence quenching assay of polyamine conjugate–DNA interactions for the analysis of lipoplex formation in gene therapy*. Journal of Pharmaceutical and Biomedical Analysis **22:** 849-859.

Goto Y., Nonaka I., and Horai S. (1990). *A mutation in the tRNA(Leu)(UUR) gene associated with the MELAS subgroup of mitochondrial encephalomyopathies*. Nature **348:** 651-653.

Gray M.W., Lang B.F., and Burger G. (2004). *Mitochondria of protists*. Annual Review of Genetics **34:** 477-524.

Gregoriadis G., Bacon A., Caparros-Wanderley W., and McCormack B. (2002). *A role for liposomes in genetic vaccination*. Vaccine **20:** 1-9.

Gresch O., Engel F.B., Nesic D., Tran T.T., England H.M., Hickman E.S., Körner I., Gan L., Chen S., Castro-Obregon S., Hammermann R., Wolf J., Müller-Hartmann H., Nix M., Siebenkotten G., Kraus G., and Luna K. (2004). *New non-viral method for gene transfer into primary cells*. Methods **33:** 151-163.

Griffiths D., Bernt W., Hole P., Smith J., Malloy A., Carr B. (2011). *Zeta potential measurement of nanoparticles by Nanoparticle Tracking Analsis (NTA)*. NSTI-Nanotech. www.nsti.org.

Gross J., Sayle S., Karow A.R., Bakowsky U., and Garidel P. (2016). *Nanoparticle tracking analysis of particle size and concentration detection in suspensions of polymer and protein samples: Influence of experimental and data evaluation parameters*. European Journal of Pharmaceutics and Biopharmaceutics **104:** 30-41.

Heller A., Brockhoff G., and Goepferich A. (2012). *Targeting drugs to mitochondria.* European Journal of Pharmaceutics and Biopharmaceutics **82:** 1-18.

Hellman L.M., and Fried M.G. (2007). *Electrophoretic mobility shift assay (EMSA) for detecting protein-nucleic acid interactions.* Nature Protocols **2:** 1849-1861.

Helvig S., Azmi I.D.M., Moghimi S.M., and Yaghmur A. (2015). *Recent Advances in Cryo-TEM Imaging of Soft Lipid Nanoparticles*. AIMS Biophysics **2:** 116-130.

Hemaprabha E. (2012). *Chemical crosslinking of proteins: A review*. Journal of Pharmaceutical and Scientific Innovation **1:** 22-26.

Hill A.B., Chen M., Chen C.K., Pfeifer B.A., and Jones C.H. (2016). *Overcoming gene-delivery hurdles: Physiological considerations for nonviral vectors*. Trends in Biotechnology **34:** 91-105.

Hirota K., and Terada H. (2012). *Endocytosis of particle formulations by macrophages and its application to clinical treatment.* In Molecular Regulation of Endocytosis. Ceresa B., ed. Intech; 414-427.

Hoekstra D, Rejman J., Wasungu L., Shi F., and Zuhorn I. (2007). *Gene delivery by cationic lipids: in and out of an endosome*. Biochemical Society Transactions **35:** 68-71.

Honary S., and Zahir F. (2013a*). Effect of zeta potential on the properties of nano-drug delivery systems - A review (Part 1).* Tropical Journal of Pharmaceutical Research **12:** 255-264.

Honary S., and Zahir F. (2013b*). Effect of zeta potential on the properties of nano-drug delivery systems - A review (Part 2).* Tropical Journal of Pharmaceutical Research **12:** 265-273.

Hong J.R. and Wu J.L. (2002). *Induction of apoptotic death in cells via Bad gene expression by infectious pancreatic necrosis virus infection*. Cell Death and Differentiation **9:** 113-124.

Horobin R.W., Trapp S., and Weissig V. (2007*). Mitochondriotropics: a review of their mode of action, and their applications for drug and DNA delivery to mammalian mitochondria.* Journal of Controlled Release **121:** 125-136.

Horton K.L., Stewart K.M., Fonseca S.B., Guo Q., and Kelley S.O. (2008*). Mitochondria-Penetrating Peptides*. Chemistry and Biology **15:** 375-382.

Huang J.G., Leshuk T., and Gu F.X. (2011). *Emerging nanomaterials for targeting subcellular organelles*. Nano Today **6:** 478-492.

Huang L., Hung M., and Wagner E. (1999). Nonviral Vectors for Gene Therapy. San Diego, California, Academic Press.

Hui S., Langer M., Zhao Y., Ross P., Hurley E., and Chan K. (1996). *The role of helper lipids in cationic liposome-mediated gene transfer*. Biophysical Journal **71:** 590-599.

Hwang T.L., Hsu C.Y., Aljuffali I.A., Chen C.H., Chang Y.T., and Fang J.Y. (2015). *Cationic liposomes evoke proinflammatory mediator release andneutrophil extracellular traps (NETs) toward human neutrophils.* Colloids and Surfaces B: Biointerfaces **128:** 119-126.

Imani R., Emami S.H., and Faghihi S. (2015). *Synthesis and characterization of an octaarginine functionalized graphene oxide nano-carrier for gene delivery applications*. Physical Chemistry Chemical Physics **17:** 6328-6339.

Immordino M.R., Dosio F., and Cattel L. (2006). *Stealth liposomes: review of the basic science, rationale, and clinical applications, existing and potential*. International Journal of Nanomedicine **1:** 297-315.

Józkowicz A., and Dulak J. (2005). *Helper-dependent adenoviral vectors in experimental gene therapy*. Acta Biochimica Polonica **52:** 589-599.

Ju J., Huan M., Wan N., Hou Y., Ma X., Jia Y., Li C., Zhou S., and Zhang B.(2016). *Cholesterol derived cationic lipids as potential non-viral gene delivery vectors and their serum compatibility.* Bioorganic and Medicinal Chemistry Letters **26:** 2401-2407.

Kasibhatla S., Amarante-Mendes G.P., Finucane D., Brunner T., Bossy-Wetzel E., and Green D.R. (2006). *Acridine orange/ethidium bromide (AO/EB) staining to detect apoptosis*. Cold Spring Harbor Protocols **3:** doi: 10.1101/pdb.prot4493.

Kawamura E., Yamada Y., Yasuzaki Y., Hyodo M., and Harashima H. (2013a). *Intracellular observation of nanocarriers modified with a mitochondrial targeting signal peptide*. Journal of Bioscience and Bioengineering **116:** 634-637.

Kawamura E., Yamada Y., and Harashima H. (2013b). *Mitochondrial targeting functional peptides as potential devices for the mitochondrial delivery of a DF-MITO-Porter*. Mitochondrion **13:** 610-614.

Khalil I.A., Kogure K., Futaki S., and Harashima H. (2006a). *High density of octaarginine stimulates macropinocytosis leading to efficient intracellular trafficking for gene expression.* The Journal Of Biological Chemistry **281:** 3544-3551.

Khalil I.A., Kogure K., Akita H., and Harashima H. (2006b). *Uptake pathways and subsequent intracellular trafficking in nonviral gene delivery*. Pharmacological Reviews **58:** 32-45.

Kim B., Seu Y., Bae Y., Kwak T., Kang H., Moon I., Hwang G., Park S., and Doh K. (2014). *Efficient delivery of plasmid DNA using cholesterol-based cationic lipids containing polyamines and ether linkages.* International Journal of Molecular Sciences **15:** 7293-7312.

Kim B., Hwang G., Seu Y., Choi J., Jin K.S., and Doh K. (2015). *DOTAP/DOPE ratio and cell type determine transfection efficiency with DOTAP-liposomes.* Biochimica et Biophysica Acta **1848:** 1996-2001.

Knowles B.B., Howe C.C., and Aden D.P. (1980). *Human hepatocelluar carcinoma cell lines secrete major plasma proteins and Hepatitis B surface antigens*. Science **209:** 497-499.

Knudsen K.B., Northeved H., Kumar P., Permin A., Gjetting T., Andresen T.L., Larsen S., Wegener K.M., Lykkesfeldt J., Jantzen K., Loft S., Møller P., and Roursgaard M. (2015). *In vivo toxicity of cationic micelles and liposomes.* Nanomedicine: Nanotechnology, Biology, and Medicine **11:** 467-477.

Koumbi D., Clement J., Sideratou Z., Yaouanc J., Loukopoulos D., and Kollia P. (2006). *Factors mediating lipofection potency of a series of cationic phosphonolipids in human cell lines.* Biochimica et Biophysica Acta **1760:** 1151-1159.

Kreiss P., Cameron B., Rangara R., Mailhe P., Aguerre-Charriol O., Airiau M., Scherman D., Crouzet J., and Pitard B. (1999). *Plasmid DNA size does not affect the physicochemical properties of lipoplexes but modulates gene transfer efficiency*. Nucleic Acids Research **27:** 3792-3798.

Kuntsche J., Horst J.C., and Bunjes H. (2011). *Cryogenic transmission electron microscopy (cryo-TEM) for studying the morphology of colloidal drug delivery systems*. International Journal of Pharmaceutics **417:** 120-137.

Larsson N., and Luft R. (1999). *Revolution in mitochondrial medicine*. FEBS Letters **455:** 199-202.

Lasic D.D. (1997). Liposomes in Gene Delivery. Boca Raton, Florida, CRC Press LLC.

Layek B., Lipp L., and Singh J. (2015). C*ell penetrating peptide conjugated chitosan for enhanced delivery of nucleic acid.* International Journal of Molecular Sciences **16:** 28912-28930.

LePecq J.B., and Paoletti C. (1967). *A fluorescent complex between ethidium bromide and nucleic acids: Physical-chemical characterisation*. Journal of Molecular Biology **1:** 87-106.

Lesage D., Cao A., Briane D., Lievre N., Coudert R., Raphael M., Salzmann J.L., and Taillandier E. (2002). *Evaluation and optimisation of DNA delivery into gliosarcoma 9L cells by a cholesterol-based cationic liposome*. Biochimica et Biophysica Acta **154:** 393-402.

Li S., and Ma Z. (2001). *Nonviral gene therapy*. Current Gene Therapy **1:** 1-35.

Liu K., Liu P., Liu R., and Wu X. (2015). *Dual AO/EB staining to detect apoptosis in osteosarcoma cells compared with flow cytometry*. Medical Science Monitor Basic Research **21:** 15-20.

Liu L., and Huang L. (2002). *Development of non-viral vectors for systemic gene delivery.* Journal of Controlled Release **78:** 259-266.

Lonez C., Vandenbranden M., and Ruysschaert J. (2008). *Cationic liposomal lipids: from gene carriers to cell signalling*. Progress in Lipid Research **47:** 340-347.

Lopes S.C.A., dos Santos Giuberti C., Guieiro Ribeiro Rocha T., dos Santos Ferreira D., Leite E.A., and Oliveira M.C. (2013). *Liposomes as Carriers of Anticancer Drugs*, Cancer Treatment - Conventional and Innovative Approaches, Prof. Letícia Rangel (Ed.), InTech,

Lucey B.P., Nelson-Rees W.A., Hutchins G.M. (2009). *Henrietta Lacks, HeLa cells, and cell culture contamination.* Archives of Pathology & Laboratory Medicine *133:* 1463-1467.

Luft R., Ikkos D., Palmieri G., Ernster L., and Afzelius B. (1962). *A case of severe hypermetabolism of nonthyroid origin with a defect in the maintenance of mitochondrial respiratory control: a correlated clinical, biochemical and morphological study*. Journal of Clinical Investigation **41:** 1776-1804.

Lui Z., and Chen B. (2004). *Caco-2 cell monolayers and its application in toxicological research.* Journal Of Hygiene Research **33:** 756-759.

Lv H., Zhang S.,Wang B., Cui S., and Yan J. (2006). *Toxicity of cationic lipids and cationic polymers in gene delivery*. Journal of Controlled Release **114:** 100-109.

Lyrawati D., Trounson A., and Cram D. (2011). *Expression of GFP in the mitochondrial compartment using DQAsome-mediated delivery of an artificial mini-mitochondrial genome*. Pharmaceutical Research **28:** 2848-2862.

Ma B., Zhang S., Jiang H., Zhao B., and Lv H. (2007). *Lipoplex morphologies and their influences on transfection efficiency in gene delivery.* Journal of Controlled Release **123:** 184-194.

Madeira C ., Loura L.M.S., Prieto M., Fedorov A., and Aires-Barros M.R. (2008). *Effect of ionic strength and presence of serum on lipoplexes structure monitorized by FRET.* BMC Biotechnology **8:** 20.

Magarkar A., Dhawan V., Kallinteri P., Viitala T., Elmowafy M., Ro´g T., and Bunker A. (2014). *Cholesterol level affects surface charge of lipid membranes in saline solution.* Scientific Reports **4:** 1-5.

Mancuso M., Filosto M., Choub A., Tentorio M., Broglio L., Padovani A., and Siciliano G. (2007). *Mitochondrial DNA-related disorders*. Bioscience Reports **27:** 31-37.

Manfredi G., Fu J., Ojaimi J., Sadlock J.E., Kwong J.Q., Guy J., and Schon E.A. (2002). *Rescue of a deficiency in ATP synthesis by transfer of MTATP6, a mitochondrial DNA encoded gene, to the nucleus*. Nature Genetics **30:** 394-399.

Manjila S.B., Baby J.N., Bijin E.N., Constantine I., Pramod K., and Valsalakumari J. (2013). *Novel gene delivery systems*. International Journal of Pharmaceutical Investigation **3:** 1-7.

Marchini C., Montani M., Amici A., Amenitsch H., Marianecci C., Pozzi P., and Caracciolo G. (2009). *Structural stability and increase in size rationalize the efficiency of lipoplexes in serum.* Langmuir **25:** 3013-3021.

Masotti A., Mossa G., Cametti C., Ortaggi G., Bianco A., Del Grosso N., Malizia D., and Esposito C. (2009). *Comparison of different commercially available cationic liposome–DNA lipoplexes: Parameters influencing toxicity and transfection efficiency*. Colloids and Surfaces B: Biointerfaces **68:** 136-44.

Mayor S., and Pagano R. E. (2007). *Pathways of clathrinin dependent endocytosis.* Nature Reviews Molecular Cell Biology **8:** 603-612.

Mazunin I.O., Volodko N.V., Starikovskaya E.B., and Sukernik R.I. (2010). *Mitochondrial genome and human mitochondrial diseases.* Molecular Biology **44:** 665-681.

Mertena O., and Gaillet B. (2016). *Viral vectors for gene therapy and gene modification approaches*. Biochemical Engineering Journal **108:** 98-115.

Meyer O., Kirpotin D., Hong K., Sternberg B., Park J.W., Woodle M. C., and Papahadjopoulos D. (1998). *Cationic liposomes coated with polyethylene glycol as carriers for oligonucleotides*. The Journal of Biological Chemistry **273:** 15621-15627.

Milane L., Trivedi M., Singh A., Talekar M., and Amiji M. (2015). *Mitochondrial biology, targets, and drug delivery*. Journal of Controlled Release **207**: 40-58.

Monteiro L.O.F. , Lopes S.C.A., Barros A.B., Magalhães-Paniago R., Malachias A., Oliveira M.C., and Leite E.A. (2016). *Phase behavior of dioleyphosphatidylethanolamine molecules in thepresence of components of pH-sensitive liposomes and paclitaxel*. Colloids and Surfaces B: Biointerfaces **144:** 276-283.

Moreira P.I., Zhu X., Wang X., Lee H., Nunomura A., Petersen R.B., Perry G., and Smith M.A. (2010). *Mitochondria: A therapeutic target in neurodegeneration*. Biochimica et Biophysica Acta **1802:** 212-220.

Motta S., Rondelli V., Cantu L., Del Favero E. , Aureli M. , Pozzi D., Caracciol G., and Brocca P. (2016*). What the cell surface does not see: The gene vector under the protein corona*. Colloids and Surfaces B: Biointerfaces **141:** 170-178.

Mountain A. (2000). *Gene therapy: the first decade*. TIBTECH **18:** 119-128.

Mukhopadhyay A., and Weiner H. (2007). *Delivery of drugs and macromolecules to mitochondria.* Advanced Drug Delivery Reviews **59:** 729-738.

Mullen C.A., Snitzer K., Culver K.W., Morgan R.A., Anderson W.F., and Blaese R.M. (1996). *Molecular analysis of T lymphocyte-directed gene therapy for adenosine deaminase deficiency: Long term expression in vivo of genes introduced with a retroviral vector*. Human Gene Therapy **49:** 807-837.

Murphy M.P., and Smith R.A.J. (2000). *Drug delivery to mitochondria: the key to mitochondrial medicine.* Advanced Drug Delivery Reviews **41:** 235-250.

Naicker K., Ariatti M., Singh M. (2014). *PEGylated galactosylated cationic liposomes for hepatocytic gene delivery*. Colloids Surfaces B Biointerfaces **122:** 482-490.

NanoSight Application Note: Zeta Potential Analysis using Z-NTA (M121A), www.nanosight.com

NanoSight, (2015a). *NTA: Principles and methodology*. Malvern Instruments Limited, www.malvern.com

NanoSight, (2015b). *Nanoscale material characterization: A Review of the use of Nanoparticle.* Malvern Instruments Limited, www.malvern.com

Nayerossadat N., Maedeh T., and Abas Ali P. (2012). *Viral and nonviral delivery systems for gene delivery.* Advanced Biomedical Research **1:** 27.

Neupert W., and Herrmann J.M., (2007). *Translocation of proteins into mitochondria*. Annual Review of Biochemistry **76:** 723-749.

Niazi A.K.., Mileshina D., Cosset A., Val R., Weber-Lotfi F., Dietrich A. (2013). *Targeting nucleic acids into mitochondria: Progress and prospects*. Mitochondrion **13:** 548-558.

Niazi I. K., Kersting N. M., Jiang N., Dremstrup K., Farina D. (2012). *Peripheral electrical stimulation triggered by self-paced detection of motor intention enhances motor evoked potentials*. IEEE Transactions on Neural Systems and Rehabilitation Engineering **20:** 595-604.

Nishikawa M., and Huang L. (2001). *Nonviral vectors in the new millennium: Delivery barriers in gene transfer*. Human Gene Therapy **12:** 861-870.

Obata Y., Saito S., Takeda N., and Takeoka S. (2009). *Plasmid DNA-encapsulating liposomes: effect of spacer between the cationic head group and hydrophobic moieties of the lipids on gene expression efficiency*. Biochimica et Biophysica Acta **1788:** 1148-1158.

O'Brien J., Wilson I., Orton T., and Pognan F. (2000). *Investigation of the Alamar Blue (resazurin) fluorescent dye for the assessment of mammalian cell cytotoxicity*. European Journal of Biochemistry **267:** 5421-5426.

Oku N., Tokudome Y., Asai T., and Tsukada H. (2000). *Evaluation of drug targeting strategies and liposomal trafficking*. Current Pharmaceutical Design **6:** 1669-1691.

Pearce S., Nezich C.L., and Spinazzola A. (2013). *Mitochondrial diseases: Translation matters*. Molecular and Cellular Neuroscience **55:** 1-12.

Percot A., Briane D., Coudert R., Reynier P., Bouchemal N., Lievre N., Hantz E., Salzmann J.L., and Cao A. (2004). *A hydroxyethylated cholesterol-based cationic lipid for DNA delivery: effect of conditioning*. International Journal of Pharmaceutics **278**: 143-163.

Ramezani M., Khoshhamdam M., Dehshahri A., Malaekeh-Nikoue B. (2009). *The influence of size, lipid composition and bilayer fluidity of cationic liposomes on the transfection efficiency of nanolipoplexes*. Colloids and Surfaces B: Biointerfaces **72:** 1-5.

Rampersad S.N. (2012). *Multiple applications of alamar blue as an indicator of metabolic function and cellular health in cell viability bioassays*. Sensors **12:** 12347-12360.

Rejman J., Wagenaar A., Engberts J.F.B.N., and Hoekstra D. (2004). *Characterization and transfection properties of lipoplexes stabilized with novel exchangeable polyethylene glycol–lipid conjugates.* Biochimica et Biophysica Acta **1660:** 41-52.

Ribble D., Goldstein N.B., Norris D.A., and Shellman Y.G. (2005). *A simple technique for quantifying apoptosis in 96-well plates*. BMC Biotechnology **5:** 12-18.

Riss T.L., Moravec R.A., Niles A.L., Duellman S., Benink H.A., Worzella T.L., and Minor L. (2013). *Cell viability assays* In Assay Guide Manual. Sittampalam G.S., Coussens N.P, ed. Creative Commons Attribution-NonCommercial-ShareAlike

Rock K.L., and Kono H. (2008). *The inflammatory response to cell death.* Annual Review of Pathology: Mechanisms of Disease **3:** 99-126.

Róg T., Pasenkiewicz-Gierula M., Vattulainen I., and Karttunen M. (2009). *Ordering effects of cholesterol and its analogues.* Biochimica et Biophysica Acta **1788:** 97-121.

Ropert C. (1999). *Liposomes as a gene delivery system*. Brazilian Journal of Medical and Biological Research **32:** 163-169.

Ross P.C., and Hui S.W. (1999). *Lipoplex size is a major determinant of in vitro lipofection efficiency.* Gene Therapy **6:** 651-659.

Ruozi B., Bellett D., Tombesi A., Tosi G., Bondioli L., Forni F., and Vandelli M.A. (2011). *AFM, ESEM, TEM, and CLSM in liposomal characterization: A comparative study*. International Journal of Nanomedicine **6:** 557-563.

Russell O., and Turnbull D. (2014). *Mitochondrial DNA disease – molecular insights and potential routes to a cure.* Experimental Cell Research **325:** 38-43.

Salvado R., Sousa F., Queiroz J., and Costa D. (2015). *Development of mitochondrial targeting plasmid DNA nanoparticles:Characterization and in vitro studies.* Colloids and Surfaces A: Physicochemical and Engineering Aspects **480:** 287-295.

Sambuy Y., De Angelis I., Ranaldi G., Scarino M.L., Stammati A., Zucco F. (2005). *The Caco-2 cell line as a model of the intestinal barrier: Influence of cell and culture related factors on Caco-2 cell functional characteristics*. Cell Biology and Toxicology **21:** 1-26.

Sanitta P., Apiratikul N., Niyomtham N., Yingyongnarongkul B., Assavalapsakul W., Panyima S., Udomki A. (2016). *Cholesterol-based cationic liposome increases dsRNA protection of yellow head virus infection in Penaeus vannamei*. Journal of Biotechnology **228:** 95-102.

Santos J., Sousa F., Quiroz J., Costa D. (2014). *Rhodamine based plasmid DNA nanoparticles for mitochondrial gene therapy.* Colloids and Surfaces B: Biointerfaces **121:** 129-140.

Santos S., Silva A.M., Matos M., Monteiro S.M., and Álvaro A.R. (2016). C*opper induced apoptosis in Caco-2 and Hep-G2 cells: Expression of caspases 3, 8 and 9, AIF and p53.* Comparative Biochemistry and Physiology C **185-186:** 138–146.

Scheibye-Knudsen M., Mitchell S.J., Fang E.F., Iyama T., Ward T., Wang J., Dunn C.A., Singh N., Veith S., Hasan-Olive M.M., Mangerich A., Wilson M.A., Mattson M.P., Bergersen L.H., Cogger V.C., Warren A., Le Couteur D.G., Moaddel R., Wilson D.M., Croteau D.L., de Cabo R., Bohr V.A. (2014). *A high fat diet and NAD^+ rescue premature aging in Cockayne Syndrome*. Cell Metabolism **20:** 840-855.

Scott V., Clark A.R., and Docherty K. (1994). *Gel Retardation Assay.* Methods in Molecular Biology. Harwood A.S. ed. New York, Humana Press: 31: 339.

Severino P., Szymanski M., Favaro M., Azzoni A.R., Chaud M.V., Santana M.H.A., Silva A.M., and Souto E.B. (2015). *Development and characterization of a cationic lipid nanocarrier as non-viral vector for gene therapy*. European Journal of Pharmaceutical Sciences **66:** 78-82.

Shim G., Kim M., Park J.Y., and Oh Y. (2013). *Application of cationic liposomes for delivery of nucleic acids.* Asian Journal of Pharmaceutical Sciences **8:** 72-81.

Siekevitz P. (1957). *Powerhouse of the Cell*. Scientific American **197:** 131-144.

Singh M. (1998). *Liposome-asialoorosomucoid complexes and their delivery of an expression vector to HepG2 cells in culture*. MSc Thesis, University of Durban-Westville.

Singh M., and Ariatti M. (2006). *A cationic cytofectin with long spacer meadiates favourable transfection in transformed human epithelial cells.* International Journal of Pharmaceutics **309:** 189-198.

Singh M., Borain J., Noor-Mahomed N., and Ariatti M. (2011). *The effect of pegylation on the transfection activity of two homologous cationic cholesteryl cytofectins*. African Journal of Biotechnology **10:** 1400-1707.

Singh M., Kisoon N., and Ariatti M. (2001). *Receptor-mediated gene delivery to HepG2 cells by ternary assemblies containing cationic liposomes and cationised asialoorosamucoid*. Drug Delivery **8**: 29-34.

Smith A.E. (1999). *Gene therapy – where are we?*. Lancet **354:** 1-4.

Smith J.G., Walzem R.L., and German B. (1993). *Liposomes as agents of DNA transfer*. Biochimica et Biophysica Acta **1154:** 327-340.

Sobell H.M., Tsai C.C., Jain S.C., and Gilbert S.G. (1977). *Visualisation of drug nucleic acid interactions at atomic resolution . III. Unifying structural concepts in understanding drug-DNA interactions and their broader implications in understanding protein-DNA interactions*. Journal of Molecular Biology **114:** 333-365.

Stepanenko A.A., and Dmitrenko V.V. (2015). *HEK293 in cell biology and cancer research: Phenotype, karyotype, tumorigenicity, and stress-induced genome-phenotype evolution*. Gene **569:** 182-190.

Stockert J.C., Blázquez-Castro A., Cañete M., Horobin R.W., Villanueva A. (2012). *MTT assay for cell viability: Intracellular localization of the formazan product is in lipid droplets*. Acta Histochemica **114:** 785-796.

Stoddart M.J. (2011). *Cell viability assays: Introduction* In Mammalian Cell Viability, Methods and Protocols. Stoddart M.J., ed. Springer New York Dordrecht Heidelberg London, Humana Press: 1-28.

Szoka Jr F.C., and Papahadjopoulos D. (1978). *Procedure for preparation of liposomes with large internal aqueous space and high capture by reverse-phase evaporation.* Proceedings of the National Academy of Sciences, USA **75:** 4194-4198.

Takano S., Aramaki Y., and Tsuchiya S. (2003). *Physicochemical properties of liposomes affecting apoptosis induced by cationic liposomes in macrophages*. Pharmaceutical Research **20:** 962-968.

Thomas P., and Smart T.G. (2005). *HEK293 cell line: A vehicle for the expression of recombinant proteins.* Journal of Pharmacological and Toxicological Methods **51:** 187-200.

Tischner C., and Wenz T. (2015). *Keep the fire burning: Current avenues in the quest of treating mitochondrial disorders.* Mitochondrion **24:** 32-49.

Torchilin V. (2003). *Liposomes: a practical approach*. **2nd Edition**. New York, Oxford University Press.

Tros de Ilarduya C., Arangoa M.A., Moreno-Aliaga M.J., Düzgüneş N. (2002). *Enhanced gene delivery in vitro and in vivo by improved transferrin-lipoplexes*. Biochimica et Biophysica Acta **1561:** 209-221.

Tros de Ilarduya C., Sun Y., and Düzgünes N. (2010). *Gene delivery by lipoplexes and polyplexes*. European Journal of Pharmaceutical Sciences **40:** 159-170.

Tuppen H.A.L., Blakely E.L., Turnbull D.M., and Taylor R.W. (2010). *Mitochondrial DNA mutations and human disease*. Biochimica et Biophysica Acta **1797:** 113-128.

Vercauteren D., Rejman J., Martens T.F., Demeester J., De Smedt S.C., Braeckmans K. (2012). *On the cellular processing of non-viral nanomedicines for nucleic acid delivery: Mechanisms and methods*. Journal of Controlled Release **161:** 566–581.

Viscomi C., Bottani B., and Zeviani M. (2015). *Emerging concepts in the therapy of mitochondrial disease*. Biochimica et Biophysica Acta **1847:** 544-557.

Von Stockum S., Nardin A., Schrepfer E., and Ziviani E. (2016). *Mitochondrial dynamics and mitophagy in Parkinson's disease: A flypoint of view*. Neurobiology of Disease **90:** 58-67.

Walther W., and Stein U. (2000). *Viral vectors for gene transfer: A review of their use in the treatment of human diseases*. Drugs **60:** 249-271.

Wang S., Cheng L., Yu F., Pan W., and Zhang J. (2006). *Delivery of different length poly(L-lysine)-conjugated ODN to Hepg2 cells using N-stearyllactobionamide-modified liposomes and their enhanced cellular biological effects*. International Journal of Pharmaceutics **311:** 82-88.

Wang B., Zhou1 J., Cui S., Yang B., Zhao Y., ZhaoY., Duan Y., and Zhang S. (2012). *Cationic liposomes as carriers for gene delivery: Physico-chemical characterization and mechanism of cell transfection*. African Journal of Biotechnology **11:** 2763-2773.

Wasungu L., and Hoekstra D. (2006). *Cationic lipids, lipoplexes and intracellular delivery of genes*. Journal of Controlled Release **116:** 255-264.

Weissig V. (2011). *From serendipity to mitochondria-targeted nanocarriers*. Pharmaceutical Research **28:** 2657-2668.

Weissig V., Boddapati S.V., Cheng S., and D'Souza G.G.M. (2006). *Liposomes and liposome-like vesicles for drug and DNA delivery to mitochondria*. Journal of Liposome Research, **16:** 249-264.

Weissig V., Boddapati S.V., Jabr L., and D'Souza G.G. (2007). *Mitochondria-specific nanotechonlogy*. Nanomedicine **2:** 275-285.

Weissig V., Cheng S.M., and D'Souza G.G. (2004). *Mitochondrial pharmaceutics*. Mitochondrion **3:** 229-244.

Weissig V., D'Souza G.G.M., and Torchilin V.P. (2001). *DQAsome/DNA complexes release DNA upon contact with isolated mouse liver mitochondria*. Journal of Controlled Release **75:** 401-408.

Wessig V. (2005). *Targeted drug delivery to mammalian mitochondria in living cells*. Expert Opinion in Drug Delivery **2:** 89-102.

Wirth T., Parker N., Ylä-Herttuala S. (2013). *History of gene therapy*. Gene **525:**162-169.

Won Y., Lim K.S., Kim Y. (2011). *Intracellular organelle-targeted non-viral gene delivery systems.* Journal of Controlled Release **152:** 99-109.

Xu L., and Anchordoquy T.J. (2008). *Cholesterol domains in cationic lipid/DNA complexes improve transfection*. Biochimica et Biophysica Acta **1778:** 2177-2181.

Xu R. (2008). *Progress in nanoparticles characterization: Sizing and zeta potential measurement.* Particuology **6:** 112-115.

Xu Y., Hui S.W., Frederik P., and Szoka Jr F.C. (1999). *Physicochemical characterization and purification of cationic liposomes*. Biophysical Journal. **77:** 341-353.

Yamada Y., Akita H., Kamiya H., Kogure K., Yamamoto T., Shinohara Y., Yamashita K., Kobayashi H., Kikuchi H., and Harashima H. (2008). *MITO-Porter: A liposome-based carrier system for delivery of macromolecules into mitochondria via membrane fusion*. Biochimica et Biophysica Acta **1778:** 423-432.

Yamada Y., Akita H., Kogure K., Kamiya H., and Harashima H. (2007). *Mitochondrial drug delivery and mitochondrial disease therapy – An approach to liposome-based delivery targeted to mitochondria*. Mitochondrion **7:** 63-71.

Yamada Y., and Harashima H. (2008). *Mitochondrial drug delivery systems for macromolecule and their therapeutic application to mitochondrial diseases.* Advanced Drug Delivery Reviews **60:** 1439-1462.

Yamada Y., and Harashima H. (2012). *Delivery of bioactive molecules to the mitochondrial genome using a membrane-fusing, liposome-based carrier, DF-MITO-Porter*. Biomaterials **33:** 1589-1595.

Yamada Y., and Harashima H. (2013). *Enhancement in selective mitochondrial association by direct modification of a mitochondrial targeting signal peptide on a liposomal based nanocarrier.* Mitochondrion **13:** 526-532.

Yamada Y., Fukuda Y., and Harashima H. (2015). *An analysis of membrane fusion between mitochondrial double membranes and MITO-Porte*r, mitochondrial fusogenic vesicles. Mitochondrion **24:** 50-55.

Yamada Y., Furukawa R., Yasuzaki Y., and Harashima H. (2011). *Dual Function MITO-Porter, a nano carrier integrating both efficient cytoplasmic delivery and mitochondrial macromolecule delivery.* Molecular Therapy **19:** 1449-1456.

Yamada Y., Kawamura E., and Harashima H. (2012). *Mitochondrial-targeted DNA delivery using a DF-MITO-Porter, an innovative nano carrier with cytoplasmic and mitochondrial fusogenic envelopes*. Journal of Nanoparticle Research **14:** 1013.

Yang S., Zheng Y., Chen J., Zhang Q., Zhao D., Han D., and Chen H. (2013). *Comprehensive study of cationic liposomes composed of DC-Chol and cholesterol with different mole ratios for gene transfection*. Colloids and Surfaces B: Biointerfaces **101:** 6-13.

Yasuzaki Y.,Yamada Y., and Harashima H. (2010). M*itochondrial matrix delivery using MITO-Porter, a liposome-based carrier that specifies fusion with mitochondrial membranes*. Biochemical and Biophysical Research Communications **397:** 181-186.

Yu M. (2012). *Somatic mitochondrial DNA mutations in human cancers*. Advances in Clinical Chemistry **57:** 99-138.

Zalipsky S., Hansen C.B., Lopes de Menezes D.E., and Allen T.M. (1996). *Long-circulating, polyethylene glycol-grafted immunoliposomes.* Journal of Controlled Release **39:** 153-161.

Zhang E., Zhang C., Su Y., Cheng T., and Shi C. (2011). *Newly developed strategies for multifunctional mitochondria-targeted agents in cancer therapy.* Drug Discovery Today **16:** 140-146.

Zhang Y., and Anchordoquy T.J. (2004). *The role of lipid charge density in the serum stability of cationic lipid/DNA complexes.* Biochimica et Biophysica Acta **1663:** 143-157.

Zhdanov R.I., Podobed O.V., and Vlassov V.V. (2002). *Cationic lipid-DNA complexes – lipoplexes – for gene transfer and therapy*. Bioelectrochemistry **58:** 53-64.

Zuhorn I.S., Visser W.H., Bakowsky U., Engberts J.B.F.N., and Hoekstra D. (2002). *Interference of serum with lipoplex-cell interaction: Modulation of intracellular processing*. Biochimica et Biophysica Acta **1560:** 25-36.

http://www.pharmainfo.net/characterization-nanoparticles/zeta (accessed 08/04/2015).
www.technologyinscience.blogspot.com (accessed 19/07/2015).
http://www.abedia.com/wiley/index.html (accessed 03/03/2016).
www.rachithscellanalogy.weebly.com (accessed 21/11/2015).
http://www.mitomap.org (accessed 20/05/2016)
http://www.plasmidfactory.com (accessed 20/02/2013).

APPENDIX A

3β [*N*-(*N'*, *N'*-dimethylaminopropane)-carbamoyl] cholesterol (CHOL-T)

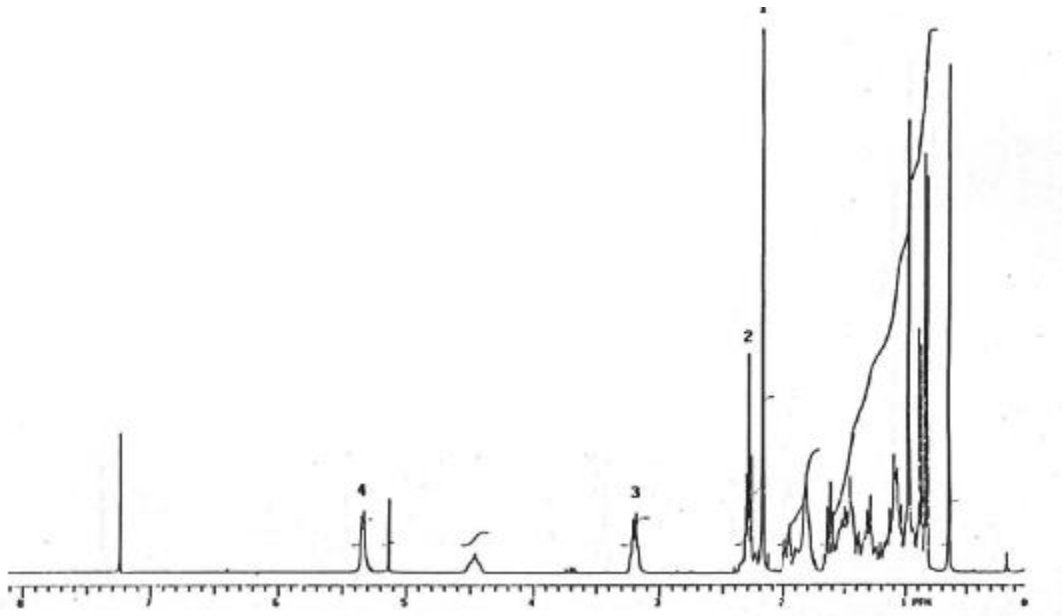

3β-[N-(hydrazino 3-{2-pyridyldithio} propionate)-carbamoyl] cholesterol (SP-CHOL)

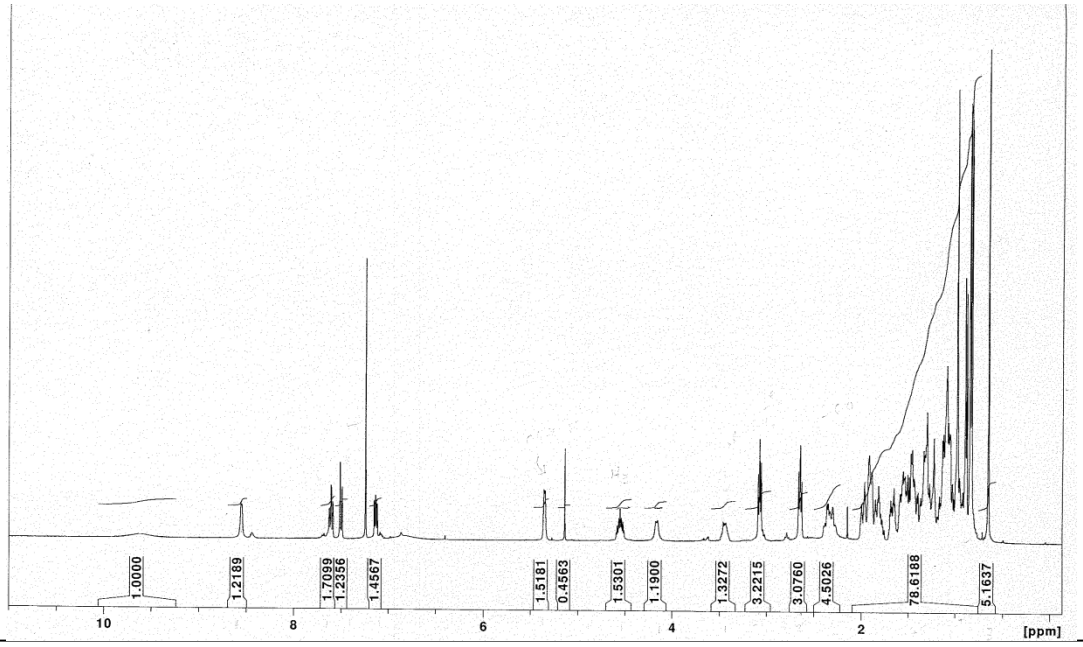

3β-[N-(hydrazino-γ-maleimidobutyryl)-carbamoyl] cholesterol (GM-CHOL)

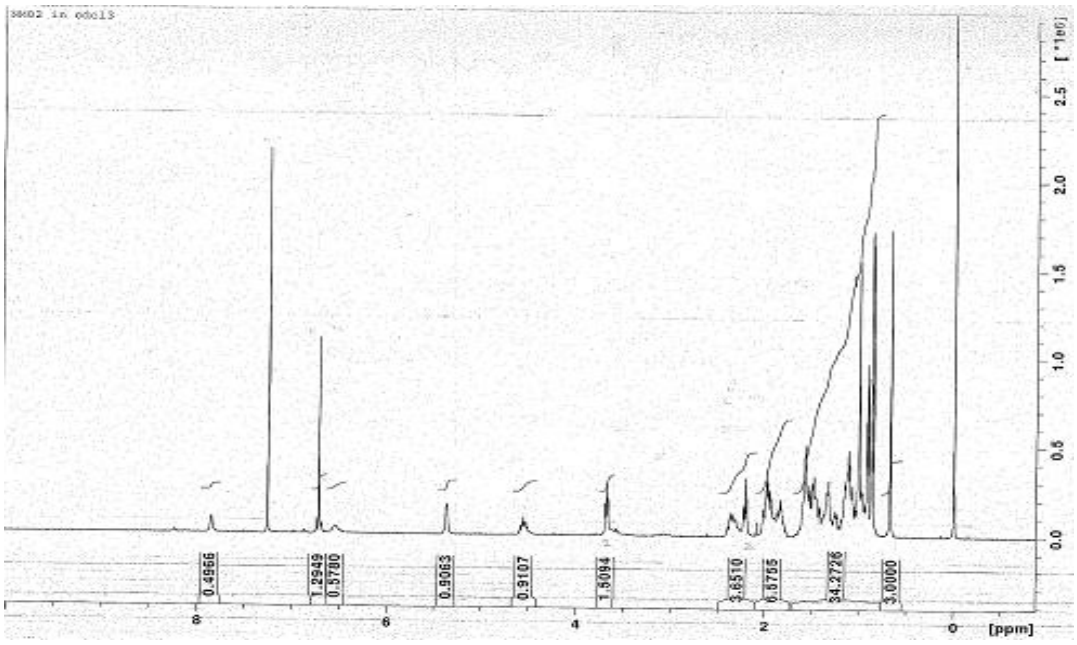

Ocataarginine (R8)

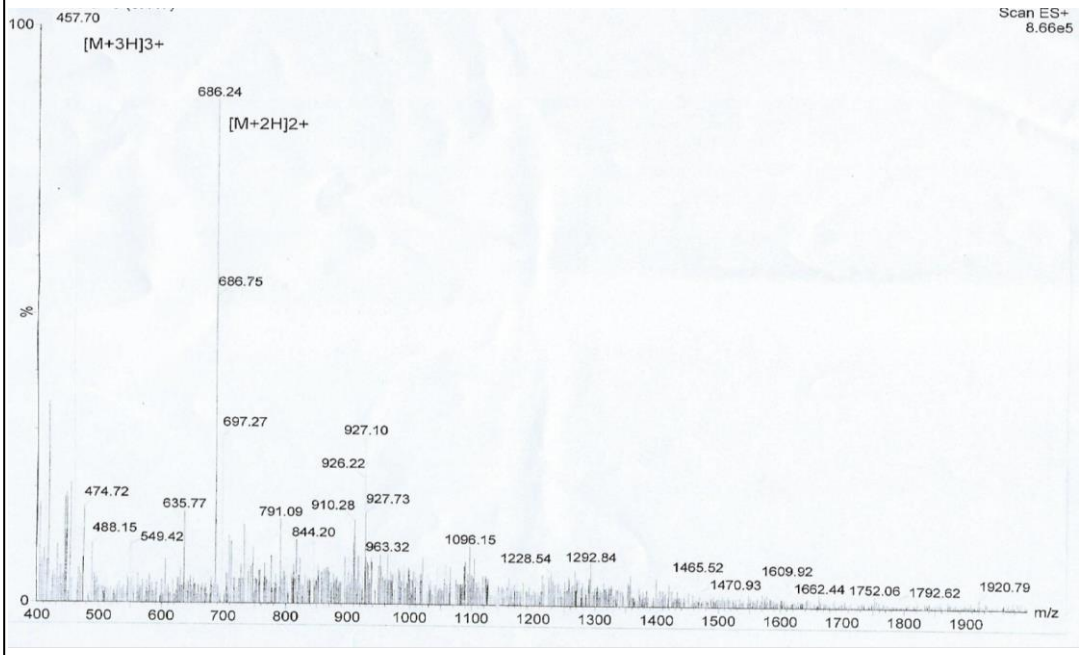

Mitochondrial Targeting Peptide (MTS)

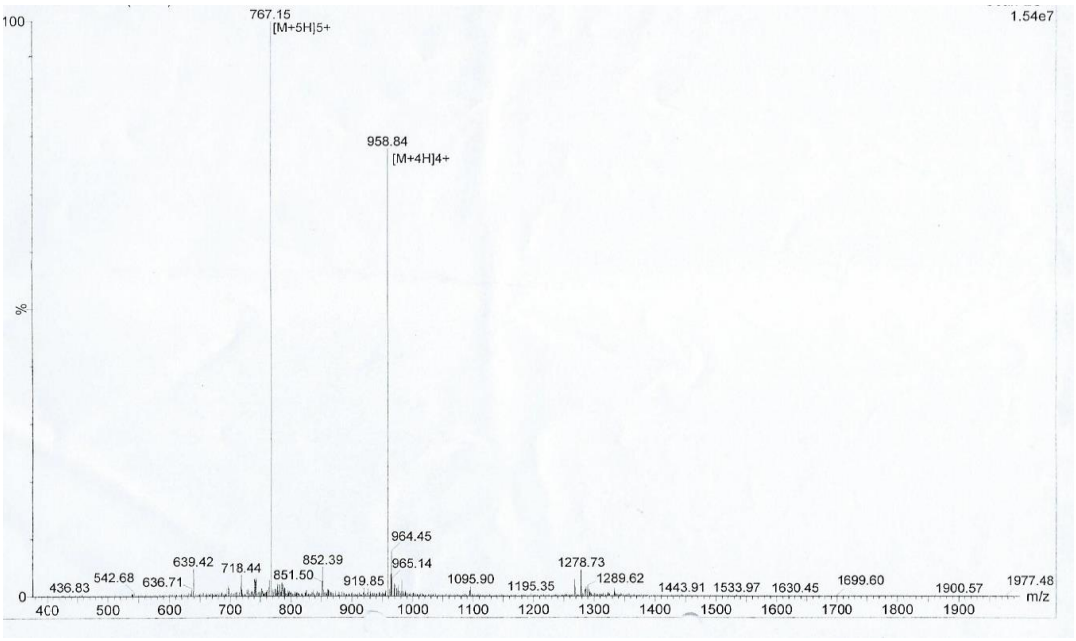

Representative NTA Report

NANOSIGHT NN2_Plex_3%HBS2 2015-12-08 13-48-42

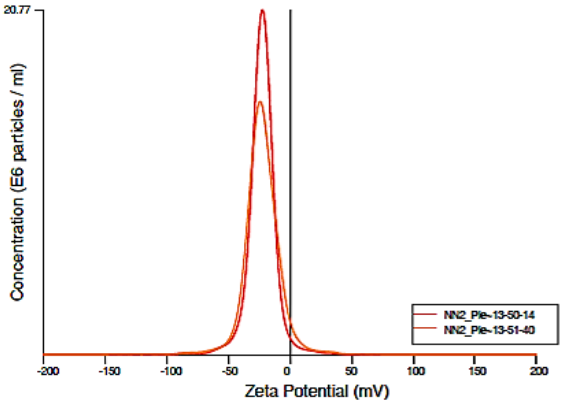

Zeta Potential / Concentration graph for Experiment:
NN2_Plex_3%HBS2 2015-12-08 13-48-42

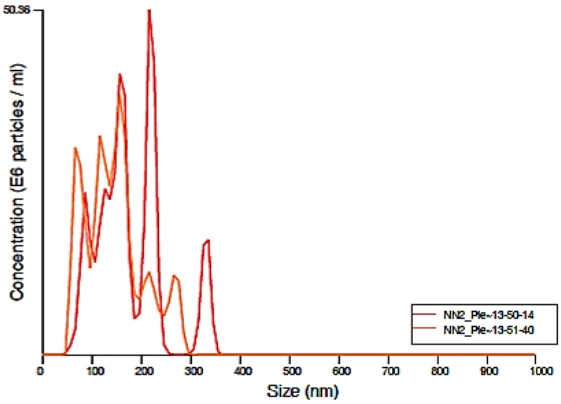

Size / Concentration graph for Experiment:
NN2_Plex_3%HBS2 2015-12-08 13-48-42

Included Files

NN2_Plex_3%HBS2 2015-12-08 13-50-14
NN2_Plex_3%HBS2 2015-12-08 13-51-40

Details

NTA Version:	NTA 3.0 0069
Script Used:	SOP Zeta Measurement 01-48-42PM 08Dec2015.txt
Time Captured:	13:48:42 08/12/2015
Operator:	Nico
Pre-treatment:	
Sample Name:	NN2_Plex_3%HBS2
Diluent:	3%HBS
Remarks:	

Capture Settings

Camera Type:	SCMOS
Camera Level:	8
Slider Shutter:	350
Slider Gain:	250
FPS	25.0
Number of Frames:	1498
Temperature:	25.0 ºC
Viscosity:	(Water) 0.9 cP
Dilution factor:	Dilution not recorded

Analysis Settings

Detect Threshold:	13
Blur Size:	Auto
Max Jump Distance:	Auto: 13.0 - 14.0 pix

Results

Stats: Mean +/- Standard Error

Mean:	155.8 +/- 16.0 nm
Mode:	186.9 +/- 31.1 nm
SD:	63.8 +/- 5.0 nm
D10:	70.3 +/- 10.6 nm
D50:	142.0 +/- 11.4 nm
D90:	233.5 +/- 7.9 nm
Concentration:	4.27e+008 +/- 9.56e+006 particles/ml
	21.7 +/- 0.5 particles/frame
	41.7 +/- 0.7 centres/frame

Zeta Settings and Results

Parabola fit complete

Adjusted r-square:	1.00
Applied Voltage:	24.0 V
Dielectric Constant:	80.00
AverageCurrent:	23.99 - 41.58 µA

Stats: Mean +/- Standard Error

Mean:	-23.2 +/- 0.1 mV
Mode:	-23.3 +/- 0.9 mV
SD:	13.6 +/- 1.0 mV
D10:	-37.2 +/- 1.4 mV
D50:	-23.8 +/- 0.3 mV
D90:	-9.8 +/- 2.1 mV

NANOSIGHT NN2_Plex_3%HBS2 2015-12-08 13-48-42

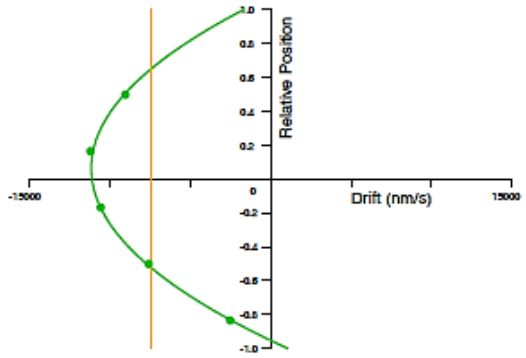

Flow profile for Experiment:
NN2_Plex_3%HBS2 2015-12-08 13-48-42

APPENDIX B

that disrupted WASP expression. We have generated two clones homozygous for the desired WAS mutation that didn't show alterations neither in the karyotype nor pluripotency. Interestingly both hESCWASKO cell lines showed significant alterations during early hematopoietic development generating higher number of CD34 CD45 hematopoietic progenitors that had altered responses to stem cell factor (SCF) but similar colony-forming-unit potential. Surprisingly, hESCWASKO cells differentiated toward the megakaryocytic lineage produced higher number of CD34 CD41 progenitors, megakaryocytes and platelets than wild-type hESCs. However, megakaryocytes and platelets derived from hESCWASKO cells have altered responses to ADP and thrombin and have increased F-actin content in basal conditions. These data corroborate and validate the hESCWASKO cell lines as a human cellular model for WAS and point to a new role for WASp on early hematopoietic differentiation as well as on megakaryocytic development.

P082

Mitochondrial Gene Targeting in Mammalian Systems using Novel 'Mitochondriotropic' Liposomes

N Narainpersad[1], M Ariatti[1], M Singh[1]

[1]*University of Kwazulu-Natal, South Africa*

Mitochondrial research has made a giant leap since the 1980/90s when mitochondrial DNA mutations were first identified as a primary cause for human diseases and the organelle's role in apoptosis was elucidated. This makes the mitochondrion a prime candidate for organelle-specific delivery of exogenous materials such as DNA and drugs, for therapy of diseases caused by mitochondrial dysfunction. Hence vector design and development is of paramount importance. The success of liposomes viz cationic liposomes, in chromosomal gene therapy make them potential

vectors for mitochondrial gene targeting. In this investigation novel 'mitochondriotropic' liposomes were synthesised to evaluate their mitochondrial localisation activities in vitro and ex vivo. Cationic cholesterol derivative, 3β [N-(N',N'-dimethylaminopropane)-carbamoyl] cholesterol (CHOL-T) was formulated with dioleoylphosphatidylethanolamine (DOPE) to produce cationic liposomes, to which a mitochondrial signalling peptide was attached via two different cross-linking agents. Size and lamellarity of liposomes and lipoplexes were assessed by zeta sizing and electron microscopy. Their ability to bind, condense and protect plasmid DNA (pBR322), was determined using the band shift, dye displacement and nuclease protection assays. In vitro cytoxicity was determined using the MTT assay in the hepatocyte-derived human cell line (HepG2). Radiolabeled DNA was used with rat liver mitochondria to determine ability of liposomes to cross the mitochondrial membrane. Confocal and fluorescence microscopy was used to determine nucleic acid localisation. These mitochondriotropic liposomes protect plasmid DNA, are well tolerated by HepG2 cells in culture and were seen to successfully traverse the mitochondrial membranes. Furthermore these liposomes showed positive mitochondrial localisation activities in vitro.

P084

Baboon retrovirus envelope pseudotyped LVs allow efficient transduction of progenitor T cells, thymocytes and adult T and B cells

A Girard[1], F Amirache[1], C Costa[1], C Lévy[1], D Lavillette[1], D Nègre[1], F Cosset[1], E Verhoeyen[1]

[1]*CIRI EVIR team, 69007 Lyon, France*

Efficient gene transfer into quiescent T and B lymphocytes for gene therapy or immunotherapy purposes may allow the treatment of several genetic dysfunctions of the hematopoietic system, such as immunodeficiencies, and the development of novel therapeutic strategies for cancers and acquired diseases. Previously, we have shown that measles virus gps LVs (MV-LVs) were able to transduce efficiently stimulated or resting T and B cells. We now showed that the newly engineered Baboon retrovirus envelope pseudotyped LVs (BAEVgp-LVs) allowed in addition to hematopoietic stem cell transduction, high level transduction of activated T and B cells and resting B cells, where VSVG-LVs fail. Moreover, both naive and memory cells were efficiently transduced and their phenotypes conserved. Since the

REVIEW

Macromolecule Delivery to Mitochondria: A Review of Delivery Strategies

Nicolisha Narainpersad, Moganavelli Singh and Mario Ariatti

Department of Biochemistry, Non-Viral Gene Delivery Laboratory, School of Life Sciences, College of Agriculture, Engineering and Science, University of KwaZulu-Natal (Westville Campus), Private Bag X54001, Durban 4000, South Africa; E-Mails: nicolisha@gmail.com (N.N); singhm1@ukzn.ac.za (M.S); ariattim@ukzn.ac.za (M.A)

Abstract

Research studies about and on mitochondria have been carried out continuously and with considerable success for over a century. In fact, since the publication of two papers in 1988, one in Science and the other in Nature revealed that mutations in the mitochondrial genome could cause human disease; mitochondrial gene targeting in gene therapy is steadily emerging to show great potential. Mitochondrial research is currently one of the fastest growing disciplines in biomedicine, so much so that it has given rise to the development of new sub-disciplines such as Mitochondrial Medicine, Mitochondrial Pharmaceutics and Mitochondrial Pharmacology. There have been a number of studies and reports of successful biomolecule delivery to the mitochondria. This review explores the experimental strategies currently being developed to deliver macromolecules including, model DNA and drug molecules to mitochondria, by discussing the theory underlying each strategy, and detailing the current progress made. Emphasis is made on the potential hurdles that must be acknowledged and overcome.

Key Words: mitochondria, delivery strategies, biomolecules